Starving to grow

The ecology and evolution of growth curve plasticity

Croll, J.C.

Publication date
2023

Document Version
Final published version

Starving to grow

The ecology and evolution of growth curve plasticity

Jasper C. Croll

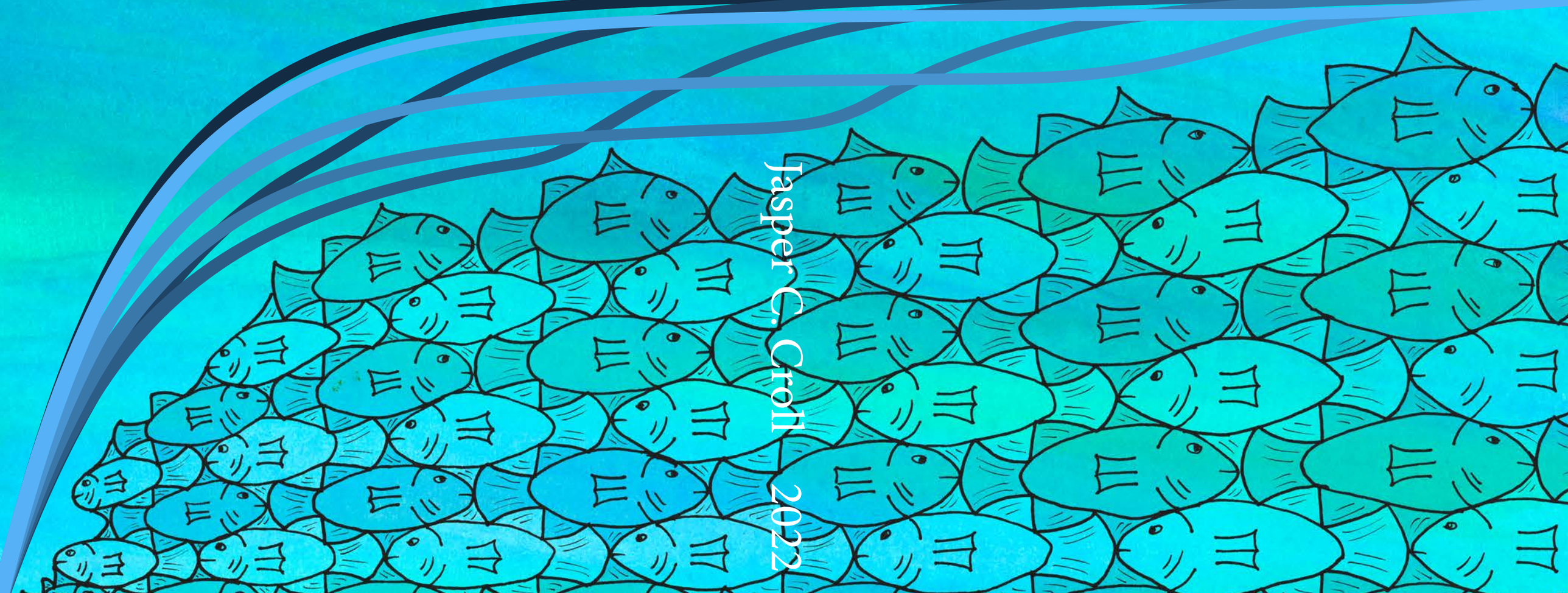

Starving to grow

Jasper C. Croll 2022

Starving to grow

The ecology and evolution
of
growth curve plasticity

by
Jasper C. Croll

Croll, J. C., 2022. Starving to grow: the ecology and evolution of growth curve plasticity

PhD thesis, Institute for Biodiversity and Ecosystem Dynamics, University of Amsterdam, The Netherlands

The research presented in this thesis was funded by the European Union's Horizon 2020 research and innovation program under the grant agreement No. 773713, also known as the Pandora Project.

Cover design: Jasper C. Croll

This thesis is printed on recycled paper

ISBN: 978-94-93260-16-0

Starving to grow

The ecology and evolution of growth curve plasticity

ACADEMISCH PROEFSCHRIFT

ter verkrijging van de graad van doctor
aan de Universiteit van Amsterdam
op gezag van de Rector Magnificus
prof. dr. ir. P.P.C.C. Verbeek
ten overstaan van een door het College voor Promoties ingestelde commissie,
in het openbaar te verdedigen in de Aula der Universiteit
op vrijdag 20 januari 2023, te 11.00 uur

door Jasper Cornelis Croll
geboren te Leidschendam

Promotiecommissie

Promotor:	prof. dr. A.M. de Roos	Universiteit van Amsterdam
Copromotor:	dr. T. van Kooten	Wageningen University & Research
Overige leden:	prof. dr. J.Z. Shamoun-Baranes	Universiteit van Amsterdam
	prof. dr. P.C. de Ruiter	Universiteit van Amsterdam
	prof. dr. K.H. Andersen	DTU Aqua
	prof. dr. M. Peck	Royal NIOZ
	prof. dr. J. van der Meer	Vrije Universiteit Amsterdam
	dr. B.T. Martin	Universiteit van Amsterdam
	dr. E.R. Burdfield Steel	Universiteit van Amsterdam

Faculteit der Natuurwetenschappen, Wiskunde en Informatica

Contents

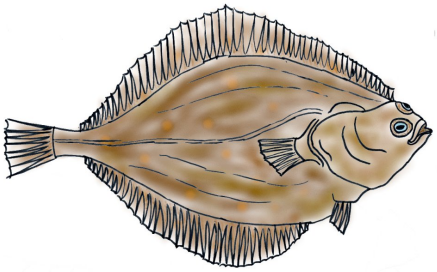

Chapter 1

General introduction

Jasper C. Croll

1.1 Ecology of body size

The body size of living organisms spans an unimaginably large range, from single cell organisms weighing only a few picograms (10^{-12} gram) on one side to large aquatic mammals weighing a couple of hundred tons (10^{9} gram) on the other side. As a consequence of the large difference in size, individuals at the extremes of this scale differ vastly in their physiology and the way they experience their environment (Bonner, 2006). For example, the smallest archaea and bacteria are so small that every single molecule in their environment is of the greatest importance. As these organisms consist of a single cell, they have to obtain their energy through direct chemical interactions with their environment and have to use chemical mechanisms to deal with stressors such as high and low temperatures. This is in stark contrast to blue whales, which can become up to 30 meters long and are therewith the largest species currently present. Blue whales roam through all major oceans and filter the water for krill and similar organisms to provide themselves with food. Part of the energy obtained this way is used to maintain a constant homeostasis, which strongly decreases the impact of external stressors on the functioning of cells and organs. Indisputably, body size is a key trait determining the ecology and physiology of species in numerous and often unknown ways.

One way scientists try to explore the effect of body size on the ecology and physiology of individuals is by comparing species with different body sizes. In this way, numerous traits were found to scale with body size (Hone and Benton, 2005; Peters, 1983). For example, larger species tend to have a higher survival rate and therefore on average live longer compared to smaller species. Meanwhile, larger species on average mature at an older age and therefore start reproducing later in life. This might have to do with the fact that larger species generally have a slower growth rate compared to smaller species and are therefore older when reaching a size at which they are physically capable of reproducing. Likewise, a larger body size generally requires more energy to be maintained and metabolic rates therefore tend to increase with size. As a consequence, larger species on average require more energy and have a higher consumption rate, but might also be able to consume a larger range of food items than smaller species. For a wide range of traits it is generally assumed that they scale following a power-law:

$$Y = Y_0 M^b \tag{1.1}$$

In which Y is the trait of interest, Y_0 is a constant to scale the trait, M is the body mass or size and b is the allometric scaling exponent. It is this allometric scaling exponent which determines the shape of the relationship between a trait and body

size. The exact values of this scaling exponent are heavily debated and are assumed to be multiples of 1/4 based on comparisons between species (Brown et al., 2000) or multiples of 1/3 based on theory about scaling of metabolic processes (Kooijman, 2010). Regardless of the qualitative form of the scaling between traits and body size, it is clear body size correlates with numerous differences between species.

When linking traits to interspecific differences in body size, it is easy to overlook the importance of body size within a species or population. By far, most of the multicellular organisms start as a single cell and end up as a full-grown individual, which can consists of trillions (10^{13}) of cells. Even after birth or hatching, a ten-, a hundred- or even a thousandfold increase in size throughout life is not uncommon. However, differences in body size within a species do not only occur due to development over time, as variation in size is also very common between individuals of the same age. Differences in size between individuals of the same age might arise because they were born with different sizes, but could also emerge from differences in their growth rates, for example because growth rates are affected by the environment. This thesis will specifically concern the ecological and evolutionary patterns that arise from intraspecific variation in body size caused by a link between individual growth rates and the environment.

1.2 Plasticity in individual growth

The effect of the environment on the expression of a trait is called phenotypic plasticity. Due to phenotypic plasticity, variation in the environment can cause differences in the phenotype of individuals with exactly the same genotype. The effect of phenotypic plasticity on a trait can be very distinct. A classic example is the defence mechanism of the water flea *Daphnia*. In the presence of a predator, *Daphnia* will produce offspring with a helmet to reduce the risk of a predator attack on the offspring, while in the absence of a predator the helmet is lacking (Krueger and Dodson, 1981). More often, the effects of plasticity on the phenotype of an individual are more subtle and might not be immediately visible, but accumulate throughout the life history of an individual. This is the case with individual growth and body size. For many species, growth rates are expected to increase with temperature or food availability, but individuals have to experience an environment for a longer period of time for environmental effects to accumulate and become visible in their body size. The physical and ecological effects of plasticity in individual growth rates might therefore have a delayed effect and might only become apparent in the size of an individual over a longer time span.

Quantifying plasticity in individual growth requires many measurements of

individual ages and sizes spanning a relatively long period of time. The ideal approach would be to follow the growth trajectory of multiple individuals in controlled environments, as has been done for *Daphnia* (McCauley et al., 1990). This study showed that the development rate of *Daphnia* increases with increasing food availability in a way that closely resembles a type II functional response. This is a clear indication that growth of *Daphnia* has a plastic component. Such experimental data is not available for most species, in which case relative size and age relationships might be obtained from annual growth rings in hard body parts such as bones, scales and even some wooden parts of plants. Several studies conducted in this way showed that in general, age is not suitable to predict the size of amphibians and reptiles (Halliday and Verrell, 1988). From this we can conclude that growth in amphibians and reptiles differs between individuals and is likely to have a plastic component. More generally, the growth rate of ectotherms can be expected to be largely plastic. Most ectotherms have weak homeostasis and as a consequence their internal condition is strongly linked to the environment. It is therefore straightforward to expect that growth in body size of ectothermic species depends on the environment as well. In contrast, endothermic species generally have a strong homeostasis and are capable of separating their internal conditions from the environment to a much larger extent. This leads to the hypothesis that the growth rate of endotherms is more static and less dependent on the environment. This is supported by observations of a very constant growth rate in ungulates. It is even observed that ungulates postpone reproduction while maintaining a constant growth rate under limited food conditions (Albon et al., 2000; Coulson et al., 2000; Skogland, 1986). Similarly, female house mice were shown to stop ovulating while maintaining a constant growth rate under low food conditions in an experimental setup (Perrigo, 1990). In general, this suggests that the growth rate of endotherms is largely fixed, while the growth rates of ectotherms contain a large plastic component.

Plasticity in individual growth is currently a topic of much interest in the field of fisheries ecology and management. Aquatic ecosystems have to withstand enormous pressure originating from human activities such as fisheries, water pollution and the emission of greenhouse gasses which accelerate climate change. Meanwhile, policymakers have to find a balance between the high economic and nutritious demand for fisheries on the one hand and the viability of fish populations on the other hand when establishing fishing quotas. To establish these fishing quotas, mathematical models are used to predict the maximum yield from a fish stock that can be sustained by the population. Classically, these models assume that all environmental impact acts on the pelagic larvae of fish, resulting

in a bottleneck early in life (May, 1974). Commonly this is modelled with a stock-recruitment relationship, which relates the number of offspring surviving the early life stages directly to the density of reproducing adults, as proposed by Ricker (1954) and Beverton and Holt (1957). After recruitment, the stock is generally modelled with an age-based model, assuming that all individuals of the same age are roughly of the same size. In other words, these models do not assume plasticity in growth to occur in fish populations after recruitment. However, recent studies have shown that individual growth in a substantial number of fish stocks correlates with stock biomass. This suggests that individual growth has a plastic part which is linked to the stock density (Zimmermann et al., 2018; Lorenzen, 2016; Schram et al., 2006; Lorenzen and Enberg, 2002). This link between stock density and individual growth can cause feedback mechanisms that could change the fishing intensity at which the maximum sustainable yield is achieved (Van Gemert and Andersen, 2018b). In addition, changes in the size structure of fish stocks due to plasticity in individual growth are important for the fisheries industry, as larger fish are often more valuable and only fish above a specified size threshold can be sold. If we add this to the human induced changes in the aquatic environment and the increase in fish stock density due to recovery from over-fishing (Rindorf et al., 2020; Wang et al., 2020; Zimmermann and Werner, 2019; Fernandes and Cook, 2013; Worm et al., 2009), it is clear that the level of growth plasticity in fish stocks becomes more important for sustainable fisheries than ever.

1.3 Energetics of individual growth

Growth in body size is a costly process, as the production of new mass requires a substantial amount of energy. Individuals have to acquire this energy through feeding and assimilation. Not all of this assimilated energy can be spent on growth, as other physiological processes need to continue as well. Energy is actually needed for all processes in the body including for example the maintenance of the chemical composition of cells, monitoring the internal and external environment, movement, feeding and last but not least the production of offspring. One can imagine that precise regulatory mechanisms are needed to distribute this energy in a correct way, especially because some processes are of vital importance, while other processes do not directly contribute to the survival of an individual. It is also clear that energy can only be spent once, which could lead to numerous trade-offs between individual life history characteristics (Stearns, 1989).

The energetic trade-offs in the life history characteristics of an individual can be made more explicit by modelling the energy flows within an individual. These

energy flows start with the absorption of energy in the body of an individual through the assimilation of compounds from the environment. Unicellular organisms and organisms with a low level of complexity, such as sponges, directly absorb molecules from the environment. In contrast, most other animals first have to collect food items, which are digested in the guts to extract energetic compounds. These compounds are then available for assimilation. Clearly, the amount of energy that can be absorbed depends on the available energy in the environment, regardless of whether this energy is in the form of chemical compounds or larger food items. After assimilation, energy can be stored and distributed among the processes within an organism. Most energy allocation schemes classify these processes into three categories, but differ in the rules that determine the division of assimilated energy among these categories (Kooijman, 2000; West et al., 2001; Hou et al., 2008; Sousa et al., 2008). The first category deals with reproductive processes. In juveniles, this category includes processes that contribute to the maturation of an individual. In adults this category includes all processes that deal with reproduction, resulting in the production of offspring. The second category deals with processes regarding somatic growth. Energy allocated to this category is used by individuals to produce new mass and to grow in size. The third category deals with somatic maintenance costs, which are costs for maintaining the current state of the body. This category is commonly used to lump together processes that cannot be included in the reproduction or growth category, such as energy expenses for movement and heat production. Nonetheless, somatic maintenance costs are generally considered to be a vital energy expense without which individuals cannot survive. The major difference between different energy allocation schemes is the order and priority in which energy is allocated to these three categories, and the way that the processes in these categories scale with body size.

The energy allocation scheme used in this thesis is based on a simple dynamic energy budget model (Jager et al., 2013) (Fig. 1.1). In this model, assimilated energy is stored in a short-term storage with a high turnover rate, from which it is directly available for usage. Energy is first distributed between somatic processes on the one hand, which is further divided between somatic growth and somatic maintenance, and reproductive processes on the other hand, which include maturation of juveniles and reproduction by adults. Energy allocated to somatic processes is directly divided among somatic maintenance and growth. The order or priority of the processes depends on whether a process is demand-driven or supply-driven. A demand-driven process requires a fixed amount of energy that only depends on the state of the body, regardless of the amount of assimilated energy. In contrast,

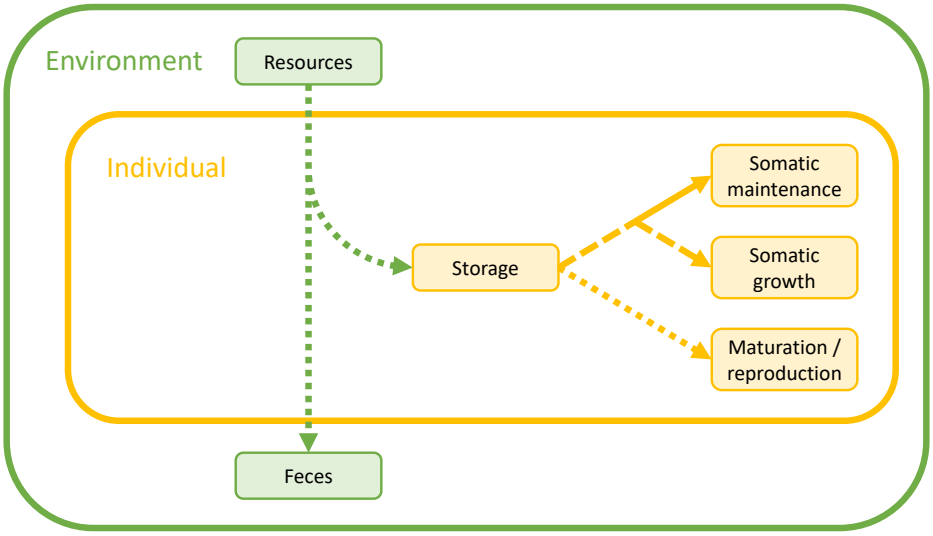

Figure 1.1: Schematic layout of the energy allocation scheme used in this thesis. Arrows indicate energy flows between components. Solid arrows indicate entirely demand-driven processes, dashed arrows indicate energy flows which could be partly demand-driven and partly supply-driven and dotted arrows indicate entirely supply-driven energy flows. This scheme also represents the order of priority of energy allocation that is assumed in this thesis.

the amount of energy used by a supply-driven process directly depends on the amount of available energy. Demand-driven processes have priority over supply-driven processes, because demand-driven processes are not flexible in the amount of energy that they require, while supply-driven processes are. Somatic maintenance costs are generally implemented as an entirely demand-driven process with the highest priority because it includes the basal processes needed to survive. In most energetic models, it is assumed that the energy allocation to both growth and reproduction depend on the amount of assimilated energy and are entirely plastic (Kooijman, 2000; West et al., 2001; Hou et al., 2008; Sousa et al., 2008; Jager et al., 2013). The energy model used in this thesis explicitly deviates from this assumption, such that somatic growth has a demand-driven and a supply-driven part. This enables individuals to grow at a more constant rate, independent of the environment. The demand-driven part of somatic growth can be interpreted as a minimum investment in somatic growth independent of the environment, while the supply-driven part of somatic growth is the additional investment in growth allowed by the amount of assimilated energy. Because energy assimilation depends on the availability of energy sources in the environment, energy investment

in supply-driven processes indirectly depends on the environment as well. In this way, supply-driven processes and in particular supply-driven growth is inherently plastic, while demand-driven processes are not plastic at all.

1.4 From individual energetics to population dynamics

Theory about individual energy allocation offers a stylized framework with which the energetic trade-offs between life history characteristics can be described. This kind of energetic theory is, however, only useful to a limited extent to answer ecological and evolutionary questions directly, because it does not account for feedback mechanisms with the environment. In addition, it is not possible to measure or observe energy fluxes in an individual directly. To bridge this gap between energetic theory and ecological questions, models of individual energy dynamics have to be connected to measurable individual traits such as body size and body condition, reproductive output and mortality. With these more tangible life history characteristics, the life history of an individual can be reconstructed. The separate life histories of individuals can be bundled together with a quantitative description of the environment to obtain a full description of a structured population. The structure in these populations arises because individuals differ in some of their life history characteristics such as age and size and can be classified based on these differences. These structured descriptions of a population are very suitable to answer questions about the ecological and evolutionary dynamics of a population, because they consider differences between individuals within a population.

The allometric scaling from dynamic energy budget theory offers a convenient way to relate schemes of individual energy allocation rules to individual life history characteristics (Kooijman, 2010). These allometric scaling laws assume that the energy content of an individual scales with the mass of an individual, while the mass of an individual relates to its volume. Meanwhile, these scaling laws assume that volume scales with length cubed while the surface area of an individual scales with length squared, which basically comes down to approaching an organism as a symmetric sphere. dynamic energy budget theory continues this line of reasoning and assumes that all important life history processes approximately scale with surface area or body volume, resulting in allometric scaling exponents in equation (1.1) which are a multiple of one-third. More precisely, energy consumption is assumed to scale with the surface area of an individual, while maintenance costs are assumed to scale with individual mass or volume. With these allometric scaling rules, an energy allocation scheme such as outlined in the previous section can be

translated to equations for growth and reproduction in terms of individual length. This commonly results in a growth curve first described by Von Bertalanffy (1938):

$$\frac{d\ell}{da} = r_B \left(\ell_{max} - \ell\right) \tag{1.2}$$

According to this description, the growth rate of an individual ($\frac{d\ell}{da}$) depends on the difference between an asymptotic size (ℓ_{max}) and the current size (ℓ) multiplied with a species-specific scalar of the growth rate (r_B). In other words, individuals grow towards an asymptotic size and the growth rate decreases when individuals approach this asymptotic size. In the first formulation of this growth curve, Von Bertalanffy (1938) already described that the asymptotic size is dependent on the individual assimilation rate while the growth rate scalar depends on the individual catabolism rate. The asymptotic size of the growth curve could therefore strongly depend on the food availability in the environment, while the growth rate scalar is generally less affected by the environment because it depends on the vital demand-driven processes in an organism.

Individuals do not live in isolation, but are part of a population in a constantly changing environment. Individuals that are born at approximately the same moment and experience approximately the same environment are likely to follow a similar growth curve and form a cohort. If the growth of individuals would be completely static and independent of the environment, all cohorts would show exactly the same growth curve. In this case, a constant relationship between age and size could be derived, and the population could be modelled using an age-based model. Fixed size-age relationships and age-based models are commonly used to establish long-term fishing quotas and fishery management strategies (Schnute and Richards, 1998). The size and age structure of a population become decoupled as soon as the individual growth rates show some plasticity. The growth curve of cohorts will start to differ, and variation within a cohort will arise as soon as growth is plastic and the environment is not constant. A population with a plastic growth rate can be modelled using physiologically structured population models, in which a population is not only structured by age, but also by a physiological trait such as size (De Roos and Persson, 2001). As these models generally neglect the variation within a cohort, physiologically structured population models are especially suitable to model populations with variation in growth between cohorts. So far, most of these models assumed that growth is an entirely supply-driven process and that the growth curves of individuals are therefore entirely plastic. As a consequence, individuals would stop growing entirely if resources fall short. It has been shown that age-structured models with static individual growth and size-structured mod-

els with entirely plastic individual growth differ strongly in their predictions about population dynamics, population dynamic cycles and the response to harvesting (Gurney and Nisbet, 1985; De Roos et al., 1990; De Roos and Persson, 2003; Persson et al., 2007; Pfaff et al., 2014). Although contrasting these extreme cases can be very informative, it is more likely that individual growth is not entirely static or plastic but consists of a plastic supply-driven growth rate on top of a basal demand-driven growth rate. This raises the question of what dynamics a structured population would exhibit if individual growth is not fully fixed nor fully plastic, but lies somewhere in between.

1.5 What to expect from this thesis

The plasticity in individual growth differs strongly between species. As is clear from the previous sections, individual growth rates are largely fixed in some species, while it is strongly dependent on the environment in other species. The impact of the environment on individual growth rates is often difficult to measure, because environmental effects on growth accumulate in the size of an individual over a longer period of time. Information on a large part of the growth history of an individual is therefore needed to disentangle the fluctuations in environmental limitation of growth over time, but in practice the age and size of an individual is often only measured once. Even if some information on the level of plasticity in individual growth is available, the population is generally simplified to an age-based model with entirely fixed growth or a size-structured model in which all growth is determined by the environment. Intermediate scenarios could arise if individual growth arises from an environment-dependent part on top of a fixed basal part, which would result in an intermediate level of plasticity in growth. So far, the ecological and evolutionary dynamics arising from an intermediate level of plasticity in individual growth did not get any attention. This thesis therefore evolves around two main questions:

How can the temporal variation in the environmental limitation of individual growth be derived from a collection of individual age and size measurements?

and

How does an intermediate level of growth plasticity shape the dynamics of a size-structured population on ecological and evolutionary time scales?

Although these questions are approached from a theoretical perspective without a particular species in mind, several chapters of this thesis turn to North Sea

fish species to demonstrate the practical application of the developed theory to natural systems. North Sea fish species are especially interesting because these populations are under high pressure from human harvesting. Due to the long history of exploitation and management, measurements of individuals from these stocks are available over a long time span. Nonetheless, little is known about the growth dynamics of these stocks and the effect of plasticity in individual growth on the management of these stocks. Altogether, this makes the North Sea fish stocks interesting populations for the application of the techniques and models discussed in this thesis.

In **chapter 2** of this thesis, I derive a method to quantify the temporal dynamics of the environmental limitation on individual growth from individual age and size measurements. To do so, I derived an expression for the size distribution of every cohort at every year and age of interest. These distributions are based on the assumption that individuals follow a Von Bertalanffy growth curve in which the asymptotic size is limited by an environmental condition that changes over time. As a consequence, variation in size at age arises between years, between cohorts and between individuals within a cohort, which are all included in the model describing the size distributions. I show that fitting the model to individual sizes and ages measured over a long time span results in a discretized approximation of the environmental limitation on individual growth.

In **chapter 3** of this thesis, I fit the model derived in chapter 2 to data of ten exploited North Sea fish species in ten ecological regions. This resulted in yearly estimates of the asymptotic sizes for all species and area combinations. These estimated asymptotic sizes summarize the temporal variation in growth and could therefore serve as a summary statistic for the environmental impact on individual growth. I show that seven of the included species show a negative trend in this asymptotic size over time. In addition, I found signs of density dependence in growth for six of the species. More importantly, cluster analysis was performed on the species and regions based on the estimated asymptotic sizes. The predicted clusters predicted with the estimated asymptotic sizes corresponded closely to the clusters expected based on the ecology of the fish species and the geographical location of the areas. This strengthens the theory that growth limitation arises through interactions with the environment.

In **chapter 4** of this thesis, I explore how the level of plasticity in individual growth affects the dynamics of a size-structured population. To do so, I first derive a detailed description of a dynamic energy budget model in which the plasticity in individual growth is variable. Herein I assume that the environment only consists of a resource, because resource availability seems the environmental factor that is

most likely to influence individual growth. I translate this dynamic energy budget model to a physiologically structured population model to explore the dynamics at the population level. The analysis reveals that the dynamics of a structured population can be limited through individual reproduction or through individual growth, which both result in qualitatively different population structures and population dynamic cycles.

In **chapter 5** of this thesis, I study the evolution of growth plasticity in the model derived in chapter 4. I show that evolution balances the individual limitation on growth and the individual limitation on reproduction, which results in the most optimal usage of consumed energy. In addition, I show that the individual energy allocation schemes determine the global endpoint of evolution, while costs scaling with plasticity only play a minor role in the evolutionary trajectory of a population. As a consequence, it is most likely to find species with an intermediate level of growth plasticity while it is very unlikely to find species in which growth is entirely plastic.

In **chapter 6** of this thesis, I parameterize the model derived in chapter 4 for four North Sea flatfish species to explore the effect of growth plasticity on the fishing intensity with maximum yield. I again find that there is a regime in which the dynamics is driven by limitation in individual reproduction and a regime in which the dynamics is driven by limitation in individual growth. In the regime driven by reproduction, the optimal harvesting intensity arises as a balance between harvesting mortality and density dependent effects on recruitment. In the regime driven by growth, density dependent effects in growth compensate for the additional mortality due to harvesting and the optimal fishing intensity is determined by a peak in recruitment. The optimal fishing intensity and composition of the catches is very different for both regimes, suggesting that it is of vital importance to know the level of density dependence in individual growth when estimating optimal harvesting regimes.

In **chapter 7** of this thesis, I discuss how growth curve plasticity affects various levels of biological organization. In addition, I discuss how plasticity and density dependence could affect fishing quotas and how the method developed in chapter 2 and 3 can advance the estimation of these quotas. Furthermore, I explore the assumptions and generalities of the models used in chapter 4 to 6. I end by concluding that species differ in the plasticity in individual growth, and that even small differences in plasticity could make a large impact on the dynamics of structured populations, especially if a population is under high pressure from human activities.

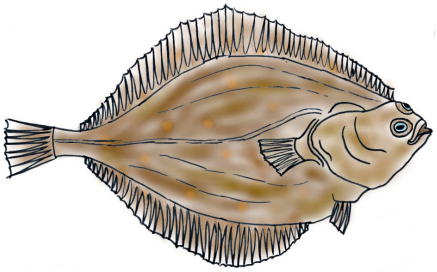

Chapter 2

Accounting for temporal and individual variation in the estimation of Von Bertalanffy growth curves

Jasper C. Croll

Tobias van Kooten

In press at *Ecology and Evolution* (2022)

Abstract

Growth and growth limitation are important indicators of density dependence and environmental limitation of populations. Estimating individual growth trajectories is therefore an important aspect of understanding and predicting the life history and dynamics of a population. Variation in individual growth trajectories arises due to variation in the environmental factors limiting individual growth. This environmental limitation can vary over time, between cohorts and between individuals within a cohort. For a complete and accurate understanding of individual growth in a population, it is important to include all these sources of variation. So far, statistical models only accounted for a subset of these factors or required an extensive growth history of individuals. Here we present a novel model describing the growth curves of cohorts in a population. This model is derived from a stochastic form of the Von Bertalanffy growth equation describing individual growth. The model is specifically tailored for use on length-at-age data in which the growth trajectory of an individual is unknown and every individual is only measured once. The presented method can also be used if growth limitation differs strongly between age or length classes. We demonstrate the use of the model for length-at-age data of North Sea plaice (*Pleuronectes platessa*) from the last thirty years. Fitting this model to length-at-age data can provide new insights in the dynamics of the environmental factors limiting individual growth and provides a useful tool for ecological research and management.

2.1 Introduction

Body size is shown to be an important indicator of many life history traits such as maturation, consumption, mortality and reproduction rates (Kooijman, 2010; Calder, 1984; Peters, 1983; Pauly, 1980; Beverton and Holt, 1959). Estimating the growth trajectory of individuals is therefore a general aspect of understanding the life history and dynamics of a population. The Von Bertalanffy growth equation is one of the most commonly used models to describe growth of individuals. It is already used to describe the growth of a wide range of species (Ramirez et al., 2021; Teleken et al., 2017; Narinç et al., 2017; Kingsley, 1979) and is especially often used for fish (Flinn and Midway, 2021; Lorenzen and Enberg, 2002). The Von Bertalanffy growth equation describes growth in terms of individual energy assimilation and catabolism rates (Von Bertalanffy, 1938). In the resulting growth curve, individuals grow towards an asymptotic length at which the catabolism rate is equal to the assimilation rate and no energy is available for growth. If we follow dynamic energy budget theory (Kooijman, 2010) and assume that assimilation scales with surface area while catabolism scales with body volume, we obtain the most commonly used form of the Von Bertalanffy growth equation:

$$\frac{d\ell_{(t,a,i)}}{dt} = r_B \left(f_t \ell_\infty - \ell_{(t,a,i)} \right) \tag{2.1}$$

Herein we indicate the length of individual i at age a and time t with $\ell_{(t,a,i)}$, which emphasizes that equation (2.1) describes the growth rate of a single individual. In this equation, individual growth is proportional to the difference between the asymptotic length ($f_t \ell_\infty$) and the current length, scaled with the Von Bertalanffy growth rate scalar (r_B). Following dynamic energy budget theory (Kooijman, 2010), the asymptotic length consists of a maximum asymptotic length (ℓ_∞) scaled with the limitation of growth by the environment through assimilation (f_t). Although individuals might vary slightly in the values of the Von Bertalanffy growth rate scalar and the asymptotic size due to genetic differences, we will only focus on environmental effects on growth because these effects can affect the growth of individuals through their life. It is commonly assumed that the asymptotic length is the only parameter in the Von Bertalanffy growth equation which depends on the environment (Kooijman, 2010; Lorenzen and Enberg, 2002). As such, the Von Bertalanffy growth equation provides an opportunity to estimate the environmental limitation on the individual growth rate.

Research on the dynamics of individual growth is generally based on one of two types of data containing age and length measurements of individuals. The first

type of data contains multiple measurements of the same individual, for example obtained through controlled experiments, mark-recapture methods or back calculation from otoliths or year-rings. This type of data generally allows for extensive correction for variation between individuals and cohorts because the growth history of individuals is known (Vincenzi et al., 2016, 2014; Shelton et al., 2013; De Graaf and Prein, 2005; Rafail, 1973). Often however, such rich individual-level data is unavailable, because individuals cannot be tagged or retrieved or because back calculation of otoliths and year-rings is often imprecise (Eveson et al., 2007). Even if these methods are successful, they only result in a relative relationship between age and length. Much more common is the second type of data, which only contains a single measurement per individual. To obtain this kind of data, individuals only have to be measured once and the age of individuals can be determined based on hard or internal body structures such as year-rings, scales, bones, teeth, and chemical composition. This is a common method for fish (Maceina et al., 2007), amphibians (Smirina, 1994), reptiles (Castanet, 1994), mammals (Read et al., 2018) and insects (Robson and Crozier, 2009). In this study, we focus on the estimation of growth curves and variation herein based on data consisting of a single observation per individual.

In data with a single age and length observation per individual, the growth history of individuals is unknown and it is difficult to deal with the different overlapping sources of variation in the length individuals have at a specified age. In addition to variation between measurements due to sampling errors (Piner et al., 2016; Taylor et al., 2005), variation in the growth rate can be separated into variation as a result of changes in the environment over time, variation in the growth history of cohorts and variation between individuals within a cohort. So far, statistical methods dealing with single observations of individual ages and lengths only deal with a subset of these sources of variation.

Variation due to changes in the environment over time is most likely to affect the asymptotic length in the Von Bertalanffy growth equation because this is the part of the growth equation that is related to the environment-dependent assimilation rate of an individual (Kooijman, 2010; Von Bertalanffy, 1938). Changes in the asymptotic size therefore affect all cohorts at a given time equally. This can be used to estimate the effect of an environmental factor on the growth of individuals. This is generally done by directly substituting the asymptotic length in the Von Bertalanffy growth equation with a linear dependency on the environmental factor of interest (De Graaf and Prein, 2005; Lorenzen and Enberg, 2002; Lorenzen, 1996; Cloern and Nichols, 1978). Although this can be useful to prove a general relationship between the growth rate and an environmental factor, the

a priori assumption of linearity is questionable.

Variation between cohorts arises due to differences in the growth history of cohorts. It is evident that cohorts in a given year differ in length due to the difference in age, but the length at a given age is likely to vary over time as well. This variation between cohorts might arise due to variation in the length at birth, but might also occur because cohorts lived at different times and therefore differ in the experienced environment (He and Bence, 2007; Wang and Thomas, 1995). A common way to correct for the growth history of individuals is to consider the average growth increment between two time points, instead of the actual length-at-age (Wang and Thomas, 1995; Lipinski and Roeleveld, 1990; Rafail, 1973). As we consider datasets that consist of independent length-at-age observations throughout years, this method can only be applied to the average length-at-age in every sampling instance and as such neglects individual variation in length-at-age and environmental limitation. In addition, this has been shown to yield less accurate estimates of the Von Bertalanffy growth parameters with a larger uncertainty (Vaughan and Kanciruk, 1982).

Similar to variation between cohorts, variation in length-at-age within cohorts arises due to differences in length at birth and differences in the experienced environment between individuals. Although individuals in the same cohort are not separated in time, they might be separated spatially or due to other ecological factors leading to variation in the experienced environment. In addition, genetic differences might cause variation between individuals as well. Consistent (genetic) differences between individuals can be accounted for by incorporating a random effect for every individual, but this is only feasible in data sets with multiple observations per individual. We focus on data sets with single observations for each individual, where this approach would only lead to extreme overfitting. Therefore, the only option to account for individual variation caused by a shared environment in datasets with single measurements is by considering the length-at-age at the population level as a distribution rather than a single value (Eveson et al., 2007; Pilling et al., 2002; Prajneshu and Venugopalan, 1999).

The different sources of variation in the length-at-age are entangled due to the autoregressive nature of individual growth processes in which the current growth rate depends on the growth history of an individual. As a consequence, variation in growth arises between individuals and cohorts and could fluctuate over time. All these sources of variation should be considered to obtain an accurate estimate of the Von Bertalanffy growth parameters of a specific species, even if we are only interested in one of the sources of variation or average growth parameters. There is currently no method available that includes all these sources of variation

simultaneously. To fill this gap, we derive a model that describes the length distribution at a given age for every cohort, which can be used for datasets with a single length and age observation per individual. Because we derived this model from a stochastic version of the Von Bertalanffy growth equation for single individuals (eq. 2.1) it simultaneously includes variation due to changes over time, variation due to differences in the growth history of cohorts and variation between individuals within a cohort. Here, we derive the model and apply it to length-at-age data of North Sea plaice (*Pleuronectes platessa*).

2.2 Methods

Model formulation

We start with the equation describing the growth trajectory of a single individual (eq. 2.1). Individuals will differ in the experienced environmental limitation and this limitation might vary over time. We therefore assume that the limiting effect of the environment at a given point in time follows a Gaussian distribution of which the mean (μ_t) and variance (σ_t^2) are allowed to vary over time:

$$f_t \sim \mathcal{N}\left(\mu_t, \sigma_t^2\right) \tag{2.2}$$

By substituting this distribution in equation (2.1) we obtain a stochastic differential equation describing the growth of an individual born at time T_b. We can solve this equation by separation of variables and integration:

$$\begin{aligned} d\ell_{(t,a,i)} =& r_B\left(\mu_t \ell_\infty - \ell_{(t,a,i)}\right) dt + r_B \sigma_t \ell_\infty dW_t \\ \ell_{(T,a,i)} =& \ell_{(T_b,0,i)} e^{-r_B(T-T_b)} + \int_{T_b}^{T} r_B \mu_t \ell_\infty e^{-r_B(T-t)} dt \\ &+ \int_{T_b}^{T} r_B \sigma_t \ell_\infty e^{-r_B(T-t)} dW_t \end{aligned} \tag{2.3}$$

The parameter $\ell_{(T_b,0,i)}$ represents the length at birth of an individual. In addition, W_t represents a Wiener process, which describes the outcome of a continuous process with independent Gaussian increments ($W_{t+u} - W_t \sim \mathcal{N}(0, u)$). The integrals in this expression cannot be solved explicitly because the dynamics of the mean and variance of the environmental limitation (μ_t, σ_t^2) are not defined. If the environmental limitation was constant over time and space ($\mu_t = \mu, \sigma_t^2 = 0$), individuals would follow a Von Bertalanffy growth curve towards a constant asymptotic length.

In this method we consider datasets in which every individual is only measured once. In the ideal situation, these individuals are selected randomly from the population. In this type of data, it is not possible to follow the growth trajectory of a single individual and fit the derived growth curve on single individuals. Instead, we describe the distribution of the length-at-age for a cohort. Because we assumed that the environmental limitation of growth follows a Gaussian distribution, the length of individuals in a given cohort at time T follows a Gaussian distribution as well. Because the expected value of the Wiener process is equal to zero, we can derive an expression for the expected mean length at time T of a cohort born at time T_b:

$$\begin{aligned} E\left[\ell_{(T,a)}\right] =& E\left[\ell_{(T_b,0,i)} e^{-r_B(T-T_b)}\right] + E\left[\int_{T_b}^{T} r_B \mu_t \ell_\infty e^{-r_B(T-t)} dt\right] \\ &+ E\left[\int_{T_b}^{T} r_B \ell_\infty \sigma_t e^{-r_B(T-t)} dW_t\right] \\ =& E\left[\ell_{(T_b,a)}\right] e^{-r_B(T-T_b)} + \int_{T_b}^{T} r_B \mu_t \ell_\infty e^{-r_B(T-t)} dt \end{aligned} \tag{2.4}$$

We omitted the indices referring to single individuals in the expression of the expected value of the length-at-age ($E[\ell_{(T,a)}]$) to make clear that this expected value is a statistic of the length-at-age distribution of a cohort rather than the length of single individuals. By using equations (2.3) and (2.4) and applying Ito's isometry rule we can also derive an expression for the expected variance in length at time T for a cohort born at time T_b:

$$\begin{aligned} V\left[\ell_{(T,a)}\right] =& E\left[\left(\ell_{(T,a,i)} - E\left[\ell_{T,a}\right]\right)^2\right] = E\left[\left(\int_{T_b}^{T} r_B \sigma_t \ell_\infty e^{-r_b(T-t)} dW_t\right)^2\right] \\ =& E\left[\int_{T_b}^{T} r_B^2 \sigma_t^2 \ell_\infty^2 e^{-2r_B(T-t)} dt\right] = \int_{T_b}^{T} r_B^2 \sigma_t^2 \ell_\infty^2 e^{-2r_B(T-t)} dt \end{aligned} \tag{2.5}$$

We assume that samples are taken with an approximately constant time interval and therefore discretize the equations characterizing the length distribution of a given cohort at time T. Under this assumption, the equations become independent of the length distribution at birth and can be applied without knowledge of the full growth history of a cohort.

$$E\left[\ell_{(T+1,a+1)}\right] = E\left[\ell_{(T_b,0)}\right] e^{-r_B(T-T_b+1)} + \int_{T_b}^{T+1} r_B \mu_t \ell_\infty e^{-r_B(T+1-t)} dt \quad (2.6a)$$

$$= E\left[\ell_{(T,a)}\right] e^{-r_B} + \int_{T}^{T+1} r_B \mu_t \ell_\infty e^{-r_B(T+1-t)} dt$$

$$V\left[\ell_{(T+1,a+1)}\right] = \int_{T_b}^{T+1} r_B^2 \sigma_t^2 \ell_\infty^2 e^{-2r_B(T+1-t)} dt \quad (2.6b)$$

$$= V\left[\ell_{(T,a)}\right] e^{-2r_B} + \int_{T}^{T+1} r_B^2 \sigma_t^2 \ell_\infty^2 e^{-2r_B(T+1-t)} dt$$

To make these equations usable, we need to make assumptions about the dynamics of the mean and the variance of the environmental limitation (μ_t and σ_t^2). These quantities only appear within the integral from time T up to time $T+1$. We therefore only have to make assumptions about the mean and variance of the environmental limitation between consecutive time points or measurements. We assume that the mean and variance of the environmental limitation between times T and $T+1$ are well approximated by the average value of these quantities in the given time interval ($\bar{\mu_T}$ and $\bar{\sigma}_T^2$). Under these assumptions, the model will approximate the growth dynamics if the interval between measurements becomes small relative to the average lifetime of an individual. Because we substitute the mean and variance of the environmental limitation by the average of these quantities over a time interval, they become independent of time in the domain of integration and we can solve the integrals in equation (2.6), which results in the final form of our model:

$$E\left[\ell_{(T+1,a+1)}\right] = E\left[\ell_{(T,a)}\right] e^{-r_B} + \bar{\mu_T} \ell_\infty \left(1 - e^{-r_B}\right) \quad (2.7a)$$

$$V\left[\ell_{(T+1,a+1)}\right] = V\left[\ell_{(T,a)}\right] e^{-2r_B} + \frac{1}{2} r_B \bar{\sigma}_T^2 \ell_\infty^2 \left(1 - e^{-2r_B}\right) \quad (2.7b)$$

Interesting to note from this formulation is that the variance in environmental limitation over a given period ($\bar{\sigma}_T^2$) has the same unit as the time constant (T). This arises because we model the length of an individual as a Brownian process which is a process with random increments. The variance of a Brownian process increases due to the random nature of the process and therefore depends on the length of the time between consecutive measurements in our model. In other words, the total variance in environmental limitation experienced by an individual increases (decreases) if the actual variation of the environment increases (decreases) or the individual experiences the environment for a longer (shorter) period of time.

To obtain a time-independent measurement of the environmental variation, we

can consider the long-term asymptotic variation in individual length ($V[\ell_{(T,\infty)}]$). This represents the variation in length that individuals would have after spending an infinitely large time in an environment with a given amount of variation in growth limitation ($\bar{\sigma}_T^2$). At this asymptotic variation in length, the loss of variation in length due to growth ($V\left[\ell_{(T,a)}\right]\left(1-e^{-2r_B}\right)$) is equal to the gain in variation in length due to variation in the environment ($\frac{1}{2}r_B\bar{\sigma}_T^2\ell_\infty^2\left(1-e^{-2r_B}\right)$). In other words, when a cohort reaches the asymptotic variation in length, the variation in length of a cohort does not change any further over time. From equation (2.7b) we can therefore derive the expression of the long term asymptotic variance in length:

$$V[\ell_{(T,\infty)}] = \frac{1}{2}r_B\bar{\sigma}_T^2\ell_\infty^2 \tag{2.8}$$

Model application

The model proposed in equation (2.7) predicts an independent Gaussian length distribution for every cohort at every discrete age and time value. Therefore, the model can be fitted to datasets containing pairs of age and length measurements using maximum likelihood estimates. The best results are obtained if individuals enter the population at approximately the same moment of the year and measurements represent a random sample of the population. This is especially important for individuals in the same age class and year. Assigning weights to the measurements allows to correct for biases in the sample, if biases are known. In addition, sample instances should approximately be evenly distributed in time and individual ages and cohorts should be characterized on the same discrete scale as sample instances. For example, measurements could be taken yearly on randomly selected individuals at a specified date. The age of individuals is consequently measured in year classes and individuals born between two measurements belong to the same cohort. Fitting the model described by equation (2.7) to a dataset with pairs of length and age measurements is done by optimizing the log likelihood through altering the value of the Von Bertalanffy scalar (r_B), the length distribution at the youngest age at every time point ($E[\ell_{T,a_{min}}]$,$V[\ell_{T,a_{min}}]$), the length distribution of all other cohorts at the first time point ($E[\ell_{T_{min},a}]$,$V[\ell_{T_{min},a}]$) and the distribution of the environmental limitation between all time points ($\bar{\mu}_T$, $\bar{\sigma}_T^2$) (Table 2.1). In the proposed model, the mean and variance of the environmental limitation always occur as a product with the maximum asymptotic length ($\bar{\mu}_T\ell_\infty$, $\bar{\sigma}_T^2\ell_\infty^2$). Therefore, the maximum asymptotic length cannot be estimated separately with this method and is incorporated as a species specific scalar of the environmental limitation. We provided an R-package (Croll, 2022) that includes a procedure for fitting the model to a dataset with pairs of age and length mea-

Table 2.1: Description of the parameters that are estimated during the model fitting procedure.

Parameter	**Description**	**Type**	**Number of parameters**
n_T	Number of sampling instances	discrete	0 (fixed value)
n_a	Number of sampled age classes	discrete	0 (fixed value)
T_{min}	Time of the first sampling instance	discrete	0 (fixed value)
a_{min}	First age class in the dataset	discrete	0 (fixed value)
r_B	Von Bertalanffy growth rate scalar	continuous	1
$E[\ell_{(T,a_{min})}]$	Expected mean length at the first age class	continuous	n_T
$V[\ell_{(T,a_{min})}]$	Variance in length at the first age class	continuous	n_T
$E[\ell_{(T_{min},a)}]$	Expected mean length at the first sampling instance	continuous	$n_a - 1$
$V[\ell_{(T_{min},a)}]$	Expected variance in length at the first sampling instance	continuous	$n_a - 1$
$\bar{\mu_T}\ell_\infty$	Mean asymptotic length	continuous	$n_T - 1$
$\bar{\sigma}^2_T\ell_\infty$	Variance in asymptotic length	continuous	$n_T - 1$

surements using maximum likelihood optimization through optimization methods available in the NLoptR-package (Johnson, 2021).

The R-package for fitting the described Von Bertalanffy growth model contains some additional features to tailor the model to specific populations. The first feature deals with the dynamics of the mean length at age when the environmental limitation is very variable. In the model described in equation (2.7) the mean length of a cohort ($E[\ell_{T,a}]$) decreases if it exceeds the asymptotic length at some time step ($\bar{\mu_T}\ell_\infty$). This is a mathematical artefact of the model that predicts that individuals will shrink in size if they are too large to be supported by the environment. Although some species might shrink in size under bad conditions, this is not realistic for all species (Kooijman, 2010). This could be solved by either assuming a log-normally distributed error structure or by simply fixing the change in the mean length-at-age to non-negative values. The first option is mathematically very complex. Instead, the package includes a version of the model in which the average length of a cohort does not decrease if the average cohort length exceeds the maximum asymptotic length. This version of the model should be used with care and only with reasonable arguments, because this method

inflates the impact of small and younger cohorts on the estimated environmental limitation. In any case we advise to first fit the model without this additional assumption, to check whether this indeed predicts large decreases in mean length of some cohorts.

The second extension available in the R-package deals with differences in environmental limitation between age and length classes. Differences in environmental limitation between age or length classes can arise if age or length classes show spatial segregation or differ in diet. The model allows specification of age or length classes and estimates separate means and variances in environmental limitation ($\bar{\mu}_{T,c}$, $\bar{\sigma}^2_{T,c}$) for every age or length class at every time step. It is important to note that this extension of the model only uses the mean length of a cohort to identify the length class and therefore all individuals in a cohort are always placed in the same length class. In addition, the number of observations per class decreases with an increase in the number of age or length classes. The incorporation of age or length classes can therefore make the model fit less accurate if there are no true differences in the environmental limitation of the selected classes.

Application to North Sea plaice

To illustrate the use of the proposed model we fit the model to a dataset with age and length measurements of plaice (*Pleuronectes platessa*) obtained from the Beam Trawl Survey (BTS). This survey is designed to monitor plaice in the North Sea and is consistently conducted in the third quarter (July to September) from 1990 onwards. The length of individuals is measured with at least 5 mm accuracy and the age of sampled individuals is obtained through otolith readings. We downloaded the datasets with individual ages and lengths recorded during the third quarter of 1990 to 2021 from the online ICES DATRAS data portal on the 1st of November 2021 (ICES, 2021a). The size distributions in the data are likely to be skewed due to size-dependent mortality in the population and biases in the sampling process. Differences between age classes and years are unlikely to affect the estimated size distributions because the model estimates a size distribution separately for every age in every year. In contrast, differences between the size classes are likely to skew the size distribution of a given age. The age-length observations were therefore weighted by the inverse of the catch per unit effort (CPUE) of the observed length. The CPUE per length indicates the probability that an individual of a given length is caught in the survey of a given year. Weighting the observations with the inverse of the CPUE corrects for any factor that affects the catch probability of a given length in a given year. After weighting of the samples, all lengths approximately had the same contribution to the dataset and visual

inspection confirmed that the data approximated the assumption that length at age in a given year follows a Gaussian distribution (judged by eye, fig. 2.7).

Starting values for the expected length at the first age in the dataset, the expected asymptotic length and the growth scalar were estimated by fitting a Von Bertalanffy growth model without considering differences between years and cohorts ($E[\ell_{(T,a_{min})}] = 120mm$, $\bar{\mu_t}\ell_\infty = 380mm$ and $r_B = 0.303y^{-1}$). Starting values for the variance in length at the lowest age class and the variance in asymptotic length were set to the variance in the youngest and oldest age class respectively ($V[\ell_{(T,a_{min})}] = 801mm^2y$ and $\bar{\sigma_t}^2\ell_\infty^2 = 5789mm^2y$).

We used the Sbplx algorithm of the NloptR package (Johnson, 2021), which is a variant of the Nelder-Mead optimization method, with a relative tolerance of 10^{-10} to optimize the likelihood of our model. The optimization was performed using a log-transformed parameter space to account for the magnitudinal difference between parameters. For comparison we fitted two versions of the model. In the first version the environmental limitation was constant over years and therefore the mean and variance of the asymptotic length were estimated as a single parameter. In the second version the environmental limitation was allowed to vary between years and the mean and variance of the asymptotic length were estimated separately for every year.

To assess the robustness of the model with yearly varying asymptotic length, we used a jackknife approach in which we repeated the analysis 31 times with data from one entire year omitted every time. This shows the impact of the samples from a given year on the model fit and gives an indication of the robustness of the method to years in which no data could be collected. Lastly, we demonstrate the use of separate age groups with a different environmental limitation in the model by splitting the plaice population in three ecological groups by age.

We used an estimation of the maximum asymptotic length ($\ell_\infty = 780$) estimated by Van der Veer et al. (2001) and scaled the estimated mean and variance in asymptotic length with this value to obtain the mean and variance in environmental limitation ($\bar{\mu_t}$,$\bar{\sigma_t}^2$).

2.3 Results

A model with a constant environmental limitation and a model with a yearly varying environmental limitation were fitted to a length-at-age dataset for North Sea plaice. The model with a yearly varying mean and variance of the environmental limitation fitted the data better compared to the model with constant mean and variance of the environmental limitation (AIC of respectively 16076750 and

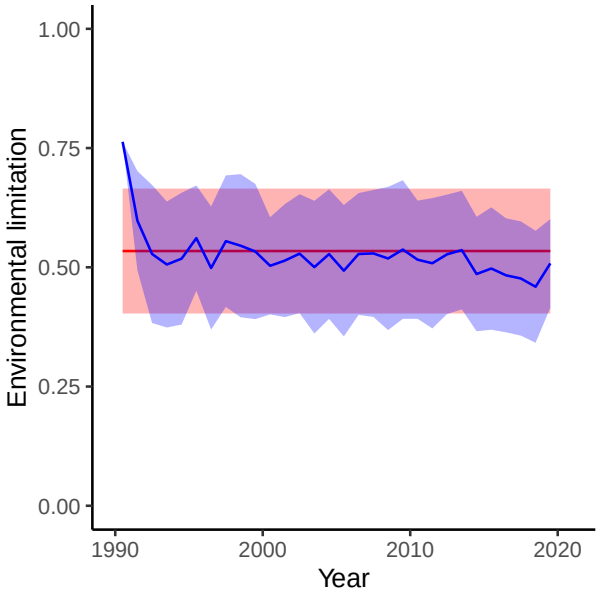

Figure 2.1: Fitted environmental limitation ($\bar{\mu}_T$) for the model with a constant environmental limitation (red) and the model with a yearly varying environmental limitation (blue). Shaded areas indicate the mean plus or minus the two times standard deviation derived from the estimated asymptotic variances ($\frac{1}{2} r_B \bar{\sigma}^2_T$).

16048031, likelihood ratio test: $p < 0.001$). This suggests that the mean and variance of the environmental limitation are likely to fluctuate between years. More precisely, the model with yearly varying environmental limitation suggests a weak downward trend in this limitation, indicating that the environmental limitation became stronger over time (Fig. 2.1, solid line). The estimated variance in the environmental limitation is slightly larger if the environmental limitation is fixed compared to the model in which the environmental limitation is allowed to fluctuate ($0.0335y$ and on average $0.0268y$ respectively). This overestimation of the variance in environmental limitation arises because the fixed limitation model accounts for the variation in the asymptotic length between years in addition to the variation in asymptotic length within a year. As expected, the models also differ slightly in the estimated parameters defining the length distribution at the youngest age. The estimates of the Von Bertalanffy growth scalar of the models ($0.2553y^{-1}$ and $0.2977y^{-1}$ respectively) are relatively close to estimates based on individual energy expenses ($0.2955y^{-1}$, (Van der Veer et al., 2001)).

The estimated model parameters lead to predictions of the length-at-age distribution for every cohort, which differ most strongly for the older age classes (Fig.

2.2). On visual inspection both the model with a constant environmental limitation and a yearly varying environmental limitation appear to fit the data points well (Fig. 2.2c-f). Note that the expected length of individuals in a cohort can shrink in the model with a yearly varying environmental limitation. This occurs if the estimated mean asymptotic length falls below the expected length of individuals in a cohort ($\bar{\mu}_T \ell_\infty < E[\ell_{(T,a)}]$). While such a decrease can realistically occur, it is sometimes a biologically impossible result. Repeating the analysis on this dataset with the restriction that the expected length of a cohort can not decrease, yields very similar results (not shown). Nonetheless, this additional restriction should be handled with care, because early tests on simulated data showed that this restriction makes the model more dependent on the data points in young age classes.

To demonstrate the robustness of the model we used a jackknife approach in which we repeated the analysis with the samples from one year omitted (Fig. 2.3). It is not unlikely that actual datasets will contain years for which there is no data, for example due to sampling problems. This analysis showed that missing samples mainly affect the estimate of the mean environmental limitation in the time step directly before and directly after the sample instance with missing data. At one of these time steps the mean environmental limitation will be overestimated while it will be underestimated in the other time step. In addition, it seems that this over- and underestimation of the mean asymptotic length becomes larger towards the start and end of the time period included in the model. A possible cause for this pattern is that these time steps include cohorts which partly fall outside the time-period covered by the data and therefore are estimated on a restricted number of ages. This could make estimates of the growth curves of these cohorts more vulnerable to missing data, which is reflected in the larger over- and underestimations of the asymptotic length in the years these cohorts are in. Indeed, the early years included in the analysis include significantly less observation than later years. Lastly, it is clear that the over- and underestimation of the mean asymptotic length due to omitted data is small compared to the variation between individuals within a cohort.

Our estimation method can also be used on populations which consist of separate ecological groups. We demonstrate this using plaice, the distribution of which has been shown to shift away from the coast with increasing length or age (Braber and De Groot, 1973; Basimi and Grove, 1985; Rijnsdorp and Vingerhoed, 2001). We divide the plaice population into three arbitrary age groups to represent this spatial shift with age, respectively a group up to 4 years old, a group from 4 to 7 years old and a group with individuals over 7 years old. The model fit yields an

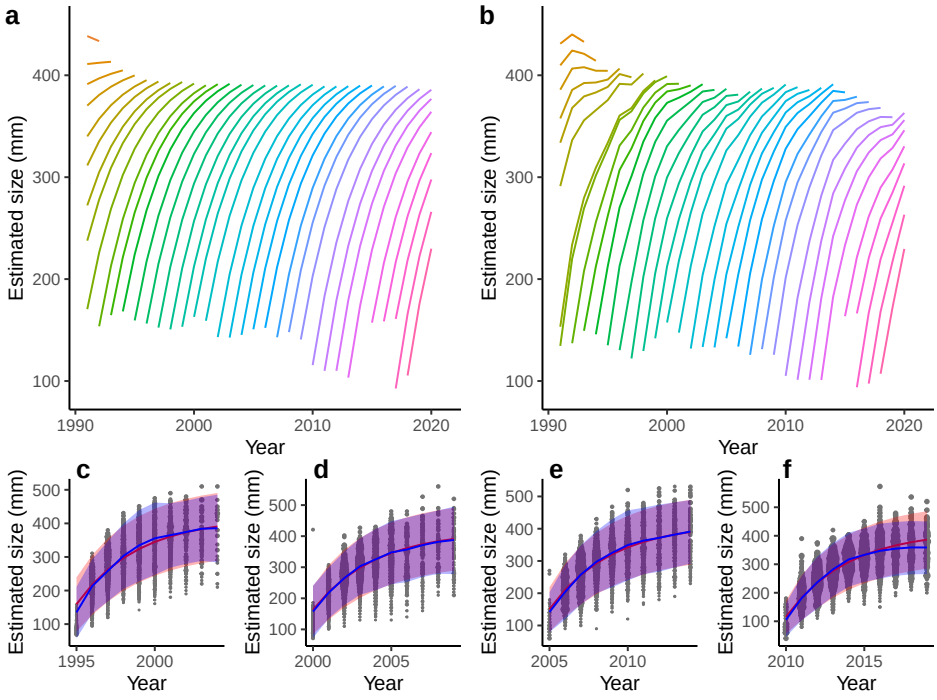

Figure 2.2: Expected value of the length-at-age ($E[\ell_{(T,a)}]$) for the model with a constant environmental limitation (a) and a yearly varying environmental limitation (b). Line colours correspond to the year of birth of the cohort. The expected length-at-age for the cohorts born in the years 1995 (c), 2000 (d), 2005 (e) and 2010 (f) are plotted separately for the model with a constant environmental limitation (red) and the model with a yearly varying environmental limitation (blue), together with the data points corresponding to the specific cohort. Shaded areas indicate the expected length plus or minus two times the standard deviation from the estimated length distribution. The size of the data points indicates the weighted number of observations of a specific age-length combination in the given cohort ranging from 1 to 60 times.

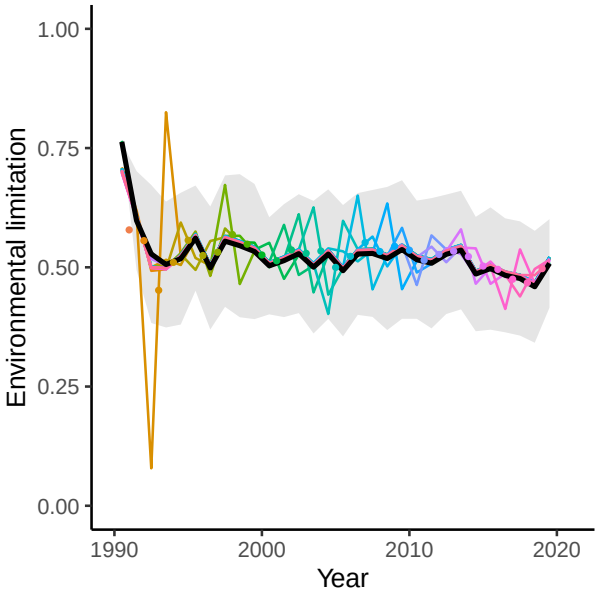

Figure 2.3: Fitted environmental limitation ($\bar{\mu}_T$) as predicted during a jackknife approach. Colours correspond to different model fits. For every model fit, the data in the year indicated by the dot is omitted from the analysis. The black line is the estimated mean environmental limitation without omitted data and the shaded area indicates the mean plus or minus the two times standard deviation derived from the estimated asymptotic variances without omitted data ($\frac{1}{2} r_B \bar{\sigma}^2_T$).

estimate of the mean and the variance of the environmental limitation for every year and group (Fig. 2.4). The model with three age groups does indeed fit the data better compared to the model without age groups (AIC of respectively 15982917 and 16048036). Despite a similar trend, year to year changes in some years differ substantially between length groups, both in magnitude and direction. Such differences could indicate relevant ecological differences between the groups. The average estimated variance in environmental limitation for the youngest age group (on average $0.0217y$) is smaller compared to the average estimated variance in environmental limitation in the model without age groups (on average $0.0268y$). This might suggest that the environmental limitation of individuals in the youngest age group is more similar to the environmental limitation of individuals in the same age group compared to the environmental limitation of individuals in other age groups. This could explain why the model with three age groups fits the data better compared to the model without age groups. In contrast, the average estimated variance in environmental limitation for the two oldest age groups (on

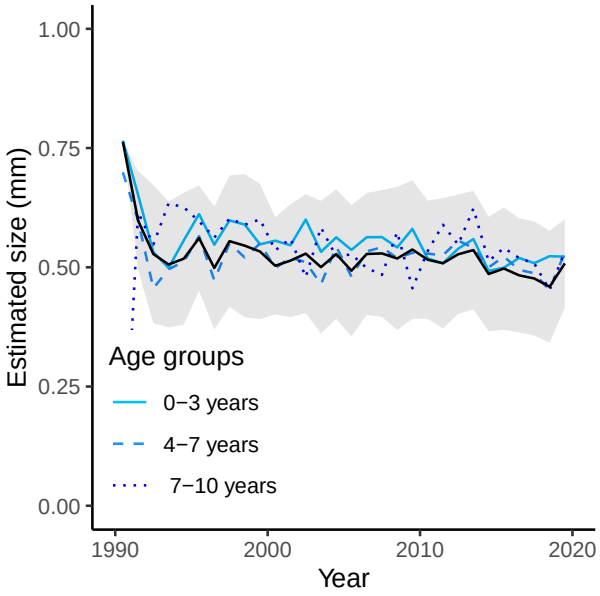

Figure 2.4: Estimated environmental limitation if three groups with separate environmental limitations are defined based on age. The black line and the shaded area indicate the mean plus or minus two times standard deviation derived from the estimated asymptotic variances if all ages are part of the same group ($\frac{1}{2} r_B \bar{\sigma}_T^2$).

average $0.0399y$ for age group 4-7 years and $0.0801y$ for age group over 7 years) is larger compared to the average estimated variance in environmental limitation in the model without age groups (on average $0.0268y$). This might suggest that the environmental limitation of some individuals in the two oldest age groups is more similar to the environmental limitation of individuals in other age groups compared to the environmental limitation of individuals in the same age groups. It is important to note that the reported variation corresponds to the fitted variation in environmental limitation and not the variation in the individual sizes. The variation in individual size is a balance between the variation in size at the previous time step and the variation in environmental limitation. The variation is size is therefore likely to increase or decrease with age, depending on the variation in size at birth. This does not hold for the variation in environmental limitation as it is independent of size and age.

2.4 Discussion

We presented a new method to estimate Von Bertalanffy growth parameters from datasets with pairs of age and length measurements and provide an R package called VBGfit (Croll, 2022) to apply this method. The method is based on a model that describes the length distribution of cohorts in a population under the assumption that cohorts partly overlap in time and experience a fluctuating environment (eq. 2.7). The model is derived from a stochastic differential equation describing the growth of a single individual in a fluctuating environment (eq. 2.1) and therefore accounts for variation due to changes in the environment over time, variation in the growth history of cohorts and variation between individuals within a cohort. Because the model is described in a discretized form, it is easy to fit on pairs of length and age measurements taken with a regular interval, which is one of the most common forms of data on population structure (Eveson et al., 2007).

Our model makes several assumptions about the underlying population structure to obtain a model applicable to datasets with random observation pairs of individual lengths and ages. First of all, we assume individuals follow a Von Bertalanffy growth curve in which only the asymptotic length fluctuates over time and between individuals (eq. 2.1). This is the most common and first proposed form of the Von Bertalanffy growth equation (Von Bertalanffy, 1938). Nonetheless, it is sometimes assumed that both the asymptotic length and the Von Bertalanffy growth rate scalar fluctuate (Eveson et al., 2007; Pilling et al., 2002). It has been shown that estimates of the asymptotic length and the Von Bertalanffy growth rate scalar are strongly correlated if both are allowed to fluctuate. Due to this correlation it might be difficult to obtain correct parameter estimates, because different sets of parameters are likely to fit the dataset equally well (Eveson et al., 2007; Pilling et al., 2002). In addition, it has been shown that only the asymptotic length or the Von Bertalanffy growth rate scalar has to fluctuate to obtain a very good prediction of the population structure and an accurate estimate of the environmental limitations when data consists of independently observed pairs of individual age and length (Eveson et al., 2007). We therefore chose to only make the asymptotic length dependent on the environmental limitation, as this has the most comprehensive substantiation in energetic theory (Kooijman, 2010). Secondly we assume that the dynamics of the environmental limitation between two measurements can be described accurately by the average environmental limitation in this period. This is a very convenient assumption borne from the discrete nature of most length-at-age data. Nonetheless, it is possible to substitute a more complex, time-dependent formulation for the environmental limitation in equa-

tion (2.6) and work out the more complex model through integration. This would lead to a more specific and less generally applicable form of the model. Thirdly we assume that the environmental limitation experienced by an individual at a given moment is drawn from a Gaussian distribution. The central limit theorem states that if a variable is influenced by many additive random factors, it will approach a Gaussian distribution. As the environmental limitation emerges from a complex ecological, chemical or physical system, it is likely to be influenced by many random factors and therefore is likely to approach a Gaussian distribution. In conclusion, most of the assumptions in this method are made to ensure that the model is as generic as possible but still applicable to the currently available datasets with length-at-age data.

Just like other methods, our model assumes that individual length is normally distributed in a cohort and therefore in the obtained samples as well. Deviations from this normal distribution can occur for example due to sampling biases or a link between individual mortality rate and individual length. Fits on simulated data showed that the value of mean environmental limitation is slightly overestimated if the contribution to the data increases with size, while the value of the mean environmental limitation is underestimated if the contribution to the data decreases with size (supplementary materials). This is comparable to a situation in which larger or smaller individuals respectively have a higher probability of ending up in the data regardless of their age. These model fits on simulated data show that the effects of length bias in the data might be relatively small. Nonetheless, it is important to correct for skewness in the individual length distribution in the data when possible. One way to do so, is to add relative weights to the samples. In our example with North Sea plaice we weighted the samples by the inverse of the catch per unit effort (CPUE) per length. The CPUE is a measure of the relative presence of a length class in the dataset in a given year. In this way, we corrected for the impact of length on the catchability of an individual, which can arise for example due to very strong length-specific mortality or harvesting probabilities. This resulted in a dataset in which individual length approximates a normal distribution of every age class in every year (Fig. 2.7). Because our model allows to add weights to every individual sample it is in theory possible to correct for biases linked to any trait of an individual including age and size. Nonetheless, it is important to note that it is not possible to correct for all biases because specific information is often lacking. Especially biases in growth due to genetic differences and habitat quality might require attention as these could directly impact growth and skew the size distributions in a population.

A novel and very important aspect of our method is that it accounts for vari-

ation caused by environmental changes over time, variation between the growth history of cohorts and variation between individuals within a cohort simultaneously. Earlier methods only account for variation due to changes over time by fitting a growth curve separately for every sampling instance, or only account for the growth history of a cohort by fitting a growth curve separately for every cohort. Similarly, more recent methods only accounted for variation between individuals (Vincenzi et al., 2014; He and Bence, 2007; Pilling et al., 2002; Prajneshu and Venugopalan, 1999; Wang and Thomas, 1995; Rafail, 1973) or variation caused by changes through time (Lorenzen and Enberg, 2002; Lorenzen, 1996; Cloern and Nichols, 1978). Due to the autoregressive nature of individual growth rates, these sources of variation are strongly intertwined and should not be considered separately. We account for this by fitting the Von Bertalanffy growth equation for all cohorts and sampling instances simultaneously. Because we derived our model from a stochastic differential equation describing individual growth, our model also accounts for variation in environmental limitation between individuals. In addition, we show that the variation between individuals is overestimated if a model does not account for changes is environmental limitation over time.

Because our model simultaneously accounts for variation between individuals and cohorts and allows variation from the environment to fluctuate over time, the model can be used for a wide range of applications. First of all, the estimated mean and variance of the asymptotic length estimated by our model can be used as a summary statistic for environmental limitation under the assumption that the sources of variation are independent. Growth of individuals is likely limited by numerous factors, which are often unknown. Our method offers a summary statistic for the cumulative distribution of all these factors. Our method is especially appropriate to estimate individual limitation in growth due to limitation through food availability. General theory about individual energy allocation links the asymptotic length of this Von Bertalanffy growth equation to the energy ingestion by individuals (Kooijman, 2010; Von Bertalanffy, 1938). The distribution of the environmental limitation estimated by our model could therefore be used as a proxy for the distribution of food availability among the individuals in a population. Estimates of individual food availability are scarce, because they commonly have to be obtained from intensive observations or analysis of stomach samples. Because our model provides a proxy of the individual food availability throughout the entire population, it can be used for more detailed analyses of the dynamics of food availability. For example, linking the estimated environmental limitation to the consumer density might reveal density-dependent feedbacks in the growth rate of individuals. The environmental limitation as a proxy for individual food

availability might also provide insight into feeding links between species. The environmental limitation in our model always appears as a product with the maximum asymptotic length ($f_t \ell_\infty$), it should therefore first be scaled by an estimate of the species-specific maximum asymptotic length before it can be compared between species. Comparison of this scaled proxy for individual food availability between species might then reveal links such as shared resources or competition.

In our example with North Sea plaice we showed that our model can be used to explore environmental segregation between length or age groups as well. The R-package (Croll, 2022) allows to split a population into a priori defined length or age groups and fits an environmental limitation separately for every length or age group. With a realistic division in length or age groups, our model could provide valuable information about growth limitation in different life stages. If for example length or age groups show very diverse patterns in environmental limitation, it is likely that the length or age groups are environmentally separated either through segregation in space or differences in diet. In this way the model could therefore yield additional understanding in the growth dynamics during various life stages.

It is often difficult to judge whether a certain division in length or age groups is valid. A way to assess the suitability of a division in age or length groups is to look at the estimated variance in environmental limitation for every group compared to the variance in environmental limitation estimated in a fit without groups. Without groups, our general model combines all length and age groups and fits a single environmental limitation for all groups. This method lumps together the variation in environmental limitation within and between age or length groups which will lead to a high estimate of the variance in environmental limitation if groups strongly differ in environmental limitation. In general, one can assume that individuals within a group are more similar to each other compared to individuals within another group. The variance in environmental limitation estimated for a single group is therefore expected to be lower compared to the variance in environmental limitation estimated for the entire population. This was only the case for the youngest age group (up to 4 years) in our example of North Sea plaice. This suggests that our arbitrary division of the population into three age groups does not accurately represent the ecology of North Sea plaice. It does demonstrate that our model can be used to verify whether a suspected division in ecological groups is likely by comparing the estimated variance in environmental limitation of a fit without ecological groups with a fit with ecological groups as is done in the example for North Sea plaice.

Lastly our method might also be applicable to management as it is able to model variation in growth through time and between individuals based on only a

limited number of parameters (Flinn and Midway, 2021). Many management models, in particular those used to estimate reference points for fish stock management, assume a fixed length distribution at a given size, while variation in growth rates is shown to be important for the response of populations to exploitation (Lorenzen and Enberg, 2002). With our model the variation in growth between years can be easily quantified, resulting in a more accurate prediction of the length-at-age for every cohort. The age-length relationships from our model then can be used to calculate a more precise estimate of the needed reference points.

In conclusion, our model provides a way to estimate growth curves and length distributions of individual cohorts based on single individual length and age observations. In our model growth is allowed to vary over time, while our model also accounts for variation between individuals and variation between cohorts. So far, these factors could only be estimated simultaneously if the growth history of individuals was known. Models for single observations of individual length and age only accounted of a subset of these factors. Our model does account for all these factors and in this way estimates a proxy for the limitation in individual growth, which may vary over time. This estimate of the limitation in individual growth is a new step in understanding patterns in individual growth based on individual field observations.

2.5 Supplementary materials

Model test on simulated data

We fitted the model to simulated data to test the sensibility of the estimated parameters to the number of observations in the data and possible biases in length in the data. To do so, we generated the population structure of a population with a constant mean and variance of the environmental limitation. To do so we used the following continuous model:

$$\frac{\partial E(\ell)}{\partial t} + \frac{\partial E(\ell)}{\partial a} = r_B \left(\mu_f \ell_\infty - E(\ell)\right) \tag{2.9}$$

$$\frac{\partial V(\ell)}{\partial t} + \frac{\partial V(\ell)}{\partial a} = 2 r_B \left(\sigma_f^2 \ell_\infty^2 - V(\ell)\right) \tag{2.10}$$

The average length at birth was determined by drawing a random value from a predetermined interval (ℓ_{0min} - ℓ_{0max}). Other parameters of the simulation were fixed (Table 2.2). The population structure was simulated over a period of 30 years and every cohort was simulated from age 0 to 10. A sample was drawn from the population structure for every year and cohort at 180 days after a new cohort

Table 2.2: Parameters used for simulating population structure.

Parameter definition	**Symbol**	**Value**	**Unit**
Von Bertalanffy growth rate scalar	r_B	0.001	d^{-1}
Maximum asymptotic length	ℓ_∞	1000	mm
Mean environmental limitation	μ_f	0.5	-
Variance in environmental limitation	σ_f^2	0.0002	-
Minimum length at birth	ℓ_{0min}	5	mm
Maximum length at birth	ℓ_{0max}	15	mm
Maximum cohort age	-	3650	d
Time between cohort starts	-	365	d
Time between cohort start and sampling	-	180	d

with age 0 is introduced to the population.

To test the influence of the number of parameters on the estimated environmental limitation, we draw 100 data sets from the simulated population structure. The number of samples varied between 10 and 100 samples per cohort per year (Fig. 2.5). The estimated mean and variance of the environmental limitation are distributed evenly around the actual mean and variance in the simulation. With an increasing number of samples, the standard error of the estimated mean and variance of the environmental limitation become smaller. In other words, the estimated mean and variance in environmental limitation become on average closer to the real mean and variance if the number of samples increases.

Another concern when estimating environmental limitations from length structures is a possible bias in the sample method. It is possible that the samples are biased towards individuals with a larger or smaller length. To test the effect of this bias on the estimated environmental limitation we sampled 100 data sets with 50 observations per cohort per year from the simulated population structure. When fitting our model we weighted the samples by individual length. The weight of a sample changed linearly with individual length ($w_i = \alpha\ell_i + \beta$). The slope of this relationship determined the strength of the bias, ranging from a sampling bias towards larger individuals ($\alpha > 0$) to a sampling bias towards smaller individuals ($\alpha < 0$). The intercept of the relation between bias weight and length is determined in such a way that the average weight of samples is equal to one ($\beta = 1 - \frac{\sum_{i=1}^{n} \alpha\ell_i}{n}$). This will ease comparison between model fits, because the weighted number of samples is equal for all datasets.

A sample bias linked to weight might result in an error in the estimation of the

mean environmental limitation, but does not affect the estimation of the variance in environmental limitation (Fig. 2.6). The mean environmental limitation is slightly overestimated if larger individuals are more likely to end up in the samples, while the mean environmental limitation is slightly underestimated when smaller individuals are more likely to end up in the sample. Although this error seems to be small, it is important to keep this bias in mind and correct for this bias when possible.

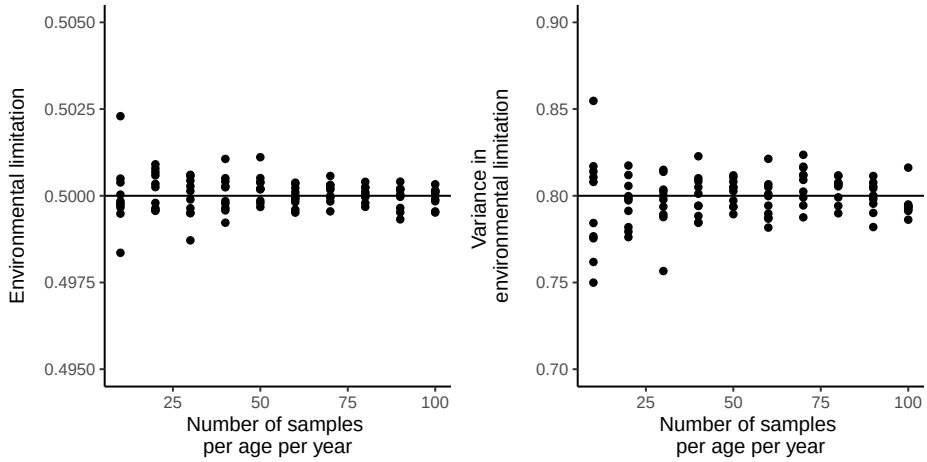

Figure 2.5: Average of the estimated mean and variance of the environmental limitation for different number of data points drawn from a simulated population structure. The black line indicates the actual values of the mean and variance in environmental limitation in the simulation.

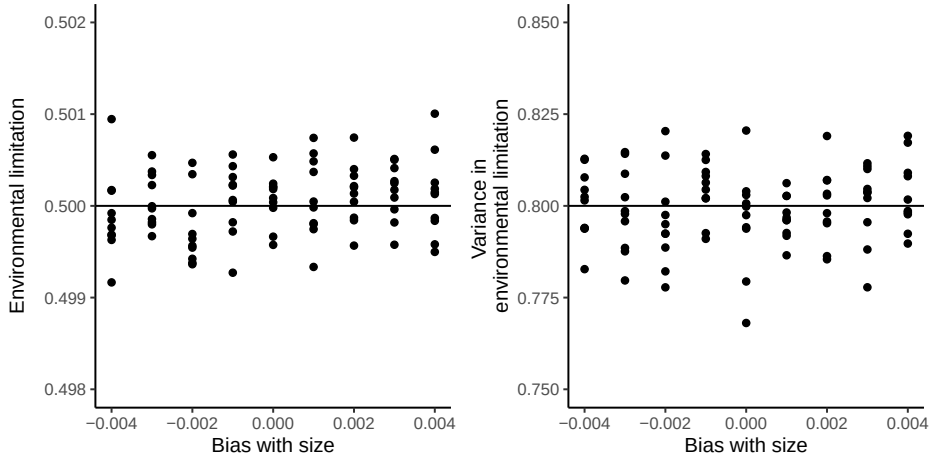

Figure 2.6: Average of the estimated mean and variance of the environmental limitation when the data contains a bias with length. A positive bias with length indicates that larger individuals contribute more to the samples, while a negative bias with length indicates that smaller individuals contribute more to the samples. The black line indicates the actual values of the mean and variance in environmental limitation in the simulation.

Supplementary figures

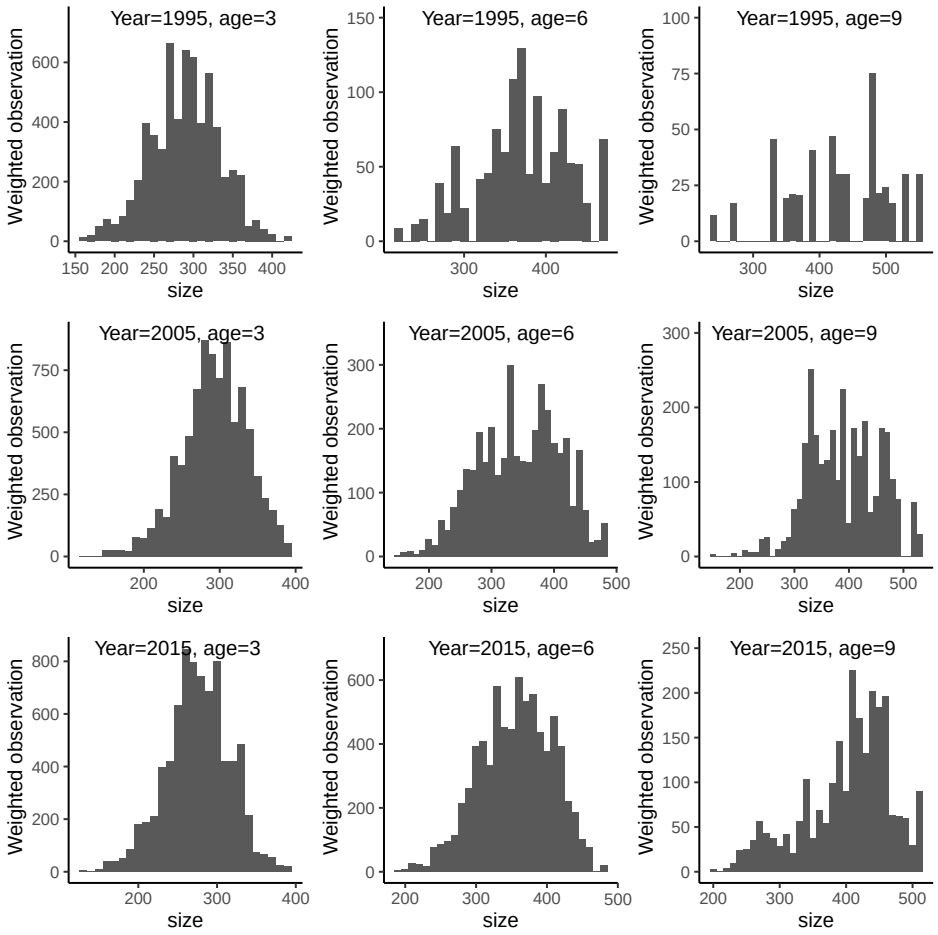

Figure 2.7: Weighted distributions of length at age at a given year. The number of observed individuals with a specific length is weighted by the inverse of the catch per unit effort of that length in the given year. The length at age seems to approximately follow a normal distribution.

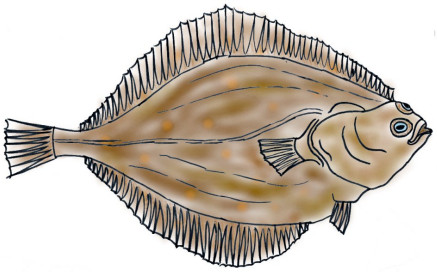

Chapter 3

Growth as measure for environmental conditions and relatedness of North Sea fish stocks

Jasper C. Croll
Quinten Mudde
Tobias van Kooten
André M. de Roos

To be submitted

Abstract

Information about the ecological connections between species is needed to make the shift from fisheries management strategies centered around single species to ecosystem-based fisheries management. Growth rates of fish strongly depend on the environment. Individual growth curves could therefore contain valuable information about the environmental conditions experienced by an individual throughout its life. In this study we explore whether estimated growth curves contain information about the competition within and between species. To do so, we estimated growth curves for ten species in North Sea roundfish areas based on size-at-age data from the NS-IBTS fish survey by fitting a Von Bertalanffy growth model with varying asymptotic size. From these model fits we extracted a relative measure for the temporal variation in growth of a stock, which can be used as indication of the experienced environmental condition. We quantified the relationship between individual growth and catch-per-unit-effort as a measure for stock biomass. In this way we found signs of density-dependent growth in at least six out of the ten species. In addition, we used cluster analysis to explore the relatedness in ecological growth condition between species and areas. Ecologically related species tend to show more similar temporal variation in ecological growth condition than ecologically more distant species. Likewise, areas that are geographically closer are more similar in ecological growth conditions compared to geographically more distant areas. This suggests that ecological conditions derived from growth curves provide a useful way to distinguish ecological groups or regions without the need for additional stomach sampling or ecological studies. We conclude that temporal variation in growth curves is a valuable summary statistic for the experienced ecology and environment of a fish stock.

3.1 Introduction

About three decades ago, general concern about the sustainability of large scale fisheries arose. Most of the commercially exploited fish stocks were in decline and showed clear signs of overexploitation (Pauly et al., 2002; Beverton, 1998; Cook et al., 1997). The widespread fear of aquatic ecosystem collapse and stock overexploitation led to a consensus about the need to reform fisheries management. The intensified management of fish stocks seems to pay off as numerous stocks show signs of recovery (Cardinale et al., 2013; Fernandes and Cook, 2013; Hutchings et al., 2010; Worm et al., 2009). Due to improvements in fisheries management, estimated stock biomass for several stocks reached sufficient numbers to produce maximum sustainable yield, which is considered a low risk scenario (Zimmermann and Werner, 2019; Froese et al., 2018).

The positive trend in the recovery of fish stocks does not mean that the current fisheries management practices cannot be improved further (Zimmermann and Werner, 2019), especially because a substantial number of global fish stocks are still overexploited (FAO, 2020). In addition, commonly used stock assessment models fail to predict large changes in the dynamics of fish stocks (Britten et al., 2021; Hilborn et al., 2020). This mismatch between predictions and reality can be partly explained by the lack of data on the dynamics of some stocks, but is likely also a result of the ecological context in which stocks are considered (Jardim et al., 2021). Most management models consider fish stocks in isolation and only use stock quantities such as the spawning stock biomass to predict the ecological dynamics of a stock. This assumption conveniently simplifies the calculation of reference points, but it is clear that environmental conditions and ecological interactions between species are important drivers of the dynamics of exploited fish stocks (Säterberg et al., 2019; Andersen et al., 2015). Based on this insight, ecosystem-based management starts to gain importance in the consideration of fishing quotas.

Ecosystem-based approaches to fisheries management have in common that they require some level of information about the ecological connections between species (Birkenbach et al., 2020; May et al., 1979). Most of the current knowledge on interactions between fish species is based on stomach samples, physiological similarities and occurrence patterns (Matley et al., 2018). Studying ecological relatedness in these ways is often time-consuming and based on limited data. In addition, the results from these studies are often inconclusive or very spatial or population specific (Cadrin, 2020; Amundsen and Sánchez-Hernández, 2019). A more general measure of the response of species to the environment is needed to understand the ecological relatedness between co-occurring species. The body

size of individuals might contain important information about the environment experienced by a stock, because fluctuations in the environment often affect the growth of individual fish (chapter 2). In this article we explore to what extent temporal variation in growth curves of fish species contain information about the experienced environment and the interactions within and between populations.

Growth in body size is an important life history process. Growth requires a substantial amount of the assimilated resources of an individual and eventually determines the size of an individual. In this way, growth is strongly linked to other life history processes such as consumption, reproduction and mortality. Growth curves of fish generally show a high degree of variation and a strong link to the environment. Changes in growth rates of fish are for example linked to changes in temperature and stock biomass (Rindorf et al., 2022; Tu et al., 2018; Lorenzen, 2008; Lorenzen and Enberg, 2002; Pauly, 1980). The link between growth rates and temperature arises because temperature affects the metabolic rates of an individual (Kooijman, 2000). In contrast, the link between growth rates and stock biomass is likely to emerge through competition. A higher stock biomass increases competition and reduces the resource availability per individual, which could be a limiting factor for individual growth. In addition, an interaction between temperature effects and competition might arise because changes in temperature might affect the food requirements of an individual, while it might also have a direct effect on the food source itself. Growth rates are even argued to respond to harvesting pressure through evolution, although similar patterns could also emerge through the effects of harvesting on the competition and food availability within a stock (Heino et al., 2015; Enberg et al., 2012). The growth curves of individuals in a stock thus contains valuable information about the environment that individuals experienced.

In this article we explore whether growth curves contain information about the environment experienced by individuals in different fish stocks. Herein we focus on environmental overlap between stocks and competition within a stock. Growth curves were fitted to fishery survey data of ten exploited North Sea fish stocks using the method developed in chapter 2. This method is tailored to fit Von Bertalanffy growth curves to size-at-age observations from fisheries surveys and accounts for variation in growth between cohorts and individuals as well as temporal variation. By applying this technique, all temporal variation in growth curves is summarized in a yearly varying asymptotic size, which we used as an indicator of the effects of environmental conditions on individual growth. We scale and normalize the asymptotic size such that it is comparable between areas and species. To gain insight into the asymptotic size as a measure for the impact of competition on

growth, we first explored trends in the scaled asymptotic size with time and stock biomass. In addition, we performed cluster analysis on the normalized asymptotic sizes to explore whether these growth curves contain information about the overlap of the environment experienced by the fish stocks.

3.2 Methods

Data collection

We used the Sex-Maturity-Age-Length-Key (SMALK) data and the Catch-Per-Unit-Effort (CPUE) per length per haul per hour data from the North Sea International Bottom Trawl Survey (NS-IBTS) to fit growth curves and estimate stock density, respectively. The data was downloaded from the ICES DATRAS database in January 2022 (ICES, 2022). The NS-IBTS is a broad scale survey conducted in the North Sea region between the British Isles, The Netherlands, Denmark and Norway. The survey uses standardized bottom trawl gear to target demersal stocks. The survey is conducted from 1965 onward and is performed throughout the year. In this study we focused on data collected in the first quarter of each year (January to March), because this quarter includes the largest number of data points and covers the largest number of years. Growth periods in this study therefore spanned from the first quarter of a year to the first quarter of the following year. We performed our analysis for ten species which are labelled as the target species of the NS-IBTS (ICES, 2020): haddock (*Melanogrammus aegefinus*), herring (*Clupea harengus*), whiting (*Merlangius merlangus*), plaice (*Pleuronectes platessa*), witch (*Glyptocephalus cynoglossus*), sprat (*Sprattus sprattus*), Norway pout (*Trisopterus esmarkii*), cod (*Gadus morhua*), mackerel (*Scomber scombrus*) and saithe (*Pollachius virens*). The data was split and analysed separately for every species and ten roundfish regions (Fig. 3.1) which are commonly used to analyse size and age relations for the NS-IBTS species (ICES, 2020).

The SMALK data reports the number of individuals observed with a specific age-length combination in every year and area. Lengths are recorded in 5 or 10 millimetre intervals and ages are recorded in years. Individuals above a predetermined, species-specific age are recorded as a plus-group. To make the SMALK data suitable for our analysis, the data of every species and area was processed in several steps. First, all data entries with missing age or size values were removed. Second, all plus-groups were removed from the data, because the exact age of these individuals was unknown, which could introduce biases when fitting growth curves. Third, early years were discarded until the first year in the data

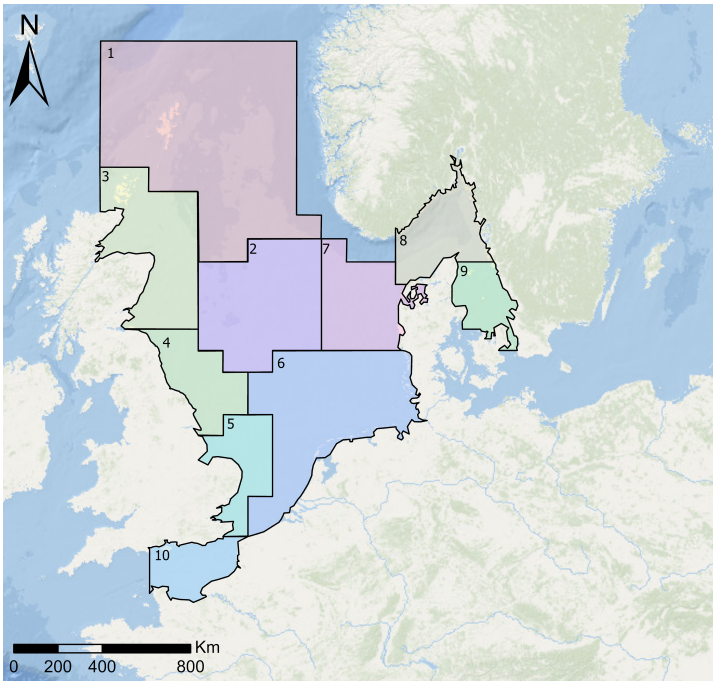

Figure 3.1: Roundfish areas used for the NS-IBTS data

contains on average at least one entry for every age. Similarly, low and high age classes were discarded until the youngest and oldest age groups contain on average at least one entry for every year. Last, areas in which the number of age and year combinations exceeded the number of observations were excluded from the analysis entirely.

The CPUE data contains a relative measure of the number of individuals caught per hour in every 5 or 10 millimetre length class for every haul in the survey. We used this metric to derive a relative proxy for the population biomass. Every length class was represented by the length midway between the length class boundaries. This length was converted to individual mass using a power scaling between individual length (ℓ) and mass (M):

$$M = a\ell^b \tag{3.1}$$

The values of a and b are species-specific scalars which are derived from fishbase (Froese and Pauly, 2021) (Table 3.1). We used the length-weight relationships from fishbase because the NS-IBTS data lacked sufficient information to construct an accurate length-weight relationship for some species. The use of the length-weight

Table 3.1: Species-specific scalars for the individual length-to-mass conversion following a power scaling ($M = a\ell^b$). Values are taken from fishbase (Froese and Pauly, 2021).

Species	**a**	**b**
Haddock	0.00646	3.08
Herring	0.00562	3.09
Whiting	0.00617	3.06
Plaice	0.00794	3.07
Witch	0.00490	3.09
Sprat	0.00575	3.06
Norway pout	0.00589	3.06
Cod	0.00676	3.08
Mackerel	0.00646	3.06
Saithe	0.00636	3.06

relationship from fishbase also minimizes the relationship between the size-at-age data used to fit the growth curves, which are used as a dependent variable in the analysis, and the estimated stock biomass, which is used as an independent variable in the analysis. The individual mass was multiplied with the CPUE per length and summed per haul to obtain the total biomass per unit effort (BPUE). The separate values of the BPUE were averaged over all hauls within a year for every area. This quantity was used as a relative proxy of the population biomass in a given area for a given year.

Fitting growth curves

The SMALK data contains pairs of age and size observations from sampled individuals. These data were used to fit the Von Bertalanffy growth models. In chapter 2 the following recurrence relations for the expected length ($E[\ell_{T,a}]$) and variance in length ($V[\ell_{T,a}]$) at time T and age a for every cohort were presented:

$$E\left[\ell_{(T+1,a+1)}\right] = E\left[\ell_{(T,a)}\right] e^{-r_B} + \bar{\mu_T}\ell_\infty \left(1 - e^{-r_B}\right) \tag{3.2a}$$

$$V\left[\ell_{(T+1,a+1)}\right] = V\left[\ell_{(T,a)}\right] e^{-2r_B} + \bar{\sigma}_T^2\ell_\infty^2 \left(1 - e^{-2r_B}\right) \tag{3.2b}$$

In this model every individual follows a Von Bertalanffy growth curve in which the Von Bertalanffy growth scalar (r_B) is a species-specific constant and the mean and variance in asymptotic size ($\bar{\mu_T}\ell_\infty$, $\bar{\sigma}_T^2\ell_\infty^2$) are allowed to fluctuate between years. We used this estimated asymptotic size as a relative estimate of the impact

of the environment on the growth of individuals in an area and year. An increase in the asymptotic size indicates that the environment of an individual becomes more favourable and the individual therefore grows faster and bigger.

The model described with equation (3.2) was fitted to the SMALK data for every species in all areas following the procedures outlined in chapter 2 and using the VBGfit package in R (Croll, 2022). This package fits the model through maximum likelihood procedures. The likelihood of the model was optimized using the Sbplx-algorithm from the NloptR package (Johnson, 2021). For every area, this resulted in one estimate of the Von Bertalanffy growth scalar (r_B), the mean and variance in size at the youngest age for every year ($E\left[\ell_{(T,a_{min})}\right]$, $V\left[\ell_{(T,a_{min})}\right]$), the mean and variance in size at all ages in the first year ($E\left[\ell_{(T_{min},a)}\right]$, $V\left[\ell_{(T_{min},a)}\right]$), and the mean and variance in asymptotic size for every year ($\bar{\mu_T}\ell_\infty$, $\bar{\sigma}_T^2\ell_\infty^2$).

From the model fits, the estimated mean asymptotic size ($\bar{\mu_T}\ell_\infty$) was used for further analysis. The time series of the mean asymptotic size were processed in three steps as described below to obtain a value of the environmental growth conditions (EGC) which were suitable for comparison between areas and species.

First, the asymptotic size estimated by the model is not reliable in years without sufficient data points (shown in chapter 2). We therefore did not include estimations of the asymptotic size for species, area and year combinations which had an average of two or fewer data points per age class. This results in a gap in some of the time series for the mean asymptotic size. These gaps did not contribute to further analysis.

Second, the asymptotic size ($\bar{\mu_T}\ell_\infty$) and the Von Bertalanffy growth scalar (r_B) cannot be estimated separately which results in a spurious relationship between the estimated asymptotic size and the Von Bertalanffy growth scalar between areas (Eveson et al., 2007; Pilling et al., 2002). This could result in a pattern in which the value and variance of the estimated asymptotic size is high in areas with a low estimated Von Bertalanffy growth scalar and the value and variance of the estimated asymptotic size is low in areas with a high estimated Von Bertalanffy growth scalar (supplementary figure 3.7). For several species we indeed found a significant relation between the mean asymptotic size and the inverse of the growth scalar ($1/r_B$). We corrected the mean asymptotic sizes of all species for this relationship by regressing the mean asymptotic size against the inverse of the growth scalar using linear models. Taking the residuals of these models removed the effect of the growth scalar on the mean asymptotic size in an area. After this correction, we still found a significant relation between the standard deviation of the mean asymptotic size and the inverse of the growth scalar ($1/r_B$) for several species. We used linear regression to quantify the relationship between the stan-

dard deviation in the mean asymptotic size and the inverse of the growth scalar. For all species, we divided the mean asymptotic size by the predicted values of these relationships to correct for the effect of the growth scalar on the amplitude of the fluctuations in the asymptotic size. These corrections resulted in a quantity of which the value and variance is independent of the Von Bertalanffy growth scalar and can be compared between areas. This quantity is still related to the estimated mean asymptotic size and contains the same information about the environment experienced by the individuals in a stock, but has different absolute values. We will therefore refer to this quantity as the corrected environmental growth condition (EGC).

Third, the corrected EGC still differs in value and variance between species. These absolute differences emerge from the physical differences between species. To enable comparison of the general patterns in corrected EGC between species, we normalized the corrected EGC of all species by subtracting the mean and dividing by the standard deviation of the corrected EGC per species. This resulted in a normalized value of the EGC. This value can be used for comparison between areas and species, because it is corrected for the possibly spurious relationship between the estimated asymptotic size and the Von Bertalanffy growth scalar as well as the absolute differences between species that are not caused by the environment.

Analysis of environmental conditions

We first analysed general trends in the corrected EGC with respect to time and BPUE using linear regression. This was done separately for every area and species combination as well as all areas combined for every species.

Then we explored the relatedness of the normalized EGC between species and between areas. Dissimilarities between species were calculated as the mean squared difference between the normalized EGC in a given year and area. Likewise, the dissimilarities between areas were calculated as the mean squared difference between the normalized EGC for a species in a year. Dissimilarities were only calculated for pairs of species or pairs of areas if they contained EGC values for at least five overlapping area-year or species-year combinations respectively. This resulted in dissimilarity matrices for the dissimilarity between all species pairs in each area and between areas for each species separately. If overlap in the time series of normalized EGC between two species or areas was insufficient, the dissimilarity between these species or areas was set to the average dissimilarity in the dissimilarity matrix. This additional step was only necessary for the dissimilarity between witch and mackerel due to several data-lacking years for these species. These dissimilarity matrices were analysed using several clustering methods (complete link-

age, average (UPGMA) and mcquitty (WPGMA)). Multiscale bootstrapping with 10,000 repeats was performed on the normalized EGC to calculate the probability of appearance of clusters using the pvclust package in R (Suzuki and Shimodaira, 2006). In this bootstrapping procedure, the normalized EGC data was resampled with replacement in which the number of samples taken varied between repeats (Shimodaira, 2002). Because the results of the various clustering methods were very similar, we only show the results from the average (UPGMA) clustering in the main text and include the results of the other clustering methods as supplementary figures (Fig. 3.5 and 3.6).

3.3 Results

Estimating environmental growth condition

We estimated the asymptotic body sizes of ten fish species in ten roundfish areas based on the size-at-age data from the NS-IBTS. In total 78 of the species-area combinations contained sufficient data to fit an asymptotic size value (Fig. 3.2). The time series of the estimated asymptotic size differed strongly in length, ranging from only one or two years to the full time span of 50 years.

Eight out of the ten species (haddock, herring, whiting, plaice, sprat, Norway pout, cod and saithe) showed a significant positive relationship between the estimated mean asymptotic size and the inverse of the growth scalar ($p < 0.05$). This relationship accounted for a substantial amount of the variation in the estimated mean asymptotic size between areas for some of the species ($0.8287 > R^2 > 0.0205$) and resulted in large differences in the estimated mean asymptotic size between areas (supplementary figure 3.7). Five of these species (haddock, whiting, plaice, Norway pout and cod) showed a significant positive relationship between the standard deviation in the estimated mean asymptotic size and the estimated growth scalar as well ($p < 0.05$, $0.9681 > R^2 > 0.608$). This relationship suggests that the amplitude of the fluctuations in the estimated mean asymptotic size increases with a decrease in the estimated growth scalar. These correlations between the estimated mean asymptotic size and the estimated growth scalar are known to arise as an artefact when fitting a Von Bertalanffy growth curve to data (Eveson et al., 2007; Pilling et al., 2002). Therefore, we corrected the estimated mean asymptotic size for this spurious relationship. After this correction, the estimated mean asymptotic size and the standard deviation herein did not correlate with the inverse of the growth scalar any more, except for cod which showed a slight positive relationship between the estimated mean asymptotic size and the inverse

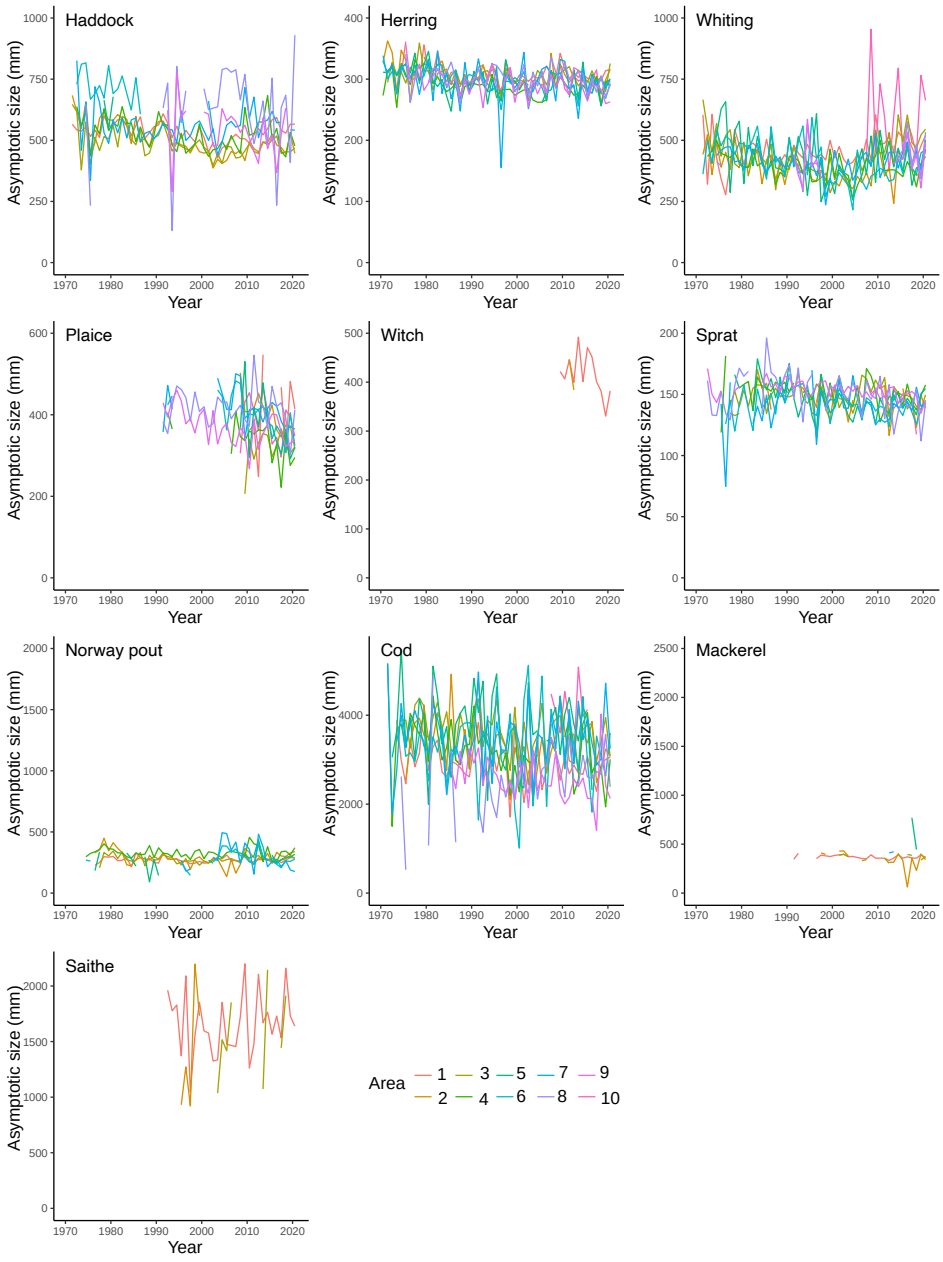

Figure 3.2: Corrected annual asymptotic sizes of ten commercially exploited fish species in ten roundfish areas in the North Sea, after correction for a possible correlation between asymptotic size and the growth scalar. Time series are interrupted for years in which data was insufficient to provide a reliable estimate of the asymptotic size.

growth scalar. This remaining relationship for cod explained a negligible amount of variation in the estimated asymptotic size between areas ($R^2 = 0.0156$ after correction against $R^2 = 0.8287$ before correction). We refer to these corrected values as the corrected EGC (Fig. 3.2).

General trend in environmental growth condition

Seven of the ten species (haddock, herring, whiting, plaice, sprat, cod and mackerel) showed a negative trend in the corrected EGC in at least one ICES area (Table 3.2). This indicates that the environmental condition decreases over time, which results in a decrease in the size-at-age over time. For five of these species (haddock, herring, plaice, sprat and cod), the negative trend in corrected EGC was also apparent on a larger scale when the data from all areas are combined.

In total 78 of the species-area combinations contained sufficient data to analyse the effect of population biomass estimated as the biomass per unit effort (BPUE) on the corrected EGC (Table 3.3). The corrected EGC was negatively correlated with BPUE for five species (haddock, herring, whiting, Norway pout and cod). For four of these species (haddock, herring, whiting and Norway pout) a negative relationship between corrected EGC and BPUE was found in at least one area. These negative correlations all occurred in roundfish areas 1 to 4, which are the more north-western areas in the North Sea. Sprat also expressed a negative relationship between the corrected EGC and BPUE in area 3, but this relationship did not persist when all areas were analysed together. In contrast to the negative correlation when all areas were analysed together, cod shows a positive correlation between the corrected EGC and BPUE in area 5.

Clustering

We clustered the ten species based on the normalized EGC in all areas and years with three cluster methods. This resulted in several consistent species clusters, occurring with every clustering method. Here we only show the results using the average (UPGMA) clustering. The first cluster consists of plaice and witch, which are the two flatfish species in our analysis (red cluster fig. 3.3). These flatfish species cluster together with two small forage fish species, herring and sprat, although with a relatively low bootstrap probability (green cluster fig. 3.3). Mackerel and Norway pout are pelagic species of intermediate length and cluster together with saithe, which is a somewhat larger pelagic species (blue cluster fig. 3.3). The last cluster consist of whiting and haddock which are both larger species that partly forage on smaller fish species (purple cluster fig. 3.3). Cod is the

Table 3.2: A significant relationship between the corrected EGC and the time variable indicates a directional trend over time. Asterisks indicate the significance of the slope ($p < 0.05$, $p < 0.01$ and $p < 0.001$ respectively). All reported areas had a significant negative relation between the environmental growth condition and the time variable ($p < 0.05$).

Species	**Overall**	**Number of areas with a negative slope**	
Haddock	**-0.0186*** **	**4/9**	(areas 2, 3, 4, 6)
Herring	**-0.0189*** **	**6/10**	(areas 1, 2, 4, 5, 6, 9)
Whiting	-0.002	**2/10**	(areas 4, 6)
Plaice	**-0.0430*** **	**4/10**	(areas 2, 4, 6, 9)
Witch	-0.1196	0/2	
Sprat	**-0.0162*** **	**3/10**	(areas 5, 9, 10)
Norway Pout	0.0023	0/7	
Cod	**-0.0130** **	**3/10**	(areas 3, 4, 9)
Mackerel	-0.0003	**1/6**	(area 3)
Saithe	0.0151	0/3	

Table 3.3: The relationship between the corrected environmental growth condition (EGC) and the biomass per unit effort (BPUE). Asterisks indicate the significance of the slope ($p < 0.05$, $p < 0.01$ and $p < 0.001$ respectively). All reported areas had a significant relationship between the EGC and the BPUE ($p < 0.05$).

Species	**Overall**	**Number of areas with significant slope**	
Haddock	$\mathbf{-3.06 \cdot 10^{-6}***}$	**1/9**	(Negative in area 3)
Herring	$\mathbf{-4.17 \cdot 10^{-7}**}$	**2/10**	(Negative in areas 2, 4)
Whiting	$\mathbf{-9.73 \cdot 10^{-7}*}$	**1/10**	(Negative in area 3)
Plaice	$-6.90 \cdot 10^{-6}$	0/10	
Witch	$-1.74 \cdot 10^{-3}$	0/2	
Sprat	$-1.12 \cdot 10^{-6}$	**1/10**	(Negative in areas 3)
Norway pout	$\mathbf{-2.21 \cdot 10^{-6}***}$	**2/7**	(Negative in areas 1, 4)
Cod	$\mathbf{-5.36 \cdot 10^{-6}**}$	**1/10**	(Positive in area 5)
Mackerel	$-1.67 \cdot 10^{-6}$	0/7	
Saithe	$-3.79 \cdot 10^{-6}$	0/3	

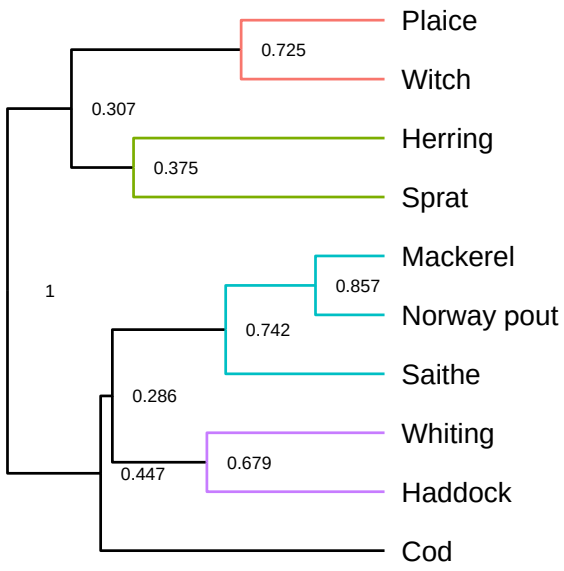

Figure 3.3: Clustering of ten North Sea fish species based on the normalized environmental growth condition for the average (UPGMA) clustering method. Small digits show the bootstrap probability, which is the fraction of bootstrap repeats in which a branch contained the depicted species. Coloured branches show clusters which arise in all clustering methods.

largest predatory fish in the data and does not cluster with the other species.

Likewise, we clustered the ten roundfish areas in this analysis based on the normalized environmental growth condition (Fig. 3.4). This resulted in a big cluster of the north-western roundfish areas 1 to 4, with a relatively high bootstrap probability (red cluster fig. 3.4). Another cluster consists of area 5 and 6 which are two large adjacent regions in the south of the North Sea (green cluster fig. 3.4). Area 8 and 9 form the Skagerrak and Kattegat areas between Denmark, Norway and Sweden which cluster together as well (blue cluster fig. 3.4). Geographically, area 7 is connected to all above-mentioned clusters, but it is unclear to which cluster area 7 belongs. This might suggest that there are some strong links between the clustered areas. Lastly, area 10 does not cluster well with any of the other areas. This is likely because area 10 is only present in the survey from 2009 onward and is relatively isolated geographically.

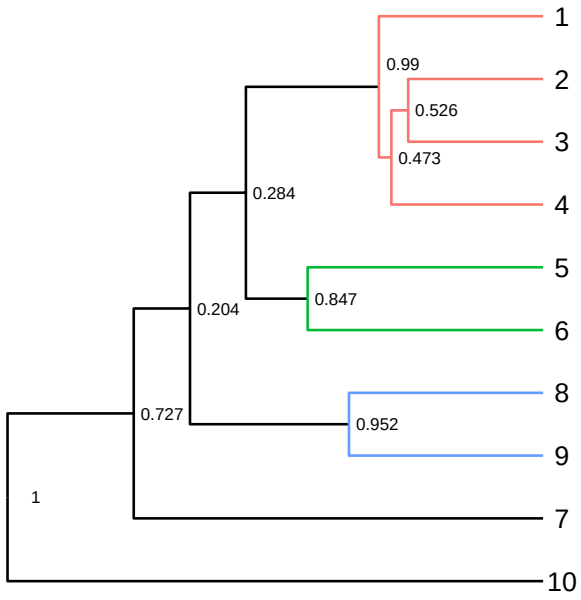

Figure 3.4: Clustering of ten roundfish areas based on the normalized environmental growth condition for the average (UPGMA) clustering method. Small digits show the bootstrap probability, which is the fraction of bootstrap repeats in which a branch contained the depicted areas. Coloured branches show clusters which arise in all clustering methods.

3.4 Discussion

We fitted Von Bertalanffy growth curves for exploited North Sea fish stocks in ten roundfish areas over a period of 50 years. The temporal variation in these growth curves was summarized in the estimated mean asymptotic size. We corrected the estimated mean asymptotic size for a possibly spurious relationship with the estimated Von Bertalanffy growth scalar and used these quantities as a corrected measure for environmental growth condition (EGC). The EGC is a summary statistic for the environmental factors that limit growth, such as food availability. Seven out of the ten species showed a negative trend in the corrected EGC over time in at least one area. In addition, corrected EGC showed a link with biomass per unit effort in at least one area for six out of ten species. More interestingly, clustering based on the normalized EGC resulted in four distinct clusters of species. These clusters consisted of the flatfish species and the forage fish species on one side and the small to intermediate pelagic species and the predatory species on the other side. Similarly, clustering of the roundfish areas resulted in three

distinct clusters, consisting of a large cluster covering the northern areas, a cluster with the southern areas and a cluster covering the Skagerrak and Kattegat.

By fitting a Von Bertalanffy growth curve in which the asymptotic size varied between years, we were able to summarize the temporal variation in growth with this asymptotic size (shown in chapter 2). The estimated asymptotic sizes showed extreme differences between areas (supplementary figure 3.7). These extreme differences arose as an artefact because the growth curves were fitted separately for every area. The asymptotic size and the Von Bertalanffy growth scalar cannot be estimated separately, resulting in a spurious relationship between the estimated asymptotic size and the Von Bertalanffy growth scalar between areas (Eveson et al., 2007; Pilling et al., 2002). We corrected for this spurious relationship to obtain an unbiased measure of the EGC. In addition, we normalized the EGC to be able to compare the EGC between species.

Because the EGC is used as a summary statistic for the environmental impact on growth, it is likely that the EGC is determined by multiple environmental factors such as food availability and temperature. Quantitatively, every environmental factor is likely to influence growth in a distinct way, but qualitatively these effects can be separated in two mechanisms. Some environmental factors such as food availability directly affect the anabolism rate of an individual. According to metabolic theory, these environmental factors only affect the asymptotic size of the growth curves (Kooijman, 2000; Von Bertalanffy, 1938). In contrast, some environmental factors, such as temperature, directly affect the catabolism rates of an individual. According to metabolic theory these processes affect the asymptotic size and the Von Bertalanffy growth scalar in opposite directions (Kooijman, 2000; Von Bertalanffy, 1938). As a consequence, factors affecting the catabolism rates of an individual will result in a negative correlation between the estimated asymptotic size and the estimated Von Bertalanffy growth scalar. This relationship is indistinguishable from the spurious relationship that might arise from the fitting procedures. Consequently, differences between areas caused by an environmental factor that affect catabolism rates will not be present in the data corrected for the spurious relationship arising from the fitting procedures. Before this correction, environmental factors affecting catabolism rates would result in a very distinctive pattern in which the estimated mean asymptotic size is negatively correlated with the estimated Von Bertalanffy growth rate and both are correlated with the environmental factor but with opposite slopes. We did not observe this pattern for the biomass-per-unit-effort (BPUE) as a predictive variable in our study. This suggests that BPUE, as a measure of population density, only affected individuals' anabolism rates but not catabolism rates. The correction for the methodological

artefact does not affect the dynamics of the estimated asymptotic size within an area because the Von Bertalanffy growth scalar is estimated as a constant parameter for every area. The corrected asymptotic size can therefore be used as a relative proxy for the environmental growth condition (EGC) within an area.

Seven out of the ten analysed stocks showed a decreasing trend in environmental growth condition over time. For five of the species this trend was even present when all areas were analysed simultaneously. This negative trend in environmental growth condition might seem counter-intuitive as most of the North Sea fish stocks are recovering over the last decades (Cardinale et al., 2013; Fernandes and Cook, 2013; Hutchings et al., 2010; Worm et al., 2009). It is important to note that studies reporting the recovery of fish stocks mainly consider the density or biomass of a stock. Stock recovery therefore indicates that the density or biomass of the stock increased. It is likely that the impact of a stock on the environment increases with the density of the stock, for example due to higher consumption or increased use of space. Recovery of a stock can, therefore, lead to deterioration of the shared environment and a decrease in EGC. It is therefore likely to observe a decrease in the EGC combined with an increase in stock biomass for recovering fish stocks, such as plaice or herring (Cardinale et al., 2013; Fernandes and Cook, 2013). However, we also reported a decrease in EGC for cod in the North Sea, while this cod stock is still heavily overfished and does not display a clear increase in biomass (Cardinale et al., 2013; Fernandes and Cook, 2013). In this situation, the decrease in EGC is not caused by the stock itself. This might be a worrying signal about the status of the stock, as both the biomass and the environment of the stock seem to deteriorate. A clear trend in EGC might therefore be an interesting addition to stock biomass as an indication of stock status.

Six of the ten analysed species showed a link between EGC and BPUE in at least one area, which suggests that growth in these species is density-dependent. Density dependence in individual growth has been shown for numerous fish stocks (Rindorf et al., 2022; Zimmermann et al., 2018; Lorenzen, 2016; Schram et al., 2006; Lorenzen and Enberg, 2002), including haddock, herring, whiting, sprat and cod for which we found this pattern as well. A common explanation for this pattern is that an increase in stock biomass results in an increase in competition for food and space and therewith a decrease in resources for individual growth. Density-dependent individual growth has previously been shown for plaice (Rijnsdorp and Van Leeuwen, 1996), mackerel (Jansen and Burns, 2015) and saithe as well (Cormon et al., 2016). We did not find an indication of density dependence in growth for these species in our analysis, even though we found a decreasing trend in EGC for these species. It is likely that we were not able to detect density

dependence in these species due to a lack of data or an inaccurate estimate of the stock biomass. For example, we were only able to estimate growth curves for plaice in most areas from 2010 onward, while the major recovery and fluctuations in stock biomass of plaice occurred before this period (ICES, 2021b). In addition, it is important to consider that stocks do live in a diverse environment with many interactions. The impact of a stock on the environment could therefore be overshadowed by other factors such as competing species or human activities. This would reduce the relative impact of the stock density on the environmental conditions and therewith reduces density dependence in growth. This could also explain the apparent positive relation between biomass per unit effort and growth of cod in roundfish area 5. An unknown confounding factor could lead to an increase in environmental conditions and therewith an increase in both growth and reproduction, resulting in an apparent positive relationship between individual size and stock density (Rindorf et al., 2022). The relationship between individual growth and stock density is therefore an interesting indicator for the relative impact of a stock on its own environmental conditions.

We performed cluster analysis on the fish species and the roundfish areas based on environmental growth condition estimated from population growth curves. This resulted in four distinct clusters of species that differentiated between forage fish species and flatfish species on one side and predatory species on the other side. Interestingly, pout and mackerel cluster together with other predatory species although only large individuals of these species feed on other fish. These clusters could be explained by a partly overlapping diet. Mackerel and pout mainly forage on crustaceans (copepods or euphausiids), while saithe, whiting and haddock feed on a mixed diet of crustaceans and forage fish (Mehl and Westgård, 1983; Hislop et al., 1991; Bromley et al., 1997). Cod is rarely associated with foraging on crustaceans, which corresponds with the result that cod clusters the furthest away from mackerel and pout (Floeter and Temming, 2003). This clustering could indicate that the non-piscivorous part of the diet from mackerel and pout has the largest impact on the experienced growth condition of a stock, possibly because most individuals within these stocks are young and not (yet) piscivorous. Another possibility is that the patterns in the growth curves of the predatory species are caused by other environmental factors than food availability, such as a similar reaction towards shifting temperatures or fishing regimes within the gadidae family. Nonetheless, the clustering of fish species based on growth curves was very similar to the clusters expected based on ecological and geographical similarities. This shows that growth curves contain valuable information about the environmental conditions encountered by a species in a specific area.

Clustering of the roundfish areas resulted in a northern cluster, a southern cluster and a cluster for the Skagerrak and Kattegat. This suggests that the EGC in geographically adjacent areas is similar. The high connectivity between the roundfish areas is further emphasized by the result that further clustering of these three clusters was inconclusive. Yet, the more global clustering of the North Sea in three regions is very clear and suggests that geographic differences in EGC are present. As a consequence, a shift in the geographical distribution of a stock is likely to influence the experienced EGC of stocks and therewith the growth and size of individuals.

Fisheries management is slowly shifting from a single-species perspective to a multi-species and ecosystem-centred perspective (Birkenbach et al., 2020; May et al., 1979). Information about the ecological overlap of species is needed to facilitate this shift. Generally, such information is collected using labor-intensive methods such as stomach sampling, physiological similarities and expert knowledge (Cadrin, 2020; Amundsen and Sánchez-Hernández, 2019; Matley et al., 2018). In this study we show that reconstructed growth curves can reveal relevant information about the ecology of a stock as well. Growth of individual fish is strongly affected by the environment (Tu et al., 2018; Lorenzen, 2008; Kooijman, 2000). Growth curves therefore contain valuable information about the ecological conditions and limitations experienced by a stock. It is likely that ecologically similar species are affected in a similar way by the environment, and that environmental conditions are similar in geographically and physically similar areas. Environmental conditions derived from growth curves could therefore provide valuable insight in the ecological relatedness between stocks and areas, based on straightforward size and age measurements. This could be further tested by comparing the results of diets and stomach samples of species with similar growth curves. Similarly, the clusters could be compared to reconstructions of the North Sea food web. In addition, estimated growth curves and EGC could be correlated to densities of other stocks to show additional ecological relationships between species such as competition and predation. Overall, growth curves appear to contain valuable information about the ecological conditions and relatedness of fish stocks and is a promising method to provide additional information about the state of a stock.

3.5 Supplementary materials

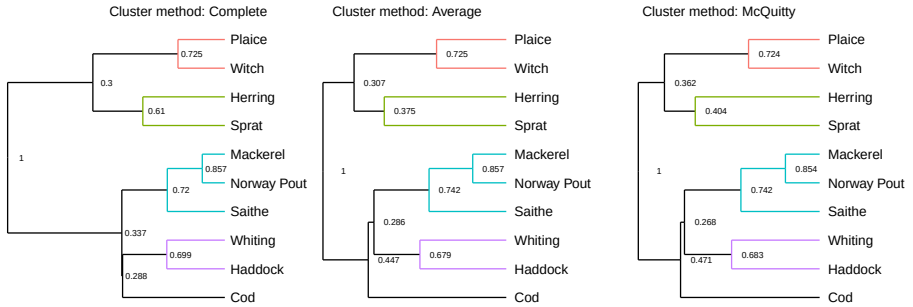

Figure 3.5: Clustering of ten North Sea fish species based on the normalized environmental growth condition for three different cluster methods. Small digits show the bootstrap probability, which is the fraction of bootstrap repeats in which a branch contained the depicted species. Coloured branches show clusters which arise in all clustering methods.

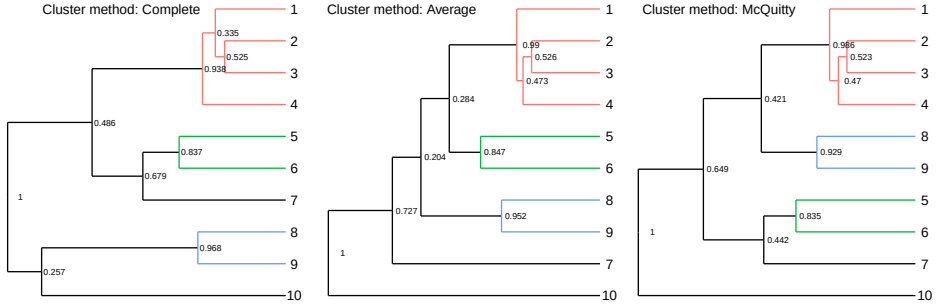

Figure 3.6: Clustering of ten roundfish areas based on the normalized environmental growth condition for three different cluster methods. Small digits show the bootstrap probability, which is the fraction of bootstrap repeats in which a branch contained the depicted areas. Coloured branches show clusters which arise in all clustering methods.

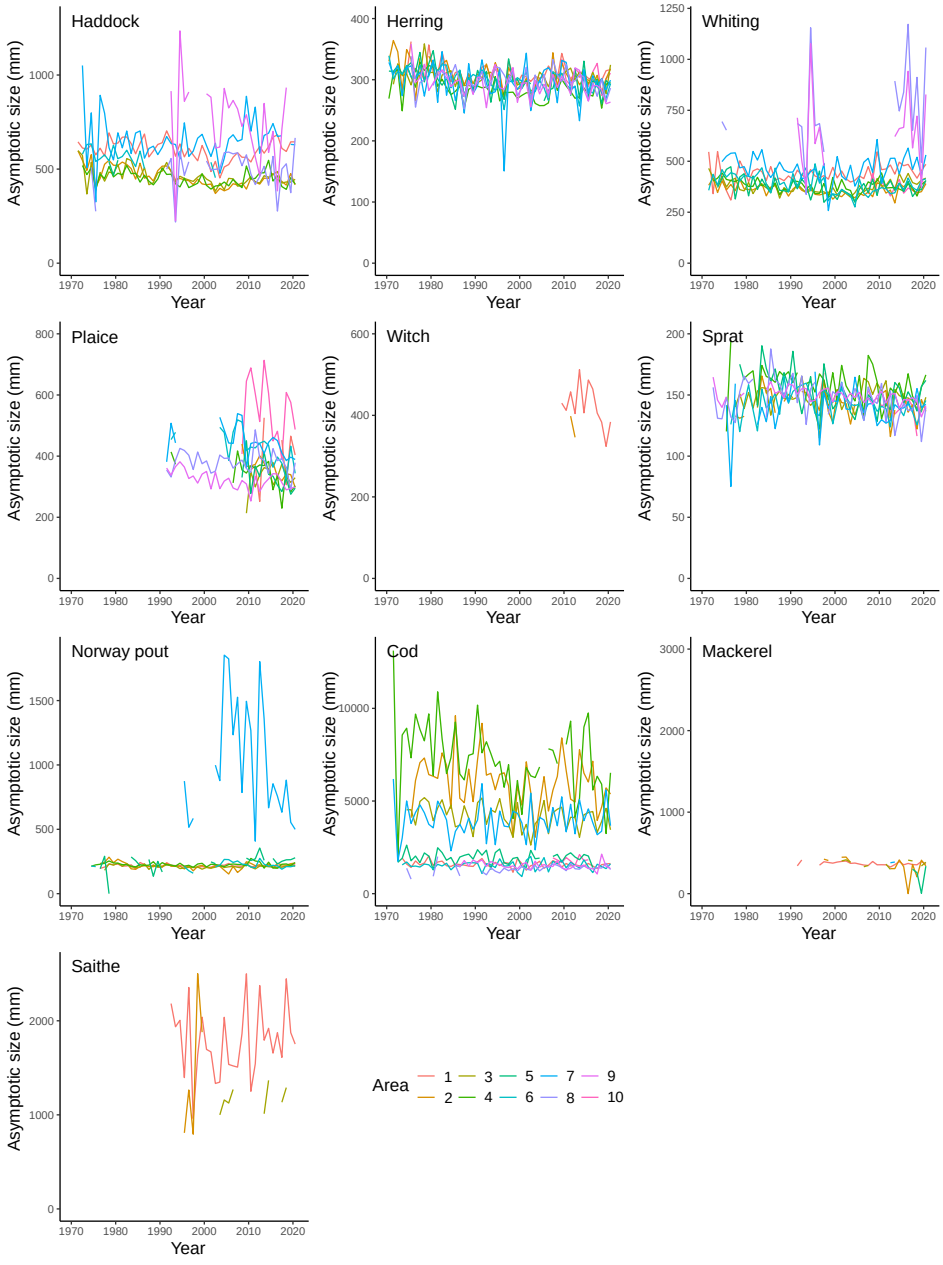

Figure 3.7: Annual asymptotic sizes of ten commercially exploited fish species in ten roundfish areas in the North Sea, before correction for a possible correlation between asymptotic size and the growth scalar. Time series are interrupted for years in which data was insufficient to provide a reliable estimate of the asymptotic size.

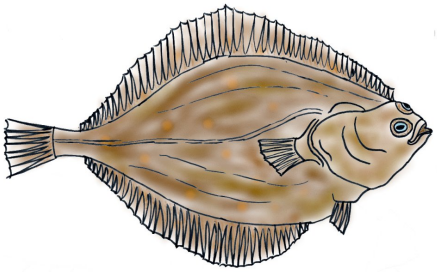

Chapter 4

The regulating effect of growth plasticity on the dynamics of structured populations

Jasper C. Croll
André M. de Roos

Published in *Theoretical ecology* (2022), 15: 95-113

Abstract

Plasticity is the extent to which life history processes such as growth and reproduction depend on the environment. Plasticity in individual growth varies widely between taxa. Nonetheless, little is known about the effect of plasticity in individual growth on the ecological dynamics of populations. In this article we analyse a physiologically structured population model of a consumer population in which the individual growth rate can be varied between entirely plastic to entirely non-plastic. We derive this population level model from a dynamic energy budget model to ensure an accurate energetic coupling between ingestion, somatic maintenance, growth, and reproduction within an individual. We show that the consumer population is either limited by adult fecundity or juvenile survival up to maturation, depending on the level of growth plasticity and the non-plastic individual growth rate. Under these two regimes we also find two different types of population cycles which again arise due to fluctuation in respectively juvenile growth rate or adult fecundity. In the end our model not only provides insight into the effects of growth plasticity on population dynamics, but also provides a link between the dynamics found in age- and size-structured models.

4.1 Introduction

Phenotypic plasticity is the difference in individual phenotypes due to the influence of the environment (Sultan and Stearns, 2005; Miner et al., 2005). It can arise if individual behaviour or individual life history processes such as growth, reproduction and mortality depend on the environment. As population dynamics arises from the accumulation of individual life histories (Miller and Rudolf, 2011), it is evident that plasticity in life history processes can strongly influence the dynamics of populations. Although plasticity is widely explored in the context of evolutionary dynamics, the effect of plasticity of life history traits on population dynamics is less well understood (Schmitz et al., 2003; Miner et al., 2005).

The population dynamic effects of plasticity in different life history processes cannot be considered separately, as many life history processes are linked through energy allocation schemes within an individual. It is therefore important to know the rules of within-individual energy allocation when considering plasticity in life history processes (Nisbet et al., 2000; Brown et al., 2004). Different frameworks have been formulated to understand individual energy allocation (Kooijman, 2000; West et al., 2001; Hou et al., 2008; Sousa et al., 2008). In general, assimilated energy is divided among maintenance, growth and reproduction, while a deficit in assimilated energy can lead to additional mortality due to starvation. If a life history process is entirely non-plastic, it does not depend on the environment and requires a predetermined amount of energy. The energy requirements of such a demand-driven process could be met through changes in behaviour to adapt the energy intake or by changes in the energy flow to other processes (Kooijman, 2010). In contrast, a purely supply-driven process is by definition plastic, because it depends entirely on the amount of assimilated energy and therefore on the food conditions of the environment. Models for individual energy allocation mainly differ in the priority of different processes (Lika and Nisbet, 2000; Kooijman, 2000; Zhang et al., 2012; Jager et al., 2013), but commonly maintenance costs are considered as a non-plastic (demand-driven) process while both growth and reproduction are considered as a plastic (supply-driven) process (but see De Roos et al. (2009) for an example of a model in which growth is incorporated as a demand-driven process).

A life history process for which plasticity strongly differs between taxa is the individual growth in body size. Environment-dependent changes in individual growth rate are observed in a wide range of ectothermic species ranging from *Daphnia* (McCauley et al., 1990) and fish (Lorenzen and Enberg, 2002; Zimmermann et al., 2018) to amphibians and reptiles (Halliday and Verrell, 1988), although some specific species in these taxa are found to be endothermic (Dickson and

Graham, 2004). In addition, it is even suggested that the growth rate of some large fossil mammals was flexible (Köhler and Moyà-Solà, 2009). This suggests that the growth rate in most ectotherms and early endotherms is plastic. In contrast, the growth rate of most modern endotherms (e.g. birds and mammals) is relatively independent of environmental influences. To maintain a constant growth rate in a fluctuating environment, it is necessary to regulate the amount of energy acquired and allocated to somatic growth. This can partly be achieved by the ability to maintain a constant homeostasis and adaptive behaviour (Kooijman, 2010). Meanwhile, the resting metabolic expenditure of endotherms exceeds that of ectotherms by an order of magnitude, even when corrected for expenditure for thermoregulation or under conditions with limited energy demand such as during torpor or hibernation (Bennett and Ruben, 1979). The additional resting metabolic expenditure in endotherms is likely used to maintain a constant energy flow to growth in order to maintain a constant somatic growth rate. This latter idea is supported by field observations of ungulates which experience delayed reproduction and decreased fecundity with low food abundance (Skogland, 1986; Clutton-Brock et al., 1987; Festa-Bianchet et al., 1995; Coulson et al., 2000; Albon et al., 2000) and laboratory observations of house mice, which stopped ovulating while maintaining growth under reduced food conditions (Perrigo, 1990). Altogether this suggests that the growth rate of endotherms is largely predetermined and non-plastic rather than supply driven.

Whereas the plasticity of life history characteristics can be considered as a continuous trait ranging from non-plastic to highly plastic (Sultan and Stearns, 2005), the individual growth rate in models of structured populations is generally assumed to be either non-plastic or entirely plastic. This results in two categories of structured models with different dynamics. For example, age-based models, such as used in fisheries management (Schnute and Richards, 1998), assume that individuals of the same age are of similar size. The growth rate of individuals is thus implicitly assumed to be independent of the environment, suggesting that individual growth is a non-plastic process (De Roos et al., 2003). In these models, the population structure is entirely determined by the individual reproduction and mortality rate. Population dynamic cycles in these models arise due to the delay between birth and maturation and the competition between different life stages (Gurney et al., 1983; Gurney and Nisbet, 1985; De Roos et al., 2003; Pfaff et al., 2014). In contrast, most size-structured models are based on a dynamic energy budget model in which individual growth is modelled as a supply-driven process. As a consequence, the individual growth rate depends on the resource density and is therefore entirely plastic (De Roos et al., 1990; De Roos and Persson, 2001). Due

to the highly plastic individual growth rate, the size-structured models can show a range of population structures and different types of population dynamic cycles, which mainly depend on the competitive strength of different life stages (De Roos et al., 2003; De Roos and Persson, 2003). Due to the discrete differences between these two classes of structured models, it is largely unclear how predictions from (age-structured) models with non-plastic growth relate to (size-structured) models with entirely plastic growth.

Although we know most about the ecological dynamics when individual growth is either entirely plastic or non-plastic, it is more likely that for most species the actual level of plasticity in individual growth lies between these two extremes. At such intermediate levels of growth plasticity, individual growth would consist of a non-plastic part representing the baseline minimum growth rate of an individual, and a plastic part, which is an environment-dependent additional increase in individual growth. This raises the question of how population dynamics changes when the plasticity in individual growth is at intermediate levels. Here we present a size-structured model in which we vary the individual growth rate from non-plastic to entirely plastic. We base this model on a simple Dynamic Energy Budget (DEB) model (Jager et al., 2013) to ensure a plausible scheme for energy allocation within an individual. Herewith we restrict ourselves to the simplest case in which the environment only consists of a single dynamic resource. Therefore, non-plastic growth in our model indicates that the individual growth rate is entirely independent of the resource density and requires a predetermined amount of energy, which could be set and regulated by genetic and chemical regulatory pathways within an individual. In contrast, entirely plastic growth indicates that the individual growth rate depends on the resource density. The growth rate is therefore completely supply driven and fluctuates accordingly. We will explore how the population dynamics in this model changes with respect to the level of growth plasticity as well as the maximum density of the resource, as an increase in the latter is generally known to destabilize the dynamics from structured population models, resulting in population dynamic cycles (De Roos et al., 1990).

4.2 Model formulation

Individual energy dynamics

As a basis for the individual energy dynamics, we use a simplified DEB model described by Jager et al. (2013). This model describes energy intake, somatic growth and reproduction in terms of energy stored in lean mass (E_m). In the

DEB theory framework, it is generally assumed that individuals of all sizes and ages have the same shape and body composition and therefore both the mass and size of an individual scale with the energy stored in lean mass. Energy ingestion (I) is assumed to scale with the resource density (R) following a Holling type II functional response ($f(R) = \frac{R}{R_h+R}$, with R_h the half saturation constant), the individual surface area ($E_m^{2/3}$) and the maximum ingestion rate per unit surface area (I_R):

$$I = I_R f(R) E_m^{2/3} = I_R \frac{R}{R_h + R} E_m^{2/3} \tag{4.1}$$

We follow DEB theory and assume assimilation efficiency in the gut is a species-specific constant. The surface-specific maximum ingestion rate times the assimilation rate is represented by α. The original energetic model by Jager et al. (2013) assumes growth is plastic and follows a κ-rule in which a fraction κ of the assimilated energy is used for somatic growth and somatic maintenance costs. The somatic maintenance costs are assumed to be non-plastic and scale with the energy stored in lean mass through the energy-specific maintenance costs (b). Covering somatic maintenance costs has priority over somatic growth. This yields the following differential equation for plastic somatic growth:

$$\frac{dE_m}{dt} = \gamma_m \left(\kappa \alpha f(R) E_m^{2/3} - b E_m \right) \tag{4.2}$$

With γ_m the conversion efficiency of assimilated energy to lean mass. These assumptions imply that individuals follow a Von Bertalanffy type of growth curve when the resource density is constant. The maximum lean mass reached by an individual is proportional to $f(R)^3$, whereas the growth rate is independent of resource density (Jager et al., 2013).

We assume individuals mature when reaching a predetermined amount of energy stored in lean mass (E_J). In adult individuals, a fraction $1 - \kappa$ of the assimilated energy is channelled to reproduction, while this fraction is used for maturation in juvenile individuals. This results in the following differential equation for the total amount of energy (E_r) invested by adults into the production of juveniles:

$$\frac{dE_r}{dt} = \gamma_r (1 - \kappa) \alpha f(R) E_m^{2/3} \tag{4.3}$$

With γ_r the conversion efficiency of assimilated energy to energy in newborn lean mass.

To formulate a version of the model with non-plastic growth, the somatic growth rate has to be decoupled from the resource density. In other words, a constant amount of energy is used for somatic growth and somatic maintenance, in-

dependent of the current resource density. To stay close to the original model with plastic growth, non-plastic somatic growth is assumed to follow a Von Bertalanffy growth trajectory as well. This results in the following differential equation for non-plastic somatic growth:

$$\frac{dE_m}{dt} = \gamma_m \left(\kappa \alpha \zeta E_m^{2/3} - b E_m \right) \tag{4.4}$$

Here we introduce a parameter ζ as a scalar modulating the non-plastic growth rate to replace the scaled functional response ($f(R)$) in the plastic growth rate. Individuals following the non-plastic growth dynamics (eq. 4.4) will therefore grow at the same rate as individuals that follow the plastic growth dynamics (eq. 4.2) with a scaled functional response ($f(R)$) equal to ζ. To capture the entire spectrum from non-plastic growth to entirely plastic growth, we introduce the parameter ϕ, which represents the extent to which growth is plastic. This results in our general formula for somatic growth:

$$\frac{dE_m}{dt} = \gamma_m \left(\phi \kappa \alpha f(R) E_m^{2/3} + (1-\phi) \kappa \alpha \zeta E_m^{2/3} - b E_m \right) \tag{4.5}$$

We assume all energy not used for somatic processes is used by juveniles for maturation and by adults for reproduction, resulting in the following expression for the investment in reproductive energy:

$$\frac{dE_r}{dt} = \begin{cases} 0 & \text{if } E_m < E_J \\ \gamma_r \left(\alpha f(R) E_m^{2/3} - \left(\phi \kappa \alpha f(R) E_m^{2/3} + (1-\phi) \kappa \alpha \zeta E_m^{2/3} \right) \right) & \text{if } E_m > E_J \end{cases} \tag{4.6}$$

With E_J the energy in lean mass corresponding to the size at which individuals mature.

Equations 4.5 and 4.6 simplify to the model described by Jager et al. (2013) if growth is entirely plastic ($\phi = 1$). In addition, notice that the investment in growth in our model is higher compared to the κ-rule model with entirely plastic growth if $f(R) < \zeta$, while investment in reproduction is higher if $f(R) > \zeta$.

By comparing the equation for the assimilated energy ($\alpha f(R) E_m^{2/3}$) with the energy used for growth (eq. 4.5), it is clear that the rate of energy supply may become insufficient to maintain the outlined energy allocation scheme. If energy supply becomes insufficient, we assume starvation and rechannelling of energy occurs. An individual could encounter three types of starvation conditions (Fig. 4.1).

Under the most severe starvation condition as a consequence of very low resource densities, ingested energy is insufficient to cover somatic maintenance costs

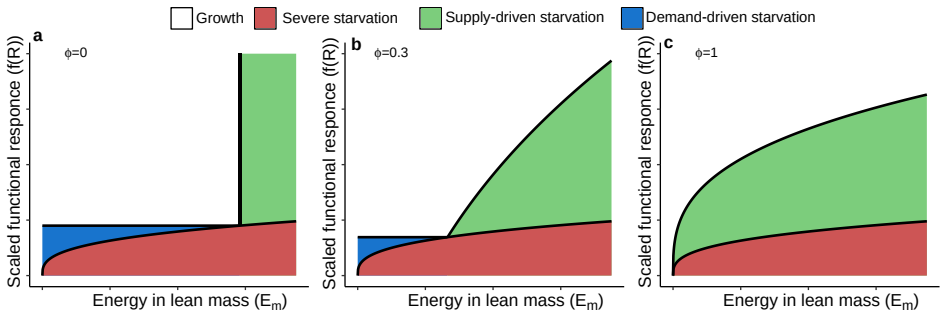

Figure 4.1: In addition to growth dynamics, individuals can encounter three types of starvation conditions, depending on the energy in lean mass and the scaled functional response of the resource density. The boundaries of these dynamics shift when growth shifts from non-plastic ($\phi = 0$) to entirely plastic ($\phi = 1$). Under severe starvation conditions (red area), assimilated energy is insufficient to cover maintenance costs. Under supply-driven starvation conditions (green area), the energy allocated to somatic processes is insufficient to cover maintenance costs. Under demand-driven starvation conditions (blue area), assimilated energy is insufficient to cover the costs for maintenance and demand-driven growth.

(red area in figure 4.1). This regime occurs when:

$$bE_m > \alpha f(R) E_m^{2/3} \tag{4.7}$$

We will refer to this condition as *severe starvation* following De Roos et al. (1990) and we will assume individuals starve instantaneously when it occurs.

Under less severe starvation conditions, ingested energy is sufficient to cover somatic maintenance costs but the energy allocated to somatic processes is not (green area in figure 4.1):

$$\alpha f(R) E_m^{2/3} > bE_m > \phi\kappa\alpha f(R) E_m^{2/3} + (1-\phi)\kappa\alpha\zeta E_m^{2/3} \tag{4.8}$$

De Roos et al. (1990) refers to this starvation condition as *mild starvation*, but we will use the term *supply-driven starvation*, because the supply of energy to somatic processes is insufficient to cover maintenance costs.

The last type of starvation occurs if the assimilated energy is insufficient to cover all energy requirements for somatic growth and maintenance:

$$\phi\kappa\alpha f(R) E_m^{2/3} + (1-\phi)\kappa\alpha\zeta E_m^{2/3} > \alpha f(R) E_m^{2/3} > bE_m \tag{4.9}$$

We will refer to this type of starvation as *demand-driven starvation*, because the

energy demand for growth is too high for the energy supplied by assimilation. From inequality (4.9), it is clear that the boundary between growth conditions and demand-driven starvation is dependent on resource density, but not on individual size (Fig. 4.1, boundary of the blue area).

Comparison of the three starvation conditions shows that all three starvation boundaries intersect at a single point ($E_m^{1/3} = \frac{\alpha\kappa}{b}\frac{1-\phi}{1-\phi\kappa}\zeta$, Fig. 4.1). If we do not take into account the conditions in which severe starvation occurs, individuals can only suffer demand-driven starvation if the energy stored in lean mass is below this critical value ($E_m^{1/3} < \frac{\alpha\kappa}{b}\frac{1-\phi}{1-\phi\kappa}\zeta$), while individuals can only suffer from supply-driven starvation if the energy stored in lean mass is above this critical value ($E_m^{1/3} > \frac{\alpha\kappa}{b}\frac{1-\phi}{1-\phi\kappa}\zeta$). In other words, small and large individuals are vulnerable to demand-driven and supply-driven starvation, respectively.

In general, we assume energy is rechannelled under starvation conditions from the energy flow with sufficient energy to the energy flow with the deficit (e.q. from maturation and reproduction to growth and somatic maintenance or vice versa). More specifically, this means that under supply-driven starvation, growth of all individuals stops and energy allocation to reproduction in adults is reduced:

$$\frac{dE_m}{dt} = 0 \tag{4.10a}$$

$$\frac{dE_r}{dt} = \begin{cases} 0 & \text{if } E_m < E_J \\ \gamma_r \left(\alpha f(R) E_m^{2/3} - bE_m\right) & \text{if } E_m > E_J \end{cases} \tag{4.10b}$$

While under demand-driven starvation, energy allocation to reproduction by adults stops and growth of all individuals is reduced:

$$\frac{dE_m}{dt} = \gamma_m \left(\alpha f(R) E_m^{2/3} - bE_m\right) \tag{4.11a}$$

$$\frac{dE_r}{dt} = 0 \tag{4.11b}$$

These rechannelling rules imply that individuals below the species-specific threshold size ($E_m^{1/3} = \frac{\alpha\kappa}{b}\frac{1-\phi}{1-\phi\kappa}\zeta$) prioritize growth if experiencing (demand-driven) starvation conditions, while individuals above the species-specific threshold size prioritize reproduction if experiencing (supply-driven) starvation conditions (Fig. 4.1b).

It is likely that the re-channelling of energy will bring additional costs such as starvation mortality. We assume starvation mortality scales with the energy deficit and is zero at the supply-driven starvation boundary and the demand-driven starvation boundary. In addition, we assume starvation mortality approaches infinity if individual energetics approaches the severe starvation boundary. As a

consequence, individuals will starve with certainty before entering severe starvation conditions. The starvation-induced mortality rate (μ_s) under supply-driven starvation we therefore assume to follow:

$$\mu_s = q_s \max\left(\frac{bE_m - \left(\phi\kappa\alpha f(R)E_m^{2/3} + (1-\phi)\kappa\alpha\zeta E_m^{2/3}\right)}{\alpha f(R)E_m^{2/3} - bE_m}, 0\right) \tag{4.12}$$

And under demand-driven starvation conditions:

$$\mu_s = q_s \max\left(\frac{\left(\phi\kappa\alpha f(R)E_m^{2/3} + (1-\phi)\alpha\kappa\zeta E_m^{2/3}\right) - \alpha f(R)E_m^{2/3}}{\alpha f(R)E_m^{2/3} - bE_m}, 0\right) \tag{4.13}$$

Growth dynamics

According to DEB theory (Kooijman, 2010), the individual body mass can be expressed in terms of energy stored in lean mass by using the mass-specific energy density (d_m). In the same way the volume can be related to the mass with the volume-specific mass (d_v) and the length can be related to the volume with a shape scaling constant (δ_m):

$$W = \frac{E_m}{d_m} = d_v V = d_v(\delta_m \ell)^3 \tag{4.14a}$$

$$\ell = \frac{V^{1/3}}{\delta_m} = \frac{W^{1/3}}{d_v^{1/3}\delta_m} = \frac{E_m^{1/3}}{d_m^{1/3}d_v^{1/3}\delta_m} \tag{4.14b}$$

Using these equalities, the individual dynamics can be expressed in terms of individual length instead of energy stored in lean mass (Table 4.1, see also the supplementary materials)(Murphy, 1983; De Roos et al., 1990). To do so, we use expressions for the investments into somatic growth ($F_g(R,\ell)$), reproduction ($F_r(R)$) and growth and reproduction together ($F_t(R,\ell) = F_g(R,\ell) + F_r(R)$), which depend on the resource density, the ultimate size under unlimited food conditions (ℓ_∞) and possibly the actual length (ℓ). Note that these investments are proportional to the energy allocation to growth and reproduction. In addition, these quantities are expressed per unit surface area and could therefore be interpreted as the (area specific) growth rate, fecundity and biomass production as well. The dynamics of the length-age relationship ($\ell(t,a)$) is defined in terms of the Von Bertalanffy growth rate (r_B) times the investments into growth ($F_g(R,\ell)$ or $F_t(R,\ell)$) in combination with the size at birth (ℓ_b), which is a boundary condition needed to solve this differential equation. Individuals mature when reaching

Table 4.1: Equations describing the population dynamics under growth conditions and supply-driven ($F_g(R,\ell) < 0$), demand-driven ($F_r(R) < 0$) and severe ($F_t(R,\ell) < 0$) starvation conditions. Notice that as long as extreme starvation does not occur ($F_t(R,\ell) > 0$) supply- and demand-driven starvation are mutually exclusive, such that $F_r(R) \leq 0$ implies $F_g(R,\ell) > 0$ and $F_g(R,\ell) \leq 0$ implies $F_r(R) > 0$.

Population age-distribution dynamics	
$\frac{\partial n}{\partial t} + \frac{\partial n}{\partial a} =$	$-\left(\mu_b + \mu_s(R,\ell)\right) n(t,a)$
$n(t,0) =$	$\int_0^{a_{max}} \beta(R,\ell(t,a)) n(t,a) da$
Energetic surpluses/deficits	
$F_g(R,\ell) =$	$(\phi f(R) + (1-\phi)\zeta)\,\ell_\infty - \ell$
$F_r(R) =$	$\left(\phi\frac{(1-\kappa)f(R)}{\kappa} + (1-\phi)\left(\frac{f(R)}{\kappa} - \zeta\right)\right)\ell_\infty$
$F_t(R,\ell) =$	$F_g(R,\ell) + F_r(R) = \frac{f(R)}{\kappa}\ell_\infty - \ell$
Length-age dynamics	
$\frac{\partial \ell}{\partial t} + \frac{\partial \ell}{\partial a} =$	$\begin{cases} r_B F_g(R,\ell) & \text{if } F_g(R,\ell) > 0 \text{ and } F_r(R) > 0 \\ r_B F_t(R,\ell) & \text{if } F_r(R) \leq 0 \text{ and } F_t(R,\ell) > 0 \\ 0 & \text{otherwise} \end{cases}$
$\ell(t,0) =$	ℓ_b
Individual fecundity	
$\beta(R,\ell) =$	$\begin{cases} r_F F_r(R)\ell^2 & \text{if } \ell_J < \ell,\ F_g(R,\ell) > 0 \text{ and } F_r(R) > 0 \\ r_F F_t(R,\ell)\ell^2 & \text{if } \ell_J < \ell,\ F_g(R,\ell) \leq 0 \text{ and } F_t(R,\ell) > 0 \\ 0 & \text{otherwise} \end{cases}$
Starvation mortality	
$\mu_s(R,\ell) =$	$\begin{cases} 0 & \text{if } F_g(R,\ell) > 0 \text{ and } F_r(R) > 0 \\ -q_s\frac{F_g(R,\ell)}{F_t(R,\ell)} & \text{if } F_g(R,\ell) \leq 0 \text{ and } F_t(R,\ell) > 0 \\ -q_s\frac{F_r(R)}{F_t(R,\ell)} & \text{if } F_r(R) \leq 0 \text{ and } F_t(R,\ell) > 0 \\ \infty & \text{if } F_t(R,\ell) \leq 0 \end{cases}$

the size at maturation (ℓ_J). The individual fecundity ($\beta(R,\ell)$) is defined in terms of the reproduction rate (r_F) times the investments into reproduction ($F_r(R)$ or $F_t(R,\ell)$). In this formulation, the parameters for the ultimate asymptotic size (ℓ_∞), Von Bertalanffy growth rate (r_B) and the reproduction rate (r_F) are composite parameters consisting of the plastic energy assimilation constant (κ), the maximum ingestion and assimilation rate (α), the energy specific somatic maintenance costs (b), the size at birth (ℓ_b) and the energy conversion efficiencies (γ_m, γ_r) from the DEB formulation (eq. 4.22). Lastly, the dynamics of the population age-distribution ($n(t,a)$) depends on the individual background mortality (μ_b) and the individual starvation mortality ($\mu_s(R,\ell)$) in combination with the population birth rate ($n(t,0)$) calculated as the total reproductive output of the population at a given time. We state that the mortality under extreme starvation conditions ($F_t(R,\ell) \leq 0$) is infinitely large to indicate that the survival probability under this condition is zero and individuals are instantaneously removed from the population.

For simplicity, we will assume the resource to be unstructured and the dynamics of the resource without consumption to be described by semi-chemostat dynamics, with a turn-over rate ν and a maximum resource density K:

$$\frac{dR}{dt} = \nu(K-R) - \int_0^{a_{max}} I_{max} f(R) \ell(t,a)^2 n(t,a) da \tag{4.15}$$

The parameter I_{max} is a scaled version of I_R, representing the ingestion rate per unit surface area in terms of length instead of energy stored in lean mass.

4.3 Mathematical analysis

Model equilibria can be calculated following the procedure described by De Roos et al. (1990). At a constant resource density $R = \bar{R}$ and hence a constant value of the functional response ($f(\bar{R})$) the consumer population can only persist if the functional response is sufficiently high for extreme and demand-driven starvation not to occur ($F_t(\bar{R},\ell), F_r(\bar{R}) > 0$), because otherwise consumers would die instantaneously or never reproduce. With a constant functional response, investment in growth and the individual size can be solved explicitly as a function of age, which results in a Von Bertalanffy growth curve:

$$F_g(\bar{R},\ell) = \left(\left(\phi f(\bar{R}) + (1-\phi)\zeta\right)\ell_\infty - \ell_b\right) e^{-r_B a} = F_{g\infty}(\bar{R}) e^{-r_B a} \tag{4.16a}$$

$$\begin{aligned} \ell(\bar{R},a) &= \ell_b + \left(1 - e^{-r_B a}\right) F_{g\infty}(\bar{R}) \\ &= \ell_b e^{-r_B a} + \left(\phi f(\bar{R}) + (1-\phi)\zeta\right)\left(1 - e^{-r_B a}\right)\ell_\infty \end{aligned} \tag{4.16b}$$

Herein we introduce $F_{g\infty}(\bar{R})$ as the lifetime investment in growth at the constant resource density $\bar{R}$ given an individual survives, which we will use as an age independent quantity for energy investment in growth (note that $F_{g\infty}(\bar{R})$ equals the integral of the product $r_B F_g(\bar{R}, \ell(\bar{R}, a))$ over the entire lifetime for an individual living at resource density $\bar{R}$). From comparing the growth curve with the supply-driven starvation condition, it is clear that individuals do not experience supply-driven starvation when living at a constant resource density $\bar{R}$ ($F_g(\bar{R}, \ell) > 0$). The Von Bertalanffy growth curve also defines the age at maturation at the constant food density ($\bar{a}_J$), which is the age at which individuals reach the size at maturation ($\ell(\bar{R}, \bar{a}_J) = \ell_J$). For individuals to reach this maturation size at the constant resource density $\bar{R}$, individuals of length ℓ_J should not experience supply-driven starvation ($F_g(\bar{R}, \ell_J) > 0$). When individuals do not experience starvation conditions, the dynamics of the population age-distribution can be simplified and solved explicitly, resulting in an expression for the density of individuals at a given age:

$$\bar{n}(a) = \bar{n}(0) e^{-\mu_b a} \tag{4.17}$$

By substituting the Von Bertalanffy growth curve (eq. 4.16) and the age distribution in equilibrium (eq. 4.17) in the expression for the population birth rate, we arrive at an expression for the lifetime reproductive output (LRO):

$$\begin{aligned} LRO =& r_F F_r(\bar{R}) \int_{\bar{a}_J}^{a_{max}} \ell(\bar{R}, a)^2 e^{-\mu a} da \\ =& r_F F_r(\bar{R}) \int_{\bar{a}_J}^{a_{max}} \left(\ell_b + \left(1 - e^{-r_B a}\right) F_{g\infty}(\bar{R})\right)^2 e^{-\mu a} da \end{aligned} \tag{4.18}$$

The lifetime reproductive output represents the average number of offspring an individual is expected to produce during its lifetime. A population is in equilibrium if every individual on average replaces itself and therefore the lifetime reproductive output in equilibrium equals one. By setting the lifetime reproductive output to one, we can solve for the functional response in equilibrium, which we indicate with $f(\tilde{R})$, because this is the only unknown in the lifetime reproductive output. The functional response and the resource density in equilibrium ($\tilde{R}$) are therefore completely determined by the growth, reproduction and mortality traits of the consumer population and hence independent of resource growth conditions.

The last step is to derive the population birth rate in equilibrium ($\tilde{n}(0)$) from the dynamics of the resource (eq. (4.15)), which together with the resource density

defines the complete equilibrium:

$$\tilde{n}(0) = \frac{\nu\left(K - \tilde{R}\right)}{I_{max} f(\tilde{R}) \int_0^{a_{max}} \ell(\tilde{R}, a)^2 e^{-\mu a} da} \tag{4.19}$$

From equation (4.19) it follows that the resource density in equilibrium equals the maximum resource density ($\tilde{R} = K$) at the persistence boundary of the consumer population ($\tilde{n}(0) = 0$). Therefore, the persistence boundary is calculated by setting the lifetime reproductive output equal to one and substituting the resource density with the maximum resource density (eq. 4.33).

The stability boundary of the model can be calculated through linearization of the dynamic equations around the equilibrium state as outlined by (De Roos et al., 1990). The derivation of the conditions determining the stability boundary is explained in detail in the supplementary materials (eq. 4.39 - 4.47).

Energetic tradeoff

At a given constant resource density $\bar{R}$ both the investments into growth ($F_{g\infty}(\bar{R})$) and the investments into reproduction ($F_r(\bar{R})$) change with the growth plasticity (ϕ). This change can be expressed as the derivative of these investments with respect to the level of growth plasticity:

$$\frac{\partial F_{g\infty}}{\partial \phi} = \left(f(\bar{R}) - \zeta\right) \ell_\infty \tag{4.20a}$$

$$\frac{\partial F_r}{\partial \phi} = -\left(f(\bar{R}) - \zeta\right) \ell_\infty \tag{4.20b}$$

The direction of a change in energy allocation due to growth plasticity is determined by the non-plastic asymptotic size ($\zeta \ell_\infty$) compared to the plastic asymptotic size ($f(\bar{R})\ell_\infty$). An increase in growth plasticity will lead to an increase in growth investments and a decrease in reproductive investments if the plastic asymptotic size exceeds the non-plastic asymptotic size ($f(\bar{R})\ell_\infty > \zeta\ell_\infty$). In contrast, an increase in growth plasticity will lead to a decrease in growth investments and an increase in reproductive investments if the non-plastic asymptotic size exceeds the plastic asymptotic size ($f(\bar{R})\ell_\infty < \zeta\ell_\infty$). It is also clear that the effect of the growth plasticity on the growth investments is always opposite to the effect on reproductive investments. This reveals a tradeoff in which an increase in investment in growth will always lead to a decrease in investment in reproduction and vice versa.

A change in growth plasticity affects the lifetime reproductive output through

both the growth investments and the reproductive investments:

$$\frac{dLRO}{d\phi} = \frac{\partial LRO}{\partial F_{g\infty}}\frac{\partial F_{g\infty}}{\partial \phi} + \frac{\partial LRO}{\partial F_r}\frac{\partial F_r}{\partial \phi} = \left(\frac{\partial LRO}{\partial F_{g\infty}} - \frac{\partial LRO}{\partial F_r}\right)\left(f(\tilde{R}) - \zeta\right)\ell_\infty \tag{4.21}$$

Explicit expressions for the partial derivatives $\frac{\partial LRO}{\partial F_{g\infty}}$ and $\frac{\partial LRO}{\partial F_r}$ are derived in the supplementary information. From equation (4.21) it is clear that the lifetime reproductive output of an individual is completely independent of the growth plasticity (ϕ) if the plastic asymptotic size equals the non-plastic asymptotic size ($f(\bar{R})\ell_\infty = \zeta\ell_\infty$). From equations (4.16) and (4.18) we can furthermore infer that the lifetime reproductive output increases with both an increase in energy allocation to growth and energy allocation to reproduction ($\frac{\partial LRO}{\partial F_{g\infty}} > 0$ and $\frac{\partial LRO}{\partial F_r} > 0$). We therefore can distinguish a parameter region in which an increase in growth investments has a larger effect on lifetime reproductive output than a similar increase in reproductive investments ($\frac{\partial LRO}{\partial F_{g\infty}} > \frac{\partial LRO}{\partial F_r}$) and a parameter region in which an increase in reproductive investments has a larger effect on lifetime reproductive output than a similar increase in growth investments ($\frac{\partial LRO}{\partial F_{g\infty}} < \frac{\partial LRO}{\partial F_r}$). We will refer to the dynamics in these regions as growth-limited and reproduction-limited dynamics respectively. Whether or not the lifetime reproductive output increases with an increase in growth plasticity depends on whether the dynamics are growth- or reproduction-limited in combination with whether the plastic asymptotic size ($f(\bar{R})\ell_\infty$) is larger or smaller than the non-plastic asymptotic size ($\zeta\ell_\infty$). Furthermore, an increase in growth plasticity (ϕ) results in a change from an increase to a decrease in lifetime reproductive output when the dynamics changes from growth to reproduction limited, assuming that the plastic asymptotic size is larger than the non-plastic asymptotic size ($f(\bar{R})\ell_\infty > \zeta\ell_\infty$). Alternatively, when the plastic asymptotic size is smaller than the non-plastic asymptotic size ($f(\bar{R})\ell_\infty < \zeta\ell_\infty$), an increase in growth plasticity (ϕ) results in a change from an increase to a decrease in lifetime reproductive output when the dynamics changes from reproduction to growth limited. The value of the growth plasticity (ϕ) at which the boundary between these two areas occurs, strongly depends on the plastic energy allocation constant (κ) but is also influenced by other parameters (eq. 4.34 - 4.37).

4.4 Numerical analysis

The persistence boundary and the stability boundary have been studied numerically as a function of model parameters using general root-finding and curve continuation procedures implemented in C (Findcurve software by De Roos (2021b)). Time dynamics of the model have been computed using the Escalator Boxcar Train

Table 4.2: Parameters used in the structured population model for *Daphnia magna* feeding on algae, derived from De Roos et al. (1990).

Parameters of the structured population model			
ϕ	Plasticity in somatic growth	varied	-
ζ	Scalar of the non-plastic growth rate	0.1 or 1	-
κ	Plastic growth energy allocation constant	0.3 or 0.9	-
ℓ_b	Length at birth	0.8	mm
ℓ_J	Length at maturation	2.5	mm
ℓ_∞	Asymptotic length under unlimited food conditions	20κ	mm
a_{max}	Maximum age	70	d
r_B	Time constant of growth	0.15	d^{-1}
r_F	Time constant of reproduction	0.00714	$mm^{-3}d^{-1}$
μ_b	Background mortality rate	0.03	d^{-1}
q_s	Starvation mortality scaling constant	0.2	d^{-1}
I_{max}	Maximum feeding rate per unit surface area	1.8	10^6 cells $mm^{-2}ml^{-1}d^{-1}$
R_h	Half saturation constant of functional response	0.14	10^6 cells ml^{-1}
ν	Semi-chemostat renewal rate	0.5	d^{-1}
K	Maximum resource density	varied	10^6 cells ml^{-1}

(EBT) method, especially designed for the numerical integration of physiologically structured population models (De Roos, 1988; De Roos et al., 1992). For the numerical analysis of the model and corresponding figures we use a parameter set representing *Daphnia magna* feeding on algae, comparable to the parameter values used by De Roos et al. (1990) (Table 4.2). We use slightly different definitions of the half saturation constant of the functional response (R_h) and the reproduction rate (r_F). Therefore, we recalculated the values of these parameters to ensure our model is numerically equivalent to the model analysed by De Roos et al. (1990) if growth is entirely plastic ($\phi = 1$). From here on we will refer to the structured *Daphnia* populations as consumers, while the unstructured algae community is referred to as the resource.

Equilibrium dynamics

In general, four different configurations of the regions with growth-limited and reproduction-limited dynamics are possible (derivation in supplementary materials eq. 4.34 - 4.37). (1) If the growth energy allocation constant κ is below a specific threshold value ($\kappa \approx 0.857$ with our parameter set) and the plastic asymptotic size exceeds the non-plastic asymptotic size ($f(\tilde{R})\ell_\infty > \zeta\ell_\infty$, Fig. 4.2a) the dynamics is always growth-limited. (2) If the plastic growth energy allocation constant κ is below the threshold value and the non-plastic asymptotic size exceeds the plastic asymptotic size, ($\kappa < 0.857$, $f(\tilde{R})\ell_\infty < \zeta\ell_\infty$, Fig. 4.2b), the dynamics is growth-limited at high growth plasticity (high ϕ) and reproduction-limited at low growth plasticity (low ϕ). (3) In contrast, if the plastic growth energy allocation constant κ is above the threshold value and the plastic asymptotic size exceeds the non-plastic asymptotic size ($\kappa > 0.857$, $f(\tilde{R})\ell_\infty > \zeta\ell_\infty$, Fig. 4.2c), the dynamics is growth-limited at low growth plasticity (low ϕ) and reproduction-limited at high growth plasticity (high ϕ). (4) Lastly, the dynamics is always reproduction-limited if the plastic energy allocation constant κ exceeds the threshold value and the non-plastic asymptotic size exceeds the plastic asymptotic size ($\kappa > 0.857$, $f(\tilde{R})\ell_\infty < \zeta\ell_\infty$, Fig. 4.2d).

With an increase or decrease of ϕ the average lifetime reproductive output increases if the growth plasticity (ϕ) approaches the boundary between growth-limited dynamics and reproduction-limited dynamics (Fig. 4.2b and c, yellow line). An increase in lifetime reproductive output with a change in ϕ implies that the lifetime reproductive output will equal 1 at a lower resource density, which hence decreases in equilibrium, while equilibrium consumer population density increases. The maximum resource density (K) needed for the consumer population to persist decreases accordingly if the growth plasticity (ϕ) approaches the boundary between the two regions (Fig. 4.2b and c, red line). In contrast, the lifetime reproductive output always increases with an increase in growth plasticity if the dynamics does not change between growth-limited dynamics and reproduction-limited dynamics. This leads to a decrease in resource density and an increase in population density at equilibrium with increasing growth plasticity. Again, the maximum resource density (K) needed for the consumer population to persist decreases accordingly (Fig. 4.2a and d, red line).

Population dynamic cycles

The bifurcation analysis revealed three parameter regions with cyclic dynamics (Fig. 4.2a and b, green lines). One of these regions occurred when the dynamics

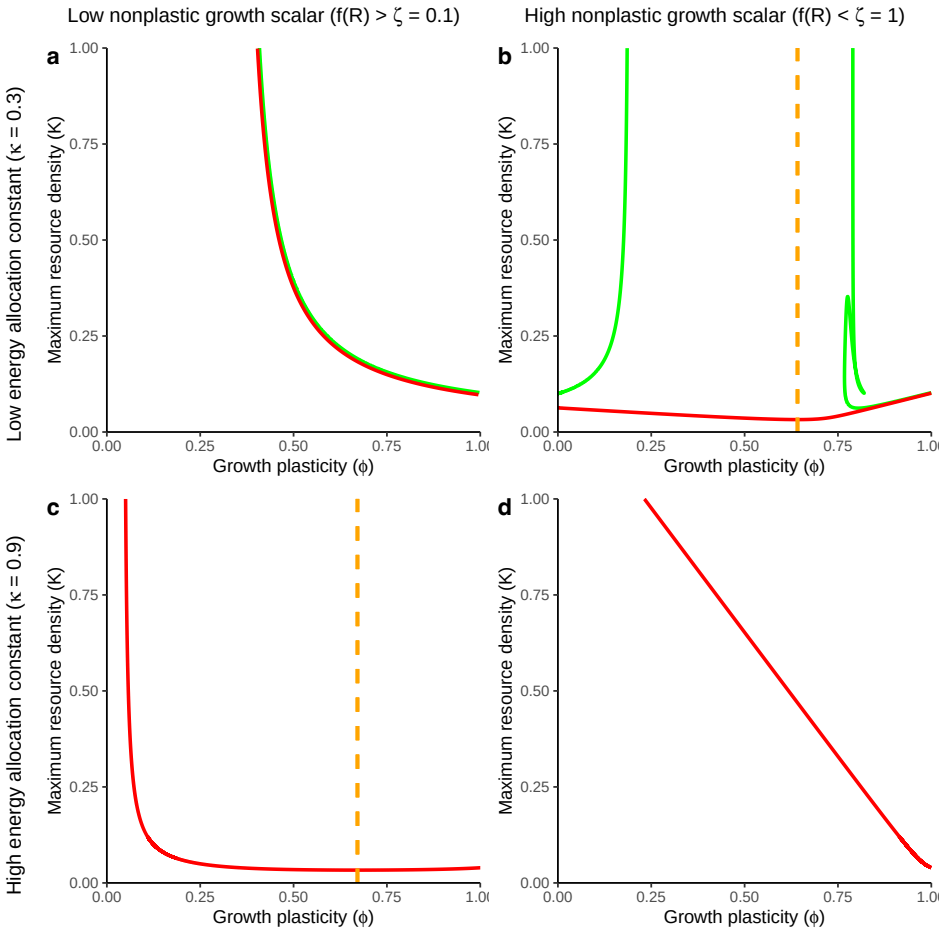

Figure 4.2: Persistence boundary (red line, numerically solved from equation (4.33)) and stability boundary (green, numerically solved from equation (4.48)) and the boundary between dynamics (yellow dashed, numerically solved from equation (4.35b)) as a function of the growth plasticity (ϕ) and the maximum resource density (K) when the plastic asymptotic size exceeds the non-plastic asymptotic size ($f(\tilde{R})\ell_\infty > \zeta\ell_\infty$) (left panels) and when the non-plastic asymptotic size exceeds the plastic asymptotic size ($\zeta\ell_\infty > f(\tilde{R})\ell_\infty$) (right panels). At the persistence boundaries (red lines), the maximum resource density is equal to the resource density in equilibrium.

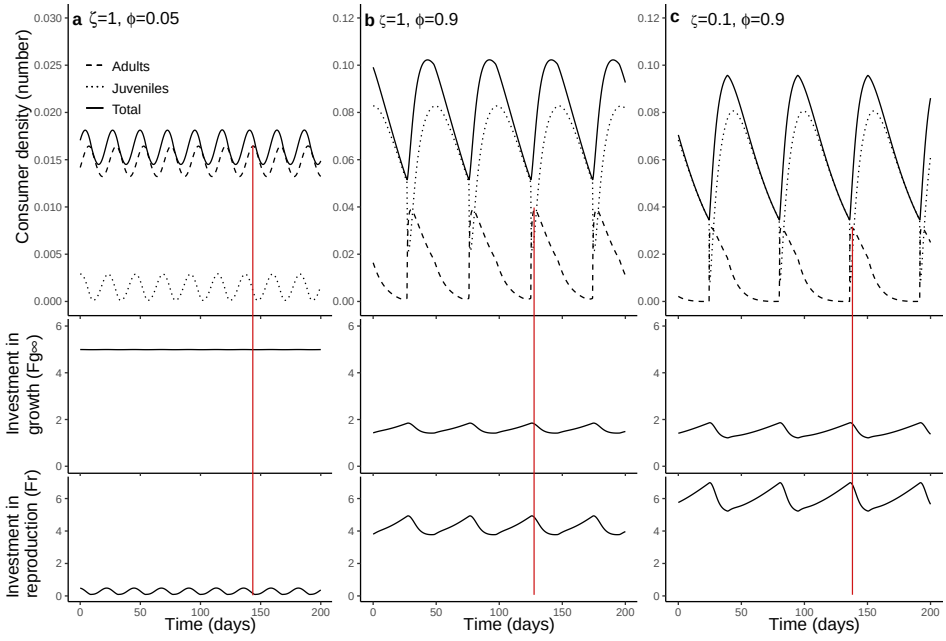

Figure 4.3: Population dynamic cycles for three combinations of ζ and ϕ with $K = 0.5$ and $\kappa = 0.3$. The surface specific total investment in growth if individuals would not die ($F_{g\infty}$) and the surface specific investment in reproduction are displaced as a measure of growth and fecundity. Note the different vertical axes for the consumer densities. The red vertical lines mark the occurrence of a peak in adult density to ease comparison between graphs.

is limited by reproduction (Fig. 4.2b, low ϕ). In these cycles (Fig. 4.3a), the area specific investment in growth ($F_{g\infty}$) and therewith the maturation rate is relatively high and constant due to the high and largely non-plastic growth rate. As a result, individuals mature at a young age and the population consists of a low number of juveniles and a high number of adults. A peak in the number of juveniles occurs simultaneously with a peak in investment in reproduction (F_r). The high density of juveniles results in a depletion of the resource, which is directly followed by a decrease in fecundity. Although individuals mature at a young age, a new large reproductive event only occurs after the consumer density has sufficiently decreased by mortality for the resource density to recover. In other words, a new cycle starts if competition between adults is reduced. As a result, the resource density and the investment in reproduction fluctuate in phase with the juvenile density but out of phase with the adult density, with a period of several times the juvenile delay. It is clear that these cycles occur due to the fluctuations in fecundity. We therefore refer to these cycles as fecundity-driven cycles.

The two other regions with cyclic dynamics occur when the dynamics is growth-limited (Fig. 4.2a and Fig. 4.2b for high ϕ). During these cycles (Fig. 4.3b and c) the area-specific investment in growth ($F_{g\infty}$) and therewith the maturation rate is very low and shows periodic increases with a large amplitude. The investment in reproduction reaches a maximum simultaneously with the maturation rate. The occurrence of the high fecundity simultaneous with the high adult density results in the production of a large cohort of juveniles. This cohort decreases the resource density, which is followed by a decrease in the fecundity and maturation rate. The juvenile cohort matures and reproduces after the consumer density has sufficiently decreased by mortality for the resource density to recover. In other words, a new cycle starts as soon as competition between juveniles is sufficiently reduced. This results in cycles dominated by a single cohort from which all individuals mature simultaneously and directly produce a new dominant cohort. Consequently, the period of the cycles is approximately equal to the juvenile delay. In addition, the periodic and simultaneous maturation of a large group of juveniles contributes to the non-symmetric shape of these cycles in comparison with the fecundity-driven cycles (Fig. 4.3). This type of cycles also occurs when the individual fecundity is assumed to be independent of the resource density (Fig. 4.4), which shows that these cycles are caused by the fluctuations in maturation rate rather than fluctuation in the fecundity. We therefore refer to this type of cycles as maturation-driven cycles.

4.5 Discussion

We analysed a model in which the individual growth rate could be varied between entirely non-plastic ($\phi = 0$) to entirely plastic ($\phi = 1$). Although the model was formulated at an individual level to ensure closed individual energy dynamics, the model was analysed at the population level. In the extreme case in which growth is entirely plastic ($\phi = 1$) the model simplified to a classic size-structured model as analysed by De Roos et al. (1990) and Kooijman and Metz (1984). It has been shown that the well-posedness of this model is difficult to show because the fecundity ($\beta(R, \ell)$) of individuals jumps from zero to a positive value at the size of maturation and the fecundity at the size at maturation ($\beta(R, \ell_J)$) is therefore undefined (Thieme, 1988). As a consequence the model is undefined if the growth rate of a cohort is exactly zero at maturation and therefore remains at the size of maturation. Although unlikely, it is difficult to predict whether this specific condition will occur based on the starting conditions. Our model has the same properties and the well-posedness of our model is therefore difficult to prove.

However, these type of models are successfully used in a wide range of applications (Baas et al., 2018; De Roos and Persson, 2001).

If growth is entirely plastic ($\phi = 1$) the individual growth rate is fully coupled to the resource density and as a consequence the age-size relationship varies per cohort if the resource density fluctuates, for example during population dynamic cycles as is observed in classic size-structured models (Fig. 4.5b). In contrast, if growth is completely non-plastic ($\phi = 0$), the model is equivalent to an age-structured model given that there is a unique relationship between age and body size. Under this extreme condition, the individual growth rate in our model only changes if the demand-driven starvation condition ($F_r < 0$) occurs, but the analysis of the model did not reveal any dynamic regimes in which individuals experienced demand-driven starvation. The growth rate is thus completely fixed if growth is non-plastic ($\phi = 0$), which results in a fixed age-size relationship even when population dynamic cycles occur (Fig. 4.5a). With the fixed age-size relationship, the model can be converted to an age-based model resembling our model with non-plastic growth. Besides linking energetic models with plastic and non-plastic growth, our model thus also connects classic age-structured models with classic size-structured models.

Our analysis divided the parameter space into a region with growth-limited and a region with reproduction-limited dynamics. In the region with growth-limited dynamics, changes in the area-specific investments in growth have a larger effect on the lifetime reproductive output than changes in the area-specific investments in reproduction. In contrast, in the region with reproduction-limited dynamics, changes in the area-specific investments in reproduction have a larger effect on lifetime reproductive output than changes in the area-specific investments in growth. At the boundary of the regions with different limiting mechanisms the consumer population exploits the resource most efficiently and can persist on the lowest resource density (Fig. 4.2). In other words, on this boundary the energy allocation to growth and reproduction is most optimal. The location of this optimum is closely related to the classic tradeoff regarding energy allocation to growth and reproduction (Stearns, 1992), in which an optimal strategy arises through avoidance of severe limitation in growth or reproduction. Although this is a very intuitive tradeoff, we tied it to the specific energy budget of individuals. Namely, an optimal energy allocation strategy can only occur if the plastic energy allocation constant is low (low κ) and the non-plastic asymptotic size exceeds the plastic asymptotic size in equilibrium ($f(\tilde{R})\ell_\infty < \zeta\ell_\infty$) or if the plastic energy allocation constant is high (high κ) and the plastic asymptotic size exceeds the non-plastic asymptotic size in equilibrium ($f(\tilde{R})\ell_\infty > \zeta\ell_\infty$). Hence, an optimal energy allocation

can only occur when energy is relatively evenly distributed between growth and reproduction to avoid severe limitation through growth and reproduction. As a consequence, evolution cannot always reach an optimal energy allocation scheme if evolution only acts on growth plasticity.

The parameter regions in which the dynamics is limited by growth or reproduction show different kinds of population dynamics cycles. In the region with growth-limited dynamics, the cycles are caused by fluctuations in maturation, which is caused by fluctuations in growth rate. These maturation-driven cycles occur because a cohort of newborn individuals outcompetes the adult individuals. This results in single cohort cycles, which are characterized by the synchronization of a high resource density with the maturation of the dominant cohort. The oscillation period of these cycles is approximately equal to the juvenile delay (De Roos et al., 2003). Single cohort cycles generally occur in models incorporating a juvenile delay and, based on the oscillation period, are mainly observed in generalist species (Murdoch et al., 2002). The type of single cohort cycles found in our model is described in more detail by De Roos et al. (2003) as juvenile-driven cycles, which occur if juvenile individuals outcompete adults because they can survive on a lower resource density. The mechanism for these juvenile-driven cohort cycles is observed in various fish species (Townsend et al., 1990; Hamrin and Persson, 1986; Townsend and Perrow, 1989) and experimental *Daphnia* populations (Murdoch and McCauley, 1985; McCauley, 1993).

In the parameter region with reproduction-limited dynamics, the cycles are caused by fluctuations in average fecundity. These fecundity-driven cycles are characterized by low amplitude oscillations with a period of more than four times the juvenile delay of the consumer. In addition, the total consumer density lacks behind the resource density. These characteristics occur because a dominant cohort of newborn individuals depletes the resource, which causes fecundity to decrease. The dominant cohort of juveniles matures before the resource density is recovered, delaying their main reproductive event until the resource density is recovered, which is far beyond the age at maturation. The fecundity-driven cycles thus differ from the reproduction driven cycles in that competition relaxes after instead of before the maturation of a dominant cohort.

The fecundity-driven cycles in our model show resemblances with various previously described types of cycles. The oscillation period of the fecundity-driven cycles is more than four times the juvenile delay of the consumer plus two times the juvenile delay of the resource, which is generally considered indicative of consumer-resource cycles (Murdoch et al., 2002). The fecundity-driven cycles indeed show an increase in resource density leading to an increase in consumer reproduction as is

found in classic non-structured models with consumer-resource cycles (Rosenzweig and MacArthur, 1963). In classic consumer-resource cycles this occurs because the resource periodically escapes the control of the consumer, which, however, cannot occur in our model, because in our model the resource follows semi-chemostat dynamics (De Roos et al., 1990). Instead, the increase in resource density in the fecundity-driven cycles is due to a relaxation of competition between consumers and are therefore different from classic consumer-resource cycles. The fecundity-driven cycles also show some resemblances with delayed-feedback cycles. One could argue that the depletion of the resource by a dominant cohort has a delayed effect, because it only affects the dominant cohort after maturation. Pfaff et al. (2014) suggested that delayed-feedback cycles can have a period of more than 4 times the juvenile delay and arise if the juvenile delay is decoupled from the resource density, which exactly occurs in the fecundity-driven cycles we found. Nonetheless, the fecundity-driven cycles do not correspond to the original description of delayed-feedback cycles from Gurney et al. (1983), because the depletion of the resource in the fecundity-driven cycles also has a direct effect on the consumer population, while Gurney et al. (1983) describe a complete separation of time between the moment of competition and the effect of competition. These resemblances between the fecundity-driven cycles, consumer-resource cycles and delayed feedback cycles at least show that very detailed knowledge is needed to disentangle different types of cycles in structured populations (Hastings, 2020).

In this article we presented a model in which we varied the plasticity in individual growth. More plastic growth is generally expected in ectotherms because the growth rate in these individuals is highly dependent on the environment, while less plastic growth is generally expected in endotherms because in these individuals, growth is generally independent of the environment. Including a non-plastic growth rate results in an additional demand-driven process in the energy allocation scheme of individuals. We assumed that a potential deficit or surplus of energy from demand-driven growth is compensated by a change in energy allocation to reproduction. Another strategy to cover a deficit in ingested energy could be to increase energy ingestion by adaptive behaviour (Kooijman, 2010). Although this strategy might weaken the tradeoff between growth and reproduction, it is unlikely that adaptive behaviour could account for the entire deficit when individuals live in a natural ecosystem, as sufficient resources should be available to increase the consumption by adaptive behaviour. In our model, the resource density is regulated by competition between consumers. Therefore, an increase in consumption due to adaptive behaviour would lead to an increase in competition and a decrease in resource density which also could enlarge the energy deficit. Even if

sufficient resource is available, ingested energy is limited by physiological and time constraints which are implemented in our model by using a type II functional response to model energy ingestion. It is therefore unlikely that adaptive behaviour can account for the full energy deficit caused by non-plastic growth and a tradeoff between energy allocation to growth and reproduction occurs.

We showed that the tradeoff between energy investment in growth and reproduction results in population dynamics regulated by respectively maturation or fecundity. Populations limited by maturation and the corresponding cohort cycles are widely explored in the context of ecological communities (De Roos et al., 2007, 2008; Persson et al., 2007; Van Leeuwen et al., 2008; Van Kooten et al., 2007), while the dynamics of populations limited by fecundity are less studied in structured populations (see De Roos et al. (2009) for an example) and is an open topic. In any case our model analysis revealed how life history strategies of species in terms of energy allocation and plasticity affect the mechanisms which limit the population and determine the type of population dynamic cycles. In this way we provide a new step in linking distinct ecological phenomena such as non-plastic growth and plastic growth, age and stage structure and populations limitation by individual growth and fecundity.

4.6 Supplementary materials

From energy flow to growth dynamics

Here we outline the calculations to transform the model in terms of individual energy dynamics into a size-based population model. We define the composite parameters ℓ_∞, r_B and r_F representing the asymptotic length of an individual, the Von Bertalanffy growth rate in length and the reproduction rate proportionally constant of an individual.

$$\ell_\infty = \frac{\kappa\alpha}{b d_m^{1/3} d_v^{1/3} \delta_m} \tag{4.22a}$$

$$r_B = \frac{b y_m}{3} \tag{4.22b}$$

$$r_F = \frac{b y_r}{\ell_b^3} \tag{4.22c}$$

Starvation boundaries

We start with reformulating the starvation boundaries (eq. 4.7 - 4.9), which also results in the equations for the area-specific energy surplus (or deficit) available

for growth (F_g), reproduction (F_r) and total biomass production (F_t). This is done by replacing the energy in lean mass (E_m) with the equivalent in terms of size ($d_m d_v (\delta_m \ell)^3$, eq. 4.14) after which we simplify the equation and substitute the composite parameters. For severe starvation conditions (eq. 4.7) this results in:

$$\begin{aligned} bE_m &> \alpha f(R) E_m^{2/3} \\ bd_m d_v (\delta_m \ell)^3 &> \alpha f(R) d_m^{2/3} d_v^{2/3} (\delta_m \ell)^2 \\ \ell &> \frac{f(R)}{\kappa} \frac{\kappa \alpha}{b d_m^{1/3} d_v^{1/3} \delta_m} \quad \Rightarrow \\ 0 &> \frac{f(R)}{\kappa} \ell_\infty - \ell = F_t(R, \ell) \end{aligned} \tag{4.23}$$

We can do the same for the supply-driven starvation condition (eq. 4.8):

$$\begin{aligned} bE_m &> \phi\kappa\alpha f(R) E_m^{2/3} + (1-\phi)\kappa\alpha\zeta E_m^{2/3} \\ bd_m d_v (\delta_m \ell)^3 &> \phi\kappa\alpha f(R) d_m^{2/3} d_v^{2/3} (\delta_m \ell)^2 + (1-\phi)\kappa\alpha\zeta d_m^{2/3} d_v^{2/3} (\delta_m \ell)^2 \\ \ell &> (\phi f(R) + (1-\phi)\zeta) \frac{\kappa \alpha}{b d_m^{1/3} d_v^{1/3} \delta_m} \quad \Rightarrow \\ 0 &> (\phi f(R) + (1-\phi)\zeta) \ell_\infty - \ell = F_g(R, \ell) \end{aligned} \tag{4.24}$$

The demand-driven starvation condition (eq. 4.9) is not dependent on the energy stored in lean mass, so we only have to simplify this condition:

$$\begin{aligned} \phi\kappa\alpha f(R) E_m^{2/3} + (1-\phi)\kappa\zeta E_m^{2/3} &> \alpha f(R) E_m^{2/3} \\ \phi\kappa f(R) + (1-\phi)\kappa\zeta &> f(R) \quad \Rightarrow \\ 0 &> \phi \frac{(1-\kappa)}{\kappa} f(R) + (1-\phi) \left(\frac{f(R)}{\kappa} - \zeta \right) = F_r(R) \end{aligned} \tag{4.25}$$

Growth rate

To derive the differential equation for the length of an individual, we have to rewrite the differential equation for the energy stored in lean mass, in terms of length.

$$\frac{d\ell}{dt} = \frac{d}{dt} \frac{E_m^{1/3}}{d_m^{1/3} d_v^{1/3} \delta_m} = \frac{1}{3 d_m^{1/3} d_v^{1/3} \delta_m E_m^{2/3}} \frac{dE_m}{dt} \tag{4.26}$$

We can now substitute the differential equation for the energy in lean mass under normal growth conditions (eq. 4.5) to derive the differential equation for growth

in length under growth conditions:

$$\begin{aligned}\frac{d\ell}{dt} &= \frac{\gamma_m}{3d_m^{1/3}d_v^{1/3}\delta_m E_m^{2/3}}\left(\phi\kappa\alpha f(R)E_m^{2/3} + (1-\phi)\kappa\alpha\zeta E_m^{2/3} - bE_m\right) \\ &= \frac{b\gamma_m}{3}\left(\left(\phi f(R) + (1-\phi)\zeta\right)\frac{\kappa\alpha}{bd_m^{1/3}d_v^{1/3}\delta_m} - \frac{E_m^{1/3}}{d_m^{1/3}d_v^{1/3}\delta_m}\right) \\ &= r_B\left(\left(\phi f(R) + (1-\phi)\zeta\right)\ell_\infty - \ell\right) \\ &= r_B F_g(R,\ell)\end{aligned} \tag{4.27}$$

In the same way we can rewrite the differential equation for energy in lean mass (eq. 4.11) under demand-driven starvation conditions:

$$\begin{aligned}\frac{d\ell}{dt} &= \frac{\gamma_m}{3d_m^{1/3}d_v^{1/3}\delta_m E_m^{2/3}}\left(\alpha f(R)E_m^{2/3} - bE_m\right) \\ &= \frac{b\gamma_m}{3}\left(\frac{\kappa\alpha}{\kappa bd_m^{1/3}d_v^{1/3}\delta_m}f(R) - \frac{E_m^{1/3}}{d_m^{1/3}d_v^{1/3}\delta_m}\right) \\ &= r_B\left(\frac{f(R)}{\kappa}\ell_\infty - \ell\right) \\ &= r_B F_t(R,\ell)\end{aligned} \tag{4.28}$$

Fecundity

To derive the fecundity in terms of number of individuals ($\beta(R,\ell)$), we have to divide the energy investment in reproduction ($\frac{dE_r}{dt}$) by the energy in lean mass of a newborn individual ($E_b = d_m d_v(\delta_m\ell_b)^3$). Under normal growth conditions (eq. 4.6), this results in:

$$\begin{aligned}\beta(R,\ell) &= \frac{\gamma_r}{E_b}\left(\alpha f(R)E_m^{2/3} - \left(\phi\kappa\alpha f(R)E_m^{2/3} + (1-\phi)\kappa\alpha\zeta E_m^{2/3}\right)\right) \\ &= \frac{\gamma_r}{d_m d_v(\delta_m\ell_b)^3}\left(\alpha f(R) - (\phi\kappa\alpha f(R) + (1-\phi)\kappa\alpha\zeta)\right)d_m^{2/3}d_v^{2/3}(\delta_m\ell)^2 \\ &= \frac{b\gamma_r}{\kappa\ell_b^3}\left(f(R) - (\phi\kappa f(R) + (1-\phi)\kappa\zeta)\right)\frac{\kappa\alpha}{bd_m^{1/3}d_v^{1/3}\delta_m}\ell^2 \\ &= \frac{r_F}{\kappa}\left(\phi(1-\kappa)f(R) + (1-\phi)\left(f(R) - \kappa\zeta\right)\right)\ell_\infty\ell^2 \\ &= r_F F_r(R)\ell^2\end{aligned} \tag{4.29}$$

We can use the same steps to derive the fecundity under supply-driven starvation conditions from equation (4.10).

$$\begin{aligned}
\beta(R,\ell) &= \frac{\gamma_r}{E_b}\left(\alpha f(R) E_m^{2/3} - bE_m\right) \\
&= \frac{\gamma_r}{d_m d_v (\delta_m \ell_b)^3}\left(\alpha f(R) d_m^{2/3} d_v^{2/3} (\delta_m \ell)^2 - b d_m d_v (\delta_m \ell)^3\right) \\
&= \frac{b\gamma_r}{\ell_b^3}\left(\frac{f(R)}{\kappa}\frac{\kappa\alpha}{b d_m^{1/3} d_v^{1/3} \delta_m} - \ell\right)\ell^2 \\
&= r_F\left(\frac{f(R)}{\kappa}\ell_\infty - \ell\right)\ell^2 \\
&= r_F F_t(R,\ell)\ell^2
\end{aligned} \tag{4.30}$$

Starvation mortality

Lastly we reformulate the equations for the starvation mortality in terms of length instead of energy stored in lean mass. For the supply-driven starvation mortality (eq. 4.12) this becomes:

$$\begin{aligned}
\mu_s(R,\ell) &= q_s \frac{bE_m - \left(\phi\kappa\alpha f(R) E_m^{2/3} + (1-\phi)\kappa\alpha\zeta E_m^{2/3}\right)}{\alpha f(R) E_m^{2/3} - bE_m} \\
&= q_s \frac{b d_m d_v (\delta_m \ell)^3 - \left(\phi\kappa\alpha f(R) + (1-\phi)\kappa\alpha\zeta\right) d_m^{2/3} d_v^{2/3} (\delta_m \ell)^2}{\alpha f(R) d_m^{2/3} d_v^{2/3} (\delta_m \ell)^2 - b d_m d_v (\delta_m \ell)^3} \\
&= q_s \frac{\ell - \left(\phi f(R) + (1-\phi)\zeta\right)\frac{\kappa\alpha}{b d_m^{1/3} d_v^{1/3} \delta_m}}{\frac{f(R)}{\kappa}\frac{\kappa\alpha}{b d_m^{1/3} d_v^{1/3} \delta_m} - \ell} \\
&= -q_s \kappa \frac{\left(\phi f(R) + (1-\phi)\zeta\right)\ell_\infty - \ell}{f(R)\ell_\infty - \kappa\ell} \\
&= -q_s \frac{F_g(R,\ell)}{F_t(R,\ell)}
\end{aligned} \tag{4.31}$$

We can do the same for the demand-driven starvation mortality (eq. 4.13):

$$\begin{aligned}\mu_s(R,\ell) &= q_s \frac{\left(\phi\kappa\alpha f(R)E_m^{2/3} + (1-\phi)\alpha\kappa\zeta E_m^{2/3} - \alpha f(R)E_m^{2/3}\right)}{\alpha f(R)E_m^{2/3} - bE_m} \\ &= q_s \frac{\left(\phi\kappa\alpha f(R) + (1-\phi)\alpha\kappa\zeta - \alpha f(R)\right) d_m^{2/3} d_v^{2/3} (\delta_m \ell)^2}{\alpha f(R) d_m^{2/3} d_v^{2/3} (\delta_m \ell)^2 - d_m d_v (\delta_m \ell)^3} \\ &= q_s \frac{\left(\phi f(R) + (1-\phi)\zeta - \frac{f(R)}{\kappa}\right) \frac{\kappa\alpha}{b d_m^{1/3} d_v^{1/3} \delta_m} \ell^2}{\frac{f(R)}{\kappa} \frac{\kappa\alpha}{b d_m^{1/3} d_v^{1/3} \delta_m} \ell^2 - \ell^3} \\ &= -q_s \frac{\left(\phi(1-\kappa) f(R) + (1-\phi)(f(R) - \kappa\zeta)\right) \ell_\infty}{f(R)\ell_\infty - \kappa\ell} \\ &= -q_s \frac{F_r(R)}{F_t(R,\ell)}\end{aligned} \tag{4.32}$$

Mathematical analysis

Persistence boundary

From equation (4.19) it follows that the resource density at the extinction boundary of the population ($\tilde{n}(0) = 0$) is equal to the maximum resource density ($\tilde{R} = K$). The existence boundary can therefore be found by setting the lifetime reproductive output (eq. 4.18) equal to one with $\tilde{R} = K$:

$$\frac{r_F}{\kappa} \left(\phi(1-\kappa) f(K) + (1-\phi)\left(f(K) - \zeta\kappa\right)\right) \ell_\infty \int_{\tilde{a_J}}^{a_{max}} \ell(K,a)^2 e^{-\mu a} da = 1 \tag{4.33}$$

Boundary between growth- and reproduction-limited dynamics

In the main text we distinguished growth-limited dynamics in which the effects through energy investments in growth exceed the effects through energy investments in reproduction ($\frac{\partial LRO}{\partial F_{g\infty}} > \frac{\partial LRO}{\partial F_r}$) and reproduction-limited dynamics in which the effects through energy investments in reproduction exceed the effects though energy investments in growth ($\frac{\partial LRO}{\partial F_{g\infty}} < \frac{\partial LRO}{\partial F_r}$). Given a constant resource density $\bar{R}$ we can obtain an explicit expression for the derivative of the lifetime reproductive output with respect to the lifetime energy investments in growth and

the energy investments in reproduction:

$$\frac{\partial LRO}{\partial F_r} = r_F \int_{a_J}^{a_{max}} \ell(\bar{R},a)^2 e^{-\mu a} da \tag{4.34a}$$

$$\frac{\partial LRO}{\partial F_{g\infty}} = r_F F_r(\bar{R}) \left(\int_{a_J}^{a_{max}} 2\ell(\bar{R},a) \left(1 - e^{-r_B a}\right) e^{-\mu a} da - \frac{\partial a_J}{\partial F_{g\infty}} \ell_J^2 e^{-\mu a_J} \right) \tag{4.34b}$$

$$\frac{\partial a_J}{\partial F_{g\infty}} = - \frac{(\ell_J - \ell_b)}{r_B \left(\left(\phi f(\bar{R}) + (1-\phi)\zeta\right)\ell_\infty - \ell_b\right)\left(\left(\phi f(\bar{R}) + (1-\phi)\zeta\right)\ell_\infty - \ell_J\right)}$$

The boundary between the regions with growth- and reproduction-limited dynamics occurs if the derivative of the lifetime reproductive output with respect to the energy investment in growth equals the derivative of the energy investment in reproduction.

$$\begin{aligned} 0 =& \frac{\partial LRO}{\partial F_{g\infty}} - \frac{\partial LRO}{\partial F_r} \qquad (4.35a)\\ =& F_r(\bar{R}) \int_{a_J}^{a_{max}} 2\ell(\bar{R},a) \left(1 - e^{-r_B a}\right) e^{-\mu a} da - \int_{a_J}^{a_{max}} \ell(\bar{R},a)^2 e^{-\mu a} da \\ & - F_r(\bar{R}) \frac{\partial a_J}{\partial F_{g\infty}} \ell_J^2 e^{-\mu a_J} \\ =& \int_{a_J}^{a_{max}} \left[2F_r(\bar{R}) \left(1 - e^{-r_B a}\right) \ell_\infty - \ell(\bar{R},a)\right] \ell(\bar{R},a) e^{-\mu a} da \qquad (4.35b)\\ & - F_r(\bar{R}) \frac{\partial a_J}{\partial F_{g\infty}} \ell_J^2 e^{-\mu a_J} \end{aligned}$$

In the extreme case in which the size at birth is zero and individuals mature directly at birth ($\ell_J = \ell_b = 0$), the age at maturation does not affect the lifetime reproductive output and equation (4.36) becomes zero if the term between squared brackets becomes zero. We can rewrite this term as:

$$\begin{aligned} &\left[2F_r(\bar{R}) \left(1 - e^{-r_B a}\right) \ell_\infty - \ell(\bar{R},a)\right] = \qquad (4.36)\\ &\quad \left(2\frac{f(\bar{R})}{\kappa} - 3\zeta - 3\left(f(\bar{R}) - \zeta\right)\phi\right) \left(1 - e^{-r_B a}\right) \ell_\infty - \ell_b e^{-r_B a} \end{aligned}$$

If we then simplify the equation further and assume that the size at birth equals zero ($\ell_b = 0$), we can obtain the following solution:

$$2\frac{f(\bar{R})}{\kappa} - 3\zeta - 3\left(f(\bar{R}) - \zeta\right)\phi = 0 \tag{4.37}$$

or

$$\kappa = \frac{2f(\bar{R})}{3\left(\phi f(\bar{R}) + (1-\phi)\zeta\right)} \tag{4.38}$$

If growth is entirely plastic ($\phi = 1$) this equality is satisfied if the plastic energy allocation constant (κ) equals two-thirds. If the functional response exceeds the non-plastic growth scalar ($f(\bar{R}) > \zeta$), the plastic energy allocation constant (κ) at which equality (4.37) is satisfied increases with decreasing growth plasticity (ϕ). In contrast, if the non-plastic growth scalar exceeds the functional response ($f(\bar{R}) < \zeta$), the plastic energy allocation constant (κ) at which equation (4.37) is satisfied decreases with decreasing growth plasticity (ϕ). In other words, $\kappa = 2/3$ represents a threshold value. If the plastic energy allocation constant (κ) is below this threshold value, the boundary between the growth-limited dynamics and the reproduction-limited dynamics occurs if the non-plastic growth scalar exceeds the functional response ($f(\bar{R}) > \zeta$). If the plastic energy allocation constant (κ) is above the threshold value, the boundary between the growth-limited dynamics and the reproduction-limited dynamics occurs if the functional response exceeds the non-plastic growth scalar ($f(\bar{R}) > \zeta$).

From equation (4.36) it is clear that a positive size at birth ($\ell_J = \ell_b > 0$) introduces an additional negative term. The introduction of this negative term decreases the threshold value of κ. From equation (4.35b) it is clear that the introduction of a size at maturation above the size at birth ($\ell_J > \ell_b > 0$) includes an additional positive term. The introduction of this positive term would increase the threshold value of κ.

Stability analysis

The stability boundaries can be found by linearization and substitution of exponential trial solutions, following De Roos et al. (1990). We first define a small perturbation in the equilibrium state of the resource, the age distribution and the individual size (ϵ_R, ϵ_n, ϵ_ℓ):

$$\epsilon_R(t) = R(t) - \tilde{R} \tag{4.39a}$$

$$\epsilon_n(t,a) = n(t,a) - \tilde{n}(a) \tag{4.39b}$$

$$\epsilon_\ell(t,a) = \ell(t,a) - \ell(\tilde{R},a) \tag{4.39c}$$

As long as these perturbations are sufficiently small, starvation conditions will not occur and the system can be described by equations which are differentiable within

their domain of definition.

$$I(R,\ell) = I_{max} f(R) \ell^2 \qquad (4.40a)$$
$$\text{for } \ell_b \leq \ell \leq (\phi f(R) + (1-\phi)\zeta)\, \ell_\infty$$
$$g(R,\ell) = r_B \left((\phi f(R) + (1-\phi)\zeta)\, \ell_\infty - \ell \right) \qquad (4.40b)$$
$$\text{for } \ell_b \leq \ell \leq (\phi f(R) + (1-\phi)\zeta)\, \ell_\infty$$
$$b(R,\ell) = \frac{r_F}{\kappa} \left(\phi(1-\kappa) f(R) + (1-\phi) \left(f(R) - \kappa\zeta \right) \right) \ell_\infty \ell^2 \qquad (4.40c)$$
$$\text{for } \ell_b \leq \ell \leq (\phi f(R) + (1-\phi)\zeta)\, \ell_\infty$$
$$d(R,\ell) = \mu_b \qquad \text{for } 0 \leq a \leq a_{max} \qquad (4.40d)$$

The perturbation in the age at maturation (ϵ_a), can be expressed in terms of the perturbation in length as shown by De Roos et al. (1990).

$$\epsilon_a(t) = \frac{-\epsilon_\ell(t, \tilde{a_J})}{g(\tilde{R}, \ell_J)} \qquad (4.41)$$

We can substitute the perturbations in the partial differential equations to formulate a linearized system of equations in which we neglect all second and higher order terms:

$$\frac{\delta \epsilon_n}{\delta t} + \frac{\delta \epsilon_n}{\delta t} = -\mu_b \epsilon_n \qquad (4.42a)$$
$$\epsilon_n(t,0) = \int_{\tilde{a_J}}^{a_{max}} \left(b(\tilde{R}, \ell(\tilde{R},a)) \epsilon_n(t,a) + b_R(\tilde{R}, \ell(\tilde{R},a)) \tilde{n}(a) \epsilon_R(t) \right. \qquad (4.42b)$$
$$\left. + b_\ell(\tilde{R}, \ell(\tilde{R},a)) \tilde{n}(a) \epsilon_\ell(t,a) da \right) - b(\tilde{R}, \ell_J) \tilde{n}(\tilde{a_J}) \epsilon_a(t)$$
$$\frac{\delta \epsilon_\ell}{\delta t} + \frac{\delta \epsilon_\ell}{\delta t} = g_R(\tilde{R}, \ell(\tilde{R},a)) \epsilon_R + g_\ell(\tilde{R}, \ell(\tilde{R},a)) \epsilon_\ell \qquad (4.42c)$$
$$\epsilon_\ell(t,0) = 0 \qquad (4.42d)$$
$$\frac{d\epsilon_R}{dt} = -\nu \epsilon_R - \int_0^{a_{max}} \left(I(\tilde{R}, \ell(\tilde{R},a)) \epsilon_n(t,a) + I_R(\tilde{R}, \ell(\tilde{R},a)) \tilde{n}(a) \epsilon_R(t) \right. \qquad (4.42e)$$
$$\left. + I_\ell(\tilde{R}, \ell(\tilde{R},a)) \tilde{n}(a) \epsilon_\ell(t,a) \right) da$$

In which the functions g_R, g_ℓ, b_R, b_ℓ, I_R and I_ℓ indicate the partial derivatives of the functions $g(R,\ell)$, $b(R,\ell)$ and $I(R,\ell)$, with respect to R and ℓ respectively.

The following step is to substitute exponential trial solutions:

$$\epsilon_R(t) = \Delta_R e^{\lambda t} \tag{4.43a}$$
$$\epsilon_n(t,a) = \Delta_n(a) e^{\lambda t} \tag{4.43b}$$
$$\epsilon_\ell(t,a) = \Delta_\ell(a) e^{\lambda t} \tag{4.43c}$$
$$\epsilon_a = \Delta_a e^{\lambda t} \tag{4.43d}$$

into the linearized system, leading to:

$$\frac{\partial \Delta_n}{\partial a} = -(\mu_b + \lambda)\Delta_n \tag{4.44a}$$
$$\Delta_n(0) = \int_{\tilde{a_J}}^{a_{max}} \big(b(\tilde{R},\ell(\tilde{R},a))\Delta_n(a) + b_R(\tilde{R},\ell(\tilde{R},a))\tilde{n}(a)\Delta_R + b_\ell(\tilde{R},\ell(\tilde{R},a))\tilde{n}(a)\Delta_\ell(a)\big)\,da - b(\tilde{R},\ell_J)\tilde{n}(\tilde{a_J})\Delta_a \tag{4.44b}$$
$$\frac{\partial \Delta_\ell}{\partial a} = g_R(\tilde{R},\ell(\tilde{R},a))\Delta_R + g_\ell(\tilde{R},\ell(\tilde{R},a))\Delta_\ell - \lambda\Delta_\ell \tag{4.44c}$$
$$\Delta_\ell(0) = 0 \tag{4.44d}$$
$$\lambda\Delta_R = -\nu\Delta_R - \int_0^{a_{max}} \big(I(\tilde{R},\ell(\tilde{R},a))\Delta_n + I_R(\tilde{R},\ell(\tilde{R},a))\tilde{n}(a)\Delta_R + I_\ell(\tilde{R},\ell(\tilde{R},a))\tilde{n}(a)\Delta_\ell(a)\big)\,da \tag{4.44e}$$

We now need to derive the explicit derivatives of the ingestion, growth and reproduction functions with respect to the resource and the size:

$$I_R(R,\ell) = I_{max} f'(R)\ell^2 \tag{4.45a}$$
$$g_R(R,\ell) = r_B \phi f'(R)\ell_\infty \tag{4.45b}$$
$$b_R(R,\ell) = r_F(1-\kappa\phi)\frac{f'(R)}{\kappa}\ell_\infty\ell^2 \tag{4.45c}$$
$$I_\ell(R,\ell) = 2I_{max} f(R)\ell \tag{4.45d}$$
$$g_\ell(R,\ell) = -r_B \tag{4.45e}$$
$$b_\ell(R,\ell) = 2r_F\left(\phi\frac{1-\kappa}{\kappa}f(R) + (1-\phi)\frac{f(R)-\kappa\zeta}{\kappa}\right)\ell_\infty\ell \tag{4.45f}$$

In which $f'(R)$ is the derivative of the functional response with respect to the resource density R.

We can solve for $\Delta_n(a)$ and $\Delta_\ell(a)$ explicitly and all quantities can be expressed

in terms of Δ_R and Δ_b which we write instead of $\Delta_n(0)$.

$$\Delta_n(a) = \Delta_b e^{-\mu_b a} e^{-\lambda a} \tag{4.46a}$$

$$\Delta_\ell(a) = \frac{r_B \phi f'(\tilde{R}) \ell_\infty}{r_B + \lambda} \left(1 - e^{-(r_B+\lambda)a}\right) \Delta_R \tag{4.46b}$$

$$\Delta_a = \frac{-\Delta_\ell(t, \tilde{a_J})}{g(\tilde{R}, \ell_J)} = -\frac{\phi f'(\tilde{R}) \ell_\infty}{\left(\phi f(\tilde{R}) + (1-\phi)\zeta\right) \ell_\infty - \ell_J} \frac{1 - e^{-(r_B+\lambda)\tilde{a_J}}}{r_B + \lambda} \Delta_R \tag{4.46c}$$

From this we directly arrive at the stability matrix:

$$S(\lambda)\Delta = \begin{pmatrix} s_{11} & s_{s12} \\ s_{21} & s_{22} \end{pmatrix} \begin{pmatrix} \Delta_b \\ \Delta_R \end{pmatrix} \tag{4.47}$$

With elements:

$$\begin{aligned}
s_{11} &= b_c(\tilde{R}) \frac{\bar{A}_s(\lambda, \tilde{a_J})}{\tilde{n}(0)} - 1 \\
s_{12} &= \frac{r_F}{\kappa}(1 - \kappa\phi) f'(\tilde{R}) \ell_\infty \bar{A}_s(0, \tilde{a_J}) \\
&\quad + b_c(\tilde{R}) \frac{\phi}{r_B + \lambda} f'(\tilde{R}) \ell_\infty \left(\frac{\left(1 - e^{-(r_B+\lambda)\tilde{a_J}}\right) \ell_J^2 e^{-\mu_b \tilde{a_J}}}{\left(\left(\phi f(\tilde{R}) + (1-\phi)\zeta\right) \ell_\infty - \ell_J\right)} + 2 r_B \bar{A}_\ell(\tilde{a_J}) \right) \\
s_{21} &= -I_R f(\tilde{R}) \frac{\bar{A}_s(\lambda, 0)}{\tilde{n}(0)} \\
s_{22} &= -\nu - \lambda - I_R f'(\tilde{R}) \left(\bar{A}_s(0,0) + 2 \frac{r_B \phi}{r_B + \lambda} f(R) \ell_\infty \bar{A}_\ell(0) \right)
\end{aligned}$$

With:

$$\begin{aligned}
b_c(\tilde{R}) &= \frac{r_F}{\kappa} \left(\phi(1-\kappa) f(\tilde{R}) + (1-\phi)\left(f(\tilde{R}) - \kappa\zeta\right)\right) \ell_\infty, \\
\bar{A}_s(s, a_{min}) &= \int_{a_{min}}^{a_{max}} \tilde{n}(0) \ell(\tilde{R}, a)^2 e^{-(\mu_b + s)a} da, \\
\bar{A}_\ell(a_{min}) &= \int_{a_{min}}^{a_{max}} \tilde{n}(0) \left(1 - e^{-(r_B+\lambda)a}\right) \ell(\tilde{R}, a) e^{-\mu_b a} da
\end{aligned}$$

In which $f'(\tilde{R})$ represents the derivative of the type II functional response with respect to the resource density in equilibrium. The eigenvalues of the system are now the roots of

$$\det(S(\lambda)) = 0 \tag{4.48}$$

Supplementary figures

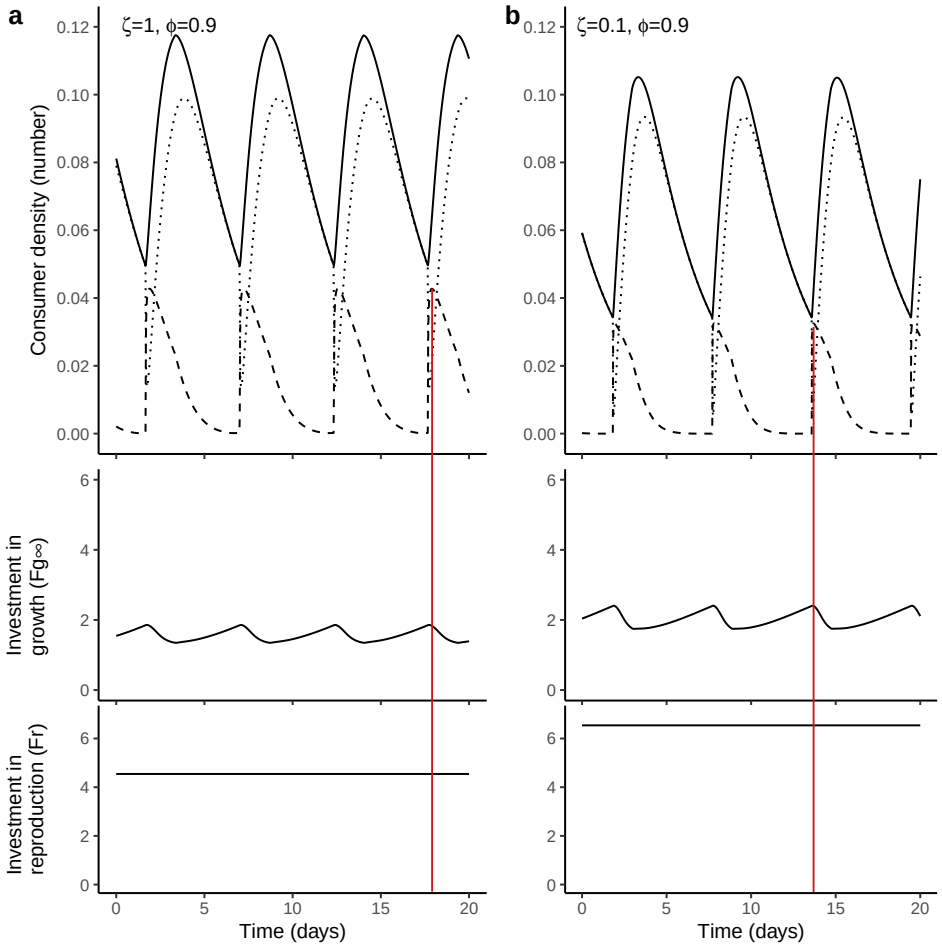

Figure 4.4: Population dynamic cycles with a resource independent fecundity. The fecundity is made independent by substituting the resource density in the function of the individual fecundity with the equilibrium resource density ($\beta(\tilde{R}, \ell(t, a))$). The cycles are the same as the cycles represented in figure 4.3b and c. This shows that this type of cycles is not caused by fluctuations in the individual fecundity. Note the different vertical axis for the consumer densities.

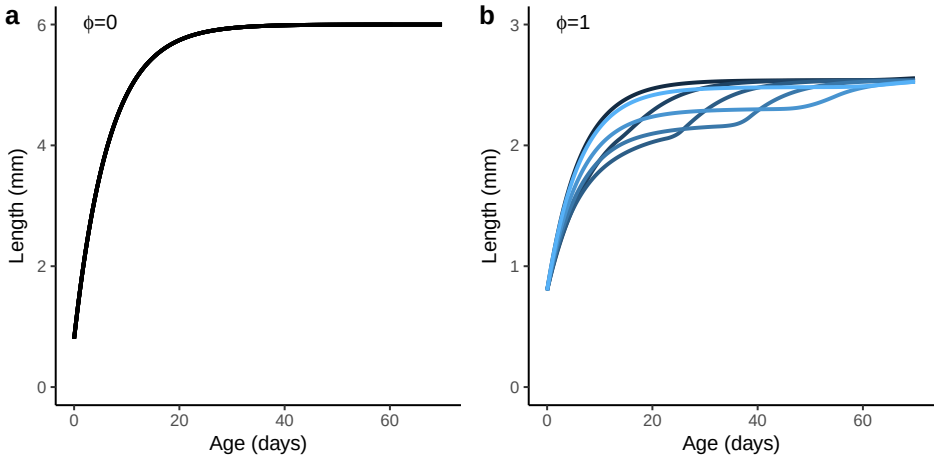

Figure 4.5: Age-size relationships at different times during population cycles if growth is non-plastic (a) or entirely plastic (b). The graphs are constructed with $K = 0.5$, $\zeta = 1$ and $\kappa = 0.3$. Differently coloured lines occur at different moments during the simulation. All age-size curves for non-plastic growth (a) do overlap. Also note the different scaling of the vertical axes.

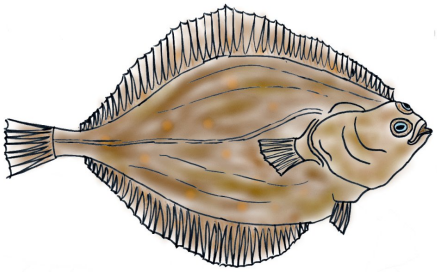

Chapter 5

The evolution of growth curve plasticity in size-structured populations

Jasper C. Croll
Tobias van Kooten
André M. de Roos

To be resubmitted

Abstract

Growth in individual body size among different species can to a greater or lesser extent depend on environmental factors such as resource availability. Individual growth curves can therefore be largely fixed or more plastic. Classic theory about phenotypic plasticity assumes that such plasticity has associated costs. In contrast, according to dynamic energy budget theory, maintaining a fixed growth rate in the face of variable resource availability would incur additional energetic costs. In this article we explore the simultaneous evolution of the degree of plasticity in individual growth curves and the rate of non-plastic, environment-independent individual growth. We explore different relations between possible additional energetic costs and the degree of growth curve plasticity. To do so, we use adaptive dynamics to analyse a size-structured population model that is based on dynamic energy budget theory to account for the energetic trade-offs within an individual. We show that simultaneous evolution of the degree of growth curve plasticity and the rate of non-plastic individual growth will drive these traits to intermediate values at first. Afterwards, the degree of growth curve plasticity might evolve slowly towards extreme values depending on whether energetic costs increase or decrease with the degree of plasticity. In addition, the analysis shows that it is unlikely to encounter species in which individual growth is entirely fixed or entirely plastic, opposing general assumptions in dynamic energy budget theory.

5.1 Introduction

Individual body size strongly affects the physiology, morphology and life history of an individual (Calder, 1984; LaBarbera, 1989; Peters, 1983). For example, body size is positively correlated with stress tolerance, fecundity, mating success and survival (Hone and Benton, 2005; Kingsolver and Pfennig, 2004; Blanckenhorn, 2000; Peters, 1983). This suggests that fitness increases with body size and therefore body size should be under strong selective pressure (Kingsolver and Huey, 2008). Comparison between taxa indeed shows an increase in species body size throughout the history of life, a pattern that is known as Cope's rule (Smith et al., 2016; Stanley, 1973). However, this interspecific trend of increasing body size does not imply that intraspecific selection pressure always results in directional selection towards faster growth rates (Gotanda et al., 2015). On the contrary, trade-off relations between individual growth rates and other life history processes such as fecundity and senescence often result in opposing selection forces (Rollinson and Rowe, 2015; Dmitriew, 2011; Blanckenhorn, 2000). This is likely to result in balancing selection towards an optimal growth rate. The optimal growth rate is likely to be species and population specific as it strongly depends on the environment and could shift with human impact or climate change (Gardner et al., 2011; Allendorf and Hard, 2009).

Individual growth curves, that is the relationship between individual body size and age, are not only determined by genetic components, but in many species also show a strong plastic response to the environment. Environment-dependent changes in individual growth curves are observed in a wide range of ectothermic species ranging from *Daphnia* (McCauley et al., 1990) and fish (Zimmermann et al., 2018; Lorenzen and Enberg, 2002) to amphibians and reptiles (Halliday and Verrell, 1988), but it is even suggested that some large fossil mammals were growing in body size at flexible rates (Köhler and Moyà-Solà, 2009). This suggests that the growth curves of most ectotherms and early endotherms is or was at least partly plastic. In contrast, modern-day endotherms (e.g. birds and mammals) might be able to sustain a more constant growth curve due to the ability to maintain a strong homeostasis (Kooijman, 2010). For example, female mice stop ovulating but maintain growth in body size if food is scarce (Perrigo, 1990). Overall this suggests that taxa not only differ in their growth rate but also differ strongly in the degree of plasticity in the individual growth curves. In this paper we will explore a mechanistic way to study the simultaneous evolution of the degree of plasticity in individual growth curves.

Evolution of a trait and the plasticity herein is often considered in the con-

text of a dynamic environment with a certain degree of unpredictability. As a consequence, phenotypic plasticity is argued to be able to both hamper and accelerate evolutionary change in a trait, while plasticity itself might be subject to selection as well (Perry et al., 2018; Levis and Pfennig, 2016; Fusco and Minelli, 2010). Plasticity decouples the phenotypic expression of a trait from the genotype of an individual and increases its dependence on the environment. Yet, the mechanisms that link a life-history trait to the environment are often unknown and are likely to have a genetic basis as well. As a consequence, plasticity and evolution of a trait are found to influence each other in several ways (Pfennig et al., 2010; Crispo, 2007). Plasticity could, for example, enable species to survive in new environmental conditions encountered through environmental change or radiation and in this way grant species more time to adapt to new environments (Levis and Pfennig, 2016; Moczek et al., 2011; Price et al., 2003). On the other hand, canalization could cause a species to lose plasticity in a trait if the environment is relatively constant (Crispo, 2007). Simultaneously, plasticity may also mask genotypes from selective forces which could reduce the total genetic change in a trait (Crispo, 2007). In general, it is suggested that an intermediate degree of plasticity is expected to favour the evolution of a trait, while fluctuating environments favour a higher degree of plasticity (Levis and Pfennig, 2016; Moczek et al., 2011; Fusco and Minelli, 2010; Price et al., 2003). Although it is clear that the environment plays an important role in the evolution of plasticity, the mechanistic link between the environment and a trait often remains vague and unconsidered.

A way to obtain a more mechanistic underpinning of the evolution of phenotypic plasticity is to consider the energy expenses or costs that are associated with phenotypic plasticity (Pigliucci, 2005). The energetic costs of plasticity could arise from numerous mechanisms and processes and strongly depend on the trait (DeWitt et al., 1998). A useful way to disentangle the energetic expenses of expressing a plastic trait is to split these expenses into the costs of expressing the trait itself and the costs of maintaining plasticity in the trait (Murren et al., 2015). Energetic costs of expressing the trait itself can be considered as the expenses that are needed to express a specific phenotype and are only paid when a phenotype is actually expressed. In contrast, energetic costs of maintaining plasticity in a trait are expenses that are always paid even if a phenotype is not expressed. This would for example include costs of monitoring the environment or costs of maintaining a complex genetic or chemical pathway to facilitate plasticity in a trait. Although maintaining plasticity in a trait might bring additional expenses, plasticity can still increase the fitness of an individual as the benefits of plasticity can outweigh the costs for maintaining plasticity. It is generally assumed that costs of maintaining

plasticity are low or have a very small impact on the evolution of plasticity (Auld et al., 2010), even though it is often difficult to disentangle the different costs of a plastic trait.

Dynamic Energy Budget (DEB) theory offers a useful way to formulate a mechanistic model about the energetic expenses regarding phenotypic plasticity in individual growth. DEB theory describes the allocation of assimilated energy to growth, reproduction and somatic maintenance costs within an individual and in this way links important life history processes (Jager et al., 2013; Kooijman, 2010). DEB models inherently incorporate the costs of expressing a specific growth rate and include a tradeoff with fecundity, because assimilated energy can only be spent once. Most DEB models use a κ-rule, in which a fraction κ of the assimilated energy is allocated to somatic growth and somatic maintenance, while a fraction $1-\kappa$ is allocated to reproduction (Jager et al., 2013; Kooijman, 2010), which implies that both the individual growth curve and individual fecundity depend on the food availability in the environment and are therefore entirely plastic. It is clear that most endothermic species deviate from the κ-rule as these species maintain a relatively constant growth curve, which is prioritized over reproduction. This fundamental tradeoff between growth and reproduction becomes especially apparent if individuals maintain a fixed growth rate under extreme conditions. This tradeoff is very clear in ungulates which show delayed reproduction and decreased fecundity under reduced food conditions (Albon et al., 2000; Coulson et al., 2000; Clutton-Brock et al., 1987; Festa-Bianchet et al., 1995; Skogland, 1986). DEB theory assumes that the κ-rule is a fundamental mechanism in individual energy allocation and that deviating from this rule requires additional mechanisms such as monitoring the environment and adaptive behaviour as well as more complex genetic and chemical system to regulate energy allocation (Kooijman, 2010). These additional mechanisms are argued to induce additional costs for deviating from the simpler and more straightforward κ-rule to maintain a more constant growth rate. This assumption contrasts with the general assumption that plasticity in a trait is costly, such that an increase in the degree of plasticity implies higher costs (Pigliucci, 2005). Whether costs increase or decrease with plasticity might, in the end, strongly depend on the type of costs and their link to the underlying chemical structure for energy allocation. Here we therefore explore both the situation in which additional costs increase with plasticity and the situation in which costs decrease with plasticity.

In this research we use a size-structured population model (formulated in chapter 4) based on a DEB model describing growth and reproduction to explore the simultaneous evolution of the degree of plasticity in the individual growth

curve and the rate of the non-plastic part of individual growth. The DEB model provides a mechanistic way to incorporate the energy expenses and costs linked to plasticity in individual growth on an individual level. The translation of the individual energetic model to a size-structured population model allows us to analyse the model at the population level. Because we are interested in how the individual energetic model affects the evolution of plasticity, we study the model in an artificial and closed condition without external influences. As a consequence, fluctuations in the environment only arise due to changes in the structure of the consumer population, for example due to evolution of the individual traits or population dynamic cycles. In this way, individuals are able to use plasticity in growth to optimize their energy allocation schemes. With this model, we will explore the situation in which costs decrease with plasticity, which is in line with DEB theory, and contrast this with the scenario in which costs increase with plasticity, which is in line with general theory about plasticity.

5.2 Methods

Model formulation

In this study we use a physiologically structured population model to describe the dynamics of a consumer population structured by age (a) and size (length ℓ). the individuals of the consumer population compete for a shared, unstructured resource (R). The energetics of individual consumers is modelled with a DEB model that forms the core of the population model. The details of this DEB model for individual energetics are presented in chapter 4 and here we provide a concise overview of its main features.

In the underlying DEB model, consumer individuals are characterized by the energy stored in lean mass. In DEB theory, it is assumed that energy in lean mass scales with the mass of an individual. Likewise, the mass is assumed to scale with the volume and the volume can be related to the cubed length (Kooijman, 2010). As a consequence, energy in lean mass scales with length cubed (ℓ^3).

We assume that individuals feed on a resource community that follows semi-chemostat dynamics with a maximum density K and a turn-over rate ν. Consumption of the resource scales with the surface area of an individual, which is assumed to be proportional to length squared (ℓ^2). In addition, the consumption rate scales with the resource density following a scaled type II functional response

($f(R) = \frac{R}{R_h+R}$, with a half saturation constant R_h) and an ingestion scalar (I_{max}).

$$\frac{dR}{dt} = \nu\,(K - R)\; - \int_0^{a_{max}} I_{max} f(R) \ell(t,a)^2 n(t,a) da \tag{5.1}$$

In which $n(t,a)$ represents the number of individuals at time t with age a. Consumed resources are assimilated in the guts and the ingestion rate times the assimilation rate is given by α. Assimilated energy is divided between somatic processes and reproductive processes. Somatic processes include growth in body size and somatic maintenance costs, which are costs for maintaining the current individual state. Reproductive processes include maturation of juveniles and the production of offspring by adults.

The model follows DEB theory in assuming that total energy allocation to somatic processes scales with individual surface area (ℓ^2). This energy allocation rate to somatic processes is furthermore assumed to be a combination of a fixed energy allocation rate and an ingestion-dependent energy allocation rate. The fixed energy allocation rate is determined by a fixed scalar (ζ) and is therefore non-plastic. In contrast, for the ingestion-dependent allocation rate we follow DEB theory by assuming that a fixed fraction κ of assimilated energy is channelled to somatic processes. Since ingestion depends on the resource availability in the environment (following $f(R)$), this ingestion-dependent allocation is plastic. In other words, allocation to growth consists of a non-plastic part scaling with ζ and a plastic part scaling with the energy availability in the environment ($f(R)$). The balance between these two energy flows determines the level of plasticity in the energy allocation to somatic processes. We introduce the parameter ϕ to vary this balance from entirely fixed growth ($\phi = 0$) to entirely plastic growth ($\phi = 1$). Energy allocated to somatic processes is first used to pay somatic maintenance costs because these costs are essential for the functioning of an individual (Kooijman, 2010). The somatic maintenance costs are independent of the environment and scale with the energy stored in lean mass and therefore with length cubed (ℓ^3) and a maintenance scalar (b). The remainder of the energy allocated to somatic processes is used for somatic growth. When there are no additional costs for plasticity we assume that energy is converted to mass with a constant efficiency (γ_m):

$$\frac{d\ell^3}{dt} = \gamma_m \left(\kappa\alpha\left(\phi f(R) + (1-\phi)\zeta\right)\ell^2 - b\ell^3\right) \tag{5.2}$$

Note that the parameter ϕ itself is constant and in particular does not depend on resource availability. This parameter provides, however, a mechanistic basis for varying levels of plasticity in the growth rate in body size and thus the growth

curve of individuals, as it influences to what extent somatic growth depends on resource availability. The value of ϕ varies between 0 and 1. Without growth curve plasticity ($\phi = 0$), energy allocation to somatic growth is determined by a fixed parameter (ζ) and is therefore independent of the environment. With full growth curve plasticity ($\phi = 1$) this energetic model simplifies to the DEB model described by Jager et al. (2013) and energy allocation to somatic growth is entirely determined by the resource density in the environment ($f(R)$).

The assimilated energy not allocated to somatic processes is allocated to maturation in juveniles and reproduction in adults. In our model consumer individuals eventually mature when reaching a predefined size (ℓ_J). Adult consumers convert the energy not used for somatic processes to reproductive energy (E_r) with a constant conversion efficiency (γ_r):

$$\frac{dE_r}{dt} = \begin{cases} \gamma_r \left(\alpha f(R) \ell^2 - \kappa\alpha \left(\phi f(R) + (1-\phi)\zeta \right) \ell^2 \right) & \text{if } \ell > \ell_J \\ 0 & \text{if } \ell < \ell_J \end{cases} \tag{5.3}$$

From equations (5.2) and (5.3) it is clear that assimilated energy might become insufficient to cover the energy required for somatic maintenance or non-plastic growth resulting in starvation. Under these conditions, individuals are forced to change their energy allocation scheme, which unavoidably results in additional plasticity. The DEB model assumes that individuals will first prioritize somatic maintenance and then non-plastic growth over other processes. To do so, individuals have to reallocate energy from reproduction to somatic processes under starvation conditions. In addition, we assume that individuals will experience starvation mortality (μ_s) on top of the fixed background mortality (μ_b). We assume that the starvation mortality increases with the energy deficit scaled with a starvation scalar (q_s). Starvation mortality ranges from 0 under normal conditions to immediate death ($\mu_s = \infty$) if individuals fail to pay all somatic maintenance costs. The specific formulation of the starvation conditions plays a minor role in the ecological and evolutionary dynamics of the model. The equations for the energy dynamics and mortality under starvation conditions are therefore outlined in more detail in the supplementary materials.

We reformulate the equation for growth (5.2) to describe the growth in length rather than the growth in length cubed. In addition, we use a conversion factor to translate the reproductive energy into the number of offspring. To express this model more succinctly we use three composite parameters representing the ultimate asymptotic size under unlimited resource conditions ($\ell_\infty = \frac{\alpha\kappa}{b}$), the time constant of growth ($r_B = \frac{\gamma_m b}{3}$) and the time constant of reproduction ($r_F = \frac{\gamma_r b}{\ell_b^3}$).

Interesting to note is that $(\phi f(R) + (1-\phi)\zeta)\,\ell_\infty$ is the actual asymptotic size of an individual taken into account the energy allocation strategy and environment of an individual. Individuals grow towards this asymptotic size with a rate r_B.

The physiologically structured population model described the dynamics at the level of the population (Table (5.1)). At the core of the population model are three equations describing the energy surplus or deficit in growth ($F_g(R,\ell)$), in reproduction ($F_r(R)$) and these two combined in terms of length ($F_t(R,\ell)$). These terms indicate the amount of energy available for growth and reproduction and the amount of energy not used for somatic maintenance. As long as these terms are positive, individuals have sufficient energy to grow and reproduce. As soon as one of these terms becomes negative, individuals do not have sufficient energy to grow, reproduce or cover somatic maintenance costs and experience starvation conditions. Although most equations in the population model are expressed in these terms for energetic surpluses or deficits, we have to derive some additional expressions to complete the model. Integrating the individual fecundity ($\beta(R,\ell)$) at a given time (t) over the entire population results in the number of individuals at birth ($n(t,0)$). The dynamics of the number of individuals at a given time and age ($n(t,a)$) is determined by the background mortality (μ_b) and starvation mortality ($\mu_s(R,\ell)$). For computational reasons we also assume that individuals die when reaching a maximum age (a_{max}). This assumption barely affects the dynamics as it is set such that almost no individual reaches this age. Individuals are born with a fixed size (ℓ_b) and grow towards an asymptotic size determined by the energy assimilation to somatic processes ($(\phi f(R) + (1-\phi)\zeta)\ell_\infty$). If the energy allocation to somatic processes is highly plastic (high ϕ), the asymptotic size largely depends on the resource availability in the environment ($f(R)\ell_\infty$) and is therefore largely plastic. This then directly results in a plastic individual growth curve. In contrast, if the energy allocation to somatic processes is largely fixed (low ϕ), the asymptotic size is largely fixed ($\zeta\ell_\infty$) and the growth rate is largely independent of the environment.

Besides the situation without additional costs associated with plasticity we explore the situation in which additional costs are associated with growth curve plasticity. We assume that these costs reduce the efficiency with which energy allocated to growth is converted into lean mass. We explore both the situation in which costs increase with individual growth curve plasticity and the situation in which costs decrease with growth curve plasticity. We introduce a separate parameter (c_g) to switch between these two situations ($c_g = 1$ and $c_g = 0$ respectively). In addition, we use the parameter c_p to scale the costs with the level of growth

Table 5.1: Equations describing the population dynamics based on the model in chapter 4.

Population age-distribution dynamics

$$\frac{\partial n}{\partial t} + \frac{\partial n}{\partial a} = -\left(\mu_b + \mu_s(R,\ell)\right) n(t,a)$$
$$n(t,0) = \int_0^{a_{max}} \beta(R,\ell(t,a)) n(t,a) da$$

Energetic surpluses/deficits

$$F_g(R,\ell) = (\phi f(R) + (1-\phi)\zeta)\,\ell_\infty - \ell$$
$$F_r(R) = \left(\phi\frac{(1-\kappa)f(R)}{\kappa} + (1-\phi)\left(\frac{f(R)}{\kappa} - \zeta\right)\right)\ell_\infty$$
$$F_t(R,\ell) = F_g(R,\ell) + F_r(R) = \frac{f(R)}{\kappa}\ell_\infty - \ell$$

Length-age dynamics

$$\frac{\partial \ell}{\partial t} + \frac{\partial \ell}{\partial a} = \begin{cases} r_B(1-c_t)F_g(R,\ell) & \text{if } F_g(R,\ell) > 0 \text{ and } F_r(R) > 0 \\ r_B(1-c_t)F_t(R,\ell) & \text{if } F_r(R) \leq 0 \text{ and } F_t(R,\ell) > 0 \\ 0 & \text{otherwise} \end{cases}$$
$$\ell(t,0) = \ell_b$$
$$c_t = \left(c_g\phi + (1-c_g)(1-\phi)\right) c_p$$

Individual fecundity

$$\beta(R,\ell) = \begin{cases} r_F F_r(R)\ell^2 & \text{if } \ell_J < \ell,\ F_g(R,\ell) > 0 \text{ and } F_r(R) > 0 \\ r_F F_t(R,\ell)\ell^2 & \text{if } \ell_J < \ell,\ F_g(R,\ell) \leq 0 \text{ and } F_t(R,\ell) > 0 \\ 0 & \text{otherwise} \end{cases}$$

Starvation mortality

$$\mu_s(R,\ell) = \begin{cases} 0 & \text{if } F_g(R,\ell) > 0 \text{ and } F_r(R) > 0 \\ -q_s\frac{F_g(R,\ell)}{F_t(R,\ell)} & \text{if } F_g(R,\ell) \leq 0 \text{ and } F_t(R,\ell) > 0 \\ -q_s\frac{F_r(R)}{F_t(R,\ell)} & \text{if } F_r(R) \leq 0 \text{ and } F_t(R,\ell) > 0 \\ \infty & \text{if } F_t(R,\ell) \leq 0 \end{cases}$$

curve plasticity (ϕ). This results in an expression for the total costs of plasticity:

$$c_t = (c_g\phi + (1 - c_g)(1 - \phi))\, c_p \tag{5.4}$$

From this expression it follows that the costs for plasticity (c_t) will increase ($c_g = 1$) from 0 to c_p or decrease ($c_g = 0$) from c_p to 0 if plasticity in the growth curve (ϕ) changes from 0 to 1. In other words, c_t indicates the fraction of energy allocated to growth that is used to cover additional costs for plasticity. This results in a reduction of the growth rate scalar from r_B to $r_B(1 - c_t)$.

Adaptive dynamics

We analyse the evolution of growth curve plasticity (ϕ) and the non-plastic growth scalar (ζ) in the described model using the adaptive dynamics framework (Brännström et al., 2013). This framework considers the invasion fitness of a rare mutant, which has a slightly different trait value compared to resident individuals, in an environment determined by the resident population in equilibrium. Because the population is in equilibrium, the environment only changes over evolutionary time and is therefore constant throughout the lifetime of an individual. As a consequence, growth curve plasticity in individual growth is not visible during the lifetime of an individual, but still affects the energy allocation of an individual. Mutant trait values that yield a positive invasion fitness can spread and take over the population, which results in a stepwise change in the trait throughout the population. Using this framework results in a fitness landscape which predicts the evolutionary trajectories towards and away from evolutionary singular strategies.

The adaptive dynamics framework assumes that the evolutionary timescale can be separated from the ecological timescale. The derivation of the invasion fitness function therefore starts with defining the ecological equilibrium of a resident population with a given trait value (ϕ, ζ). In physiologically structured population models, the equilibrium conditions can be derived using the expression for the lifetime reproductive output of an individual (De Roos, 1997). The lifetime reproductive output represents the average number of offspring an individual produces during its lifetime. In equilibrium the resource density is constant and individuals therefore do not experience starvation conditions. As a consequence the lifetime reproductive output of an individual in equilibrium ($LRO(\tilde{R})$) is given by an expression in which only the scaled resource density ($f(\tilde{R})$) is unknown (derivation

in the supplementary materials and chapter 4):

$$LRO(\tilde{R}) = r_F F_r(\tilde{R}) \int_{\tilde{a_J}}^{a_{max}} \tilde{\ell}(a)^2 e^{-\mu_b a} da \tag{5.5}$$

$$\tilde{\ell}(a) = \ell_b e^{-r_B(1-c_t)a} + \left(\phi f(\tilde{R}) + (1-\phi)\zeta\right)\left(1 - e^{-r_B(1-c_t)a}\right)\ell_\infty$$

$$\tilde{a_J} = \frac{1}{r_B(1-c_t)} \ln\left(\frac{\left(\phi f(\tilde{R}) + (1-\phi)\zeta\right)\ell_\infty - \ell_b}{\left(\phi f(\tilde{R}) + (1-\phi)\zeta\right)\ell_\infty - \ell_J}\right)$$

Herein we denoted the equilibrium value of a variable with a tilde. In equilibrium every individual should exactly replace itself and the lifetime reproductive output should therefore be equal to one. This can be used to numerically compute the resource density in equilibrium ($\tilde{R}$). We refrain from calculating the consumer density in equilibrium as is done in chapter 4 because this is not necessary to compute the invasion fitness of a mutant individual.

To calculate the invasion fitness of a mutant, we consider the lifetime reproductive output of a mutant individual in an environment set by the resident population in equilibrium. We assume that the difference between the mutant trait value and the resident trait value is sufficiently small to prevent mutant individuals from experiencing starvation mortality in an environment set by the resident population in equilibrium. We can therefore use the same expression for the lifetime reproductive output for mutant and resident individuals (eq. 5.5). A mutant trait value can spread through the population if the lifetime reproductive output of a mutant individual ($LRO_m(\tilde{R})$) exceeds the lifetime reproductive output of a resident individual in equilibrium ($LRO_r(\tilde{R})$), which is always equal to one. The invasion fitness of a mutant can therefore be closely approximated by the natural logarithm of the lifetime reproductive output of the mutant in an environment set by the resident population in equilibrium, scaled by the average age at reproduction of a resident individual in equilibrium (T_r) (Metz and Leimar, 2011):

$$S_m(\tilde{R}) = \frac{\ln\left(LRO_m(\tilde{R})\right)}{T_r(\tilde{R})} \tag{5.6}$$

$$T_r(\tilde{R}) = \int_0^{a_{max}} a\beta(\tilde{R}, \tilde{\ell}) e^{-\mu_b a} da$$

Note that the average age at reproduction of a resident individual in equilibrium (T_r) is always positive and therefore never affects the qualitative form of the fitness landscape. The local selection gradient represents the direction and rate of evolutionary change in a trait (Geritz et al., 1998). For the degree of growth curve plasticity (ϕ) and the non-plastic growth rate scalar (ζ) these selection gradients

are therefore given as:

$$D_\phi(\tilde{R}) = \frac{1}{T_r}\left[\frac{\partial}{\partial \phi_m} \ln\left(LRO_m(\tilde{R})\right)\right]_{\phi_m=\phi_r} \tag{5.7a}$$

$$D_\zeta(\tilde{R}) = \frac{1}{T_r}\left[\frac{\partial}{\partial \zeta_m} \ln\left(LRO_m(\tilde{R})\right)\right]_{\zeta_m=\zeta_r} \tag{5.7b}$$

The full expression for the selection gradients is given in the supplementary material (eq. 5.16 and eq. 5.17).

We refer to the collection of points at which one of the selection gradients is equal to zero as an evolutionary isocline ($D_\phi(\tilde{R}) = 0$ or $D_\zeta(\tilde{R}) = 0$). A singular strategy occurs if both selection gradients are equal to zero, which is at the intersection of an evolutionary isocline for the growth curve plasticity and an evolutionary isocline for the non-plastic growth scalar. In this article we explore the fitness landscape around these singular strategies without additional costs for growth curve plasticity ($c_p = 0$), if costs increase with growth curve plasticity ($c_g = 1$) and if costs decrease with growth curve plasticity ($c_g = 0$). We use general root finding and curve continuation procedures implemented in C (De Roos, 2021b) for the continuation of the isoclines ($LRO = 1$ and $D_\phi = 0$ or $D_\zeta = 0$) with respect to the growth curve plasticity (ϕ) and the non-plastic growth scalar (ζ). In addition, we perform this analysis for two values of the somatic energy allocation scalar (κ) because this parameter strongly influences the configuration of the fitness landscape. Bifurcation over other parameters showed that the presented fitness landscapes cover all biologically relevant scenarios. In addition, we verify the evolutionary behaviour of the traits around the evolutionary isoclines in terms of convergence- and evolutionary stability by plotting the sign of the invasion fitness for combinations of resident and mutant trait values in so-called Pairwise Invasibility Plots (PIPs) (Geritz et al., 1998). An evolutionary isocline is convergence stable if evolution drives a trait value towards the isocline and evolutionary stable if evolution cannot drive the trait value away from the isocline in any direction. For the model analysis we will use a parameter set for *Daphnia* feeding on algae adapted from De Roos et al. (1990) (Table 5.2).

Dynamic simulations

To corroborate the evolutionary analysis using adaptive dynamics we also carry out numerical simulations of both the ecological and evolutionary dynamics using the escalator-boxcar-train method (EBT) (De Roos, 1988), a numerical method specifically designed to study the dynamics of structured population models. During these simulations, the ecological dynamics and evolutionary dynamics occur at

Table 5.2: Parameters used in the structured population model for *Daphnia magna* feeding on algae, derived from De Roos et al. (1990).

Parameters of the structured population model			
ϕ	Growth curve plasticity	varied	-
ζ	Scalar of the non-plastic growth rate	varied	-
κ	Somatic energy allocation scalar	0.3 or 0.9	-
ℓ_b	Length at birth	0.8	mm
ℓ_J	Length at maturation	2.5	mm
ℓ_∞	Asymptotic length under unlimited food conditions	20κ	mm
a_{max}	Maximum age	70	d
r_B	Time constant of growth	0.15	d^{-1}
r_F	Time constant of reproduction	0.00714	$\mathrm{mm}^{-3}\mathrm{d}^{-1}$
μ_b	Background mortality rate	0.03	d^{-1}
q_s	Starvation mortality scaling constant	0.2	d^{-1}
I_{max}	Maximum feeding rate per unit surface area	1.8	10^6 cells $\mathrm{mm}^{-2}\mathrm{ml}^{-1}\mathrm{d}^{-1}$
R_h	Half saturation constant of functional response	0.14	10^6 cells ml^{-1}
ν	Semi-chemostat renewal rate	0.5	d^{-1}
K	Maximum resource density	0.5	10^6 cells ml^{-1}
c_g	Relation between costs and plasticity	0 or 1	-
c_p	Additional plasticity costs scalar	0.4	-
p_m	Mutation probability for a specific mutation	0.01	-
d_m	Mutation effect on trait	0.01	-

the same timescale, because every day new mutations occur during a reproductive event. As a consequence, the compositions of the consumer population changes constantly and is not in equilibrium. Similarly, the resource density therefore is not in equilibrium and changes due to the changes in the structure of the consumer population as well as population dynamic cycles (Chapter 4). This results in more realistic conditions in which individuals have to deal with a constantly changing environment, which could affect the evolution of the level of growth curve plasticity.

In the EBT method the population is subdivided into cohorts consisting of individuals born at approximately the same time. In our simulations, a new cohort will be formed once a day and all offspring are always born with age 0 and length ℓ_b. We split a cohort into multiple sub-cohorts consisting of genetically identical individuals such that the differential equations can be solved separately for every sub-cohort. When a new cohort is formed based on the reproductive output of the current population, we assume that a mutation occurs with probability p_m for each trait and that this mutation has an effect of size d_m on either the growth curve plasticity (ϕ) or the non-plastic growth scalar (ζ). We assume that mutations can affect traits in both directions, resulting in either an increase or decrease in growth curve plasticity or an increase or decrease in non-plastic growth rate, such that selection can drive these trait values in both directions. As a result, a fraction $1 - 4p_m$ of the offspring will have the same trait values as the parent cohort. In addition, four sub-cohorts with mutants are produced, which differ from the parent cohort in either the growth curve plasticity ($\phi - d_m$ or $\phi + d_m$) or the non-plastic growth scalar ($\zeta - d_m$ or $\zeta + d_m$). A fraction p_m of the offspring is allocated to each of the mutant sub-cohorts. If the trait values of a mutant cohort fall outside the range of the allowed trait values ($0 \leq \phi \leq 1$, $0 \leq \zeta \leq 1$), the trait values of the mutant sub-cohort are reset to the trait values of the parent cohort. Simulations are started from a population dynamic attractor for the resident population, obtained by running the model 5000 time-steps with a given parameter-set and a mutation probability of zero. Afterwards simulations are continued with a non-zero mutation probability until the number of cohorts, the average trait values and the resource density become constant with a precision of 10^{-6}, which indicates that the population has reached an evolutionary and ecological attractor (which took at least 5000 time-steps). We will depict the evolving trait values of the simulated trajectories using black solid lines in the same graphs as the fitness landscapes computed with adaptive dynamics.

5.3 Results

We first consider the situation in which maintaining a plastic or non-plastic growth curve does not incur additional costs in the form of a reduced conversion efficiency ($c_p = 0$, fig. 5.1). We found two evolutionary isoclines for the degree of growth curve plasticity ($D_\phi(\tilde{R}) = 0$) and two evolutionary isoclines for the non-plastic growth scalar ($D_\zeta(\tilde{R}) = 0$). The first isocline for the growth curve plasticity ($D_\phi(\tilde{R}) = 0$) occurs when the non-plastic growth scalar is equal to the scaled resource density in the environment ($\zeta = f(\tilde{R})$, fig. 5.1, blue dashed line). At this isocline the plastic growth rate is equal to the non-plastic growth rate and as a consequence a mutation in growth curve plasticity does not affect the fitness of an individual. Selection in the non-plastic growth scalar will drive the population away from this evolutionary isocline for growth curve plasticity. We will therefore refer to this isocline as the trivial evolutionary isocline for growth curve plasticity (ϕ). The direction of the selection gradient for growth curve plasticity is opposite at different sides of this trivial isocline for growth curve plasticity.

Similarly, an evolutionary isocline for the non-plastic growth scalar ($D_\zeta(\tilde{R}) = 0$) occurs if growth is entirely plastic ($\phi = 1$, fig. 5.1 red dashed line). At this isocline the life history and fitness of an individual is not affected by the non-plastic growth scalar. Evolution in growth curve plasticity will drive the population away from this evolutionary isocline for some values of the non-plastic growth scalar. We therefore refer to this isocline as the trivial evolutionary isocline for the non-plastic growth scalar (ζ).

The second evolutionary isocline for the growth curve plasticity and the non-plastic growth scalar ($D_\phi(\tilde{R}) = 0$, $D_\zeta(\tilde{R}) = 0$) occur on the same manifold in the parameter space in absence of additional costs for growth curve plasticity (Fig. 5.1, purple line; see eq. 5.16 and eq. 5.17 for corroboration that these isoclines coincide when $c_p = 0$). This manifold represents a collection of singular points. All combinations of trait values on this manifold have the same fitness which results in evolutionary neutrality on the manifold. Nonetheless, the singular points on the manifold are invasion and convergence stable against mutants with trait values which are not on the manifold (Fig. 5.6 and 5.7). The manifold therefore forms a collection of evolutionary endpoints with the same fitness. We will refer to this manifold as the main ESS-manifold. Time simulations revealed two different evolutionary trajectories towards this main ESS-manifold (Fig. 5.1, black lines). If the initial point of the trajectory and the main manifold occur at the same side of the trivial evolutionary isocline for growth curve plasticity, selection will drive the growth curve plasticity and the non-plastic growth scalar directly towards the

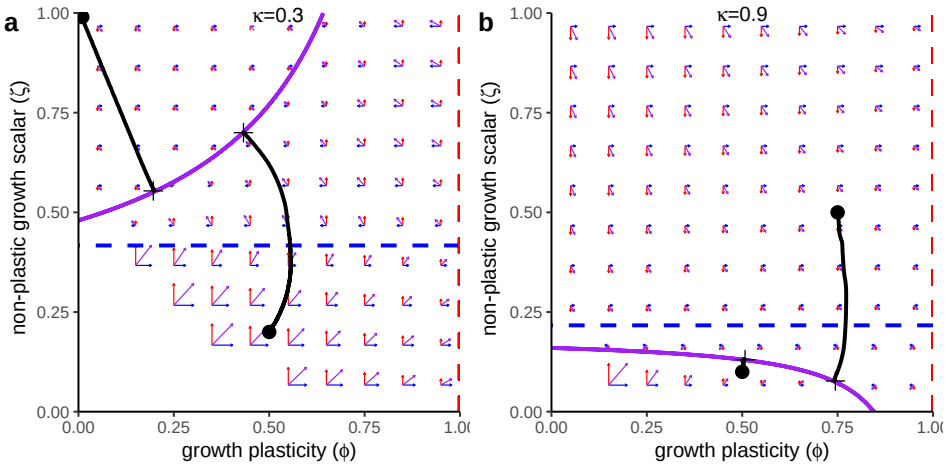

Figure 5.1: Selection gradients and evolutionary trajectories for the evolution of the growth curve plasticity (ϕ) and the non-plastic growth scalar (ζ) without additional costs for plasticity ($c_p = 0$) for $\kappa = 0.3$ (left) and $\kappa = 0.9$ (right). Blue, red and purple arrows show the selection gradient for the growth curve plasticity (ϕ), non-plastic growth scalar (ζ) and combination of both respectively. Blue, red and purple lines indicate evolutionary isoclines for the growth curve plasticity (ϕ), non-plastic growth scalar (ζ) and overlapping instances of these isoclines. Solid lines represent evolutionary isoclines which are convergence and evolutionary stable for the parameter under consideration. Because these isoclines overlap in this situation, these lines form a manifold that is evolutionary neutral for all parameter combinations on the manifold and evolutionary stable against invasion of mutants with parameter combinations not on the manifold. Dashed lines represent evolutionary isoclines which are evolutionary neutral for the parameter under consideration. Black lines show the average trait values from time simulations of evolutionary trajectories starting at the parameter values marked with a dot.

main manifold. On the other hand, if the initial point of the trajectory and the main ESS-manifold occur at opposite sides of the trivial evolutionary isocline for growth curve plasticity, selection will first drive the growth curve plasticity and non-plastic growth scalar towards the trivial isocline for growth curve plasticity. At this isocline the direction of selection for the growth curve plasticity changes and selection drives the growth curve plasticity and the non-plastic growth scalar towards the main ESS-manifold.

Introducing a cost increasing with growth curve plasticity ($c_g = 1, c_p = 0.4$) changes the location of the evolutionary isoclines in the parameter space relatively little but does so differently for the evolutionary isoclines of the growth curve plasticity and the non-plastic growth scalar (Fig. 5.2). First of all, the trivial

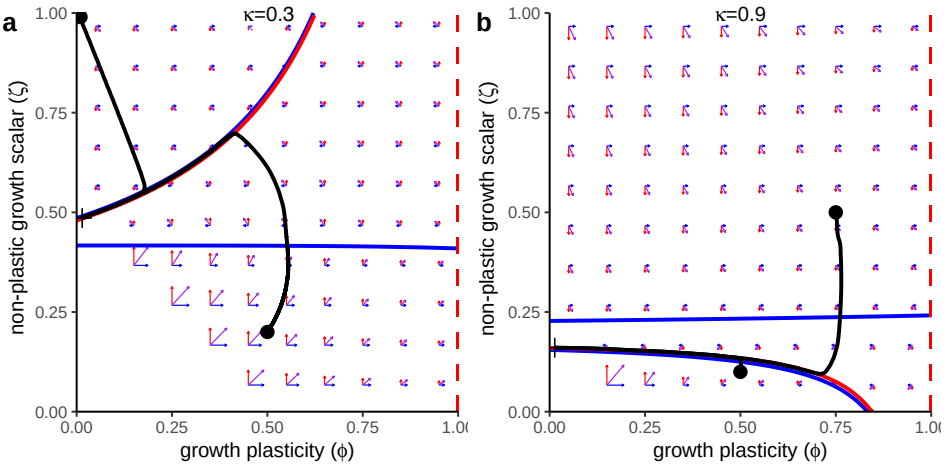

Figure 5.2: Selection gradient and evolutionary trajectories for the evolution of the growth curve plasticity (ϕ) and the non-plastic growth scalar (ζ) with costs increasing with growth curve plasticity ($c_g = 1, c_p = 0.4$) for $\kappa = 0.3$ (left) and $\kappa = 0.9$ (right). Blue, red and purple arrows show the selection gradient for the growth curve plasticity (ϕ), non-plastic growth scalar (ζ) and combination of both respectively. Blue and red lines indicate evolutionary isoclines for the growth curve plasticity (ϕ) and the non-plastic growth scalar (ζ). Solid lines represent evolutionary isoclines that are convergence and evolutionary stable for the parameter under consideration. Dashed lines represent evolutionary isoclines that are evolutionary neutral for the parameter under consideration. Black lines show the average trait values from time simulations of evolutionary trajectories starting at the parameter values marked with a dot.

evolutionary isocline for growth curve plasticity (Fig. 5.2, almost horizontal blue line) slightly curves when growth is not entirely non-plastic ($\phi > 0$), which makes this evolutionary isocline an evolutionary attractor when only considering the evolution in growth curve plasticity (Fig. 5.6 and 5.7). In addition, the main isocline for growth curve plasticity shifts away from the main isocline for the non-plastic growth scalar (Fig. 5.2, red and blue curved lines). As a consequence, selection on the non-plastic growth scalar will drive the population away from the main isocline for growth curve plasticity, while close to the main isocline for the non-plastic growth scalar the selection gradient for the growth curve plasticity is negative. As a result, the growth curve plasticity and the non-plastic growth scalar will first evolve towards the main isoclines, similar to the situation without additional costs for growth curve plasticity (Fig. 5.2, black lines). But as soon as the population trait values are between these main isoclines, the trait values will remain between these isoclines and slowly evolve towards lower growth curve plasticity. Inter-

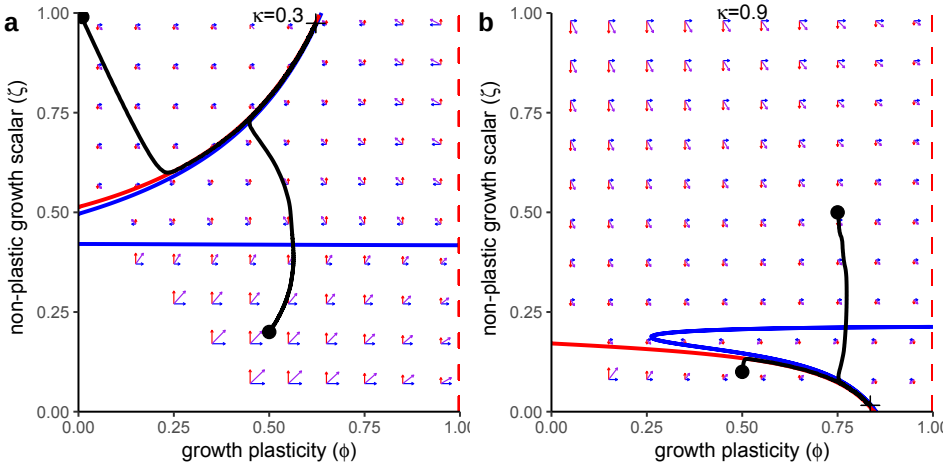

Figure 5.3: Selection gradient and evolutionary trajectories for the evolution of the growth curve plasticity (ϕ) and the non-plastic growth scalar (ζ) with costs decreasing with growth curve plasticity ($c_g = 0, c_p = 0.4$) for $\kappa = 0.3$ (left) and $\kappa = 0.9$ (right). Blue, red and purple arrows show the selection gradient for the growth curve plasticity (ϕ), non-plastic growth scalar (ζ) and combination of both respectively. Blue and red lines indicate evolutionary isoclines for the growth curve plasticity (ϕ) and the non-plastic growth scalar (ζ). Solid lines represent evolutionary isoclines that are convergent and evolutionary stable for the parameter under consideration. Dashed lines represent evolutionary isoclines that are evolutionary neutral for the parameter under consideration. Black lines show the average trait values from time simulations of evolutionary trajectories starting at the parameter values marked with a dot.

estingly, selection gradients and the time series reveal that the initial evolution towards the main isoclines is much faster compared to the evolution towards low growth curve plasticity between the main isoclines (length of arrows fig. 5.2 and supplementary videos).

Introducing a cost decreasing with growth curve plasticity ($c_g = 0$, $c_p = 0.4$) shifts the location of the isoclines in the opposite direction compared to the situation in which costs increase with growth curve plasticity (Fig. 5.3). The trivial isocline for growth curve plasticity remains an evolutionary attractor when only considering the evolution of growth curve plasticity (Fig. 5.6 and 5.7). Although sometimes very slightly, costs decreasing with plasticity decreases the distance between the trivial and the main isoclines for growth curve plasticity if growth is not entirely plastic ($\phi < 1$, blue lines fig. 5.3). For some parameter settings this can even cause these isoclines to collide and form a single isocline in the relevant parameter space (Fig. 5.3b). In this situation, evolution always drives the pop-

ulation towards a relatively high degree of growth curve plasticity. Furthermore, we see again that evolution of the non-plastic growth scalar drives the population away from the main isocline for growth curve plasticity, but this time the selection gradient for growth curve plasticity is positive around the main isocline for the non-plastic growth scalar. As a consequence, evolution will drive the population first towards the main isoclines, from which the population evolves between these isoclines towards a higher level of growth curve plasticity. The directional evolution between the main isoclines will eventually stop when the non-plastic growth scalar reaches a physiological maximum or minimum value. Again the evolution towards the main isoclines is relatively fast compared to the evolution between the main isoclines (length of arrows fig. 5.3 and supplementary videos).

5.4 Discussion

We studied the combined evolution of plasticity in individual growth curves and the non-plastic growth rate. To do so, we modelled a size-structured consumer population feeding on a single shared resource. In this model, plasticity in individual growth curves (ϕ) determines the fraction of the individual growth rate that depends on the scaled resource availability in the environment ($f(R)$), while the non-plastic growth rate is determined by an environment-independent scalar (ζ). Additional costs scaling with plasticity (c_t) were incorporated as a reduction in the conversion efficiency from energy to lean mass. This might be plausible under the assumption that these costs result from an increase in chemical complexity of the regulatory mechanism, but other costs associated with plasticity, such as additional monitoring of the environment are more likely to increase the somatic maintenance costs of an individual. This would result in a more complex equation for individual growth in which the growth scalar (r_B) and the asymptotic size (ℓ_∞) respond in opposite directions to a change in additional costs. The implementation of costs as increased somatic maintenance costs result in the same evolutionary patters as costs incorporated as a decreased conversion efficiency (Supplementary information).

We analysed the model using the adaptive dynamics framework (Brännström et al., 2013) by defining an expression for the invasion fitness based on the lifetime reproductive output of mutant individuals in an equilibrium of the resident population. We furthermore corroborated the results of the adaptive dynamics approach using numerical simulations of the ecological and evolutionary dynamics. Evolution will always drive the population uphill towards a peak in the invasion fitness, which is a singular strategy. Because we consider the consumer population in a

one-dimensional environment consisting of a single resource community, a peak in the invasion fitness corresponds to a minimum in the resource density (supplementary materials, eq. 5.18-5.21). In our model, a decrease in resource density can only be caused by an increase in consumption by the entire population, from which it follows that evolution on the growth curve plasticity and the non-plastic growth scalar actually optimize the resource consumption by the consumer population. Individuals with a degree of growth curve plasticity and non-plastic growth rate closer to the singular strategy also have a higher lifetime reproductive output in an environment without competition (chapter 4). This shows that evolution not only optimizes the energy consumption of the population but also the efficiency of energy allocation at an individual level.

In our model, evolution always ends on the main evolutionary isoclines. These main evolutionary isoclines occur when a trait value yields the most optimal energy allocation scheme, when only considering evolution in that specific trait. At these main isoclines, individuals most optimally divide the assimilated energy between growth and reproduction (chapter 4) and these isoclines are always convergence and evolutionary stable in our model when considering the evolution in only one trait (Fig. 5.6 and 5.7). The main isoclines for the growth curve plasticity and the non-plastic growth scalar occur at the same combinations of parameter values if no additional costs for maintaining a plastic or non-plastic growth curve are included (Fig. 5.1). As a consequence, the strategies on this main ESS-manifold are invasion stable against strategies outside the manifold but evolutionary neutral for points on the manifold. As a consequence, combined evolution will drive both the growth curve plasticity and the non-plastic growth scalar towards this main ESS-manifold and evolution can end in a wide range of strategies on this main ESS-manifold depending on the strategies present in the population at the start of the trajectory. The incorporation of costs that increase or decrease with growth curve plasticity slightly shifts the location of the main isoclines such that combined evolution will eventually drive the population towards one of the extreme ends of these isoclines (Fig. 5.2 and 5.3). Logically, if costs increase with growth curve plasticity, the population will end up between the main isoclines at the side with the lowest degree of growth curve plasticity. If costs decrease with growth curve plasticity, the population will end up between the main isoclines at the side with the highest degree of growth curve plasticity. General theory about plasticity assumes that energetic costs for maintaining plasticity increase with the degree of plasticity, which limits the evolution of plasticity (Pigliucci, 2005). This corresponds with the evolution towards a low level of growth curve plasticity if energetic costs increase with plasticity. In contrast, DEB theory assumes that the κ-rule is a fundamental

mechanism in all organisms and that a deviation from this rule is costly (Kooijman, 2010). Under this assumption growth curves are entirely plastic and a decrease in growth curve plasticity would result in an increase in energetic costs. This corresponds with the evolution towards a high degree of growth curve plasticity if energetic costs decrease with plasticity found in our model. In other words, assumptions about the energetic costs for maintaining plasticity based on DEB theory and classic theory about plasticity result in contradicting conclusions about the evolution of plasticity in individual growth curves.

Our model clearly shows the contribution of different types of expenses scaling with plasticity to the evolution of growth curve plasticity. In our model the expenses of expressing a plastic growth curve are determined by the individual energy allocation schemes, which depend amongst others on the plastic growth energy allocation constant (κ). The individual energy allocation schemes determine the global location for the main isoclines in the parameter space. For example, at low values of the plastic growth energy allocation constant (κ), the main isoclines occur at relatively high values of the non-plastic growth scalar (Fig. 5.1a, 5.2a and 5.3a). In this situation the non-plastic growth rate exceeds the plastic growth rate. In contrast, at high values of the somatic energy allocation scalar (κ) the main isoclines occur at relatively low values of the non-plastic growth scalar (Fig. 5.1b, 5.2b and 5.3b). In this situation, the plastic growth rate exceeds the non-plastic growth rate. We could therefore state that the individual energy assimilation schemes and therewith the expenses for expressing a specific growth rate determine the global position of the main isoclines. In addition, the simulated trajectories show that evolution towards these main isoclines is relatively fast. In contrast, costs that are directly linked to the degree of growth curve plasticity determine the final destination of the evolutionary process. For example, if additional costs increase with plasticity, the population will evolve towards lower plasticity, while if costs decrease with plasticity the population will evolve towards a higher degree of growth curve plasticity (Fig. 5.2 and 5.3). In addition, the selection gradient and the simulated trajectories show that evolution along these main isoclines is much slower than evolution towards the main isoclines. We could therefore argue that individual energy allocation schemes and expenses for expressing a specific growth rate determine the global evolutionary trajectory for growth curve plasticity, while the exact way additional costs scale with the growth curve plasticity determines the precise endpoint of evolution. This adds to the general hypothesis that costs for maintaining plasticity only play a minor role compared to costs for expressing a trait in the evolution of plasticity because a major part of the evolutionary trajectory is determined by the energy tradeoff within an individual

(Auld et al., 2010).

Several energetic costs might be involved in maintaining growth curve plasticity. We assumed a linear relationship between the costs for maintaining growth curve plasticity and the degree of growth curve plasticity. As a consequence, evolution drives the growth curve plasticity to one of the extreme values along the main isoclines. A non-monotonic relation between the costs for maintaining growth curve plasticity and the degree of growth curve plasticity is likely to alter the relative location of the main isoclines. For example, if costs for plasticity would increase toward extreme values of the growth curve plasticity, we expect balancing selection along the main isoclines to drive the growth curve plasticity towards intermediate values. In contrast, if costs for plasticity would decrease toward extreme values of the growth curve plasticity, we expect disruptive selection along the main isoclines to drive the growth curve plasticity towards one of the extreme values depending on the starting conditions.

We also found two trivial evolutionary isoclines that occur at very specific conditions in our model. Such an isocline occurs for the growth curve plasticity (ϕ) if the plastic growth rate and the non-plastic growth rate are equal ($f(\tilde{R}) = \zeta$, fig. 5.1), because in this case a shift in growth curve plasticity does not affect the total growth rate of an individual. As a consequence, individuals with different degrees of growth curve plasticity have the same fitness and growth curve plasticity will not change due to selection. This trivial isocline for growth curve plasticity is not an evolutionary endpoint, because evolution of other traits such as the non-plastic growth scalar could easily drive the population away from these strategies. Nonetheless, the occurrence of this trivial manifold for growth curve plasticity suggests that the selection pressure on the level of phenotypic plasticity becomes stronger if a change in growth curve plasticity has a larger impact on the phenotype of an individual.

It is also suggested that phenotypic plasticity can mask genotypes from selective forces and therefore hamper the evolution of a trait (Crispo, 2007; Price et al., 2003). It could be argued that this occurs at the trivial isocline for the non-plastic growth scalar (ζ). This trivial isocline occurs if growth is entirely plastic ($\phi = 1$, fig. 5.1-5.3). As a consequence, the individual growth rate does not have a non-plastic component that is scaled by the non-plastic growth scalar and selection does not affect the non-plastic growth scalar. This only occurs at an extreme condition in the model and it is likely that evolution in another trait such as the degree of growth curve plasticity will drive natural populations away from this trivial isocline. It is therefore unlikely that growth curve plasticity will entirely mask a non-plastic part of growth from evolutionary pressure. Nonetheless, the

occurrence of this trivial isocline for the non-plastic growth scalar suggests that the selection pressure on the non-plastic growth rate decreases with an increasing degree of growth curve plasticity.

In this study we focused on the effect of an individual energetic mechanism on the evolution of growth curve plasticity. We therefore chose to consider a structured consumer population feeding on a single resource in closed conditions. In the adaptive dynamics analysis, the resource is in population dynamic equilibrium and therefore does not fluctuate during the lifetime of an individual. As a consequence, evolution results in the optimization of individual life histories through optimization of the individual energy allocation scheme. Interestingly, this suggests that plasticity in growth might evolve even when the environment is constant, although the same optimal energy allocation scheme could arguably be achieved through the evolution of other individual traits such as the plastic energy allocation constant (κ) as well. During the dynamic simulations, the resources were not in equilibrium and followed transient dynamics. Changes in the resource density occur through population dynamic cycles (chapter 4) as well as changes in the structure of the consumer population. It is generally expected that fluctuations in the environment would favour a more plastic life history strategy (Levis and Pfennig, 2016; Moczek et al., 2011; Fusco and Minelli, 2010; Price et al., 2003). Surprisingly, the results from the dynamic simulations seem to barely differ from the predictions from the adaptive dynamics framework. This might suggest that optimization of the individual life histories is a stronger selective force for the level of growth curve plasticity than environmental fluctuations. It is important to note that in our model, all fluctuations in the environment are generated by the system itself. It is likely that externally driven fluctuations in the environment have a stronger effect on the level of growth curve plasticity. These fluctuations could for example cause different types of starvation dynamics depending on the underlying energy allocation schemes of an individual (chapter 4). Whether and how external environmental fluctuations would affect the evolution of growth curve plasticity in combination with a mechanistic description of individual energy allocation is still an open question and our model offers a suitable framework to study this.

This study can at least inform us about the evolution of plasticity in the light of the optimization of individual energy allocation dynamics. Our model supports the suggestion that taxa are likely to strongly differ in the plasticity in their growth curves and the non-plastic growth rate. It is generally suggested that growth curves of ectotherms are largely plastic while growth curves of endotherms are largely static (McCauley et al., 1990; Lorenzen and Enberg, 2002; Zimmermann et al., 2018; Halliday and Verrell, 1988; Köhler and Moyà-Solà, 2009;

Kooijman, 2010). An explanation of this could be that costs decrease with plasticity in ectotherms, because they need additional chemical or genetic mechanisms to maintain a constant growth curve. In contrast, endotherms have strong homeostasis and therefore might need additional mechanisms to monitor the environment (Kooijman, 2010). If these mechanisms are costly, costs might increase with plasticity, which could explain evolution towards lower plasticity in growth curves. Interestingly, our model suggests that it is possible for a population to evolve towards entirely non-plastic growth curves, while a strategy with entirely plastic growth curves is not evolutionary stable. This contrasts with DEB theory which argues that a κ-rule mechanism for energy allocation is most efficient for individuals (Kooijman, 2010). Independent of this, our model suggests that it is unlikely that growth curves are entirely plastic or entirely non-plastic in most species, because even if maintaining a plastic or non-plastic growth curve induces additional costs, evolution is likely to drive plasticity towards intermediate values at first, after which the evolution towards extreme values is very slow. It is more likely to find species with an intermediate degree of growth curve plasticity on the trajectory towards more extreme values. Similarly, the total growth rate of individuals is most likely at intermediate values, due to the tradeoff with other life history characteristics such as reproduction in this model (Gardner et al., 2011; Allendorf and Hard, 2009). Unfortunately, it is hard to disentangle the plastic and non-plastic components of individual growth curves and the evolution herein for a specific species as the difference between plastic and non-plastic growth only becomes visible under extreme conditions. Therefore, there might even be more variation in individual growth rates and the plasticity herein than we currently expect.

5.5 Supplementary materials

Energy dynamics under starvation

From equations (5.2) and (5.3) it is clear that the energy flow can become insufficient to cover demand-driven processes such as maintenance costs and growth. This would lead to starvation conditions which require a rechannelling of the assimilated energy. Three different types of starvation conditions can be distinguished.

Under supply-driven starvation, the energy supplied to somatic processes is insufficient to cover somatic maintenance costs ($\kappa\alpha\left(\phi f(R)+(1-\phi)\zeta\right)\ell^2 < b\ell^3$). Under this condition some of the energy is reallocated from reproductive processes to cover somatic maintenance costs. As a consequence, somatic growth stops and

reproduction is reduced. In contrast, under demand-driven starvation the assimilated energy is insufficient to cover the energy demand by non-plastic growth and somatic maintenance ($\alpha f(R)\ell^2 < \kappa\alpha\left(\phi f(R) + (1-\phi)\zeta\right)\ell^2$). Under this condition we assume that all energy is used to cover the energy demand by non-plastic growth and somatic maintenance as these are both demand-driven processes determined by the internal state of an individual. As a consequence reproduction stops and growth is reduced. Under severe starvation conditions, assimilated energy is insufficient to cover somatic maintenance costs ($\alpha f(R)\ell^2 < b\ell^3$) and both growth and reproduction stop immediately. This results in the following equations for energy allocation to growth and reproduction:

$$\frac{d\ell^3}{dt} = \begin{cases} \gamma_m(1-c_t)\left(\kappa\alpha\left(\phi f(R) + (1-\phi)\zeta\right)\ell^2 - b\ell^3\right) \\ \qquad \text{if } b\ell^3 < \kappa\alpha\left(\phi f(R) + (1-\phi)\zeta\right)\ell^2 < \alpha f(R)\ell^2 \\ \gamma_m(1-c_t)\left(\alpha f(R)\ell^2 - b\ell^3\right) \\ \qquad \text{if } b\ell^3 < \alpha f(R)\ell^2 < \kappa\alpha\left(\phi f(R) + (1-\phi)\zeta\right)\ell^2 \\ 0 \qquad \text{otherwise} \end{cases} \tag{5.8a}$$

$$\frac{dE_r}{dt} = \begin{cases} \gamma_r\alpha\left((1-\kappa)f(R) + (f(R)-\kappa\zeta)\right)\ell^2 \\ \qquad \text{if } b\ell^3 < \kappa\alpha\left(\phi f(R) + (1-\phi)\zeta\right)\ell^2 < \alpha f(R)\ell^2 \\ \gamma_r\left(\alpha f(R)\ell^2 - b\ell^3\right) \\ \qquad \text{if } \kappa\alpha\left(\phi f(R) + (1-\phi)\zeta\right)\ell^2 < b\ell^3 < \alpha f(R)\ell^2 \\ 0 \qquad \text{otherwise} \end{cases} \tag{5.8b}$$

Additionally, we assume that starvation conditions lead to an increase in mortality. We assume that starvation mortality scales with the energy deficit of an individual and a starvation mortality scalar (q_s). Under extreme conditions it can even occur that the assimilated energy is insufficient to cover somatic maintenance costs ($\alpha f(R)\ell^2 < b\ell^3$). We assume that individuals will starve instantaneously under these extreme starvation conditions. This results in the following expressions for the starvation mortality:

$$\mu_s = \begin{cases} 0 \qquad \text{if } b\ell^3 < \kappa\alpha\left(\phi f(R) + (1-\phi)\zeta\right)\ell^2 < \alpha f(R)\ell^2 \\ q_s\frac{b\ell^3 - \kappa\alpha(\phi f(R) + (1-\phi)\zeta)\ell^2}{\alpha f(R)\ell^2 - b\ell^2} \\ \qquad \text{if } \kappa\alpha\left(\phi f(R) + (1-\phi)\zeta\right)\ell^2 < b\ell^3 < \alpha f(R)\ell^2 \\ q_s\frac{\kappa\alpha(\phi f(R) + (1-\phi)\zeta)\ell^2 - \alpha f(R)\ell^2}{\alpha f(R)\ell^2 - b\ell^3} \\ \qquad \text{if } b\ell^3 < \alpha f(R)\ell^2 < \kappa\alpha\left(\phi f(R) + (1-\phi)\zeta\right)\ell^2 \\ \infty \qquad \text{if } \alpha f(R)\ell^2 < b\ell^3 \end{cases} \tag{5.9}$$

Together this results in the formulation of the population dynamics under supply-driven ($F_g(R,\ell) < 0$), demand-driven ($F_r(R) < 0$) and severe ($F_t(R,\ell) < 0$) starvation conditions in equation (5.1) in the main text.

Derivation of ecological equilibrium

In equilibrium the density of the resource is constant ($\tilde{R}$). As a consequence, starvation conditions can not occur in equilibrium (chapter 4). Therefore, we can simplify the differential equation for the number of individual at a given age in equilibrium ($\tilde{n}(a)$):

$$\frac{\partial n}{\partial a} = -\mu_b \tilde{n}(a) \tag{5.10}$$

Because the number of individuals at birth in equilibrium ($\tilde{n}(0)$) is constant, this equation can be solved explicitly:

$$\tilde{n}(a) = \tilde{n}(0) e^{-\mu_b a} \tag{5.11}$$

Similarly, the differential equation of the growth rate in equilibrium simplifies to:

$$\frac{\partial \ell}{\partial a} = r_B \left(1 - c_t\right) \left(\left(\phi f(\tilde{R}) - (1-\phi)\zeta\right) \ell_\infty - \ell\right) \tag{5.12}$$

We solve this differential condition by using the boundary condition of the length at birth ($\ell(0) = \ell_b$):

$$\tilde{\ell}(a) = \ell_b e^{-r_B(1-c_t)a} + \left(\phi f(\tilde{R}) + (1-\phi)\zeta\right) \left(1 - e^{-r_B(1-c_t)a}\right) \ell_\infty \tag{5.13}$$

By substituting the length at maturation (ℓ_J) in this equation, we can rearrange the equation to express the age at maturation (a_J):

$$\tilde{a_J} = \frac{1}{r_B(1-c_t)} \ln\left(\frac{\left(\phi f(\tilde{R}) + (1-\phi)\zeta\right) \ell_\infty - \ell_b}{\left(\phi f(\tilde{R}) + (1-\phi)\zeta\right) \ell_\infty - \ell_J}\right) \tag{5.14}$$

With an explicit expression for the density at age, the size at age and the age at maturation, we can evaluate the integral of the individual fecundity to sum the reproductive rate of all adults resulting in the number of individuals at birth:

$$\tilde{n}(0) = \int_0^{a_{max}} \beta(\tilde{R}, \tilde{\ell}(a)) \tilde{n}(t,a) da = \int_{a_J}^{a_{max}} r_F F_r(\tilde{R}) \tilde{n}(0) e^{-\mu a} da \tag{5.15}$$

We can divide both sides of this expression by the number of individuals at birth in equilibrium ($\tilde{n}(0)$). This yield the expression for the lifetime reproductive output

in equilibrium given in equation 5.5.

Mathematical expressions of the selection gradients

The explicit expressions for the selection gradients are derived by differentiating the function $LRO(\tilde{R})$ (equation 5.5) with respect to ϕ and ζ, respectively, resulting in:

$$
\begin{aligned}
&D_\phi(\tilde{R}) = \\
&\frac{r_F\left(f(\tilde{R})-\zeta\right)\ell_\infty}{T_r(\tilde{R})LRO_m(\tilde{R})}\left[\int_{\tilde{a_J}}^{a_{max}}\left(2\left(1-e^{-r_B(1-c_t)a}\right)F_r(\tilde{R})-\tilde{\ell}(a)\right)\tilde{\ell}(a)e^{-\mu_b a}da\right. \\
&\left.+\frac{\left(\ell_J-\ell_b\right)F_r(\tilde{R})\ell_J^2 e^{-\mu_b\tilde{a_J}}}{r_B(1-c_t)\left(\left(\phi f(\tilde{R})+(1-\phi)\zeta\right)\ell_\infty-\ell_b\right)\left(\left(\phi f(\tilde{R})+(1-\phi)\zeta\right)\ell_\infty-\ell_J\right)}\right] \\
&-\frac{(2c_g-1)c_p r_F F_r(\tilde{R})}{T_r(\tilde{R})LRO_m(\tilde{R})}\left(\frac{\ell_J^2\tilde{a_J}e^{-\mu_b\tilde{a_J}}}{(1-c_t)}\right. \\
&\left.+2r_B\left(\left(\phi f(\tilde{R})+(1-\phi)\zeta\right)\ell_\infty-\ell_b\right)\int_{\tilde{a_J}}^{a_{max}}\tilde{\ell}(a)e^{-\mu_b a}e^{-r_B(1-c_t)a}ada\right)
\end{aligned}
\tag{5.16}
$$

$$
\begin{aligned}
&D_\zeta(\tilde{R}) = \\
&\frac{r_F\left(1-\phi\right)\ell_\infty}{T_r(\tilde{R})LRO_m(\tilde{R})}\left[\int_{\tilde{a_J}}^{a_{max}}\left(2\left(1-e^{-r_B(1-c_t)a}\right)F_r(\tilde{R})-\tilde{\ell}(a)\right)\tilde{\ell}(a)e^{-\mu_b a}da\right. \\
&\left.+\frac{\left(\ell_J-\ell_b\right)F_r(\tilde{R})\ell_J^2 e^{-\mu_b\tilde{a_J}}}{r_B(1-c_t)\left(\left(\phi f(\tilde{R})+(1-\phi)\zeta\right)\ell_\infty-\ell_b\right)\left(\left(\phi f(\tilde{R})+(1-\phi)\zeta\right)\ell_\infty-\ell_J\right)}\right]
\end{aligned}
\tag{5.17}
$$

The lifetime reproductive output of the resident in equilibrium ($LRO_r(\tilde{R})$) is always equal to one and therefore cancels out in these equations. The numerator of the fraction before the squared brackets represents the effect of a change in ϕ or ζ on the asymptotic size of an individual. The term between the squared brackets represents the effect of a change of the asymptotic size on the fecundity, size and age at maturation of an individual. Note that the terms between squared brackets in both selection gradients are equal. The second term of the selection gradient for the growth curve plasticity deals with the additional costs scaling with plasticity and only occurs if there is a cost for maintaining a plastic or non-plastic growth curve ($c_p \neq 0$). An isocline arises if the selection gradient is equal to zero. If there are no additional costs scaling with plasticity ($c_p = 0$) the second term of the selection gradient for growth curve plasticity is equal to zero. In this case it is clear that the selection gradient for growth curve plasticity is equal to zero ($D_\phi(\tilde{R}) = 0$) if the non-plastic growth scalar is equal to the scaled resource density ($\zeta = f(\tilde{R})$) or if the term between square brackets is equal to zero. Similarly, the

selection gradient for the non-plastic growth scalar is zero ($D_\zeta(\tilde{R})$=0) if the growth curve plasticity is equal to one ($\phi = 1$) or if the term between squared brackets is equal to zero. Setting the term between square brackets equal to zero thus yields a manifold at which the isoclines for the growth curve plasticity and non-plastic growth scalar overlap as long as there are no additional costs for maintaining a plastic or non-plastic growth rate.

Deriving the isoclines becomes somewhat more complicated if additional costs for maintaining a plastic or a non-plastic growth curve are involved ($c_p \neq 0$). It is at least clear that costs increasing with plasticity ($c_g = 1$) decrease the selection gradient for growth curve plasticity ($D_\phi(\tilde{R})$), while costs decreasing with growth curve plasticity ($c_p < 0$) increase the selection gradient for growth curve plasticity ($D_\phi(\tilde{R})$).

We can also derive the derivative of the lifetime reproductive output with respect to the resource density:

$$\begin{aligned}
&\frac{\partial LRO(\tilde{R})}{\partial \tilde{R}} = \frac{\partial LRO(\tilde{R})}{\partial f(\tilde{R})}\frac{\partial f(\tilde{R})}{\partial \tilde{R}} \\
&\frac{\partial LRO(\tilde{R})}{\partial f(\tilde{R})} = \\
&\frac{r_F \ell_\infty}{\kappa}\int_{\tilde{a_J}}^{a_{max}} \left(2\phi\kappa\left(1-e^{-r_B(1-c_t)a}\right)F_r(\tilde{R}) + (1-\phi\kappa)\tilde{\ell}(a)\right)\tilde{\ell}(a)e^{-\mu_b a}da \\
&+ \frac{r_F\phi\ell_\infty\left(\ell_J-\ell_b\right)F_r(\tilde{R})\ell_J^2 e^{-\mu_b a_J}}{r_B(1-c_t)\left(\left(\phi f(\tilde{R})+(1-\phi)\zeta\right)\ell_\infty-\ell_b\right)\left(\left(\phi f(\tilde{R})+(1-\phi)\zeta\right)\ell_\infty-\ell_J\right)} \\
&\frac{\partial f(\tilde{R})}{\partial \tilde{R}} = \frac{R_h}{\left(\tilde{R}+R_h\right)^2}
\end{aligned} \tag{5.18}$$

All terms in the derivative of the lifetime reproductive output with respect to the resource density in equilibrium are positive. This shows that an increase in resource density will always result in an increase in the lifetime reproductive output of an individual.

Now we will consider the change in resource density ($\tilde{R}$), growth curve plasticity (ϕ) and non-plastic growth scalar (ζ) over evolutionary time (τ). We assume that ecological time is relatively fast compared to evolutionary time and therefore assume that the population is always in ecological equilibrium and therefore the lifetime reproductive output is always equal to one ($\tilde{LRO} = 1$). As a consequence, the lifetime reproductive output does not change over evolutionary time and changes in the resource density, growth curve plasticity and non-plastic growth

scalar are always due to evolutionary change:

$$\frac{dL\tilde{R}O}{d\tau} = \frac{\partial LRO(\tilde{R})}{\partial \tilde{R}}\frac{d\tilde{R}}{d\tau} + \frac{\partial LRO(\tilde{R})}{\partial \phi}\frac{d\phi}{d\tau} = 0 \tag{5.19}$$

$$\frac{dL\tilde{R}O}{d\tau} = \frac{\partial LRO(\tilde{R})}{\partial \tilde{R}}\frac{d\tilde{R}}{d\tau} + \frac{\partial LRO(\tilde{R})}{\partial \zeta}\frac{d\zeta}{d\tau} = 0 \tag{5.20}$$

We can rearrange these expressions using the chain rule and the inverse function theorem:

$$\frac{d\tilde{R}}{d\phi} = \frac{\frac{d\tilde{R}}{d\tau}}{\frac{d\phi}{d\tau}} = -\frac{1}{\frac{\partial LRO(\tilde{R})}{\partial \tilde{R}}}\frac{\partial LRO(\tilde{R})}{\partial \phi} \tag{5.21}$$

$$\frac{d\tilde{R}}{d\zeta} = \frac{\frac{d\tilde{R}}{d\tau}}{\frac{d\zeta}{d\tau}} = -\frac{1}{\frac{\partial LRO(\tilde{R})}{\partial \tilde{R}}}\frac{\partial LRO(\tilde{R})}{\partial \zeta} \tag{5.22}$$

Because the derivative of the lifetime reproductive output with respect to the resource density is always positive, these expressions show that a change in resource density due to a shift in a trait value is opposite to the change in lifetime reproductive output. The isoclines studied in this article occur at a maximum of the lifetime reproductive output with respect to the trait value of interest. This maximum in lifetime reproductive output thus corresponds with a minimum in resource density. This shows that evolution in this system minimizes the resource density in the system which can only occur through maximizing the consumption by the consumer population.

Costs as part of the somatic maintenance

It could be argued that costs for plasticity scale with individual body mass and therefore arise as a part of the somatic maintenance costs. The energy dynamics without starvation could then be described as:

$$\frac{d\ell^3}{dt} = \gamma_m \left(\kappa\alpha\left(\phi f(R) + (1-\phi)\zeta\right)\ell^2 - b(1+c_t)\ell^3\right) \tag{5.23}$$

This incorporation of additional costs for plasticity results in a less intuitive implementation of the costs in the individual growth functions, as the maintenance costs both affect the asymptotic size as well as the time constant for growth.

$$\frac{d\ell}{da} = (1+c_t)r_B\left(\left(\phi f(R) + (1-\phi)\zeta\right)\frac{\ell_\infty}{(1+c_t)} - \ell\right) \tag{5.24}$$

This results in the following equation for the length at age in equilibrium:

$$\tilde{\ell}(a) = \ell_b e^{-(1+c_t)r_B a} + (\phi f(R) + (1-\phi)\zeta)\left(1 - e^{-(1+c_t)r_B a}\right)\frac{\ell_\infty}{1+c_t} \tag{5.25}$$

From this expression we can also derive the new expression for the age at maturation under equilibrium conditions:

$$\tilde{a_J} = \frac{1}{(1+c_t)r_B}\ln\left(\frac{\left(\phi f(\tilde{R}) + (1-\phi)\zeta\right)\ell_\infty - (1+c_t)\ell_b}{\left(\phi f(\tilde{R}) + (1-\phi)\zeta\right)\ell_\infty - (1+c_t)\ell_J}\right) \tag{5.26}$$

Because maintenance costs are only paid after the division of energy between somatic processes and reproduction, the equation for the energy surplus of reproduction remains the same:

$$F_r(\tilde{R}) = \left(\phi\frac{(1-\kappa)f(\tilde{R})}{\kappa} + (1-\phi)\left(\frac{f(\tilde{R})}{\kappa} - \zeta\right)\right)\ell_\infty \tag{5.27}$$

This again can be combined with the expression for the lifetime reproductive output:

$$LRO(\tilde{R}) = r_F F_r(\tilde{R})\int_{\tilde{a_J}}^{a_{max}} \tilde{\ell}(a)^2 e^{-\mu_b a} da \tag{5.28}$$

From this model we can derive a new expression for the selection gradient of the degree of growth curve plasticity (ϕ) and the non-plastic growth scalar (ζ) (eq. 5.29 and 5.30).

If we compare these selection gradients to the selection gradients for the situation in which additional costs for maintaining plasticity only affect the growth scalar (eq. 5.17), it is clear that the selection gradient for the non-plastic growth scalar is the same except for the new incorporation of the plasticity costs (c_t). Similarly, the first term in the selection gradient for the level of growth curve plasticity is the same except for the new location of the plasticity costs (5.16). The second term from the selection gradient for growth curve plasticity has an opposite sign compared to the selection gradient in the main article, because the effect of the plasticity costs on the growth scalar changed sign. This new formulation adds a third term, which incorporates the effects of costs for growth curve plasticity on the asymptotic size.

We can create the analogues of figures 5.2 and 5.3 with this alternative model formulation (see fig. 5.4 and 5.5). Comparison shows that costs incorporated as increased somatic maintenance costs show the same evolutionary patterns as costs incorporated as decreased conversion efficiency.

$$D_\phi(\tilde{R}) = \frac{r_F\left(f(\tilde{R})-\zeta\right)\ell_\infty}{T_r(\tilde{R})(1+c_t)LRO_m(\tilde{R})}\left[\int_{\tilde{a_J}}^{a_{max}}\left(2\left(1-e^{-(1+c)r_B a}\right)F_r(\tilde{R})-(1+c_t)\tilde{\ell}(a)\right)\tilde{\ell}(a)e^{-\mu_b a}da\right.$$
$$\left.+\frac{(1+c_t)\left(\ell_J-\ell_b\right)F_r(\tilde{R})\ell_J^2 e^{-\mu\tilde{a_J}}}{r_B\left(\left(\phi f(\tilde{R})+(1-\phi)\zeta\right)\ell_\infty-(1+c_t)\ell_b\right)\left(\left(\phi f(\tilde{R})+(1-\phi)\zeta\right)\ell_\infty-(1+c_t)\ell_J\right)}\right]$$
$$+\frac{(2c_g-1)\,c_p r_F F_r(\tilde{R})}{T_r(\tilde{R})LRO_m(\tilde{R})}\left(\frac{\ell_J^2\tilde{a_J}e^{-\mu\tilde{a_J}}}{(1+c_t)}+2r_B\int_{\tilde{a_J}}^{a_{max}}\left(\left(\phi f(\tilde{R})+(1-\phi)\zeta\right)\frac{\ell_\infty}{(1+c_t)}-\ell_b\right)\tilde{\ell}(a)e^{-\mu a}e^{-(1+c)r_B a}ada\right)$$
$$-\frac{(2c_g-1)\,c_p r_F F_r(\tilde{R})\left(\phi f(\tilde{R})+(1-\phi)\zeta\right)\ell_\infty}{T_r(\tilde{R})(1+c_t)^2LRO_m(\tilde{R})}\left[\int_{\tilde{a_J}}^{a_{max}}2\left(1-e^{-(1+c)r_B a}\right)\tilde{\ell}(a)e^{-\mu a}da\right.$$
$$\left.+\frac{(1+c_t)\left(\ell_J-\ell_b\right)\ell_J^2 e^{-\mu\tilde{a_J}}}{r_B\left(\left(\phi f(\tilde{R})+(1-\phi)\zeta\right)\ell_\infty-(1+c_t)\ell_b\right)\left(\left(\phi f(\tilde{R})+(1-\phi)\zeta\right)\ell_\infty-(1+c_t)\ell_J\right)}\right] \tag{5.29}$$

$$D_\zeta(\tilde{R}) = \frac{r_F\left(1-\phi\right)\ell_\infty}{T_r(\tilde{R})(1+c_t)LRO_m(\tilde{R})}\left[\int_{\tilde{a_J}}^{a_{max}}\left(2\left(1-e^{-r_B(1+c_t)a}\right)F_r(\tilde{R})-(1+c_t)\tilde{\ell}(a)\right)\tilde{\ell}(a)e^{-\mu_b a}da\right.$$
$$\left.+\frac{(1+c_t)\left(\ell_J-\ell_b\right)F_r(\tilde{R})\ell_J^2 e^{-\mu_b\tilde{a_J}}}{r_B\left(\left(\phi f(\tilde{R})+(1-\phi)\zeta\right)\ell_\infty-\ell_b\right)\left(\left(\phi f(\tilde{R})+(1-\phi)\zeta\right)\ell_\infty-\ell_J\right)}\right] \tag{5.30}$$

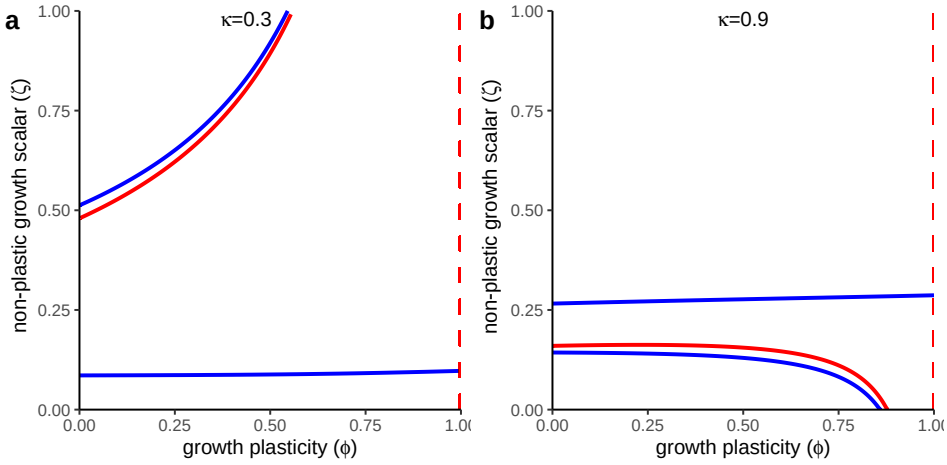

Figure 5.4: Isoclines for the evolution of the growth curve plasticity (ϕ) and the non-plastic growth scalar (ζ) with costs increasing with growth curve plasticity ($c_g = 1, c_p = 0.4$), incorporated as an increase in somatic maintenance costs. Blue and red lines represent evolutionary isoclines for the growth curve plasticity (ϕ) and the non-plastic growth scalar (ζ) respectively. Solid lines represent evolutionary isoclines that are convergent and evolutionary stable for the parameter under consideration. Dashed lines represent evolutionary isoclines that are evolutionary neutral for the parameter under consideration. Incorporating costs as an increase in somatic maintenance results in the same evolutionary patterns as costs incorporated as decreased conversion efficiency (Fig. 5.2).

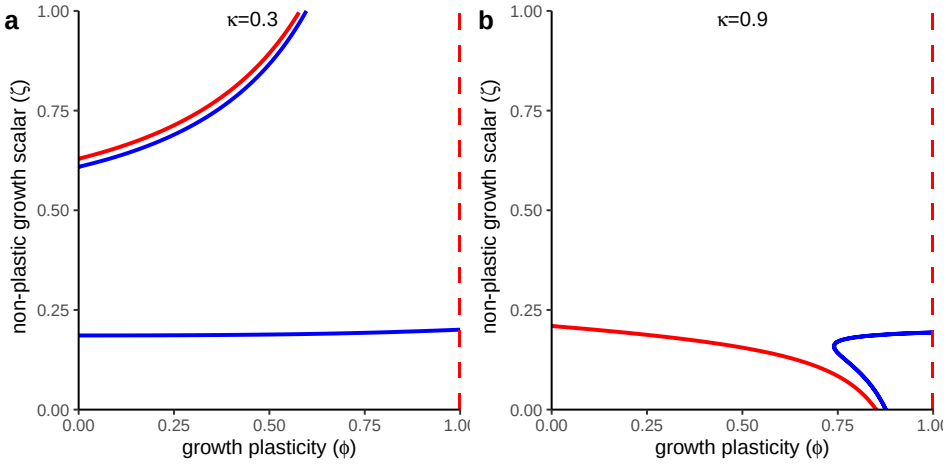

Figure 5.5: Isoclines for the evolution of the growth curve plasticity (ϕ) and the non-plastic growth scalar (ζ) with costs decreasing with growth curve plasticity ($c_g = 0, c_p = 0.4$), incorporated as an increase in somatic maintenance costs. Blue and red lines represent evolutionary isoclines for the growth curve plasticity (ϕ) and the non-plastic growth scalar (ζ) respectively. Solid lines represent evolutionary isoclines that are convergent and evolutionary stable for the parameter under consideration. Dashed lines represent evolutionary isoclines that are evolutionary neutral for the parameter under consideration. Incorporating costs as an increase in somatic maintenance results in the same evolutionary patterns as costs incorporated as decreased conversion efficiency (Fig. 5.3).

Supplementary videos

Supplementary videos show the EBT-simulations for the evolution of the growth curve plasticity (ϕ) and non-plastic growth rate (ζ) for various parameter combinations. The black lines in figures 5.1, 5.2 and 5.3 correspond to the average trait values in the simulations shown in the videos.

Supplementary figures

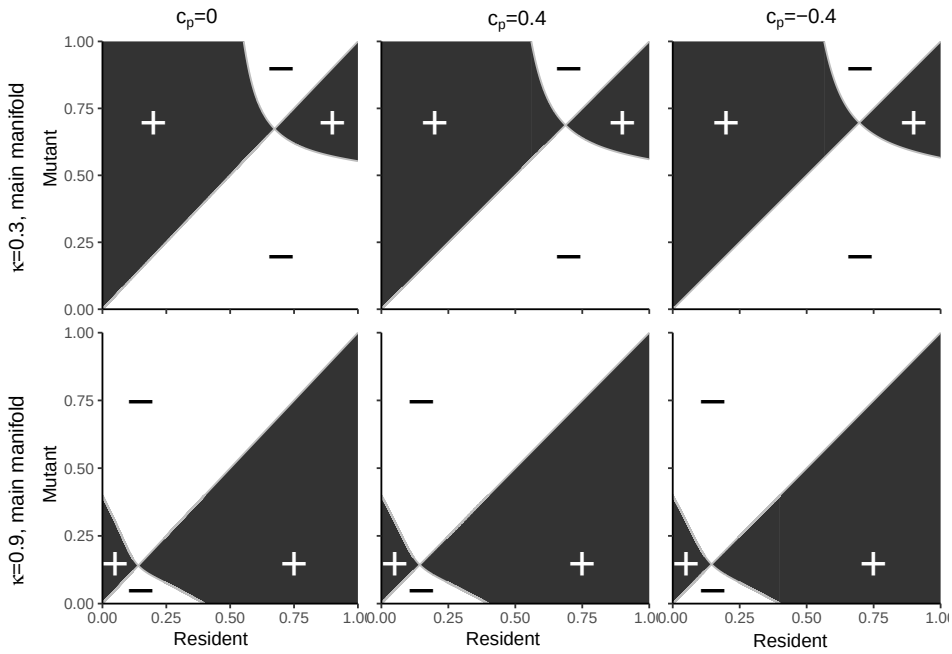

Figure 5.6: Pairwise Invasibility Plots (PIPs) for the non-plastic growth scalar (ζ) at different parameter combinations on the isoclines for growth curve plasticity in figures 5.1 to 5.3. These PIPs only consider evolution for the non-plastic growth scalar and assume a constant value for the growth curve plasticity (ϕ). Grey lines indicate instances at which the invasion fitness of the mutation is equal to zero ($S_m(\tilde{R}) = 0$), while the invasion fitness is positive ($S_m(\tilde{R}) > 0$) in black areas and negative ($S_m(\tilde{R}) < 0$) in white areas. A singular strategy arises if an isocline at which the invasion fitness is equal to zero intersects with the main diagonal. A singular strategy is convergence and invasion stable if the horizontal line through the singular strategy lies within areas with a positive invasion fitness. The singular strategy is evolutionary stable if the vertical line through the invasion fitness completely lies within areas with a negative invasion fitness.

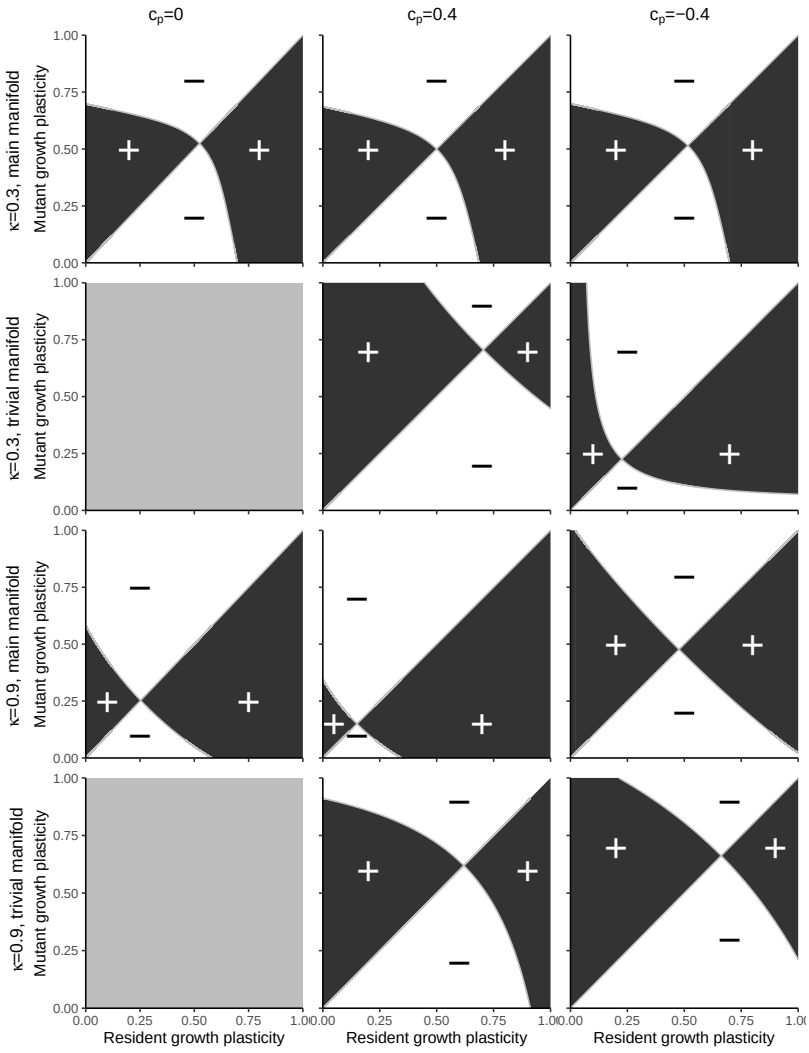

Figure 5.7: Pairwise Invasibility Plots (PIPs) for the growth curve plasticity (ϕ) at different parameter combinations on the isoclines for growth curve plasticity in figures 5.1 to 5.3. These PIPs only consider evolution for the growth curve plasticity and assume a constant value for the non-plastic growth scalar (ζ). Grey lines and areas indicate instances at which the invasion fitness of the mutation is equal to zero ($S_m(\tilde{R}) = 0$), while the invasion fitness is positive ($S_m(\tilde{R}) > 0$) in black areas and negative ($S_m(\tilde{R}) < 0$) in white areas. A singular strategy arises if an isocline at which the invasion fitness is equal to zero intersects with the main diagonal. A singular strategy is convergence and invasion stable if the horizontal line through the singular strategy lies within areas with a positive invasion fitness. The singular strategy is evolutionary stable if the vertical line through the invasion fitness completely lies within areas with a negative invasion fitness.

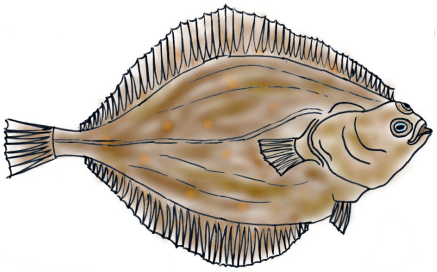

Chapter 6

The consequences of density-dependent individual growth for sustainable harvesting and management of fish stocks

Jasper C. Croll
Tobias van Kooten
André M. de Roos

Submitted manuscript

Abstract

Density dependence is likely to act as a regulatory mechanism in fish stocks that are recovering from overfishing. In general, density dependence in fish stocks is assumed to only occur in reproduction and early life stages and is therefore usually modelled as a stock-recruitment relationship. Recent research shows that density dependence can also reduce individual growth in body size later in life. In this study we show how optimal fishing effort changes with the strength of density dependence in individual growth for four stocks of North Sea flatfish species. Using size-structured population models we show that density dependence arises due to a mechanistic link between the resource availability and life history processes at the individual level. We furthermore show that the stock response to harvesting is either driven by changes in individual reproduction when density dependence in individual growth is weak or by changes in individual growth rate when individual growth is strongly affected by density dependence. These two types or regimes are separated by a sudden shift in dynamics. It is therefore of great importance to account for density dependence in growth when managing fish stocks.

6.1 Introduction

Density dependence is a key factor when establishing sustainable fisheries. Without density-dependent regulation, fish stocks would either exponentially grow or decline, depending on the fishing pressure and environmental conditions. Compensatory density dependence counteracts this exponential change in stock density through negative feedback mechanisms which link individual life history characteristics such as growth, reproduction and mortality to the density of the stock (Herrando-Pérez et al., 2012; Rose et al., 2001). As a consequence, unharvested fish stocks are limited by these density-dependent mechanisms and are expected to fluctuate around a constant density as long as the environment does not show directional changes. Harvesting is expected to lead to a decrease in stock abundance and therefore a change in density-dependent life history rates resulting in an increase of individual biomass production. This is also known as surplus production, which is the additional production by an individual compared to the case without harvesting. Classically, maximum sustainable yield is achieved when the total surplus production of a stock is equal to the additional mortality due to harvesting (Lassen et al., 2014).

In models underlying fishery management, density dependence is almost always assumed to act only in very early life stages. Generally, fish have a very large reproductive output in the form of numerous eggs, while only a small number of these offspring make it to the juvenile life stage. This indicates a high mortality rate in the larval stage, which is attributed to strong density-dependent mortality (May, 1974). Density dependence in early life stages is often summarized with a stock-recruitment relationship, which relates the number of small individuals that are recruited to the population to the current density or biomass of the spawning stock (Rothschild, 2000). The most widely used stock-recruitment relationships are formulated by Beverton and Holt (1957) and Ricker (1954). These relationships try to account for all density-dependent effects in both the reproduction by the stock and the mortality of larvae and juveniles up to the size or age at which individuals enter the explicitly modelled part of the stock. By assuming all density dependence is covered by a stock-recruitment relationship, it is indirectly assumed that larger individuals do not experience density dependence in growth and that they follow a fixed size-at-age trajectory. Recent studies have however shown that a substantial fraction of stocks appears to exhibit density-dependent growth (Zimmermann et al., 2018; Lorenzen, 2016; Schram et al., 2006; Lorenzen and Enberg, 2002).

With stocks increasingly recovering from overfishing (Rindorf et al., 2020; Wang

et al., 2020; Zimmermann and Werner, 2019; Fernandes and Cook, 2013; Worm et al., 2009), density dependence in growth may start to play an important role in the management of exploited fish stocks (Van Gemert and Andersen, 2018a). In addition to density-dependent recruitment, density-dependent growth potentially offers another mechanism to compensate for a decrease in stock biomass due to harvesting. In general, harvesting causes a truncated age distribution, resulting in fewer old and hence large individuals. At the same time, harvesting reduces the density and hence relaxes the density-dependent reduction of growth, causing the exact opposite effect: an increased growth rate. If this response is strong enough, it can even lead to a positive relationship between harvesting intensity and the harvestable biomass in the stock (De Roos et al., 2007). Models assuming density-independent growth might therefore be inappropriate to predict the response to harvesting of a stock with density-dependent growth and the maximum sustainable yield for these stocks. This might be especially important if regulations not only restrict effort but also restrict catches based on length, such as the minimum landing sizes which are widely used in fishery management, because density-dependent growth will strongly affect which part of the individuals of the stock reaches a particular size set for management purposes. Therefore, it is important to understand how optimal harvesting strategies change with the level of density dependence in individual growth.

In this study we explore how the optimal fishing intensity changes with a change in density dependence in individual growth for four North Sea flat fish species. To do so we use a size-structured model in which density dependence arises because individuals feed on the same resource community. The model is derived from a dynamic energy budget model (chapter 4) which specifies the dynamics of individuals given their physiological state and the environment they interact with. Density-dependent growth occurs if individual growth depends on the resource consumption and is therefore plastic. In contrast, growth is density independent and hence non-plastic if it does not depend on the resource consumption. We therefore vary the strength of density dependence in individual growth by changing the level of plasticity in the individual growth rate. Understanding how fishing intensity with maximum sustainable yield changes with the strength of density dependence and the level of plasticity in individual growth provides insight on how to optimize the harvesting of exploited fish stocks.

6.2 Methods

Model description

We use the physiologically structured population model described in chapter 4 to model the harvested fish stocks. The individual dynamics in this model is derived from a Dynamic Energy Budget (DEB) model to ensure closed individual energy dynamics. This DEB model is briefly discussed in the supplementary materials. Density dependence in growth and reproduction arises through the interaction of the stock with a resource community. As a consequence, density dependence in individual growth can be altered by changing the dependence of somatic growth on the individual resource assimilation rate. This creates a gradient ranging from entirely non-plastic growth ($\phi = 0$), in which somatic growth does not depend on the assimilation rate and is therefore density independent, to entirely plastic growth ($\phi = 1$) in which somatic growth fully depends on the assimilation rate and is therefore entirely density dependent. We will use the equilibrium conditions of the model as an approximation of the long term average stock densities from which we calculate total biomass yield, harvested undersized biomass and total harvested biomass. Because individuals do not experience starvation under equilibrium conditions we present a simplified form of the model sufficient to calculate the model equilibria. We provide a more detailed description of the model derivation in the supplementary materials and summarize the model equations below (Table 6.1).

The population model uses a simplified DEB model, describing the energy allocation within an individual (Jager et al., 2013; De Roos et al., 1990), to mechanistically represent the dynamics at the level of an individual. In DEB theory, the energy content of an individual is generally assumed to scale with length cubed (ℓ^3), which allows us to describe feeding, growth and reproduction at the individual level in terms of length. Ingestion is assumed to scale with individual surface area (length squared, ℓ^2), the individual feeding level ($f(R)$ described as a type II functional response of individual feeding on the resource density R) and a proportionality constant (I_{max}) representing the maximum individual ingestion rate per unit surface area. The assimilated energy is subdivided into a part allocated to somatic processes consisting of maintenance and growth and a part allocated to maturation in juveniles or reproduction in adults. In case growth is entirely non-plastic, a fixed amount of energy, determined by a scalar ζ, is allocated to somatic processes. This results in a density-independent growth rate. In case growth is entirely plastic, a fraction κ of the assimilated energy is allocated to somatic processes, resulting in a resource- and density-dependent somatic growth rate (Jager et al., 2013). For intermediate levels of plasticity in growth, the asymptotic size

Table 6.1: Model equations defining the equilibrium dynamics derived in the model described in chapter 4.

Individual dynamics		
Survival	$\frac{\partial s}{\partial a} =$	$-\left(\mu_b + \mu_h(\ell(a))\right) s(a)$
Growth	$\frac{\partial \ell}{da} =$	$r_B \left((\phi f(R) + (1-\phi)\zeta)\, \ell_\infty - \ell(a)\right)$
Harvesting mortality	$\mu_h(\ell) =$	$\frac{F}{1 + e^{-c_s(\ell - \ell_H)}}$
Reproduction	$\beta(R,\ell) =$	$\begin{cases} 0 & \text{if } \ell < \ell_J \\ \frac{r_F}{\kappa}\left(\phi(1-\kappa)f(R) + (1-\phi)\left(f(R) - \kappa\zeta\right)\right)\ell_\infty \ell^2 & \\ & \text{if } \ell > \ell_J \end{cases}$
Characteristics at birth		
Survival	$s(0) =$	1
Growth	$\ell(0) =$	ℓ_b
Stock quantities		
Birthrate	$n(0) =$	$\int_{a_J}^{a_{max}} \beta(R, \ell(a)) n(0) s(a) da$
Consumption	$I =$	$\int_0^{a_{max}} I_{max} f(R) n(0) s(a) \ell(a)^2 da$
Yield	$Y =$	$\int_{a_{min}}^{a_{max}} d_v \mu_h(\ell(a)) n(0) s(a) (\delta_m \ell(a))^3 da$
Undersized catches	$U =$	$\int_0^{a_{min}} d_v \mu_h(\ell(a)) n(0) s(a) (\delta_m \ell(a))^3 da$
Resource dynamics		
Equilibrium condition		$\nu\left(K - R\right) - I = 0$

of an individual is a weighted average of the plastic and non-plastic allocation to growth, weighted by ϕ and $(1-\phi)$, respectively. Individuals grow towards this asymptotic size, which is given by $(\phi f(R) + (1-\phi)\zeta)\,\ell_\infty$, with ℓ_∞ the ultimate length under ad-libidum food conditions and r_B a scalar of the Von Bertalanffy growth rate.

We assume individuals mature and start reproducing at a fixed size (ℓ_J) and in equilibrium individuals reach this size at a specific age a_J. The energy available for reproduction, is the part of the assimilated energy that is not used for somatic growth or maintenance processes. This energy is used by juveniles to mature and

by adults to reproduce. The energy investment in reproduction is scaled with a reproduction scalar (r_F) which captures the conversion from energy to eggs and the mortality during the larval stage, resulting in the individual fecundity (β). This fecundity function defines the adult density and the number of newborn individuals in this model ($n(0)$).

Mortality consists of a constant background mortality (μ_b), and mortality due to fishing ($\mu_h(\ell)$). Fishing mortality equals the product of the fishing effort (F) and the individual catchability (c_ℓ) which is among others determined by the mesh size of the fishing gear. We assume catchability follows a sigmoid function of length:

$$c_\ell = \frac{1}{1 + e^{-c_s(\ell - \ell_H)}} \tag{6.1}$$

In which ℓ_H is the size at which the catchability is half the maximum value and determines the size selectivity of the gear. The parameter c_s determines the steepness of the catchability curve. The harvested individuals are divided into yield which consists of all individuals above the minimum market size (ℓ_{min}) and undersized catches which are all individuals below the minimum market size (ℓ_{min}). In equilibrium, individuals reach the minimum market size at a specific age a_{min}.

We use semi-chemostat dynamics to model an unstructured resource community. We use this type of dynamics to represent a resource community because it is likely to be more realistic than logistic growth dynamics, especially if a part of the resource community is not available for consumption. Semi-chemostat dynamics results in a constant productivity of the resource community (Persson et al., 1998).

Model parametrization

The model is analysed for four North Sea flatfish species: plaice (*Pleuronectes platessa*), flounder (*Platichthys flesus*), dab (*Limanda limanda*) and sole (*Solea solea*) (Table 6.2). These species belong to three separate families and differ strongly in the energy allocation and growth rates. Values for the maximum ingestion rate (I_{max}), plastic growth allocation fraction (κ), maximum age (a_{max}), individual growth parameters (r_B and ℓ_∞) as well as the parameters to convert individual size to individual mass (d_v and δ_m) are derived from DEB parameters reported by Van der Veer et al. (2001). The non-plastic growth scalar (ζ) is set to 0.9 for all species. This is supplemented with values for the size at maturation (ℓ_J) from Fishbase (Froese and Pauly, 2021).

Due to the lack of information about the dynamics of the larval stages, we do not explicitly model the larval stage. Instead, we only explicitly model individuals

Table 6.2: Overview of parameter values for four North Sea flatfish species derived from dynamic energy budget parameters derived by Van der Veer et al. (2001), complemented with values from fishbase (Froese and Pauly, 2021).

Parameter		**Plaice**	**Flounder**	**Dab**	**Sole**	
Growth plasticity	ϕ	0-1	0-1	0-1	0-1	-
Plastic growth allocation fraction	κ	0.85	0.65	0.85	0.9	-
Non-plastic growth allocation scalar	ζ	0.9	0.9	0.9	0.9	-
Size at settlement	ℓ_b	10	10	10	10	mm
Size at maturation	ℓ_J	308	244	214	303	mm
Ultimate size	ℓ_∞	780	560	510	750	mm
Minimum landing size	ℓ_{min}	270	240	230	240	mm
Catchability size selectivity	ℓ_H	270	240	230	240	mm
Steepness of catchability curve	c_ℓ	0.1	0.1	0.1	0.1	mm^{-1}
Fishing effort	F	varied	varied	varied	varied	d^{-1}
Background mortality	μ_b	0.2739	0.2739	0.2739	0.2739	$10^{-3}\mathrm{d}^{-1}$
Growth rate scalar	r_B	0.9257	0.9257	0.9257	0.9257	$10^{-3}\mathrm{d}^{-1}$
Fecundity scalar	r_F	0.0102	0.5903	0.0234	0.7854	$10^{-3}\mathrm{mm}^{-3}\mathrm{d}^{-1}$
Maximum ingestion rate	I_{max}	4.8902	4.7088	3.1190	3.8966	$10^{-9}\mathrm{J\ mm}^{-2}\mathrm{d}^{-1}$
Half saturation constant	R_h	0.978	0.739	1.112	1.571	$10^9\mathrm{J}$
Shape coefficient	δ_m	0.219	0.224	0.213	0.192	-
Volume specific mass	d_v	1	1	1	1	$10^{-9}\mathrm{gmm}^{-3}$
Maximum age	a_{max}	10950	5475	4380	7300	d
Resource growth rate	ν	0.1	0.1	0.1	0.1	d^{-1}
Maximum resource density	K	8.801	6.651	10.007	14.139	$10^9\mathrm{J}$

starting from benthic settlement, which is approximately around 10 mm (Fonds, 1979). In this simplification we assume that the pelagic larvae do not interfere with the dynamics of the benthic population because they do not overlap in space and diet. In contrast to traditional approaches, we ignore density dependence in early life stages, but we do correct for the high mortality during the egg and larval stage by incorporating the survival of the larval stage derived from fishbase (Froese and Pauly, 2021) in the reproduction parameter (r_F).

The background mortality rate for all individuals is set to 0.1 per year, which is a common value in the assessment of fish stocks. The fishing mortality is size dependent and is scaled by the fishing effort (F). Caught individuals are divided into yield, which are all catches above the minimum landing size (ℓ_{min}), and undersized catches, which are all catches below the minimum landing size (European council, 1996). We assume that fishermen try to maximize their yield while minimizing the amount of undersized catches. We therefore set the size-selectivity parameter of the fishing mortality function (ℓ_H) equal to the minimum landing size and assume a steep catchability curve ($c_s = 0.1$).

The parameterization of the resource dynamics (ν and κ) only scales the density of the fish stock and therewith the absolute value of harvested biomass (De Roos et al., 1990). We therefore chose to parameterize the resource dynamics in terms of energy available for the fish stock instead of the number of food items, to avoid unnecessary conversions of quantities. In addition, we parameterized the resource dynamics in such a way that the stock with density-dependent growth and the stock with density independent growth are similar at extreme overfishing and go extinct at exactly the same harvesting intensity. This corresponds to the assumption that extreme overfishing would decrease the stock to a level at which the stock is not influenced by density-dependence. Density dependence will start to affect the stock as soon as fishing mortality decreases as is currently aimed for in many stocks.

Model analysis

The stock is in equilibrium if the resource density (R) and the birthrate of the stock ($n(0)$) are constant. Table 6.1 specifies the equations determining the density and size distribution of the stock in an equilibrium state, which are needed in order to calculate the fishing effort at which the long term maximum sustainable yield is obtained (F_{MSY}). With a constant resource density, the individual size ($\ell(a)$)

and survival ($s(a)$) can be expressed as a function of age:

$$\ell(a) = \ell_b e^{-r_B a} + (\phi f(R) + (1-\phi)\zeta)\left(1 - e^{-r_B a}\right)\ell_\infty \tag{6.2}$$

$$s(a) = e^{-\left(\mu_b a + \int_0^a \mu_h(\ell(a))da\right)} \tag{6.3}$$

The fixed age-size relationship in equilibrium also defines the age at which individuals reach the size at maturation and mature:

$$a_J = \frac{1}{r_B}\ln\left(\frac{(\phi f(R) + (1-\phi)\zeta)\,\ell_\infty - \ell_b}{(\phi f(R) + (1-\phi)\zeta)\,\ell_\infty - \ell_J}\right) \tag{6.4}$$

in a similar fashion, the fixed age-size relationship determines the age a_{min} at which individuals reach the minimum landing size:

$$a_{min} = \frac{1}{r_B}\ln\left(\frac{(\phi f(R) + (1-\phi)\zeta)\,\ell_\infty - \ell_b}{(\phi f(R) + (1-\phi)\zeta)\,\ell_\infty - \ell_{min}}\right) \tag{6.5}$$

If we substitute the expressions for the size and survival at a given age and the age at maturation in the equation for the population birth rate, we obtain an expression for the lifetime reproductive output of an individual:

$$LRO = \int_{a_J}^{a_{max}} \beta(R,\ell)s(a)da \tag{6.6}$$

This represents the expected reproductive output of an individual throughout its lifetime. In equilibrium, every individual should on average replace itself and the lifetime reproductive output should therefore be equal to one. This condition determines the resource density in equilibrium (R). Using the equilibrium values of the resource density (R), the individual size ($\ell(a)$) and survival at age ($s(a)$), an expression for the population birth rate in equilibrium ($n(0)$) can be derived from the equilibrium condition for the resource:

$$n(0) = \frac{\nu(K-R)}{\int_0^{a_{max}} I_{max} f(R) s(a) \ell(a)^2 da} \tag{6.7}$$

With the expressions for the equilibrium conditions we will calculate the yield (Y), undersized catches (U) and several life history characteristics of individuals as a function of the fishing effort (F) for stocks with entirely plastic growth ($\phi = 1$) and entirely non-plastic growth ($\phi = 0$). To do so we will use general root-finding and curve-continuation procedures implemented in C (De Roos, 2021b).

Maximum sustainable yield is obtained at the fishing effort at which the yield

(Y) from the stock is highest (F_{MSY}). The fishing effort with maximum sustainable yield can be obtained by evaluating the derivative of the yield function with respect to the fishing effort:

$$\frac{dY}{dF} = 0 \tag{6.8}$$

This expression is itself dependent on the level of growth plasticity (ϕ). The FindCurve software package (De Roos, 2021b) can be used to explore how the fishing effort with maximum sustainable yield (F_{MSY}) changes with changing levels of growth plasticity.

6.3 Results

Processes determining F_{MSY}

The yield at a given fishing effort depends on various mechanisms affecting the life history of individuals. We compare these mechanisms in a stock with entirely non-plastic ($\phi = 0$) and therefore density-independent growth and a stock with entirely plastic ($\phi = 1$) and therefore density-dependent growth. Here we only discuss the figures of plaice (Fig. 6.1) and flounder (Fig. 6.2). The figures of sole and dab are very similar to the figures of respectively plaice and founder and are therefore added in the supplementary materials (Fig. 6.4 and 6.5).

The yield from a stock (Fig. 6.1 and 6.2, first row) is determined by the harvesting mortality and the stock biomass density above the minimum landing size. The stock biomass density results from the individual mortality (Fig. 6.1 and 6.2, third row) and the population reproductive output (Fig. 6.1 and 6.2, fourth row). The population reproductive output itself depends on the adult density and the resource availability through the relationship between the individual fecundity and the resource density. An increase in fishing effort leads to an increase in the mortality rate up to the minimum landing size (Fig. 6.1 and 6.2, third row) as well as the mortality rate at larger sizes. The increased mortality relaxes competition, which has a positive effect on recruitment. Overall, this results in a dome-shaped relationship between fishing effort and recruitment (Fig. 6.1 and 6.2, fourth row).

The individual growth rate in the stock with plastic growth is lower compared to the stock with non-plastic growth, because it is limited through density-dependent effects (Fig. 6.1 and 6.2, second row). Individuals with plastic growth therefore take longer to reach the minimum landing size and as a consequence have a higher probability of dying before reaching the minimum landing size (Fig. 6.1 and 6.2, third row). The individual growth rate in a stock with non-plastic growth is independent of the environment and therefore does not change with an

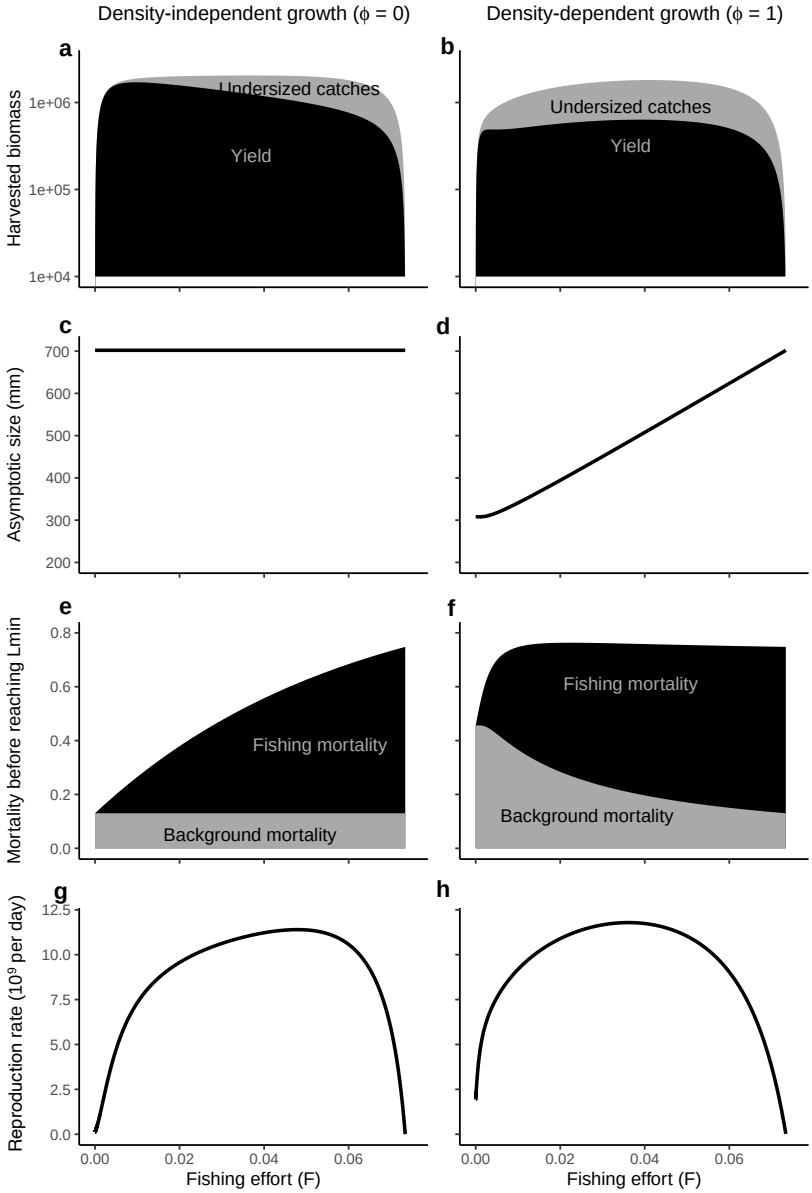

Figure 6.1: Harvested biomass, asymptotic size, mortality before reaching the minimum landing size (ℓ_{min}) and the population reproductive output for a plaice stock with an entirely non-plastic and therefore density-independent individual growth rate and an entirely plastic and therefore entirely density-dependent individual growth rate.

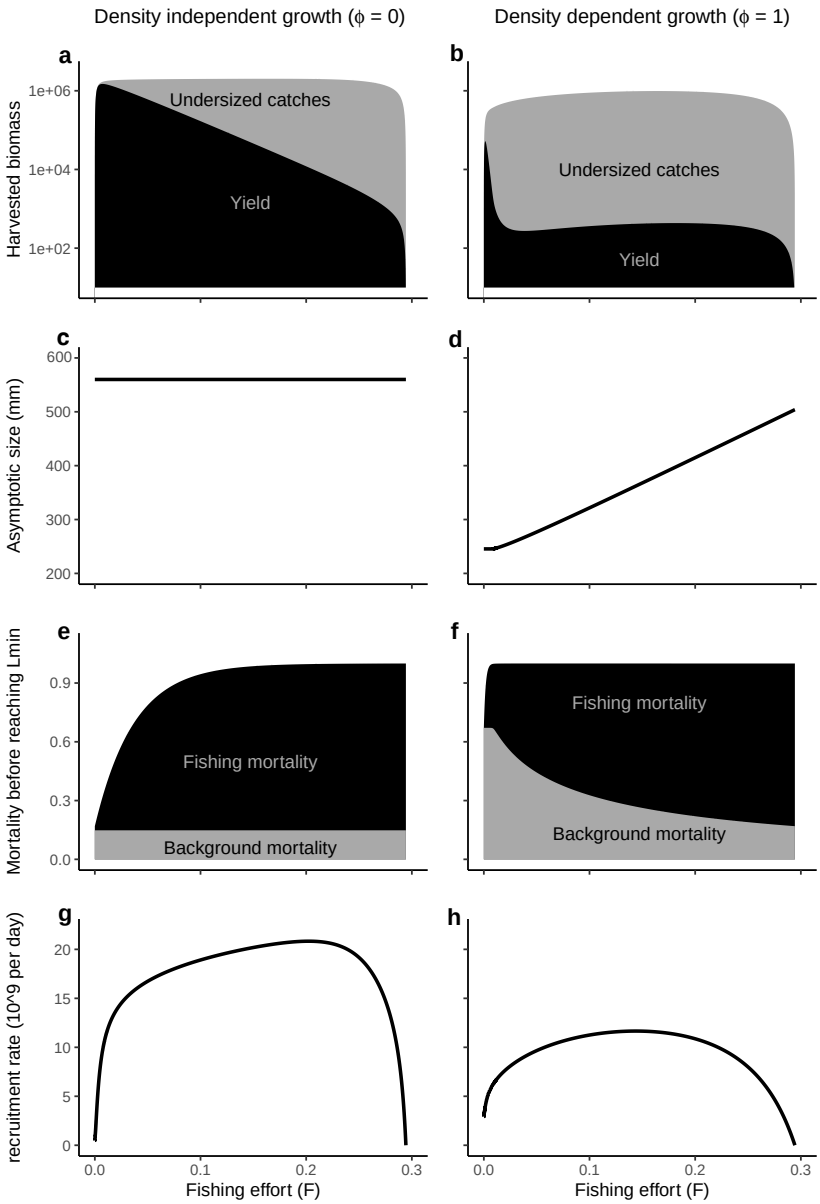

Figure 6.2: Harvested biomass, asymptotic size, mortality before reaching the minimum landing size (ℓ_{min}) and the population reproductive output for a flounder stock with an entirely non-plastic and therefore density-independent individual growth rate and an entirely plastic and therefore entirely density-dependent individual growth rate.

increase in fishing effort (Fig. 6.1 and 6.2, second row). As a consequence, the total background mortality before individuals reach the minimum landing size does not change with fishing effort if growth is non-plastic (Fig. 6.1 and 6.2, third row). In contrast, the individual growth rate in a stock with plastic growth is dependent on the resource density. As an increase in the overall mortality relaxes competition in the stock, the growth rate of individual with density-dependent growth increases with fishing effort (Fig. 6.1 and 6.2, second row). Because individuals grow faster, they reach the minimum landing size at a younger age and therefore with a lower overall background mortality. At intermediate to high fishing effort, the decrease in background mortality balances the increase in mortality due to harvesting and as a consequence, the total mortality up to the minimum harvesting size does not change with fishing effort (Fig. 6.1 and 6.2, third row). Differences in the total mortality and the change in total mortality with fishing effort determine at what fishing effort maximum sustainable yield (F_{MSY}) is achieved. In stocks with non-plastic, density-independent growth, the fishing effort with maximum sustainable yield is determined by the interplay between density-dependent effects as captured by the fecundity-resource relationship and the additional mortality due to fisheries. In the stock with plastic, density-dependent growth, a peak in yield arises at two different values of the fishing effort (Fig. 6.1 and 6.2, fourth row). The peak in yield that arises at very low fishing effort is caused by the same balance between the fecundity-resource relationship and mortality as described for the stock without density-dependent growth. In contrast, at a high fishing effort, the increase in mortality due to fisheries is balanced by an increase in the individual growth rate. As a consequence, a second peak in yield from a stock with entirely plastic growth occurs at the fishing effort for which a peak in recruitment occurs. The maximum yield of a plaice stock with density-dependent growth is obtained at relatively high fishing effort, while the maximum yield of a flounder stock with density-dependent growth is obtained at very low fishing effort. Interestingly, at low fishing efforts the harvested biomass mainly consists of yield while at high fishing efforts the harvested biomass mainly consists of undersized individuals.

F_{MSY} as function of growth plasticity

So far we considered only the two extreme situations of entirely plastic ($\phi = 1$) and entirely non-plastic ($\phi = 0$) growth. It is more likely that growth in fish stocks is largely but not entirely plastic. We therefore calculated how the fishing effort at which maximum sustainable yield of individuals above the minimum market size (F_{MSY}) changes with growth plasticity (Fig. 6.3). The value of the fishing effort at

which maximum sustainable yield occurs can differ an order of magnitude between species and with the level of growth curve plasticity. Despite the quantitative differences, all four species show a comparable pattern over the growth plasticity gradient. The growth plasticity gradient corresponds to a gradient in density dependence in individual growth. This gradient can be split into two regions. In the first region, density dependence mainly affects the population reproductive output and therefore the fishing effort at which maximum sustainable yield (F_{MSY}) occurs is mainly determined by the balance between reproduction and mortality. In other words, the dynamics in this region is driven by changes in reproduction. This region occurs at relatively low growth plasticity. In the second region, density dependence also affects the individual growth rate, which balances the additional mortality due to harvesting. In other words, the dynamics in this region is driven by changes in growth rate. This region occurs at relatively high growth plasticity.

For all species, F_{MSY} is higher in the region with high growth plasticity compared to the region with low growth plasticity (Fig. 6.3). At the intersection of these two regions, an optimum in yield arises at both a high and a low fishing effort, and these optima are separated by a local minimum in yield. Flounder differs from the three other species in that the local minimum does not connect the two optima for maximum sustainable yield (Fig. 6.3b). This pattern arises because for flounder growth is limited by density-dependent effects to such an extent that individuals barely reach the minimum market size. In addition, for plaice and sole, a second local optimum and minimum in yield occurs at relatively low fishing effort for stocks with high density dependence in growth (high growth plasticity, fig. 6.3a and d). Overall, F_{MSY} is lowest on the transition between the distinct regions with high and low growth plasticity and density dependence in individual growth.

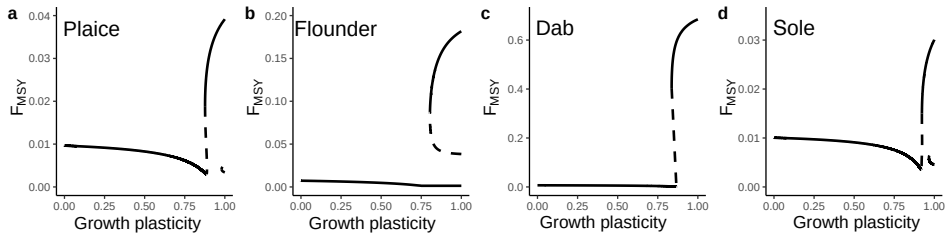

Figure 6.3: The dependence of fishing efforts with maximum sustainable yield (F_{MSY}) on the growth plasticity of four North Sea flatfish species. Lines indicate values of the fishing effort at which the yield is at a maximum value (solid lines) or minimum value (dashed lines).

6.4 Discussion

We modelled four North Sea flatfish species using a model in which we could alter the level of density dependence in individual growth by changing the strength of the growth plasticity. The non-plastic part of growth ($(1-\phi)\zeta$) can be interpreted as a basal growth rate which is always expressed independent of the environment. The plastic part of growth ($\phi f(R)$) represents additional growth on top of the basal growth rate which is only expressed if allowed by the environment. We assumed that the plastic part of growth is determined by the amount of resource available to the stock. As a consequence, the plastic part of growth becomes density dependent because an increase in consumption due to an increase in stock density results in a decrease in the resource density. Although a fixed age-size relationship is often assumed for fish stocks, general energetic theory (Kooijman, 2010) suggests that growth of endothermic species such as fish is largely plastic (high value of ϕ), which corresponds to recent observations of density-dependent growth in several fish stocks (Zimmermann et al., 2018; Lorenzen, 2016; Schram et al., 2006; Lorenzen and Enberg, 2002).

We showed that the gradient of growth plasticity can be divided into a region in which density-dependent effects in individual growth play a minor role in determining the fishing effort with maximum sustainable yield (F_{MSY}) and a region in which density-dependent effects in individual growth play a major role in determining the fishing effort with maximum sustainable yield (F_{MSY}) (Fig 6.3). Maximum sustainable yield arises as a balance between the additional mortality due to harvesting and the increase in biomass production due to the reduction of density-dependent effects. If growth is largely density independent, this balance is fully determined by the harvesting mortality and the stock reproductive output. In contrast, strong density dependence in growth counteracts the effect of increased mortality, which shifts the maximum sustainable yield to higher fishing effort. The occurrence of these two distinct regions shows that the occurrence of density dependence in growth plays a major role in the response of a stock to harvesting.

We have assumed a single resource governed by semi-chemostat dynamics, which feeds the entire fish stock. This is a pragmatic way to implement density-dependent growth. Many fish species gradually change diet or habitat as they grow (Persson et al., 1998), which complicates resource dynamics and can partly decouple density-dependent effects on growth across size ranges. The effects of these additional interactions on the resource availability strongly depend on the diet overlap between and within the species and the connectivity of the resource

community across its habitat. These additional interactions could weaken the density-dependent effects through competition, which affects both growth and reproduction in our model. It is nonetheless unlikely that density-dependent effects would disappear completely due to these additional interactions as density dependence is needed to regulate fish stocks and is indeed observed in many fish stocks (Zimmermann et al., 2018; Lorenzen, 2016; Schram et al., 2006; Lorenzen and Enberg, 2002).

The relationship between the stock and the number of new recruits in our model arises due to the competition for resources and consists of two parts. The first part of this relationship consists of the reproduction rate of adult individuals. Density dependence in this reproduction rate arises due to the dependence of the individual fecundity on the individual resource consumption. Modelling density-dependent effects in reproduction through resource consumption instead of an explicit stock-recruitment relationship enables us to incorporate a more complex and mechanistic description of density dependence. In addition, it allows a direct link between density dependence in reproduction and density dependence in growth through dynamic energy budget theory (Kooijman, 2010). The second part of the relationship between the stock and the number of new recruits in our model arises from the survival up to settlement. Due to the lack of information about the dynamics during the larvae stage, we assume that the survival from egg to settlement can be approximated by a constant value. This is in line with classic stock-recruitment models (Rothschild, 2000; Beverton and Holt, 1957; Ricker, 1954) which map the stock density of one year to the density of recruited individuals in the following year. Strong density dependence during the larval stage would offer another balancing mechanism against the increased harvesting mortality because it would likely flatten the response of recruitment to changes in fishing effort (Fig. 6.1 and 6.2, fourth column). It is likely that this would dampen the effect of a change in fishing effort on the stock biomass which could mask density dependence in fecundity or growth as long as fishing effort would not approach the extinction boundaries of the stock.

The effect of fishing intensity on the size distribution of a stock could provide a first indication whether density-dependent individual growth plays an important role in the dynamics of the stock (Fig. 6.1 and 6.2, second column). Individuals with largely density-independent growth can reach a large size without fisheries. If fishing mortality increases, individuals will be harvested before reaching a large size. Harvesting increases mortality and as a consequence, the size distribution of a stock with density-independent individual growth shifts towards lower sizes if fishing intensity increases. In contrast, individuals with largely density-dependent

growth will, given the same mortality, stay smaller, because growth is limited through competition. Harvesting decreases competition and as a consequence, the size distribution of a stock with density-dependent individual growth shifts towards larger sizes. Such a direct relation between harvesting intensity and an increased growth rate is for example already shown in sole and plaice (Rijnsdorp and Van Leeuwen, 1996; Millner and Whiting, 1996) and could play an important role in the response of the ecosystem to harvesting and predation in both sea and lake systems (Van Leeuwen et al., 2008; Persson et al., 2007; De Roos et al., 2003). Shifts in the size distribution of the stock due to density-dependent growth can act on relatively short timescales. Nonetheless, these patterns are often attributed to fisheries-induced evolution even though evolution tends to act on longer timescales (Andersen and Brander, 2009). More direct measures of evolution, such as the use of genetic markers, could help to disentangle the effects of fisheries-induced evolution and density-dependent effects in individual growth. Nonetheless, the response of the size distribution of the stock to harvesting might be an important first indication of the underlying processes determining the dynamics of the stock, although other factors such as fisheries-induced evolution should be considered when exploring the dynamics of the size distribution of a stock in more detail.

Density-dependent regulation of fish stocks has long been assumed to only occur early in life and hence accounted for by the stock-recruitment relationship, even though it has become increasingly clear that many fish stocks also experience density dependence in growth (Zimmermann et al., 2018; Schram et al., 2006; Lorenzen and Enberg, 2002). Changes towards smaller individuals with a decrease in fishing intensity might give a first indication of density dependence in individual growth. Nonetheless, caution is needed because signs that indicate overfishing in stocks with density-independent growth, such as the absence of large individuals, might indicate the recovery of a stock with density dependence in growth. In addition, stocks with density-dependent growth have a different composition compared to stocks with density-independent growth and therefore have different optimal harvesting strategies. A first step towards more sustainable fisheries is to explore the strength of density dependence in growth and recruitment in more detail. Especially if density dependence has a large impact on the dynamics of the stock, it is important to incorporate this additional mechanism into models for predicting optimal yield. This can only be done by incorporating a descriptive relationship between the stock abundance and the growth rate in a stock assessment model as is for example done by Lorenzen (1996) or by using an ecosystem-based assessment method in which the individual growth rate depends on the food intake as is done in the density-dependent model presented here. Notwithstanding, our

results show that stocks in which density dependence in individual growth is relatively strong exhibit completely different dynamics compared to stocks in which density dependence in individual growth is relatively weak. This strongly affects the fishing strategies with which maximum sustainable yield can be obtained. Understanding and quantifying the mechanisms of density dependence is therefore of vital importance for the sustainable management of fish stocks.

6.5 Supplementary materials

Underlying equations of the dynamic energy budget model

In the underlying Dynamic Energy Budget (DEB) model, individuals are characterized by the energy stored in lean mass (E_m). In DEB theory, it is assumed that energy in lean mass scales with the mass of an individual through the mass specific energy density (d_m). Likewise, the mass is assumed to scale with the volume through the mass density (d_v) and the volume can be related to the length cubed using a shape coefficient (δ_m) (Kooijman, 2010).

All life history processes are expressed in terms of the energy stored in the lean mass of an individual. Energy ingestion is assumed to scale with the surface area of an individual, and thus with lean mass to the power two-third ($E_m^{2/3}$). In addition, the ingestion rate scales with the resource density following a scaled type II functional response ($f(R) = \frac{R}{R_h+R}$), with a half saturation constant R_H. The ingestion rate furthermore scales with the maximum ingestion rate scalar I_{max}, which represents the maximum ingestion rate per unit surface area. If we assume assimilation efficiency is constant, we can express the total assimilated energy as $\alpha f(R) E_m^{2/3}$, in which α represents the maximum ingestion rate per unit surface area times the assimilation efficiency.

The energy dynamics of individuals with plastic growth are based on the DEB model specified by Jager et al. (2013). This model assumes that a fraction κ of the assimilated energy is used for somatic processes, while the remainder of the energy is used for maturation in juveniles and reproduction in adults (E_r). The energy allocated to somatic processes is first used to cover maintenance costs, which scale with the energy stored in lean mass through the energy specific maintenance costs (b). The remainder of the energy allocated to somatic processes is converted to lean mass with conversion efficiency y_m. Likewise, the conversion efficiency of ingested energy to reproductive energy is y_r. This results in the following model

for energy usage within an individual with plastic growth:

$$\frac{dE_m}{dt} = y_m(\kappa\alpha f(R)E_m^{2/3} - bE_m) \tag{6.9a}$$

$$\frac{dE_r}{dt} = y_r(1-\kappa)\alpha f(R)E_m^{2/3} \tag{6.9b}$$

The growth dynamics from this model is density dependent, because the growth in lean mass depends on the energy consumption of the individual and hence on the resource density R, which might be depressed by population foraging (De Roos and Persson, 2002; De Roos et al., 2003). To obtain the growth equation for an individual with density-independent growth, we decouple the energy allocation to somatic processes from energy assimilation, by scaling energy allocation to somatic processes with a constant value (ζ) instead of the scaled resource density. As in the model with density-dependent growth, we assume that all energy not used for somatic growth and maintenance is used for reproduction. This results in the following equation for the growth in lean mass for individuals with density-independent growth:

$$\frac{dE_m}{dt} = y_m(\kappa\alpha\zeta E_m^{2/3} - bE_m) \tag{6.10a}$$

$$\frac{dE_r}{dt} = y_r(\alpha f(R)E_m^{2/3} - \kappa\alpha\zeta E_m^{2/3}) = y_r\alpha(f(R) - \kappa\zeta)E_m^{2/3} \tag{6.10b}$$

We combine the equation for the energy dynamic with and without density dependence in growth. To do so, we assume that the level of plasticity in individual growth is given by a separate parameter (ϕ). This resulted in our final formulation of the individual energetic model:

$$\frac{dE_m}{dt} = y_m\left(\phi\kappa\alpha f(R)E_m^{2/3} + (1-\phi)\kappa\alpha\zeta E_m^{2/3} - bE_m\right) \tag{6.11a}$$

$$\frac{dE_r}{dt} = y_r\left(\alpha f(R)E_m^{2/3} - \left(\phi\kappa\alpha f(R)E_m^{2/3} + (1-\phi)\kappa\alpha\zeta E_m^{2/3}\right)\right) \tag{6.11b}$$

To convert the energy dynamics of a single individual to the dynamics of the entire population, we follow allometric scaling from dynamic energy budget theory (Kooijman, 2000). We assume that the energy stored in lean mass scales with the mass of an individual through the mass-specific energy density (d_m) and likewise the mass scales with the volume through the mass density (d_v) and the volume can be related to the length cubed using a shape coefficient (δ_m).

$$\ell = \frac{V^{1/3}}{\delta_m} = \frac{W^{1/3}}{d_v^{1/3}\delta_m} = \frac{E_m^{1/3}}{d_m^{1/3}d_v^{1/3}\delta_m} \tag{6.12}$$

By using these rules, the equations for the individual energy dynamics can be re-written for individual growth in length ($g(\ell, R)$). To derive the individual fecundity ($\beta(\ell, R)$) from the energy equations we need to know the energy per egg which we estimated by Van der Veer et al. (2001). In addition, we use some composite parameters representing the asymptotic size under unlimited food conditions (ℓ_∞), the Von Bertalanffy growth rate scalar (r_B) and the individual fecundity scalar (r_F):

$$\ell_\infty = \frac{\alpha\kappa}{b d_m^{1/3} d_v^{1/3} \delta_m} \tag{6.13a}$$

$$r_B = \frac{\gamma_m b}{3} \tag{6.13b}$$

$$r_F = \frac{b\gamma_r}{\ell_b^3} \tag{6.13c}$$

This eventually results in the model described in table 6.1.

Supplementary figures

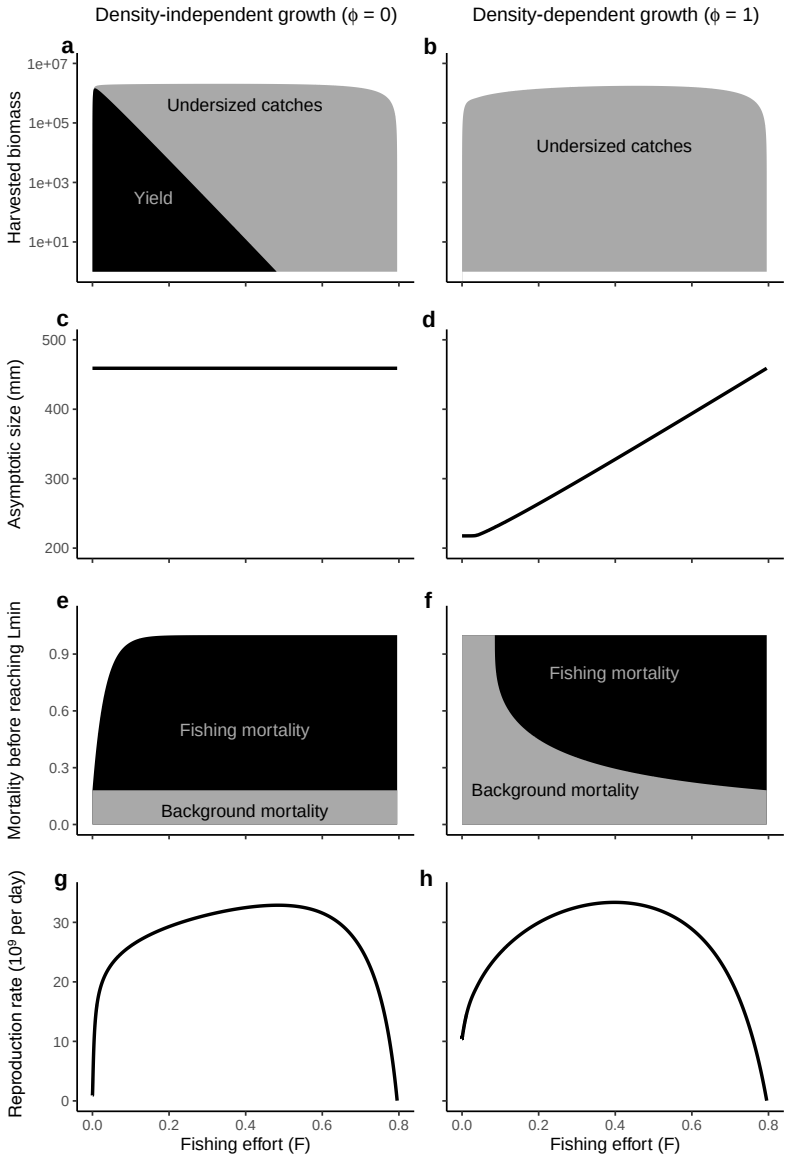

Figure 6.4: Harvested biomass, asymptotic size, mortality before reaching the minimum landing size (ℓ_{min}) and the population reproductive output for a dab stock with an entirely non-plastic and therefore density-independent individual growth rate and an entirely plastic and therefore entirely density-dependent individual growth rate.

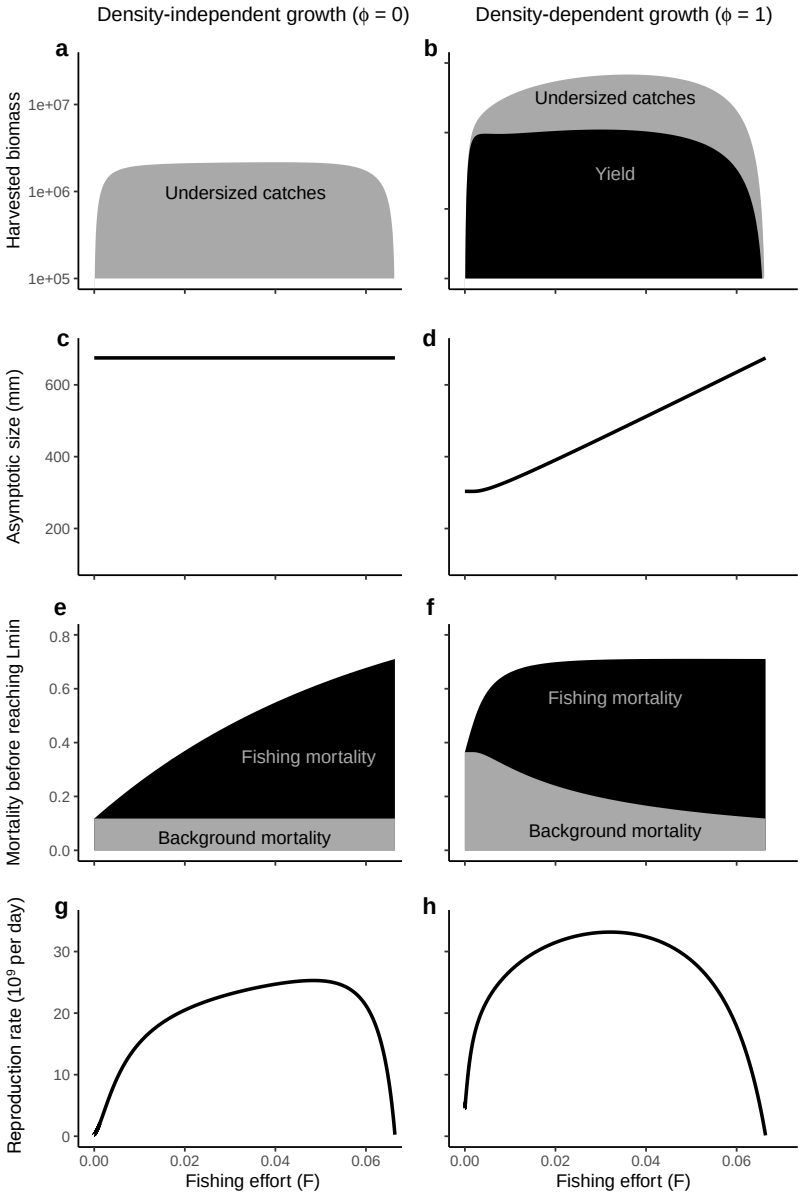

Figure 6.5: Harvested biomass, asymptotic size, mortality before reaching the minimum landing size (ℓ_{min}) and the population reproductive output for a sole stock with an entirely non-plastic and therefore density-independent individual growth rate and an entirely plastic and therefore entirely density-dependent individual growth rate.

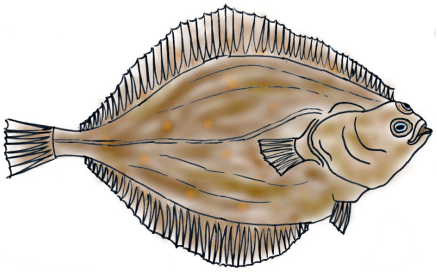

Chapter 7

General discussion

Jasper C. Croll

All organisms grow in size throughout their life. The growth rate of an organism determines its size, which is linked to numerous other life history characteristics such as consumption, maturation, reproduction and survival (Hone and Benton, 2005; Peters, 1983). Variation in the growth rate of individuals will lead to variation in the size of individuals at a given age. Some of this variation in growth might result from the genetic differences between individuals, while some of the variation in growth might arise due to differences in the environment experienced by an individual. Environmental factors that are commonly argued to affect the growth rate of individuals are resource availability and temperature. The level of plasticity in the growth curve of an individual determines the extent to which growth depends on environmental factors. Individuals with a low level of growth curve plasticity will follow a largely fixed growth trajectory, while a substantial part of the growth trajectory of individuals with a largely plastic growth curve is determined by the experienced environment. The growth curves of birds and mammals are often observed to be largely fixed (Albon et al., 2000; Coulson et al., 2000; Skogland, 1986; Perrigo, 1990), while insects, fish, amphibians and reptiles often seem to have a high level of growth curve plasticity (McCauley et al., 1990; Halliday and Verrell, 1988; Köhler and Moyà-Solà, 2009).

Plasticity in growth curves affects many levels of biological organization, ranging from individual energy allocation schemes up to the ecological and evolutionary dynamics of multi-species communities and ecosystems. To understand how growth curve plasticity arises and affects individuals and populations, this thesis considered the effects of growth curve plasticity on several levels of biological organization.

7.1 Individual energetics

Growth in body size requires energy and all energy used to grow cannot be used for other processes such as reproduction. This results in a tradeoff in which different life history processes compete for the available energy. In chapter 4, I constructed a dynamic energy budget model to quantify this tradeoff in energy allocation. This model forms the basis for the ecological and evolutionary analyses in chapters 4 to 6 as well as a more theoretical underpinning for the individual equations in chapter 2. This model assumes that resource availability is the major environmental factor that influences an individual. The model therefore reduces the environment to the dynamics of a single resource. Individuals acquire energy through consumption and assimilation of the resource. The level of growth curve plasticity is altered by changing the dependence of the individual growth rate on the amount of assimi-

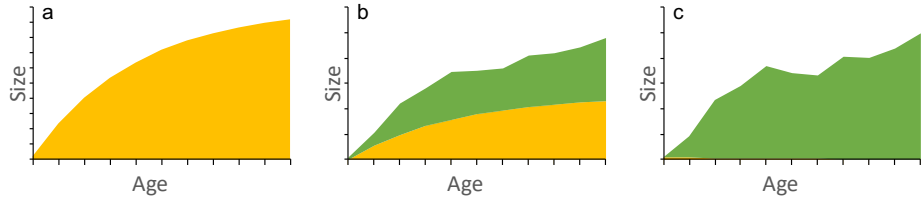

Figure 7.1: Partition of growth into a basal part, which results from a fixed amount of energy allocated to growth (yellow), and an additional part which results from plastic energy allocation to growth when allowed by the environment (green). The composition of growth can shift from entirely fixed (left) to entirely plastic (right).

lated energy. The growth curve of an individual is static if a fixed amount of energy is allocated to growth, while the level of growth curve plasticity increases if the amount of energy available for individual growth becomes more dependent on the amount of assimilated energy. In this formulation, the non-plastic part of growth could be considered as a minimum basal growth rate required by an individual, while the plastic part of growth represents the additional growth allowed by the environment (Fig 7.1). The level of growth curve plasticity then determines which fraction of growth consists of the minimum basal growth rate and which fraction consists of additional environment-dependent growth.

The absolute amount of energy allocated to growth is a central concept in the formulation of the dynamic energy budget model used in this thesis. I chose this as a starting point for the model formulation because this provided a clear direct link between the individual energy allocation scheme and the individual growth curve. Another way to describe the energy allocation of an individual is to quantify the fraction of assimilated energy which is allocated to somatic processes such as growth and maintenance ($\kappa_{realised}$), rather than the absolute amount of energy allocated to these processes. This quantity can be derived easily from equation (4.5):

$$\kappa_{realised} = \left(\phi + (1-\phi)\frac{\zeta}{f(R)}\right)\kappa \tag{7.1}$$

in which ϕ represents the level of growth plasticity, ζ a scalar for the amount of energy reserved for basal growth, $f(R)$ a measure of the total amount of assimilated energy and κ a scalar of the fraction of energy allocated to growth and maintenance. From this equation it is clear that the fraction of energy allocated to growth becomes more dependent on the environment if the level of plasticity in growth decreases. This might seem contradicting at first, but it merely implies that individuals have to deviate from a fractional energy allocation scheme

to maintain a constant growth rate in a fluctuating environment.

Although the dynamic energy budget model used in this thesis is far from all-encompassing, it shows the importance of the tradeoff between individual investment in growth and reproduction. In chapter 4 and 5, I show that this tradeoff arises if two conditions are met:

1. An independent increase in the energy investment in either growth or reproduction should lead to an increase in the total lifetime energy investment in offspring;

2. The total amount of energy available for growth and reproduction combined should be limited, such that an increase in energy allocation to growth is linked to a decrease in energy allocation to reproduction and vice versa.

The first condition ensures that an increase in energy investment in growth or reproduction has a potential benefit for an individual. It is straightforward that an increase in energy investment in reproduction leads to a higher total energy investment in offspring. The link between energy investment in growth and the total lifetime investment in offspring is less clear. An increased investment in growth could lead to maturation at a younger age and higher survival up to maturation and therefore a longer reproductive period. In addition, an increased growth rate is likely to result in a larger individual size at a given age. If energy consumption increases faster with size than the energy required by life history processes other than reproduction, the net amount of energy available for reproduction will increase with size. In our model an increased investment in growth leads to an increase in lifetime energy investment in offspring through all these processes. In general, the occurrence of these mechanisms depends on the exact formulation of the dynamic energy budget model, maturation conditions and metabolic scaling used (Kooijman, 2000; West et al., 2001; Hou et al., 2008; Sousa et al., 2008; Brown et al., 2000).

The second condition for the tradeoff between individual investment in growth and reproduction ensures the link between growth and reproduction which results in the actual tradeoff. This condition relates to one of the basic assumptions of energy budget modelling in which the available energy is limited by assimilation and can only be spent once. Although energy budget models sometimes strongly differ in order and priority of the different processes, they all follow this assumption (Kooijman, 2000; West et al., 2001; Hou et al., 2008; Sousa et al., 2008). This condition also ensures that the tradeoff between growth and reproduction arises independent of the environmental factors that influence growth. Namely, an environmental factor affecting the energy allocation to growth indirectly also affects the

energy availability for reproduction. It is therefore likely that the tradeoff between growth and reproduction plays a role in the dynamics resulting from growth curve plasticity regardless of the specific assumptions made about the energy allocation within an individual and the environmental factors influencing growth.

Unfortunately, individual energy dynamics is often impossible to measure. I therefore translated the energy budget model used in this thesis to equations in terms of individual length using the allometric scaling proposed in dynamic energy budget theory (Kooijman, 2000). As a result, individuals will follow a Von Bertalanffy growth curve in which individuals grow towards an asymptotic size (Von Bertalanffy, 1938). The asymptotic size of this growth curve is likely to fluctuate with the environment, because the asymptotic size is directly linked to individual assimilation rates. Some environmental factors, such as temperature, might influence individual catabolism rates and therefore affect the asymptotic size as well as the rate at which individuals grow towards this asymptotic size. Statistical studies have shown that it is not possible to distinguish fluctuations in the asymptotic size from fluctuations in the growth rate when fitting Von Bertalanffy growth curves to observational data (Eveson et al., 2007; Pilling et al., 2002). In addition, in chapter 5 I show that it does not matter for the evolution of growth curve plasticity whether additional costs for plasticity only affect the asymptotic size of the Von Bertalanffy growth equation or both the asymptotic size and the growth rate. All together this suggests that it does not matter which aspects of the Von Bertalanffy growth equation are affected by plasticity when studying the ecological and evolutionary dynamics of a population.

7.2 Population structure

The structure of a population arises because individuals within a population differ in one or several of their life history characteristics. In this thesis, I considered populations that are structured by age and size. The age of individuals does not depend on the environment and is therefore only used to divide the population into cohorts of individuals that are born at roughly the same moment. The size structure of a population might be more dynamic, depending on the level of growth curve plasticity in the population. In chapter 2, I showed that the variation in the size structure of a population can be considered within a cohort, between cohorts and as a population metric (Fig. 7.2).

A cohort consists of individuals born at the same time and arises if individuals within a cohort have similar life history characteristics. In chapter 2 and 3, I assumed that the sizes within a cohort follow a Gaussian distribution and the size

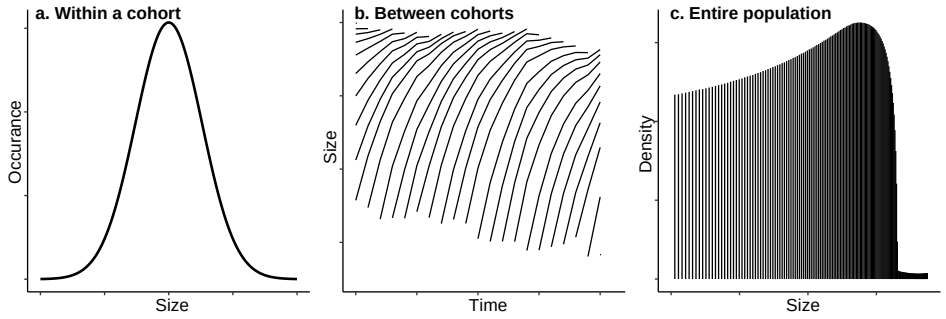

Figure 7.2: Throughout this thesis, size distributions of a population are considered within a cohort (a), between cohorts (b) and for the entire population (c).

structure of a cohort is therefore bell shaped. It is convenient to assume that the size distribution of a cohort follows a Gaussian distribution because in this case only the mean and variance are needed to quantify the exact shape of the distribution. In chapter 2, I showed that the corrected size structure at a given age of North Sea plaice can indeed be approximated by a Gaussian distribution. Nonetheless, it is likely that the size distribution of a cohort will become skewed when individuals grow older, due to size-dependent effects. For fish stocks, size-selective fisheries could be an important factor skewing the size distribution of a cohort. For example, if fisheries would target large fish, it is likely that the size distribution of a cohort shifts towards the smaller individuals because larger individuals have a higher fishing mortality. Starvation mortality could have a similar effect on the size distribution of cohorts. According to the energetic model used in chapter 4 to 6, larger individuals need more energy for maintenance and are therefore more likely to starve due to a lack of resources. As a consequence, the larger individuals of a cohort have a higher probability of dying when resources become scarce. Because of this, variation within a cohort is often neglected in structured population models including the models used in chapter 4 to 6 (De Roos and Persson, 2001; De Roos, 1997). Instead, it is generally assumed that all individuals within a cohort are exactly similar. It would be an interesting challenge to make the models used in this thesis more specific by deriving a quantity for the skewness of the size distribution of a cohort which can account for size-specific effects.

Cohort structures arise if individuals are born at approximately the same time. Cohorts are most distinct if reproductive events are clustered for example due to seasonal reproduction. In structured population models, clustered reproduction can also arise due to population cycles in which maturation or reproduction is

limited by competition for resources as found in chapter 4 and other work on structured population models (De Roos and Persson, 2003; De Roos et al., 1990). The cohort structure of a population vanishes if reproductive events become less discrete or if the time between reproductive events becomes very short. All models in this thesis divide the population into cohorts for mathematical purposes. In chapter 2 and 3 the division in cohorts is very crude as all individuals born in the same year are grouped together. In contrast, reproduction in the simulations in chapter 4 to 6 is almost continuous as a new cohort is formed every day.

The growth curves of cohorts differ if growth is at least partly plastic and the environment fluctuates over time. If growth is entirely static, all individuals would follow the same growth trajectory. Only genetic variation could then cause minor differences in the growth curves of individuals. As a consequence, the average size structure of the population would scale with the age structure of the population and the population could be modelled as an age-structured model in which an individual of a given age has a specific size or size distribution. This approach is commonly used in models for fisheries management (Schnute and Richards, 1998). However, if the environment is fluctuating and growth is at least partly plastic, cohorts can differ in their growth curves. These differences arise because cohorts are born at different points in time and therefore experience different environmental conditions. Models that explicitly take size structure into account are needed to model populations in which growth depends on the environment. In the deterministic models used in chapter 4, fluctuations in the environment only arise due to population dynamic cycles, but in chapter 3, I show that the environment experienced by harvested North Sea fish stocks is never constant.

The level of growth curve plasticity always affects the structure of the entire population, even if the population is in equilibrium and the environment is constant. From chapter 4 it is clear that the size structure of a population is very similar to the age structure of the population if growth is largely fixed. In this case a population consists of both small and large individuals and individuals mature relatively quickly. In contrast, growth is hampered due to competition if growth is largely plastic. As a consequence, individuals stay small and mature late in life resulting in a truncated size distribution of the population (De Roos et al., 1990). From chapter 6 it is clear that this difference in population structure also translates to the yield from exploited fish stocks. Harvesting from a population with largely non-plastic growth yields relatively large and valuable catches. In contrast, harvesting from a population with largely plastic growth often yields small and undersized catches unless the population is heavily over-fished. The level of plasticity in individual growth thus does not only affect the structure of a cohort or

population but even affects the way humans should interact with the population.

7.3 Ecological dynamics

Natural populations never exist in isolation but are always part of a larger ecosystem. One of the most important aspects of the ecosystem are the resources available for a population, regardless of whether these resources consist of inorganic compounds, plants or animals. A consumer population is strongly limited by the amount of resources available in the environment and simultaneously affects the dynamics of the resources through consumption. Understanding and modelling the interactions of consumers and resources has been a recurring topic in ecological research (Hastings, 2020; Berryman, 1992; Tilman et al., 1982; Rosenzweig and MacArthur, 1963). The interaction between consumer and resource is a key factor in the dynamics explored in chapter 4. In this model, the consumer population depletes the resources, which in turn limits the consumer. In this way, two types of dynamics emerge. The first type of dynamics arises if a decrease of the resource density has a larger impact on growth than on reproduction. In this case the population is mainly limited by growth and a bottleneck at maturation occurs. The second type of dynamics arises if reproduction is more limited by a decrease in the resource density than growth. In this case the population suffers from reduced fecundity, resulting in a bottleneck at reproduction. In chapter 6, I show that these limiting mechanisms also drive the response of a consumer population to additional mortality such as harvesting. In chapter 5, I furthermore show that evolution will minimize the limitation in growth and reproduction, resulting in balancing selection. Whether growth or reproduction is more limited by the resources depends on the energy allocation schemes of an individual and especially on the level of growth curve plasticity.

The population dynamic cycles explored in chapter 4 clearly demonstrate how competition can limit a population through growth and reproduction. In both types of cycles, a newborn cohort depletes the resources, which results in an increase in competition within the population. Maturation-driven cycles emerge if competition mainly affects growth and maturation while fecundity-driven cycles emerge if competition mainly affects individual fecundity. Several types of population dynamic cycles have been observed in structured population models. These cycles are often characterized by the amplitude and the period relative to the juvenile delay (Murdoch et al., 2002). Differentiating population cycles based on their amplitude and period might be useful when dealing with field observations, but is not very informative about the mechanisms causing the cycles. For example,

Table 7.1: Overview of cycles occurring in structured population models ordered based on the life stage that is the superior competitor and the life history processes that suffers from the strongest limitation due to competition.

		Superior competitor	
		Juveniles	Adults
Limiting process	Maturation	Maturation-driven cycles / Juvenile-driven cohort cycles	Adult-driven cohort cycles / Parental effect cycles
	Reproduction	Fecundity-driven cycles / Delayed-feedback cycles	Consumer-resource cycles

the fecundity-driven cycles found in chapter 4 are similar to consumer-resource cycles and delayed feedback cycles when considering the cycle period, but differ in the mechanisms causing the cycles (Murdoch et al., 2002; Pfaff et al., 2014; Rosenzweig and MacArthur, 1963). A more insightful way to classify the population dynamic cycles occurring in structured population models would be based on the mechanisms causing the population dynamic cycles. Two important aspects in classifying these cycles are the competitive superior life stage and the life history process that is most strongly affected by competition. A population is often split into juveniles and adults as the two most important life stages. Individuals are born as juveniles and have to mature into adults before they can start reproducing. Maturation and reproduction might therefore be considered as two of the most important processes that can limit a population. In addition, I define the competitive superior life stage as the life stage which can persist on the lowest resource density and therefore is able to deplete the resources to the lowest level. Which life stage is superior depends on the minimum amount of resources that an individual in a specific life stage needs to persist and the rate at which an individual in a specific life stage can acquire these resources from the environment. Population dynamic cycles in structured populations could be classified by considering the superior life stage and the life history process that is most strongly affected by competition (Table 7.1).

In the model used in chapter 4 juveniles are always competitively superior to adults. In this model, individual maintenance costs increase faster with size than the individual ingestion rate. Larger individuals therefore need more energy to cover maintenance costs than small individuals, while they acquire the resources to

do so at a relatively slower rate. Because juveniles are smaller than adults, juveniles can persist on a lower resource density and therefore are competitively superior. This corresponds to the observation that the resources are depleted after a large cohort of juveniles is produced. The maturation-driven cycles found in chapter 4 arise because growth and therefore maturation is limited by a lack of resources. These cycles are previously described as juvenile-driven cohort cycles (De Roos et al., 1990, 2003). Interesting to note is that the term juvenile-driven cohort cycles emphasizes the competitive superior life stage while the term maturation-driven cycles emphasizes the limited life history process. The fecundity-driven cycles found in chapter 4 arise because competition limits the reproduction by adults. The dynamic characteristics of these cycles are very comparable to previously described delayed feedback cycles (Pfaff et al., 2014; Gurney et al., 1983; Gurney and Nisbet, 1985). The major difference between the fecundity-driven cycles described in chapter 4 and delayed-feedback cycles is the way competition affects fecundity. In fecundity-driven cycles, an external resource is reduced by juveniles. As a result, reproduction by adults is directly reduced and remains low until the resource recovers. In delayed-feedback cycles, competition affects some endogenous character of an individual during the juvenile stage which then affects reproduction of that specific individual later in life. The major difference between fecundity-driven cycles and delayed-feedback cycles is thus whether the effect of competition is conveyed through an exogenous or endogenous factor and therefore affects either the entire population or only specific individuals.

Cycles can also emerge if adults are competitively superior. Cycles in which adults are competitively superior but competition mainly affects maturation are previously described as adult-driven cohort cycles (De Roos et al., 2003; De Roos and Persson, 2003). In these cycles, adults are competitively superior because they can persist at a lower resource density. In these models an adult cohort constantly reproduces but simultaneously depresses the resource density such that juveniles cannot mature. Similar to fecundity-driven cycles, these adult-driven cohort cycles are based on exogenous factors to convey the effect of competition. Cannibalism is another example of an exogenous way in which adults can affect juveniles, which can lead to population dynamic cycles (Claessen et al., 2004). Herein adults are the superior life stage because juveniles function as an additional resource for adults, while the limiting life history process is reproduction because an increased adult density decreases the probability of a juvenile to survive up to maturation. An endogenous mechanism that can convey effects from adults to juveniles would result in parental effects, which is indeed hypothesized to cause population dynamic cycles (Inchausti and Ginzburg, 2009). To my know-

ledge, cycles in which adults are competitively superior and competition mainly affects reproduction have not been observed in structured population models. One could argue that classic consumer-resource cycles fall into this category, because these cycles arise in models which only model reproducing adults without a delay or structure (Rosenzweig and MacArthur, 1963). However, it is important to note that classic consumer-resource cycles only arise if the resource can periodically escape the control of the consumer. This might indicate that a combination of a competitively superior adult stage and competition-limited reproduction is insufficient to cause population dynamic cycles without additional mechanisms. It is clear that the classification proposed here does not provide an all-inclusive framework for classifying population dynamic cycles. Other processes such as seasonality, stochastic environments, community dynamics and evolution might cause cycles as well (Barraquand et al., 2017). Nonetheless, I want to emphasize that it is important to consider the mechanisms causing population dynamic cycles rather than only using descriptive statistics when classifying cycles. The classification proposed here could provide a start in the context of structured populations.

Obviously consumers and resources are not the only components of an ecosystem. Individuals have to deal with many different resources and might interact with other species through multiple processes such as competition and predation simultaneously. For example, in chapter 3 I show that some North Sea fish species with a similar ecology also experience the environment in a more similar way which suggests that they are also strong competitors. As a consequence, the dynamics of ecosystems become vastly complex. One way to tackle this complexity is by simplifying the size-structured models to stage-structured models with juveniles and adults. With these simplified models it has been shown that size-structure and plasticity in growth can facilitate coexistence of competitors and persistence of higher trophic levels (De Roos et al., 2008; Van Leeuwen et al., 2008). These patterns arise because predation and consumption decrease the competition between prey species, which will change the size structure of the prey population if growth is largely plastic. The shift in size distribution of the prey enables the persistence of an additional competitor or top-predator which benefits from the shifted structure of the prey population. In chapter 6 I showed that the same mechanisms determine the yield from a fish stock with largely plastic growth, resulting in high yield at high fishing intensities. It has even been shown that communities in which all species are plastic in the maturation rate are more stable and can contain more species compared to communities in which the juvenile-adult ratio is fixed (De Roos, 2021a). It is still an open question whether size structure can facilitate the persistence of multiple competitors, top-predators and large communities

if growth of some of the species is partly or entirely non-plastic.

7.4 Improving fisheries management

Chapter 2, 3 and 6 of this thesis are framed in the context of harvested fish stocks and use data and parameters from exploited fish species. Relatively recent developments in the management of fish stocks make the results from this thesis especially relevant for the field of fisheries management. Due to increased and strict management, numerous stocks show signs of recovering from over-fishing (Zimmermann and Werner, 2019; Cardinale et al., 2013; Fernandes and Cook, 2013; Hutchings et al., 2010; Worm et al., 2009). When recovering, fish stocks will increase in density and as a consequence competition between individuals within a stock will increase. To accurately predict the effect of increased competition on the fish stocks, it is important to understand which life history processes are mostly affected by competition (Van Gemert and Andersen, 2018a). Traditional methods for modelling fish stocks use a stock-recruitment relationship to model density dependence, in which the number of new individuals entering the stock is related to the number of reproducing adults in the stock (Rothschild, 2000; Beverton and Holt, 1957; Ricker, 1954). This assumes that only reproduction and recruitment are limited by the environment, while numerous stocks have shown signs of density dependence in other life history processes as well (Zimmermann et al., 2018; Lorenzen, 2016; Lorenzen and Enberg, 2002). The results from chapter 6 show that it cannot be determined whether a fish stock is limited by growth or reproduction as long as the stock is over-fished. Nonetheless, growth-limited stocks and reproduction-limited stocks will become very different as soon as fishing intensity decreases. It is therefore important to keep a close eye on the dynamics of recovering fish stocks and adjust the models used for management purposes accordingly.

The results from chapter 3 show that the growth curves of North Sea fish stocks are very variable. Both the mean and variance in the size-at-age differ strongly between years. Classic models for establishing fisheries reference points are based on individual ages instead of sizes and therefore do not allow for fluctuations in the size-at-age distribution over time. As a consequence, a fixed size distribution is assumed for every age. A first improvement of these models would be to assume a separate size distribution for every cohort in every year. For most exploited fish species it is unlikely to have sufficient data to fit an independent size distribution for every cohort in every year. Instead, the model proposed in chapter 2 can be used. This is a descriptive model which fits a size distribution for every cohort

in every year while taking into account the size distributions of other cohorts and years. In this way the number of parameters that needs to be estimated is reduced and the model can provide an interpolation for cohorts with missing data. The model in chapter 2 is developed as a descriptive model for the dynamics of the size-structure of a population. The changes in the size distribution of cohorts are summarized in two variables representing the environmental impact on the growth curves of cohorts and individuals. These two variables need to be extrapolated to make predictions about the future structure of a population. It is likely that a variable size distribution for every cohort will improve the predictions of fisheries management models substantially because many factors in fisheries, such as the catchability of an individual, are related to the size of individuals.

Models for fisheries management can furthermore be improved by incorporating a description of the environmental dynamics. In this way, the environment does not only affect the dynamics of a fish stock, but the stock also affects the dynamics of the environment. If the growth model described in chapter 2 is coupled to a dynamic description of the environment, it becomes very similar to the model used in chapter 6. Models used for fisheries management might be a bit more complex compared to the models in chapter 6, for example due to a more complex description of the environment or the stock recruitment relationship. Nonetheless, the model in chapter 6 provides useful insight in the response of fish stocks to harvesting. The model for example shows that changes in the competition within a stock could affect the size distribution of a stock through the environment. As a consequence, it is likely to achieve maximum sustainable yield at a higher fishing intensity if growth is largely plastic compared to a situation in which growth is largely static. In addition, it might be beneficial to target the most abundant or most competitive life-stage of a stock to reduce the competition within the stock, because this allows the remaining individuals to grow faster and reproduce more. For some stocks this might imply that fisheries should also target small juvenile individuals. This is against common fisheries policies aimed to reduce the mortality of small undersized individuals. Nonetheless, the optimal harvesting strategies are likely to be highly species-specific and can only be considered by including a dynamic size-structure and a dynamic description of the environment. Including these factors in fisheries management models would therefore be an interesting step to improve fisheries management.

Meanwhile, fisheries management is slowly changing from a single-species perspective to a multi-species perspective. This change arose from the realization that many stocks in an ecosystem interact and harvesting of one species is likely to affect other species as well. The proposed approaches range from combining data

from multiple species in one statistical model to multi-species models and models in which individuals are only ordered by a trait and not by species (Jardim et al., 2021; Säterberg et al., 2019; Trochta et al., 2018; Andersen et al., 2015). It is important to consider interactions between multiple species and the environment, but these models require extensive knowledge about the ecological connections between species and the way species interact with the environment (Birkenbach et al., 2020; May et al., 1979). Information on these interactions is often difficult or time-consuming to acquire. In chapter 3, I show that trends in growth curves contain information about the experienced environment of a population. Ecologically similar species tend to be more similar in the dynamics of the size-at-age structure. Summary statistics of the variation in growth might therefore be a useful indicator of the ecological relatedness of species. One of the main advantages of using growth curves to indicate ecological relatedness is the availability of data. Size and age measurements are widely collected for many species through surveys and are already used for the assessment of many species. Using this data to construct the ecological relatedness thus does not require additional surveys or measurements. Variation in growth could therefore become a central concept in understanding and gaining information about the ecological dynamics and interactions of harvested fish stocks.

7.5 Evolutionary dynamics

Taxa in the animal kingdom differ vastly in the level of growth curve plasticity. It is tempting to divide these taxa into two extreme categories consisting of species with a very plastic growth curve and species with an entirely fixed growth curve. Insects (McCauley et al., 1990), fish (Zimmermann et al., 2018; Lorenzen and Enberg, 2002), amphibians and reptiles (Halliday and Verrell, 1988) are observed to have a high level of plasticity in their growth curve, while the growth curves of mammals and birds are thought to be largely fixed (Perrigo, 1990; Albon et al., 2000; Coulson et al., 2000; Clutton-Brock et al., 1987; Festa-Bianchet et al., 1995; Skogland, 1986). A common consensus is therefore that the growth curve of endotherms is fixed while the growth curve of ectotherms is largely plastic. This is in contrast to the results in chapter 5 which predict that a whole range of intermediate levels of growth curve plasticity can be found in nature. This mismatch between observations and predictions could occur because some mechanisms might mask a part of the plasticity in growth curves. For example, endotherms have a high metabolic rate and are therefore expected to live in environments with a high and constant resource availability (Nagy, 2005; Clarke, 2019). The plasticity in growth

curves would be less visible if the resource availability is relatively constant. Individuals could also show behaviour that increases or decreases the ingestion rate under specific conditions. By actively changing their ingestion rate, individuals can regulate the amount of energy available for growth, which could result in a constant growth rate, even if the underlying energy allocation mechanisms allow for plastic growth (Kooijman, 2000). Interesting to note is that behaviour could only mask plasticity in growth if there are sufficient resources available in the environment, which might not always be the case. Experiments in which individuals are grown or starved on various resource levels are needed to determine the actual level of growth curve plasticity of an individual.

It is interesting to speculate how differences in growth curve plasticity between endotherms and ectotherms might arise even if these differences are less distinct than suggested. In general, endothermic individuals are able to regulate their body temperature independent of the environment, while the body temperature of ectothermic individuals always depends on environmental factors. Birds and mammals are the primary examples of endothermic individuals because they maintain a very constant body temperature, but some insects, fish and reptiles have been shown to regulate their body temperature independent of the environment as well (Ciezarek et al., 2019; Zermoglio et al., 2018; Seymour et al., 2009; Dickson and Graham, 2004). Meanwhile, the processes that drive the evolution of endothermy itself are unclear and many factors ranging from increased aerobic activity to increased parental care are suggested to influence the evolution of endothermy (Farmer, 2000; Bennett and Ruben, 1979; Ruben, 1995). Endothermy might even be a by-product of the optimization of the energy balance of an individual, just like the evolution of growth curve plasticity in chapter 5 (Seebacher, 2020).

The major difference between endotherms and ectotherms is the degree in which the internal environment of an individual depends on the external environment. The internal environment of ectotherms strongly depends on the external environment. It might therefore be costly for ectotherms to decouple their growth rate from the external environment. On the other hand, the internal environment of endotherms is already decoupled from the external environment. It might therefore be costly for endotherms to monitor the external environment and make their growth rate plastic. In this case, the model in chapter 5 predicts that evolution would slowly drive ectotherms towards a higher level of growth curve plasticity, while endotherms are driven to a lower level of growth curve plasticity. This is in line with the observation that the growth rate of large fossil mammals was at least partly plastic, while the growth rate of modern mammals seems almost entirely static (Köhler and Moyà-Solà, 2009).

A high and constant body temperature is of vital importance for the survival and functioning of endotherms. As a consequence, endothermic individuals spend a substantial amount of energy on the production of heat (Nagy, 2005; Clarke, 2019). In the model used in chapters 4 and 5 this would translate to high somatic maintenance costs. For endotherms, it might therefore be especially important to ensure a sufficient energy supply to these somatic processes, even in a strongly fluctuating environment. One way to do so is by fixing the energy allocation to somatic processes including growth. Under these conditions, fluctuations in the environment would only result in strong fluctuations in reproductive output as observed in many ungulate species (Perrigo, 1990; Albon et al., 2000; Coulson et al., 2000; Clutton-Brock et al., 1987; Festa-Bianchet et al., 1995; Skogland, 1986). This furthermore predicts that high somatic maintenance costs in combination with a strongly fluctuating environment would result in evolution towards a low level of growth curve plasticity. It would be very interesting to test this prediction with the models used in chapter 5 as well as observations on individual energy expenses. In addition, a more detailed understanding of the mechanisms underlying the energy allocation to physical processes such as growth and heat production is needed to disentangle the relation between growth curve plasticity and endothermy. Until then, it is unclear whether a low level of growth curve plasticity evolves due to endothermy or whether endothermy and the level of growth curve plasticity are both just the result of the evolutionary optimization of individual energy dynamics.

7.6 Conclusion

Growth curve plasticity is the extent to which the growth rate of an individual depends on environmental factors such as the resource availability. The level of growth curve plasticity is determined by an underlying individual energy allocation scheme. Endothermic species are often assumed to have a largely fixed growth rate while ectothermic species are generally expected to have a higher level or growth curve plasticity. Similarly, theoretical models often assume that growth is entirely fixed or entirely plastic, while evolutionary analysis of the level of growth curve plasticity suggests that these extremes are unlikely to occur in nature. The level of growth curve plasticity might rather be at some intermediate value.

The level of growth curve plasticity strongly affects the growth curves of individuals and therewith the variation in size within and between cohorts as well as the size structure of the entire population. Variation in growth can therefore be used as an indicator of the environment experienced by a population. This might be useful in for example fisheries management, because information about

the ecological relatedness of stocks is often missing while size and age data is often sufficiently available from surveys.

Meanwhile, growth and individual size are linked to numerous life history characteristics determining the dynamics of a population. Because growth curve plasticity is determined by the energy allocation scheme of an individual, it causes a tradeoff between energy investment in growth and energy investment in reproduction. As a consequence, either maturation or individual fecundity is limited by the environment and eventually determines the dynamics of the population. Populations limited by maturation and fecundity strongly differ in the response to external influences such as harvesting and the type of population dynamic cycles that can emerge. The level of growth curve plasticity and the individual life history processes that limit the population are therefore central in understanding the dynamics of structured populations.

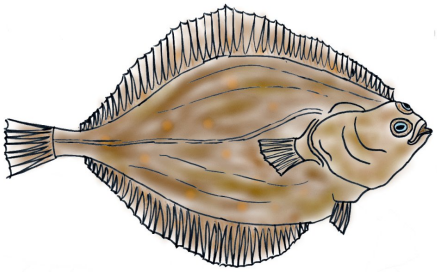

Bibliography

Albon, S. D., Coulson, T. N., Brown, D., Guinness, F. E., Pemberton, J. M., and Clutton-Brock, T. H. (2000). Temporal changes in key factors and key age groups influencing the population dynamics of female red deer. *Journal of Animal Ecology*, 69(6):1099–1110.

Allendorf, F. W. and Hard, J. J. (2009). Human-induced evolution caused by unnatural selection through harvest of wild animals. *Proceedings of the National Academy of Sciences*, 106:9987–9994.

Amundsen, P.-A. and Sánchez-Hernández, J. (2019). Feeding studies take guts–critical review and recommendations of methods for stomach contents analysis in fish. *Journal of Fish Biology*, 95(6):1364–1373.

Andersen, K. H. and Brander, K. (2009). Expected rate of fisheries-induced evolution is slow. *Proceedings of the National Academy of Sciences*, 106(28):11657–11660.

Andersen, K. H., Brander, K., and Ravn-Jonsen, L. (2015). Trade-offs between objectives for ecosystem management of fisheries. *Ecological Applications*, 25(5):1390–1396.

Auld, J. R., Agrawal, A. A., and Relyea, R. A. (2010). Re-evaluating the costs and limits of adaptive phenotypic plasticity. *Proceedings of the Royal Society B: Biological Sciences*, 277(1681):503–511.

Baas, J., Augustine, S., Marques, G. M., and Dorne, J.-L. (2018). Dynamic energy budget models in ecological risk assessment: from principles to applications. *Science of the Total Environment*, 628:249–260.

Barraquand, F., Louca, S., Abbott, K. C., Cobbold, C. A., Cordoleani, F., DeAngelis, D. L., Elderd, B. D., Fox, J. W., Greenwood, P., Hilker, F. M., et al. (2017). Moving forward in circles: challenges and opportunities in modelling population cycles. *Ecology letters*, 20(8):1074–1092.

Basimi, R. A. and Grove, D. J. (1985). Estimates of daily food intake by an inshore population of *Pleuronectes platessa* L. off eastern Anglesey, North Wales. *Journal of Fish Biology*, 27(4):505–520.

Bennett, A. F. and Ruben, J. A. (1979). Endothermy and activity in vertebrates. *Science*, 206(4419):649–654.

Berryman, A. A. (1992). The orgins and evolution of predator-prey theory. *Ecology*, 73(5):1530–1535.

Beverton, R. J. H. (1998). Fish, fact and fantasy: a long view. *Reviews in Fish Biology and Fisheries*, 8(3):229–249.

Beverton, R. J. H. and Holt, S. J. (1957). *On the dynamics of exploited fish populations*. Fish and Fisheries series 11. Springer Science & Business Media.

Beverton, R. J. H. and Holt, S. J. (1959). A review of the lifespans and mortality rates of fish in nature, and their relation to growth and other physiological characteristics. In Wolstenholme, G. E. W. and M., O., editors, *Ciba foundation symposium-the lifespan of animals (colloquia on ageing)*, volume 5, pages 142–180.

Birkenbach, A. M., Cojocaru, A. L., Asche, F., Guttormsen, A. G., and Smith, M. D. (2020). Seasonal harvest patterns in multispecies fisheries. *Environmental and Resource Economics*, 75(3):631–655.

Blanckenhorn, W. U. (2000). The evolution of body size: what keeps organisms small? *The quarterly review of biology*, 75(4):385–407.

Bonner, J. T. (2006). *Why size matters*. Princeton University Press.

Braber, L. and De Groot, S. J. (1973). The food of five flatfish species (Pleuronectiformes) in the southern North Sea. *Netherlands Journal of Sea Research*, 6(1-2):163–172.

Brännström, Å., Johansson, J., and Von Festenberg, N. (2013). The hitchhiker's guide to adaptive dynamics. *Games*, 4(3):304–328.

Britten, G. L., Duarte, C. M., and Worm, B. (2021). Recovery of assessed global fish stocks remains uncertain. *Proceedings of the National Academy of Sciences*, 118(31):e2108532118.

Bromley, P. J., Watson, T., and Hislop, J. R. G. (1997). Diel feeding patterns and the development of food webs in pelagic 0-group cod (*Gadus morhua* L.), haddock (*Melanogrammus aeglefinus* L.), whiting (*Merlangius merlangus* L.), saithe (*Pollachius virens* L.), and norway pout (*Trisopterus esmarkii* Nilsson) in the northern North Sea. *ICES Journal of Marine Science*, 54(5):846–853.

Brown, J. H., Gillooly, J. F., Allen, A. P., Savage, V. M., and West, G. B. (2004). Toward a metabolic theory of ecology. *Ecology*, 85(7):1771–1789.

Brown, J. H., West, G. B., and Enquist, B. J. (2000). Scaling in biology: patterns and processes, causes and consequences. volume 87 of *Santa Fe Institute Studies on the sciences of complexity*. Oxford University Press.

Cadrin, S. X. (2020). Defining spatial structure for fishery stock assessment. *Fisheries Research*, 221:105397.

Calder, W. A. (1984). *Size, function, and life history*. Harverd University Press.

Cardinale, M., Dörner, H., Abella, A., Andersen, J. L., Casey, J., Döring, R., Kirkegaard, E., Motova, A., Anderson, J., Simmonds, E. J., et al. (2013). Rebuilding EU fish stocks and fisheries, a process under way? *Marine Policy*, 39:43–52.

Castanet, J. (1994). Age estimation and longevity in reptiles. *Gerontology*, 40(2-4):174–192.

Ciezarek, A. G., Osborne, O. G., Shipley, O. N., Brooks, E. J., Tracey, S. R., McAllister, J. D., Gardner, L. D., Sternberg, M. J., Block, B., and Savolainen, V. (2019). Phylotranscriptomic insights into the diversification of endothermic *Thunnus tunas*. *Molecular biology and evolution*, 36(1):84–96.

Claessen, D., De Roos, A. M., and Persson, L. (2004). Population dynamic theory of size–dependent cannibalism. *Proceedings of the Royal Society of London. Series B: Biological Sciences*, 271(1537):333–340.

Clarke, A. (2019). Energy flow in growth and production. *Trends in Ecology & Evolution*, 34(6):502–509.

Cloern, J. E. and Nichols, F. H. (1978). A Von Bertalanffy growth model with a seasonally varying coefficient. *Journal of the Fisheries Board of Canada*, 35(11):1479–1482.

Clutton-Brock, T. H., Albon, S. D., and Guinness, F. E. (1987). Interactions between population density and maternal characteristics affecting fecundity and juvenile survival in red deer. *The Journal of Animal Ecology*, 56:857–871.

Cook, R., Sinclair, A., and Stefansson, G. (1997). Potential collapse of North Sea cod stocks. *Nature*, 385(6616):521–522.

Cormon, X., Ernande, B., Kempf, A., Vermard, Y., and Marchal, P. (2016). North Sea saithe *Pollachius virens* growth in relation to food availability, density dependence and temperature. *Marine Ecology Progress Series*, 542:141–151.

Coulson, T., Milner-Gulland, E. J., and Clutton-Brock, T. (2000). The relative roles of density and climatic variation on population dynamics and fecundity rates in three contrasting ungulate species. *Proceedings of the Royal Society of London. Series B: Biological Sciences*, 267(1454):1771–1779.

Crispo, E. (2007). The Baldwin effect and genetic assimilation: revisiting two mechanisms of evolutionary change mediated by phenotypic plasticity. *Evolution: International Journal of Organic Evolution*, 61(11):2469–2479.

Croll, J. C. (2022). VBGfit package for R. https://doi.org/10.5281/zenodo.6797840.

De Graaf, G. and Prein, M. (2005). Fitting growth with the Von Bertalanffy growth function: a comparison of three approaches of multivariate analysis of fish growth in aquaculture experiments. *Aquaculture Research*, 36(1):100–109.

De Roos, A. M. (1988). Numerical methods for structured population models: the escalator boxcar train. *Numerical methods for partial differential equations*, 4(3):173–195.

De Roos, A. M. (1997). A gentle introduction to physiologically structured population models. In Caswell, H. and S., T., editors, *Structured-population models in marine, terrestrial, and freshwater systems*, volume 18 of *Population and community biology series*, pages 119–204. Springer.

De Roos, A. M. (2021a). Dynamic population stage structure due to juvenile-adult asymmetry stabilizes complex ecological communities. *Proceedings of the National Academy of Sciences*, 118(21):e2023709118.

De Roos, A. M. (2021b). FindCurve package v0.1.0 for R. https://doi.org/10.5281/zenodo.5642759.

De Roos, A. M., Diekmann, O., and Metz, J. A. J. (1992). Studying the dynamics of structured population models: a versatile technique and its application to Daphnia. *The American Naturalist*, 139(1):123–147.

De Roos, A. M., Galic, N., and Heesterbeek, H. (2009). How resource competition shapes individual life history for nonplastic growth: ungulates in seasonal food environments. *Ecology*, 90(4):945–960.

De Roos, A. M., Metz, J. A. J., Evers, E., and Leipoldt, A. (1990). A size dependent predator-prey interaction: who pursues whom? *Journal of Mathematical Biology*, 28(6):609–643.

De Roos, A. M. and Persson, L. (2001). Physiologically structured models: from versatile technique to ecological theory. *Oikos*, 94(1):51–71.

De Roos, A. M. and Persson, L. (2002). Size-dependent life-history traits promote catastrophic collapses of top predators. *Proceedings of the National Academy of Sciences*, 99(20):12907–12912.

De Roos, A. M. and Persson, L. (2003). Competition in size-structured populations: mechanisms inducing cohort formation and population cycles. *Theoretical population biology*, 63(1):1–16.

De Roos, A. M., Persson, L., and McCauley, E. (2003). The influence of size-dependent life-history traits on the structure and dynamics of populations and communities. *Ecology Letters*, 6(5):473–487.

De Roos, A. M., Schellekens, T., Van Kooten, T., and Persson, L. (2008). Stage-specific predator species help each other to persist while competing for a single prey. *Proceedings of the National Academy of Sciences*, 105(37):13930–13935.

De Roos, A. M., Schellekens, T., Van Kooten, T., Van de Wolfshaar, K., Claessen, D., and Persson, L. (2007). Food-dependent growth leads to overcompensation in stage-specific biomass when mortality increases: the influence of maturation versus reproduction regulation. *The American Naturalist*, 170(3):E59–E76.

DeWitt, T. J., Sih, A., and Wilson, D. S. (1998). Costs and limits of phenotypic plasticity. *Trends in Ecology & Evolution*, 13(2):77–81.

Dickson, K. A. and Graham, J. B. (2004). Evolution and consequences of endothermy in fishes. *Physiological and Biochemical Zoology*, 77(6):998–1018.

Dmitriew, C. M. (2011). The evolution of growth trajectories: what limits growth rate? *Biological Reviews*, 86(1):97–116.

Enberg, K., Jørgensen, C., Dunlop, E. S., Varpe, Ø., Boukal, D. S., Baulier, L., Eliassen, S., and Heino, M. (2012). Fishing-induced evolution of growth: Concepts, mechanisms and the empirical evidence. *Marine ecology*, 33(1):1–25.

European council (1996). Council regulation (EC) No. 2406/96 Laying down common marketing standards for certain fishery products. *Official Journal of the European Communities*, 334(1):1–15.

Eveson, J. P., Polacheck, T., and Laslett, G. M. (2007). Consequences of assuming an incorrect error structure in Von Bertalanffy growth models: a simulation study. *Canadian Journal of Fisheries and Aquatic Sciences*, 64(4):602–617.

FAO (2020). The state of world fisheries and aquaculture 2020. In *Sustainability in action.* FAO.

Farmer, C. G. (2000). Parental care: the key to understanding endothermy and other convergent features in birds and mammals. *The American Naturalist*, 155(3):326–334.

Fernandes, P. G. and Cook, R. M. (2013). Reversal of fish stock decline in the Northeast Atlantic. *Current Biology*, 23(15):1432–1437.

Festa-Bianchet, M., Jorgenson, J. T., Lucherini, M., and Wishart, W. D. (1995). Life history consequences of variation in age of primiparity in bighorn ewes. *Ecology*, 76(3):871–881.

Flinn, S. A. and Midway, S. R. (2021). Trends in growth modeling in fisheries science. *Fishes*, 6(1):1.

Floeter, J. and Temming, A. (2003). Explaining diet composition of North Sea cod (*Gadus morhua*): prey size preference vs. prey availability. *Canadian Journal of Fisheries and Aquatic Sciences*, 60(2):140–150.

Fonds, M. (1979). Laboratory observations on the influence of temperature and salinity on development of the eggs and growth of the larvae of *Solea solea* (Pisces). *Marine Ecology Progress Series*, 1(9):91–99.

Froese, R. and Pauly, D. (2021). Fishbase. https://www.fishbase.org.

Froese, R., Winker, H., Coro, G., Demirel, N., Tsikliras, A. C., Dimarchopoulou, D., Scarcella, G., Quaas, M., and Matz-Lück, N. (2018). Status and rebuilding of European fisheries. *Marine Policy*, 93:159–170.

Fusco, G. and Minelli, A. (2010). Phenotypic plasticity in development and evolution: facts and concepts. *Philosophical Transactions of the Royal Society B: Biological Sciences*, 365(1540):547–556.

Gardner, J. L., Peters, A., Kearney, M. R., Joseph, L., and Heinsohn, R. (2011). Declining body size: a third universal response to warming? *Trends in Ecology & Evolution*, 26(6):285–291.

Geritz, S. A. H., Kisdi, E., Metz, J. A. J., et al. (1998). Evolutionarily singular strategies and the adaptive growth and branching of the evolutionary tree. *Evolutionary ecology*, 12(1):35–57.

Gotanda, K. M., Correa, C., Turcotte, M. M., Rolshausen, G., and Hendry, A. P. (2015). Linking macrotrends and microrates: Re-evaluating microevolutionary support for cope's rule. *Evolution*, 69(5):1345–1354.

Gurney, W. S. C. and Nisbet, R. M. (1985). Fluctuation periodicity, generation separation, and the expression of larval competition. *Theoretical Population Biology*, 28(2):150–180.

Gurney, W. S. C., Nisbet, R. M., and Lawton, J. H. (1983). The systematic formulation of tractable single-species population models incorporating age structure. *The Journal of Animal Ecology*, 52(2):479–495.

Halliday, T. R. and Verrell, P. A. (1988). Body size and age in amphibians and reptiles. *Journal of Herpetology*, 22(3):253–265.

Hamrin, S. F. and Persson, L. (1986). Asymmetrical competition between age classes as a factor causing population oscillations in an obligate planktivorous fish species. *Oikos*, 47(2):223–232.

Hastings, A. (2020). Predator–prey cycles achieved at last. *Nature*, 577:172–173.

He, J. X. and Bence, J. R. (2007). Modeling annual growth variation using a hierarchical Bayesian approach and the Von Bertalanffy growth function, with application to lake trout in southern Lake Huron. *Transactions of the American Fisheries Society*, 136(2):318–330.

Heino, M., Pauli, B. D., and Dieckmann, U. (2015). Fisheries-induced evolution. *Annual Review of Ecology, Evolution, and Systematics*, 46:461–480.

Herrando-Pérez, S., Delean, S., Brook, B. W., and Bradshaw, C. J. A. (2012). Density dependence: an ecological Tower of Babel. *Oecologia*, 170(3):585–603.

Hilborn, R., Amoroso, R. O., Anderson, C. M., Baum, J. K., Branch, T. A., Costello, C., De Moor, C. L., Faraj, A., Hively, D., Jensen, O. P., et al. (2020). Effective fisheries management instrumental in improving fish stock status. *Proceedings of the National Academy of Sciences*, 117(4):2218–2224.

Hislop, J. R. G., Robb, A. P., Bell, M. A., and Armstrong, D. W. (1991). The diet and food consumption of whiting (*Merlangius merlangus*) in the North Sea. *ICES Journal of Marine Science*, 48(2):139–156.

Hone, D. W. E. and Benton, M. J. (2005). The evolution of large size: how does Cope's Rule work? *Trends in Ecology & Evolution*, 20(1):4–6.

Hou, C., Zuo, W., Moses, M. E., Woodruff, W. H., Brown, J. H., and West, G. B. (2008). Energy uptake and allocation during ontogeny. *Science*, 322(5902):736–739.

Hutchings, J. A., Minto, C., Ricard, D., Baum, J. K., and Jensen, O. P. (2010). Trends in the abundance of marine fishes. *Canadian Journal of Fisheries and Aquatic Sciences*, 67(8):1205–1210.

ICES (2020). *Manual for the North Sea International Bottom Trawl Surveys. Series of ICES Survey Protocols SISP 10-IBTS 10, Revision 11. 102 pp.* ICES.

ICES (2021a). ICES BTS (Beam Trawl Survey) dataset. https://www.ices.dk/data/data-portals/Pages/DATRAS.aspx.

ICES (2021b). Plaice (pleuronectes platessa) in subarea 4 (North Sea) and subdivision 20 (Skagerrak). *Report of the ICES Advisory Committee*.

ICES (2022). ICES NS-IBTS (North Sea International Bottom Trawl Survey) dataset. https://www.ices.dk/data/data-portals/Pages/DATRAS.aspx.

Inchausti, P. and Ginzburg, L. R. (2009). Maternal effects mechanism of population cycling: a formidable competitor to the traditional predator–prey view. *Philosophical Transactions of the Royal Society B: Biological Sciences*, 364(1520):1117–1124.

Jager, T., Martin, B. T., and Zimmer, E. I. (2013). DEBkiss or the quest for the simplest generic model of animal life history. *Journal of theoretical biology*, 328:9–18.

Jansen, T. and Burns, F. (2015). Density dependent growth changes through juvenile and early adult life of North East Atlantic Mackerel (*Scomber scombrus*). *Fisheries Research*, 169:37–44.

Jardim, E., Azevedo, M., Brodziak, J., Brooks, E. N., Johnson, K. F., Klibansky, N., Millar, C. P., Minto, C., Mosqueira, I., Nash, R. D. M., et al. (2021). Operationalizing ensemble models for scientific advice to fisheries management. *ICES Journal of Marine Science*, 78(4):1209–1216.

Johnson, S. G. (2021). The nlopt nonlinear-optimization package.

Kingsley, M. C. S. (1979). Fitting the Von Bertalanffy growth equation to polar bear age–weight data. *Canadian Journal of Zoology*, 57(5):1020–1025.

Kingsolver, J. G. and Huey, R. B. (2008). Size, temperature, and fitness: three rules. *Evolutionary Ecology Research*, 10(2):251–268.

Kingsolver, J. G. and Pfennig, D. W. (2004). Individual-level selection as a cause of Cope's rule of phyletic size increase. *Evolution*, 58(7):1608–1612.

Köhler, M. and Moyà-Solà, S. (2009). Physiological and life history strategies of a fossil large mammal in a resource-limited environment. *Proceedings of the National Academy of Sciences*, 106(48):20354–20358.

Kooijman, S. A. L. M. (2000). *Dynamic energy and mass budgets in biological systems*. Cambridge university press.

Kooijman, S. A. L. M. (2010). *Dynamic energy budget theory for metabolic organisation*. Cambridge university press.

Kooijman, S. A. L. M. and Metz, J. A. J. (1984). On the dynamics of chemically stressed populations: the deduction of population consequences from effects on individuals. *Ecotoxicology and environmental safety*, 8(3):254–274.

Krueger, D. A. and Dodson, S. I. (1981). Embryological induction and predation ecology in *Daphnia pulex*. *Limnology and oceanography*, 26(2):219–223.

LaBarbera, M. (1989). Analyzing body size as a factor in ecology and evolution. *Annual review of ecology and systematics*, 20:97–117.

Lassen, H., Kelly, C., and Sissenwine, M. (2014). ICES advisory framework 1977–2012: from F_{max} to precautionary approach and beyond. *ICES Journal of Marine Science*, 71(2):166–172.

Levis, N. A. and Pfennig, D. W. (2016). Evaluating 'plasticity-first' evolution in nature: key criteria and empirical approaches. *Trends in Ecology & Evolution*, 31(7):563–574.

Lika, K. and Nisbet, R. M. (2000). A dynamic energy budget model based on partitioning of net production. *Journal of Mathematical Biology*, 41(4):361–386.

Lipinski, M. R. and Roeleveld, M. A. (1990). Minor extension of the Von Bertalanffy growth theory. *Fisheries research*, 9(4):367–371.

Lorenzen, K. (1996). A simple Von Bertalanffy model for density-dependent growth in extensive aquaculture, with an application to common carp (*Cyprinus carpio*). *Aquaculture*, 142(3-4):191–205.

Lorenzen, K. (2008). Fish population regulation beyond "stock and recruitment": the role of density-dependent growth in the recruited stock. *Bulletin of Marine Science*, 83(1):181–196.

Lorenzen, K. (2016). Toward a new paradigm for growth modeling in fisheries stock assessments: embracing plasticity and its consequences. *Fisheries Research*, 180:4–22.

Lorenzen, K. and Enberg, K. (2002). Density-dependent growth as a key mechanism in the regulation of fish populations: evidence from among-population comparisons. *Proceedings of the Royal Society of London. Series B: Biological Sciences*, 269(1486):49–54.

Maceina, M. J., Boxrucker, J., Buckmeier, D. L., Gangl, R. S., Lucchesi, D. O., Isermann, D. A., Jackson, J. R., and Martinez, P. J. (2007). Current status and review of freshwater fish aging procedures used by state and provincial fisheries agencies with recommendations for future directions. *Fisheries*, 32(7):329–340.

Matley, J. K., Maes, G. E., Devloo-Delva, F., Huerlimann, R., Chua, G., Tobin, A. J., Fisk, A. T., Simpfendorfer, C. A., and Heupel, M. R. (2018). Integrating complementary methods to improve diet analysis in fishery-targeted species. *Ecology and Evolution*, 8(18):9503–9515.

May, R. C. (1974). Larval mortality in marine fishes and the critical period concept. In Blaxter, J. H. S., editor, *The early life history of fish*, pages 3–19. Springer.

May, R. M., Beddington, J. R., Clark, C. W., Holt, S. J., and Laws, R. M. (1979). Management of multispecies fisheries. *Science*, 205(4403):267–277.

McCauley, E. M. W. W. (1993). Internal versus external causes of dynamics in a freshwater plant-herbivore system. *The American Naturalist*, 141(3):428–439.

McCauley, E. M. W. W., Murdoch, W. W., and Nisbet, R. M. (1990). Growth, reproduction, and mortality of *Daphnia pulex* Leydig: life at low food. *Functional Ecology*, 4(4):505–514.

Mehl, S. and Westgård, T. (1983). The diet and consumption of mackerel in the North Sea.

Metz, J. A. J. and Leimar, O. (2011). A simple fitness proxy for structured populations with continuous traits, with case studies on the evolution of haplo-diploids and genetic dimorphisms. *Journal of Biological Dynamics*, 5(2):163–190.

Miller, T. E. X. and Rudolf, V. H. W. (2011). Thinking inside the box: community-level consequences of stage-structured populations. *Trends in Ecology & Evolution*, 26(9):457–466.

Millner, R. S. and Whiting, C. L. (1996). Long-term changes in growth and population abundance of sole in the North Sea from 1940 to the present. *ICES Journal of Marine Science*, 53(6):1185–1195.

Miner, B. G., Sultan, S. E., Morgan, S. G., Padilla, D. K., and Relyea, R. A. (2005). Ecological consequences of phenotypic plasticity. *Trends in Ecology & Evolution*, 20(12):685–692.

Moczek, A. P., Sultan, S., Foster, S., Ledón-Rettig, C., Dworkin, I., Nijhout, H. F., Abouheif, E., and Pfennig, D. W. (2011). The role of developmental plasticity in evolutionary innovation. *Proceedings of the Royal Society B: Biological Sciences*, 278(1719):2705–2713.

Murdoch, W. W., Kendall, B. E., Nisbet, R. M., Briggs, C. J., McCauley, E., and Bolser, R. (2002). Single-species models for many-species food webs. *Nature*, 417(6888):541–543.

Murdoch, W. W. and McCauley, E. (1985). Three distinct types of dynamic behaviour shown by a single planktonic system. *Nature*, 316(6029):628–630.

Murphy, L. F. (1983). A nonlinear growth mechanism in size structured population dynamics. *Journal of theoretical biology*, 104(4):493–506.

Murren, C. J., Auld, J. R., Callahan, H., Ghalambor, C. K., Handelsman, C. A., Heskel, M. A., Kingsolver, J. G., Maclean, H. J., Masel, J., Maughan, H., et al. (2015). Constraints on the evolution of phenotypic plasticity: limits and costs of phenotype and plasticity. *Heredity*, 115(4):293–301.

Nagy, K. A. (2005). Field metabolic rate and body size. *Journal of Experimental Biology*, 208(9):1621–1625.

Narinç, D., Narinç, N. Ö., and Aygün, A. (2017). Growth curve analyses in poultry science. *World's Poultry Science Journal*, 73(2):395–408.

Nisbet, R. M., Muller, E. B., Lika, K., and Kooijman, S. A. L. M. (2000). From molecules to ecosystems through dynamic energy budget models. *Journal of animal ecology*, 69:913–926.

Pauly, D. (1980). On the interrelationships between natural mortality, growth parameters, and mean environmental temperature in 175 fish stocks. *ICES journal of Marine Science*, 39(2):175–192.

Pauly, D., Christensen, V., Guénette, S., Pitcher, T. J., Sumaila, U. R., Walters, C. J., Watson, R., and Zeller, D. (2002). Towards sustainability in world fisheries. *Nature*, 418(6898):689–695.

Perrigo, G. (1990). Food, sex, time, and effort in a small mammal: energy allocation strategies for survival and reproduction. *Behaviour*, 114(1-4):191–205.

Perry, B. W., Schield, D. R., and Castoe, T. A. (2018). Evolution: plasticity versus selection, or plasticity and selection? *Current Biology*, 28(18):R1104–R1106.

Persson, L., Amundsen, P.-A., De Roos, A. M., Klemetsen, A., Knudsen, R., and Primicerio, R. (2007). Culling prey promotes predator recovery alternative states in a whole-lake experiment. *Science*, 316(5832):1743–1746.

Persson, L., Leonardsson, K., De Roos, A. M., Gyllenberg, M., and Christensen, B. (1998). Ontogenetic scaling of foraging rates and the dynamics of a size-structured consumer-resource model. *Theoretical population biology*, 54(3):270–293.

Peters, R. H. (1983). *The ecological implications of body size*, volume 2 of *Cambridge studies in ecology*. Cambridge University Press.

Pfaff, T., Brechtel, A., Drossel, B., and Guill, C. (2014). Single generation cycles and delayed feedback cycles are not separate phenomena. *Theoretical Population Biology*, 98:38–47.

Pfennig, D. W., Wund, M. A., Snell-Rood, E. C., Cruickshank, T., Schlichting, C. D., and Moczek, A. P. (2010). Phenotypic plasticity's impacts on diversification and speciation. *Trends in Ecology & Evolution*, 25(8):459–467.

Pigliucci, M. (2005). Evolution of phenotypic plasticity: where are we going now? *Trends in Ecology & Evolution*, 20(9):481–486.

Pilling, G. M., Kirkwood, G. P., and Walker, S. G. (2002). An improved method for estimating individual growth variability in fish, and the correlation between Von Bertalanffy growth parameters. *Canadian Journal of Fisheries and Aquatic Sciences*, 59(3):424–432.

Piner, K. R., Lee, H.-H., and Maunder, M. N. (2016). Evaluation of using random-at-length observations and an equilibrium approximation of the population age structure in fitting the Von Bertalanffy growth function. *Fisheries Research*, 180:128–137.

Prajneshu and Venugopalan, R. (1999). Von Bertalanffy growth model in a random environment. *Canadian Journal of Fisheries and Aquatic Sciences*, 56(6):1026–1030.

Price, T. D., Qvarnström, A., and Irwin, D. E. (2003). The role of phenotypic plasticity in driving genetic evolution. *Proceedings of the Royal Society of London. Series B: Biological Sciences*, 270(1523):1433–1440.

Rafail, S. Z. (1973). A simple and precise method for fitting a Von Bertalanffy growth curve. *Marine biology*, 19(4):354–358.

Ramirez, M. D., Popovska, T., and Babcock, E. A. (2021). Global synthesis of sea turtle Von Bertalanffy growth parameters through Bayesian hierarchical modeling. *Marine Ecology Progress Series*, 657:191–207.

Read, F. L., Hohn, A. A., and Lockyer, C. H. (2018). A review of age estimation methods in marine mammals with special reference to monodontids. *NAMMCO Scientific Publications*, 10.

Ricker, W. E. (1954). Stock and recruitment. *Journal of the Fisheries Board of Canada*, 11(5):559–623.

Rijnsdorp, A. D. and Van Leeuwen, P. I. (1996). Changes in growth of North Sea plaice since 1950 in relation to density, eutrophication, beam-trawl effort, and temperature. *ICES Journal of Marine Science*, 53(6):1199–1213.

Rijnsdorp, A. D. and Vingerhoed, B. v. (2001). Feeding of plaice *Pleuronectes platessa* L. and sole *Solea solea* (L.) in relation to the effects of bottom trawling. *Journal of Sea Research*, 45(3-4):219–229.

Rindorf, A., Gislason, H., Burns, F., Ellis, J. R., and Reid, D. (2020). Are fish sensitive to trawling recovering in the northeast atlantic? *Journal of Applied Ecology*, 57(10):1936–1947.

Rindorf, A., Van Deurs, M., Howell, D., Andonegi, E., Berger, A., Bogstad, B., Cadigan, N., Elvarsson, B. Þ., Hintzen, N., Savina Roland, M., et al. (2022). Strength and consistency of density dependence in marine fish productivity. *Fish and Fisheries*, 23(4):812–828.

Robson, S. K. and Crozier, R. H. (2009). An evaluation of two biochemical methods of age determination in insects (pteridines and lipofuscins) using the ant *Polyrhachis sexpinosa* Latrielle (hymenoptera: Formicidae). *Australian Journal of Entomology*, 48(2):102–106.

Rollinson, N. and Rowe, L. (2015). Persistent directional selection on body size and a resolution to the paradox of stasis. *Evolution*, 69(9):2441–2451.

Rose, K. A., Cowan Jr, J. H., Winemiller, K. O., Myers, R. A., and Hilborn, R. (2001). Compensatory density dependence in fish populations: importance, controversy, understanding and prognosis. *Fish and Fisheries*, 2(4):293–327.

Rosenzweig, M. L. and MacArthur, R. H. (1963). Graphical representation and stability conditions of predator-prey interactions. *The American Naturalist*, 97(895):209–223.

Rothschild, B. J. (2000). "fish stocks and recruitment": the past thirty years. *ICES Journal of Marine Science*, 57(2):191–201.

Ruben, J. (1995). The evolution of endothermy in mammals and birds: from physiology to fossils. *Annual review of physiology*, 57(1):69–95.

Säterberg, T., Casini, M., and Gårdmark, A. (2019). Ecologically sustainable exploitation rates—a multispecies approach for fisheries management. *Fish and Fisheries*, 20(5):952–961.

Schmitz, O. J., Adler, F. R., and Agrawal, A. A. (2003). Linking individual-scale trait plasticity to community dynamics: Trait plasticity and community dynamics. *Ecology*, 84(5):1081–1082.

Schnute, J. T. and Richards, L. J. (1998). Analytical models for fishery reference points. *Canadian Journal of Fisheries and Aquatic Sciences*, 55(2):515–528.

Schram, E., Van der Heul, J. W., Kamstra, A., and Verdegem, M. C. J. (2006). Stocking density-dependent growth of Dover sole (*Solea solea*). *Aquaculture*, 252(2-4):339–347.

Seebacher, F. (2020). Is endothermy an evolutionary by-product? *Trends in Ecology & Evolution*, 35(6):503–511.

Seymour, R. S., White, C. R., and Gibernau, M. (2009). Endothermy of dynastine scarab beetles (*Cyclocephala colasi*) associated with pollination biology of a thermogenic arum lily (*Philodendron solimoesense*). *Journal of Experimental Biology*, 212(18):2960–2968.

Shelton, A. O., Satterthwaite, W. H., Beakes, M. P., Munch, S. B., Sogard, S. M., and Mangel, M. (2013). Separating intrinsic and environmental contributions to growth and their population consequences. *The American Naturalist*, 181(6):799–814.

Shimodaira, H. (2002). An approximately unbiased test of phylogenetic tree selection. *Systematic biology*, 51(3):492–508.

Skogland, T. (1986). Density dependent food limitation and maximal production in wild reindeer herds. *The Journal of Wildlife Management*, 50(2):314–319.

Smirina, E. M. (1994). Age determination and longevity in amphibians. *Gerontology*, 40(2-4):133–146.

Smith, F. A., Payne, J. L., Heim, N. A., Balk, M. A., Finnegan, S., Kowalewski, M., Lyons, S. K., McClain, C. R., McShea, D. W., Novack-Gottshall, P. M., et al. (2016). Body size evolution across the geozoic. *Annual Review of Earth and Planetary Sciences*, 44:523–553.

Sousa, T., Domingos, T., and Kooijman, S. A. L. M. (2008). From empirical patterns to theory: a formal metabolic theory of life. *Philosophical Transactions of the Royal Society B: Biological Sciences*, 363(1502):2453–2464.

Stanley, S. M. (1973). An explanation for Cope's rule. *Evolution*, 27(1):1–26.

Stearns, S. C. (1989). Trade-offs in life-history evolution. *Functional ecology*, 3(3):259–268.

Stearns, S. C. (1992). *The evolution of life histories*. Oxford university press.

Sultan, S. E. and Stearns, S. C. (2005). Environmentally contingent variation: phenotypic plasticity and norms of reaction. In Hallgrímsson, B. and Hall, B. K., editors, *Variation*, chapter 14, pages 303–332. Elsevier, Oxford.

Suzuki, R. and Shimodaira, H. (2006). Pvclust: an R package for assessing the uncertainty in hierarchical clustering. *Bioinformatics*, 22(12):1540–1542.

Taylor, N. G., Walters, C. J., and Martell, S. J. D. (2005). A new likelihood for simultaneously estimating Von Bertalanffy growth parameters, gear selectivity, and natural and fishing mortality. *Canadian Journal of Fisheries and Aquatic Sciences*, 62(1):215–223.

Teleken, J. T., Galvão, A. C., and Robazza, W. d. S. (2017). Comparing non-linear mathematical models to describe growth of different animals. *Acta Scientiarum. Animal Sciences*, 39:73–81.

Thieme, H. R. (1988). Well-posedness of physiologically structured population models for *Daphnia magna*. *Journal of Mathematical Biology*, 26(3):299–317.

Tilman, D., Kilham, S. S., and Kilham, P. (1982). Phytoplankton community ecology: the role of limiting nutrients. *Annual review of Ecology and Systematics*, 13:349–372.

Townsend, C. R. and Perrow, M. R. (1989). Eutrophication may produce population cycles in roach, *Rutilus rutilus* (L.), by two contrasting mechanisms. *Journal of Fish Biology*, 34(1):161–164.

Townsend, C. R., Sutherland, W. J., and Perrow, M. R. (1990). A modelling investigation of population cycles in the fish *Rutilus rutilus*. *The Journal of Animal Ecology*, 59(2):469–485.

Trochta, J. T., Pons, M., Rudd, M. B., Krigbaum, M., Tanz, A., and Hilborn, R. (2018). Ecosystem-based fisheries management: perception on definitions, implementations, and aspirations. *PloS one*, 13(1):e0190467.

Tu, C.-Y., Chen, K.-T., and Hsieh, C.-H. (2018). Fishing and temperature effects on the size structure of exploited fish stocks. *Scientific reports*, 8(1):1–10.

Van der Veer, H. W., Kooijman, S. A. L. M., and Van der Meer, J. (2001). Intra- and interspecies comparison of energy flow in North Atlantic flatfish species by means of dynamic energy budgets. *Journal of Sea Research*, 45(3-4):303–320.

Van Gemert, R. and Andersen, K. H. (2018a). Challenges to fisheries advice and management due to stock recovery. *ICES Journal of Marine Science*, 75(6):1864–1870.

Van Gemert, R. and Andersen, K. H. (2018b). Implications of late-in-life density-dependent growth for fishery size-at-entry leading to maximum sustainable yield. *ICES Journal of Marine Science*, 75(4):1296–1305.

Van Kooten, T., Persson, L., and De Roos, A. M. (2007). Size-dependent mortality induces life-history changes mediated through population dynamical feedbacks. *The American Naturalist*, 170(2):258–270.

Van Leeuwen, A., De Roos, A. M., and Persson, L. (2008). How cod shapes its world. *Journal of Sea Research*, 60(1-2):89–104.

Vaughan, D. S. and Kanciruk, P. (1982). An empirical comparison of estimation procedures for the Von Bertalanffy growth equation. *ICES Journal of Marine Science*, 40(3):211–219.

Vincenzi, S., Crivelli, A. J., Munch, S., Skaug, H. J., and Mangel, M. (2016). Trade-offs between accuracy and interpretability in Von Bertalanffy random-effects models of growth. *Ecological applications*, 26(5):1535–1552.

Vincenzi, S., Mangel, M., Crivelli, A. J., Munch, S., and Skaug, H. J. (2014). Determining individual variation in growth and its implication for life-history and population processes using the Empirical Bayes method. *PLoS computational biology*, 10(9):e1003828.

Von Bertalanffy, L. (1938). A quantitative theory of organic growth (inquiries on growth laws. II). *Human biology*, 10(2):181–213.

Wang, Y., Wang, Y., Liang, C., Zhang, H., and Xian, W. (2020). Assessment of 12 fish species in the northwest Pacific using the CMSY and BSM methods. *Frontiers in Marine Science*, 7:1–11.

Wang, Y.-G. and Thomas, M. R. (1995). Accounting for individual variability in the Von Bertalanffy growth model. *Canadian Journal of Fisheries and Aquatic Sciences*, 52(7):1368–1375.

West, G. B., Brown, J. H., and Enquist, B. J. (2001). A general model for ontogenetic growth. *Nature*, 413(6856):628–631.

Worm, B., Hilborn, R., Baum, J. K., Branch, T. A., Collie, J. S., Costello, C., Fogarty, M. J., Fulton, E. A., Hutchings, J. A., Jennings, S., et al. (2009). Rebuilding global fisheries. *Science*, 325(5940):578–585.

Zermoglio, P. F., Castelo, M. K., and Lazzari, C. R. (2018). Endothermy in the temperate scarab *Cyclocephala signaticollis*. *Journal of insect physiology*, 108:10–16.

Zhang, L., Lin, Z., and Pedersen, M. (2012). Effects of growth curve plasticity on size-structured population dynamics. *Bulletin of mathematical biology*, 74(2):327–345.

Zimmermann, F., Ricard, D., and Heino, M. (2018). Density regulation in northeast atlantic fish populations: density dependence is stronger in recruitment than in somatic growth. *Journal of Animal Ecology*, 87(3):672–681.

Zimmermann, F. and Werner, K. M. (2019). Improved management is the main driver behind recovery of Northeast Atlantic fish stocks. *Frontiers in Ecology and the Environment*, 17(2):93–99.

Summary

Starving to grow: the ecology and evolution of growth curve plasticity

The size of living organisms spans an unimaginably large range, from single-cell organisms to large aquatic mammals. The size of an organism is linked to numerous life history processes such as consumption, reproduction and survival and determines the way an organism experiences its environment. It is therefore unsurprising that individual body size is a key factor in the life history and ecology of an organism.

Species not only differ in their body size, but also in the rate at which they grow. Individuals of some species grow fast and reach their maximum size at a young age, while individuals of other species might grow slowly but keep growing throughout their entire life. The rate at which an individual can grow and the size an individual can reach is governed by the amount of energy available for the growth of an individual. Individuals acquire energy through consumption and assimilation of resources. The acquired energy is used to fuel life history processes such as growth and reproduction, but also to maintain the current state of the body. This results in a tradeoff between these processes because assimilated energy can only be spent once. As a consequence, the growth rate of an individual is strongly determined by the physiological rules an individual uses to allocate energy to growth and other processes.

Interestingly, species differ in the amount in which their individual growth rate depends on the environment. Some species, such as most mammals and birds, display a very constant growth rate independent of the experienced environment. For these species, the size of an individual can be predicted relatively accurately based on its age. In contrast, the growth rate of other species, such as insects, fish and amphibians, strongly depends on the environment and especially the amount of resources that are available. The extent to which the growth of an individual depends on the environment is the level of growth curve plasticity of an individual. The level of growth curve plasticity arises from the energy allocation schemes used by individuals and strongly affects the ecological dynamics of a population.

If growth is largely plastic, individuals of the same age can differ strongly in size, even within the same population. These differences in size arise because individuals experienced different environments. Individuals could for example experience differences in the environment due to chance or because they live in different

places. In addition, the environment can also change over time, which causes variation in size between individuals born at different points in time. Variation in size therefore contains valuable information about the environment experienced by individuals. In chapter 2, I developed a method to quantify the variation in the environment based on size and age measurements of individuals that can only be measured once during their life, which is for example the case for wild fish. In addition, I showed that a model which accounts for temporal fluctuations in the environment predicts the size of individuals more accurately compared to a model in which the environment is assumed to be constant. In chapter 3, I used this model to characterize the temporal trends in the experienced environment for ten exploited North Sea fish stocks in ten North Sea regions. Analyses of these trends revealed that the experienced environment is more similar for ecologically similar species and within geographically connected regions. This suggests that variation in growth can be a useful summary statistic for ecological relatedness of fish stocks, which is especially useful in the transition towards ecosystem-based fisheries management.

The environment thus affects the life history of an individual, but individuals can in their turn also affect the environment, for example through consumption of the resource. This results in a feedback loop in which the resource density and the consumer population mutually limit each other. The level of growth curve plasticity affects the energy allocation scheme of an individual and determines to what extent growth in size is dependent on the resources in the environment. In chapter 4, I show that this can result in a consumer population limited by growth and a consumer population limited by reproduction. These two regimes differ vastly in the structure of the consumer population and the type of population dynamic cycles that can emerge. The dynamics of a consumer population limited by growth is mainly affected by fluctuations in the survival up to maturation, while the dynamics of a consumer population limited by reproduction is mainly affected by fluctuations in individual fecundity. In chapter 5, I show that evolution balances the limitation in growth and reproduction. Evolution is therefore expected to drive a population towards an intermediate level of growth curve plasticity. This is in sharp contrast with common theory about the evolution of plasticity and energy budget theory, which often assume that the level of growth curve plasticity will evolve to extreme values.

The level of growth curve plasticity strongly affects the response of a fish stock to harvesting. Classic models of fisheries management are structured by age rather than size and therefore assume a low level of growth curve plasticity, while most fish species have been shown to maintain a largely plastic growth rate. In chapter 6, I

show that yield from fish stocks with a low level of growth curve plasticity is highest at a relatively low fishing intensity. Unfortunately, under these conditions, a large part of the catches is undersized and cannot be sold on the market. In contrast, yield from a fish stock with a high level of growth curve plasticity is highest at a relatively high fishing intensity. This is again paired with the harvesting of numerous undersized individuals. Interestingly, for some stocks with a high level of growth curve plasticity, a second harvesting intensity with high yield arises at which the amount of undersized catches is relatively low.

All together, this thesis shows how growth curve plasticity affects all levels of biological organization, from individual energetics to the ecological and evolutionary dynamics of entire populations. On the individual level, growth curve plasticity is tightly intertwined with the energy allocation schemes of an individual and the energetic trade-offs between life history processes. Fluctuations in the environment accumulate in the size of individuals if growth is largely plastic. As a consequence, the level of growth curve plasticity strongly influences the structure of a population. The size-structure of a population might therefore contain valuable information on the experienced environment. Meanwhile, the structure of a population also influences the impact of a population on the environment. The level of growth curve plasticity therefore strongly affects the type of dynamics that can arise from the mutual interactions between the populations and its environment. Overall, it is clear that growth curve plasticity is an important factor when considering the dynamics of structured populations on any level of biological organization.

Samenvatting

Vast en zeker groeien: de ecologie en evolutie van plasticiteit in groeicurves

De lichaamsgrootte van levende organismen bestrijkt een ongelofelijk groot bereik, variërend van eencellige organismen tot aan grote aquatische zoogdieren. De grootte van een organisme houdt verband met veel verschillende levensprocessen, zoals consumptie, reproductie en overleving, en is daarnaast belangrijk voor de manier waarop een organisme zijn omgeving ervaart. Het is dan ook niet verrassend dat de lichaamsgrootte van een individu een sleutelrol speelt in zijn ontwikkeling en ecologie.

Diersoorten verschillen niet alleen in hun lichaamsgrootte, maar ook in de snelheid waarmee ze groeien. Individuen van sommige soorten groeien snel en bereiken hun maximumlengte op jonge leeftijd, terwijl individuen van andere soorten hun hele leven langzaam doorgroeien. De snelheid waarmee een individu groeit en de lengte die een individu kan bereiken, hangt af van de hoeveelheid energie die beschikbaar is voor groei. Individuen vergaren energie door voedsel te consumeren en te verteren. De vergaarde energie wordt gebruikt voor levensprocessen zoals groei en reproductie, maar ook voor het onderhouden van het huidige lichaam. Omdat energie maar één keer gebruikt kan worden, veroorzaakt dit een wisselwerking tussen verschillende levensprocessen. Hierdoor hangt de snelheid waarop individuen groeien vooral af van de regels die bepalen hoe individuen vergaarde energie gebruiken.

Soorten verschillen in de mate waarin de groei van een individu afhangt van de omgeving. Bij sommige soorten, zoals de meeste vogels en zoogdieren, is de groeisnelheid zeer constant en onafhankelijk van de omgeving. De grootte van individuen van deze soorten kan geschat worden op basis van hun leeftijd. Dit is niet het geval bij de meeste andere soorten, zoals insecten, vissen en amfibieën, waarbij de groeisnelheid sterk afhangt van de omgeving en vooral de beschikbaarheid van voedsel. Hoe sterk de groeisnelheid van een individu bepaald wordt door de omgeving hangt af van de mate van plasticiteit in de groeicurve. De mate van groeiplasticiteit wordt bepaald door de regels voor energiegebruik van een organisme en heeft een grote impact op de ecologische dynamiek van een populatie.

Bij een hoge mate van groeiplasticiteit kunnen individuen van dezelfde leeftijd sterk verschillen in lichaamsgrootte, zelfs als deze individuen uit dezelfde populatie komen. Deze verschillen ontstaan doordat individuen de omgeving verschil-

lend ervaren. Dit kan veroorzaakt worden door toeval, maar individuen kunnen bijvoorbeeld ook in een ander gebied leven. Daarnaast kan de omgeving veranderen, waardoor het moment waarop een individu geboren is, bepalend is voor de omgeving die hij ervaart. De variatie in lichaamsgrootte bevat dus belangrijke informatie over de ervaren omgeving. In hoofdstuk 2 ontwikkel ik een methode die gebruikt kan worden om de variatie in de omgeving te schatten op basis van metingen van lengte en leeftijd van individuen die maar één keer gemeten kunnen worden, zoals het geval is bij vissen uit de zee. Daarnaast laat ik zien dat een model dat rekening houdt met temporale fluctuaties in de omgeving beter in staat is om de grootte-structuur van een populatie te voorspellen dan een model dat aanneemt dat de omgeving constant is. In hoofdstuk 3 gebruik ik dit model om een schatting te maken van de fluctuaties in de omgeving van tien commerciële vispopulaties in tien verschillende regio's van de Noordzee. De analyse van deze fluctuaties laat zien dat vissen met eenzelfde ecologie en vissen in verbonden regio's op een vergelijkbare manier beïnvloed worden door de omgeving. Dit suggereert dat variatie in groei van vissen een belangrijke maat kan zijn voor de ecologische verwantschap van vispopulaties. Dit kan bijvoorbeeld gebruikt worden in de transitie naar een nieuwe manier van visserij management die rekening houdt met het gehele ecosysteem.

De omgeving beïnvloedt niet alleen de levensloop van een individu, maar een individu beïnvloedt ook zijn omgeving, bijvoorbeeld door het eten van voedsel. Hierdoor ontstaat er een wisselwerking waarbij de voedselbron en de consumentenpopulatie elkaar wederzijds beïnvloeden. De mate van groeiplasticiteit beïnvloedt de regels voor energiegebruik van een individu en bepaalt in welke mate de groei van een individu afhangt van het voedsel in de omgeving. In hoofdstuk 4 laat ik zien dat dit kan leiden tot een consumentenpopulatie gelimiteerd door groei en een consumentenpopulatie gelimiteerd door reproductie. Deze twee regimes laten grote verschillen zien in de structuur van de consumentenpopulatie en de dynamische cycli die kunnen ontstaan in de populatie. De dynamiek van een consumentenpopulatie gelimiteerd door groei ontstaat voornamelijk door fluctuaties in de overleving tot het moment waarop individuen volwassen worden, terwijl de dynamiek van consumentenpopulaties gelimiteerd door reproductie voornamelijk ontstaat door fluctuaties in de reproductie van individuen. In hoofdstuk 5 laat ik zien dat evolutie leidt tot een balans tussen de limitatie in groei en de limitatie in reproductie. Het is daarom te verwachten dat een populatie zal evolueren richting een gedeeltelijk plastische groei. Dit staat in schril contrast met klassieke theorieën over evolutie van plasticiteit en energietheorie, die voorspellen dat de mate van groeiplasticiteit zal evolueren richting extreme waarden.

De reactie van een vispopulatie op visserij wordt sterk bepaald door de mate van plasticiteit in groei. Klassieke modellen voor visserij volgen de leeftijdsstructuur van een populatie en gaan daardoor uit van een lage mate van groeiplasticiteit, terwijl veel vissoorten een hoge mate van groeiplasticiteit laten zien. In hoofdstuk 6 laat ik zien dat de opbrengst van een vispopulatie met een lage mate van groeiplasticiteit het hoogste is bij een relatief lage visserij-intensiteit. Helaas worden er in dit geval ook veel vissen gevangen die te klein zijn om te verkopen. De opbrengst van vispopulaties met een hoge mate van groeiplasticiteit is daarentegen het hoogst bij een relatief hoge mate van visserij-intensiteit. Ook dit gaat samen met het vangen van een grote hoeveelheid vis die te klein is om te verkopen. Voor sommige vispopulaties met een hoge mate van groeiplasticiteit is er een tweede visserij intensiteit met een hoge opbrengst, waarbij het aantal te kleine vissen dat gevangen wordt, beperkt is.

In het geheel laat dit proefschrift zien hoe plasticiteit in groei invloed heeft op alle niveaus van biologische organisatie, van individuele energiehuishouding tot de ecologische en evolutionaire dynamiek van populaties. Op het niveau van een individu is groeiplasticiteit sterk verbonden met de regels voor energiegebruik en de wisselwerking tussen levensprocessen. Als groei sterk afhangt van de omgeving, bouwen schommelingen in de omgeving zich op in de lichaamsgrootte van een individu. Hierdoor wordt de structuur van een populatie sterk beïnvloed door de mate van plasticiteit in groei. Aan de andere kant kan de lengtestructuur van een populatie daardoor waardevolle informatie bevatten over de omgeving waarin een populatie heeft geleefd. Ondertussen beïnvloedt de structuur van een populatie ook de impact van een populatie op de omgeving. Hierdoor heeft de mate van groeiplasticiteit een sterke invloed op de dynamiek die voortkomt uit de interacties tussen een populatie en de omgeving. Uit dit proefschrift is in ieder geval duidelijk geworden dat plasticiteit op elk biologisch organisatieniveau een belangrijke factor is voor de dynamiek van een gestructureerde populatie.

Acknowledgements

Until a few months before I started my PhD project, I did not envision an academic career. This all of a sudden changed when André and Tobias informed me about a PhD project that might be of my interest. It felt like a split-second decision and before I knew, I left my previous job and embarked on my PhD journey. At first, I was sceptic whether I could find my way in a project about fish, but in the end I have never regretted the decision to accept this PhD position. Many challenges presented themselves during my PhD project, but I truly enjoyed tackling most of them. The most unexpected challenge was the Covid-19 pandemic, which shut down a large part of academia, including the university, teaching, conferences and many social activities for almost two years. I was lucky to receive a large amount of guidance and support during this period. I would like to sincerely thank everyone who was involved in my PhD project in either a personal or academic way, and want to thank some of those people explicitly.

Tobias, thank you for the warm and personal approach you took throughout the entire project. It did not matter whether I had to deal with complex new ideas, unexpected feedback or the rejection of a manuscript, you were always one of the first people to support me. Even if I wandered off to topics which were less familiar to you, you managed to provide me with constructive support and feedback. Meanwhile, you motivated me to broaden my horizon through literature, talks, conferences and courses. You even dragged me to the annual ICES WGECO working group, which was one of the most intense academic experiences I have had so far. You truly enriched my PhD project in numerous ways.

André, thank you for the inexhaustible and sincere interest in both me as a person as well as my academic ideas. From the start, it was clear that you valued an involved personal conversation just as much as a profound academic discussion and you were able to seamlessly switch between them. This created an honest and open atmosphere in which any issue and idea could be discussed. I especially enjoyed the meetings in which we sat down for hours to fill the whiteboard with numerous equations and graphs. More than once we could not come to a solution or did not agree at the end of a meeting, but the sharp comments and questions always helped me forward. Thanks to you, I always dived in a bit deeper than I thought I could.

In addition, I would like to thank Quinten for working together with me on the research presented in the third chapter of this thesis. I enjoyed supervising your master project and it was great to see how it grew into an entire manuscript. You introduced me to new statistical methods, which I would never have looked into

otherwise. I think we can be proud of the work we did together.

I want to thank the ECODYN group from WMR for the time I spent with them during my project. I especially enjoyed the personal interactions during the first one and a half year of my PhD project. Working at WMR showed me a more practical approach to science and pushed me to think about the applications of my work.

I also wish to thank all the people from IBED that interacted with me one way or another during my PhD project. It is great to be part of an institute with this many interests. I am especially thankful for all the interesting meetings and discussions we had with the TCE and TE groups. I also enjoyed being involved in the dynamical systems course, the theoretical ecology course and quantitative biology course. It was great to interact with students and think about ways to set up or improve these courses together with all other teachers and assistants.

In addition, I want to mention my fellow PhDs from IBED and especially the PhDs from TCE. I am happy that they accepted me as a chair of the IBED PhD and post-doc council during the Covid Pandemic. I want to thank all the other members of the council for the elaborate meetings and our joined effort to get the best for PhD students and post-docs in difficult times. I also want to thank the PhDs and other members from TCE for showing me the social side of doing a PhD project, the great times in the office and the strange lunch conversations, even if the amount of bird related conversations was sometimes a bit too much for me.

In addition, I want to explicitly thank Sara. During your master project and your PhD project, you often felt as my closest colleague. From all PhDs, you were the one that knew most about the topic of my thesis and you spent a substantial amount of time reading through the first versions of the introduction and discussion of this thesis. It was great to have you around during my PhD project.

Of course, I also got a lot of support from friends and family outside academia. My mother, father, brother and sister spent a great amount of effort to understand my work. It is amazing to realize that they always supported me all these years, even if they did not exactly understand what I was doing. Similarly, my friends from scouting Flevo provided me with the necessary distractions and time away from my project. They were always looking for stupid jokes about my work, which in the end was a sign for me that they care.

Most importantly, I need to thank my partner, Sanne. She has been around for my entire PhD project. She motivated me to go on when I needed it. She was always around to discuss setbacks and celebrate milestones. She read through all my manuscripts several times, even if it did not make any sense to her at all. Sanne, you did way more than I can describe here. Thank you.

Author contributions

2. Accounting for temporal and individual variation in the estimation of Von Bertalanffy growth curves

J. C. Croll and T. van Kooten

Both authors contributed to the conceptualization of the study. JCC derived and tested the model, analysed the examples and wrote the manuscript. TvK commented on model testing, analyses of the examples and the manuscript text.

3. Growth as measure for environmental conditions and relatedness of North Sea fish stocks

J. C. Croll, Q. Mudde, T. van Kooten and A. M. de Roos

JCC and QM contributed to the conceptualization of the study and wrote the manuscript. QM processed the data and tested early versions of the model. JCC developed the model and performed the final analysis. TvK and AMdR commented on the results and the manuscript text.

4. The regulating effect of growth plasticity on the dynamics of structured populations

J. C. Croll and A. M. de Roos

Both authors contributed to the conceptualization of the study. JCC formulated and analysed the model and wrote the manuscript. AMdR commented on the model formulation, the results and the manuscript.

5. The evolution of growth curve plasticity in size-structured populations

J. C. Croll, T. van Kooten and A. M. de Roos

JCC came up with the initial concept of the study, performed the model analysis and wrote the manuscript. TvK and AMdR commented on the model, the results and the manuscript.

6. The consequences of density-dependent individual growth for sustainable harvesting and management of fish stocks

J. C. Croll, T. van Kooten and A. M. de Roos

All authors contributed to the conceptualization of the study. JCC derived and analysed the model and wrote the manuscript. TvK and AMdR commented on model testing, the results and the manuscript text.

Author affiliations

Jasper C. Croll is at the:
Institute for Biodiversity and Ecosystem Dynamics (IBED), University of Amsterdam, P.O. Box 94240, 1090GE Amsterdam, The Netherlands.

André M. de Roos it at the:
Institute for Biodiversity and Ecosystem Dynamics (IBED), University of Amsterdam, P.O. Box 94240, 1090GE Amsterdam, The Netherlands.

Tobias van Kooten is at:
Wageningen Marine Research (WMR), Wageningen University and Research, P.O. Box 68, 1970AB IJmuiden, The Netherlands.

Quinten Mudde studied at the:
Institute for Biodiversity and Ecosystem Dynamics (IBED), University of Amsterdam, P.O. Box 94240, 1090GE Amsterdam, The Netherlands.